

A Dissertation

entitled

Catalysts with Increased Surface Affinity for Chemical Recycling of PET Waste

by

Hossein Abedsoltan

Submitted to the Graduate Faculty as partial fulfillment of the requirements for the

Doctor of Philosophy Degree in Chemical Engineering

Dr. Maria R. Coleman, Committee Chair

Dr. G. Glenn Lipscomb, Committee Member

Dr. Dong-Shik Kim, Committee Member

Dr. Constance A. Schall, Committee Member

Dr. Defne Apul, Committee Member

Dr. Scott Molitor, Acting Dean
College of Graduate Studies

The University of Toledo
August 2022

Copyright 2022 HOSSEIN ABEDSOLTAN

This document is copyrighted material. Under copyright law, no parts of this document may be reproduced without the expressed permission of the author.

An Abstract of
Catalysts with Increased Surface Affinity for Chemical Recycling of PET Waste

by

Hossein Abedsoltan

Submitted to the Graduate Faculty as partial fulfillment of the requirements for the
Doctor of Philosophy Degree in Chemical Engineering

The University of Toledo

August 2022

Polyethylene terephthalate (PET) is used in packaging and textile industries such as in productions of water bottles and packaging of soft drinks. As the PET products have short lifetimes, they turn into waste rapidly. Since the market for PET products has been constantly expanding, the rate of PET waste has been increased. This may negatively affect the environment and living species. In addition, PET is produced from fossil fuels, a limited resource that should be reserved to decrease the adverse effects of its applications on the environment. Therefore, recycling has been proposed as a resolution to PET waste.

Chemical recycling can decompose PET to the associated oligomers and monomers. This may provide an alternative resource for reproduction of PET and subsequently PET products. In this dissertation, hydrolysis was studied- a technique for chemically recycling of PET waste. In chemical recycling, the factors affecting the rate of PET decomposition are PET shape, PET size, reaction temperature, reaction pressure,

catalyst type, catalyst concentration, and surface wetting. Few studies are reported on surface wetting. So, the main interest of this dissertation was to explore the effect of surface wetting on the rate of PET decomposition in hydrolysis reactions.

In this dissertation, series of catalysts were introduced that could increase the rate of PET decomposition due to the better surface wetting of PET particles occurring with the solutions of these catalysts during the hydrolysis of PET. This effect was explored by applying a shrinking core model to interpret the kinetics data of TPA yield for calculations of reaction rate constants. These constants were correlated to the partition coefficient and distribution coefficient values of catalysts for the octanol/water system to indirectly study the PET/water system in hydrolysis. This revealed the role of functional group in catalyst structure as a determining factor for the hydrophobicity of catalyst solution, which may result in better surface wetting of PET. Moreover, the contact angle measurements were conducted to illustrate the effect of surface wetting. This work can be used to determine catalysts with higher surface affinity that may increase the rate of decomposition in chemically recycling of PET waste.

This dissertation is dedicated to my parents,

Ladan Bahramali and Mohammadjafar Abedsoltan,

For their endless love and support.

Acknowledgements

I'd like to thank my family members including my parents and my brother for the support and love they have given me through my life. I would like to thank my dear Bahar for her love, attention, and companionship along the journey I had during my Ph.D. studies.

I would like to thank Dr. Maria R. Coleman, my Ph.D. academic advisor. I am glad that we could work on the interesting topic of chemical recycling of PET. I am thrilled with the results achieved during my research. I'd like to thank my committee members Dr. Dong-Shik Kim, Dr. Lipscomb, Dr. Schall, and Dr. Apul. Their valuable comments on my research work helped better this dissertation. I was a teaching assistant for Dr. Dong-Shik Kim for the separation processes course and chemical process & simulation design course. I'm grateful that he nominated me three times for the outstanding teaching assistant award. I had this honor to have graduate courses with Dr. Lipscomb in membrane science and green engineering applications.

I would like to thank Corey Grice of Center for Materials and Sensor Characterization at the College of Engineering. I'm grateful that he trained me with most of the material characterization techniques including TGA, FTIR, UV-VIS, SEM, and TEM. I would like to thank Dr. Yong-Wah Kim of the NMR facility, the Department of Chemistry and Biochemistry, for training me on how to do the NMR analysis. Last but not least, I would like to thank my colleagues Kunal, Shahab, Matin, Surachet, Chinedu, Abdullah, Ehsan, Sedi, Sabrina, Emily, Ebuka, and Umberto.

Table of Contents

Abstract.....	iii
Acknowledgements.....	vi
Table of Contents.....	vii
List of Tables.....	xviii
List of Figures.....	xxi
List of Abbreviations.....	xxxii
List of Symbols.....	xxxv
Preface.....	xxxvii
1.....	1
Introduction.....	1
1.1 Overview.....	1
1.2 Hypothesis.....	2
1.3 Research Objectives.....	3

1.4 Organization of the dissertatio	6
2.....	7
A review on recycling techniques of polyethylene terephthalate with the focus on hydrolysis.....	7
2.1 Abstract	7
2.2 Introduction: Polyethylene terephthalate (PET) and the importance of recycling.....	8
2.3 Direct strategy for PET waste management.....	12
2.4 Chemical recycling of PET	13
2.5 PET Hydrolysis	20
2.5.1 Neutral hydrolysis	21
2.5.2 Alkaline hydrolysis.....	24
2.5.2.1 Background	24
2.5.2.2 Issued patents for PET alkaline hydrolysis.....	27
2.5.2.3 Phase transfer agents as catalysts for PET alkaline hydrolysis.....	27
2.5.2.4 Alternative heating methods: microwave and ultrasound.....	28
2.5.2.5 PET alkaline hydrolysis: recent studies	29
2.5.3 Acid hydrolysis	31

2.5.3.1 Background.....	31
2.5.3.2 Issued patents for PET acid hydrolysis.....	32
2.5.3.3 Enzymes as catalysts for PET acid hydrolysis.....	36
2.5.3.4 PET acid hydrolysis: recent studies	37
2.6. Conclusions.....	39
3.....	41
Materials and Methods.....	41
3.1 Materials.....	41
3.2 Experimental Methods	41
3.2.1 Synthesis of poly (4-styrene sulfonic acid) (PSSA) catalyst.....	41
3.2.2 Aryl sulfonic acids as catalysts for PET hydrolysis	43
3.2.3 Synthesis of DBU-LA catalyst	44
3.2.4 Synthesis of DBU sulfate (DBU-SO ₄) catalyst	45
3.2.4.1 Synthesis in acetonitrile as the solvent	45
3.2.4.2 Synthesis in water as the solvent.....	46
3.2.5 Syntheses of DBU-OA and DBU-CA catalysts	46

3.2.5.1 Synthesis in water as the solvent.....	46
3.2.5.2 Synthesis in methanol as the solvent.....	48
3.2.6 Titration measurements	49
3.2.7 pH tape strips.....	50
3.2.8 Contact angle measurements	50
3.2.9 Ethyl acetate hydrolysis reactions	51
3.2.10 PET hydrolysis reactions.....	51
3.3 Thermal Characterization.....	54
3.4 Structural Characterization	54
3.4.1 Fourier Transform-Infrared Spectroscopy (FTIR).....	54
3.4.2 Nuclear Magnetic Resonance Spectroscopy (NMR)	54
3.4.3 Scanning Electron Microscopy (SEM)	55
4.....	56
Poly (4-Styrenesulfonic Acid): A Recoverable and Reusable Catalyst for Acid Hydrolysis of Polyethylene Terephthalate	56
4.1 Highlights.....	57
4.2 Abstract	57

4.3 Graphical abstract	58
4.4 Keywords	58
4.5 Introduction	59
4.6 Experimental	61
4.6.1 Materials	61
4.6.2 PSSA catalyst synthesis.....	61
4.6.3 Titration measurements	62
4.6.4 PET hydrolysis reactions.....	62
4.6.5 Characterization of recovered PSSA and TPA.....	63
4.6.6 Contact angle measurements	64
4.6.7 Ethyl acetate hydrolysis (Model System).....	64
4.7 Results and Discussion.....	65
4.7.1 Temperature effect on the reaction kinetics	65
4.7.2 Catalyst concentration effect on acid hydrolysis reaction.....	72
4.7.3 Hydrolysis of ethyl acetate (Model System)	75
4.7.4 Mechanism for the acid hydrolysis of PET	77

4.7.5 Reutilization experiments with PSSA catalyst	79
4.8 Conclusions	81
4.9 Acknowledgements	82
4.10 Supplementary Material	83
4.10.1 Water content in the as-synthesized (Fresh) PSSA	83
4.10.2 Confirmation of TPA structure.....	84
4.10.3 Confirmation of PSSA structure.....	86
4.10.4 PSSA recovery yield	89
5.....	90
Aryl sulfonic acid catalysts: Effect of pendant group structure on activity in hydrolysis of polyethylene terephthalate (PET)	
5.1 Abstract	91
5.2 Graphical abstract	92
5.3 Study description.....	92
5.4 Keywords	92
5.5 Introduction	93
5.6 Experimental section.....	95

5.6.1. Materials	95
5.6.2 PET hydrolysis	96
5.6.3 Ethyl acetate hydrolysis.....	98
5.6.4 Contact angle measurements.....	98
5.6.5 Recovered TPA characterization.....	99
5.7. Results and Discussion	99
5.7.1 Shrinking core model for PET hydrolysis.....	99
5.7.3 Effect of catalyst concentration the TPA yield	102
5.7.4 Effect of reaction temperature on the TPA yield	104
5.7.5. Ethyl acetate hydrolysis, homogeneity effect on the reaction rate and activation energy	108
5.7.6 Wetting studies of catalyst solutions on the PET surface	110
5.7.7 Octanol/water distribution coefficients of the catalysts.....	112
5.8 Conclusions	116
5.9 Acknowledgements	117
5.10 Supporting Information.....	118
5.10.1 Confirmation of the structure of recovered terephthalic acid (TPA)	118

5.10.2 Effect of catalyst concentration on PET conversions (%).....	121
5.10.3 Reaction temperature effect on PET conversions (%), PET hydrolysis	122
5.10.4 Fitting the shrinking core model to PET hydrolysis kinetic data.....	123
6.....	125
DBU-acid ionic liquids: transformation of weak acids to basic ionic liquids as more thermally stable and higher active catalysts for PET hydrolysis	125
6.1. Abstract	125
6.2. Introduction.....	126
6.3. Results and Discussion.....	127
6.3.1 The acidity of the individual components for hydrolysis of PET	127
6.3.2 TGA of the catalysts used for hydrolysis of PET.....	128
6.3.3 Preliminary results for TPA yield (%) for 2M solutions of ionic liquids	129
6.3.4 Effect of catalyst concentration hydrolysis kinetics at 150°C.....	131
6.3.4.1 Shrinking core model to fit the kinetics data of TPA yield (%)	131
6.3.4.2 Comparison of catalytic activity DBU and organic acids at 150°C..	132
6.3.4.3 Catalytic activity of DBU-acid ionic liquids at 150°C	135
6.3.4.4 Comparison of times to achieve 90% TPA at 150°C.....	137

6.3.4.5 Reaction rate constants for catalysts studied at 150°C	138
6.3.5 Effect of reaction temperature on TPA yield (%), 2M catalyst solutions	139
6.3.5.1 Shrinking core model to fit the kinetics data of TPA yield (%)	139
6.3.5.2. Reaction kinetics for 2 M DBU and acid solutions	140
6.3.5.3. Reaction kinetics for 2 M DBU-acid ionic liquids	141
6.3.5.4. Time to achieve 90% TPA yield for 2 M solutions of catalysts	142
6.3.5.5 Reaction rate constants at 2 M catalyst solution.....	143
6.3.5.6 Activation energy for 2M solutions of catalysts.....	144
6.3.6 Wetting studies of the tested catalysts for hydrolysis of PET.....	146
6.4 Comparison with ionic liquids reported as catalysts for hydrolysis of PET ..	149
6.5 Conclusions	152
7.....	153
Conclusions and Future Work	153
7.1. Conclusions.....	153
7.1.1 Overall outcomes for hydrolysis of PET with presented catalysts.....	153
7.1.2 Comparison of catalysts used for hydrolysis of PET	160

7.2. Future work	167
References	169
A	245
Supporting Information for Chapter 6	245
B	266
The chemical structures of tested catalysts in Chapter 6	266
C	268
FTIR results for Chapter 6	268
D	274
¹ H NMR results for Chapter 6	274
E	284
TGA results for DBU and DBU-acid ionic liquids	284
F	285
Comparisons of tested catalysts for hydrolysis of PET	285
G	289
Octanol/water partition coefficient (P) values	289

H..... 291

Apparent reaction rate constant as the function of the contact angle value
..... 291

List of Tables

4-1	Specific reaction rate constants (k) obtained with 2 M aqueous solutions of PSSA and H ₂ SO ₄ as a function of the reaction temperature.	71
4-2	Apparent reaction rate constants (K) vs catalyst concentration (H ⁺), based on the shrinking-core model and TPA recovery with PSSA and H ₂ SO ₄ catalysts at T _{reaction} =150°C.	75
5-1	Apparent reaction rate constants (K _a values) as a function of the catalyst concentration for PET hydrolysis at T _{Reaction} = 150°C.	104
5-2	Apparent reaction rate constants (K) for the 2M catalyst solutions as function of reaction temperature for PET hydrolysis.	106
5-3	Apparent reaction rate constants (K values) for the ethyl acetate hydrolysis with 0.5M PTSA, 2-NSA, and 1,5-NDSA solutions [43].	108
5-4	Reported reaction conditions to achieve more than 90% TPA yield for PET acid hydrolysis.	116
6-1	The acidity (pK _x) values of the tested components as catalysts for hydrolysis of PET. The values are based on dissociation in water at 25°C [501, 502].	128
6-2	The water content of the catalysts, determined by TGA curves.	129
6-3	TPA yield (%) for 2M solutions of DBU-acid ionic liquids for hydrolysis of PET at T _R = 150°C and t _R = 10 hours.	130
6-4	Reaction time needed to achieve more than 90% TPA yield at T _R =150°C.	137

6-5	Apparent reaction rate constants (K_a) as a function of the catalyst concentration for PET hydrolysis at 150°C.	138
6-6	Reaction time needed to achieve more than 90% TPA yield for 2M catalyst solutions at reaction temperature of 130°C, 140°C and 150°C.	143
6-7	Apparent reaction rate constant (K_a values) as a function of the reaction temperature for 2M catalyst solutions for PET hydrolysis.	144
6-8	Activation energies for 2M solutions of the tested catalysts for PET hydrolysis.	145
6-9	Comparison of this study with the reported ionic liquids as catalysts for hydrolysis of PET.	150
7-1	The required reaction time to achieve more than 90% TPA yield, 4M catalyst concentration, $T_R = 150^\circ\text{C}$ (Hydrolysis of PET in water).....	161
A-6-S1	Results of pH tape strips and estimated $[\text{H}^+]$ values for the synthesized DBU-SO ₄ in water, equimolar ratio of DBU to H ₂ SO ₄	250
A-6-S2	Results of pH tape strips and estimated $[\text{H}^+]$ values for the synthesized DBU-OA in water, equimolar ratio of DBU to OA.....	251
A-6-S3	Results of pH tape strips and estimated $[\text{H}^+]$ values for the synthesized DBU-OA in water, titration molar ratio of DBU (2.08) to OA (1).	251
A-6-S4	Results of pH tape strips and estimated $[\text{H}^+]$ values for the synthesized DBU-CA in water, equimolar ratio of DBU to CA.	252
A-6-S5	Results of pH tape strips and estimated $[\text{H}^+]$ values for the synthesized DBU-CA in water, titration molar ratio of DBU (3.61) to CA (1).....	253
A-6-S6	Results of pH tape strips and estimated $[\text{H}^+]$ values for the synthesized DBU-SO ₄ in organic solvent, equimolar ratio of DBU to H ₂ SO ₄	254

A-6-S7	Results of pH tape strips and estimated $[\text{OH}^-]$ values for the synthesized DBU-LA, equimolar ratio of DBU to LA.....	255
A-6-S8	Results of pH tape strips and estimated $[\text{OH}^-]$ values for the synthesized DBU-OA in organic solvent, structural molar ratio of DBU (2) to H_2SO_4 (1).	255
A-6-S8	Results of pH tape strips and estimated $[\text{OH}^-]$ values for the synthesized DBU-CA in organic solvent, structural molar ratio of DBU (3) to CA (1).	256
A-6-S9	Specific reaction rate constants (k_{sp} values), PET hydrolysis at $T_{\text{R}} = 150^\circ\text{C}$	260
A-6-S10	Specific reaction rate constants (k_{sp} values) as a function of the reaction temperature for 2M catalyst solutions for PET hydrolysis.	265

List of Figures

2-1	The two paths for the synthesis of PET.....	10
2-2	Schematic diagram of PET chemical recycling techniques.....	14
2-3	Glycolysis of PET.....	16
2-4	Alcoholysis of PET.....	17
2-5	Methanolysis of PET.	17
2-6	Aminolysis of PET.	19
2-7	Ammonolysis of PET.	19
2-8	Schematic of PET particles distributed in a hydrolysis reaction medium.	21
2-9	Neutral hydrolysis of PET to TPA and EG.	22
2-10	Alkaline hydrolysis of PET with NaOH, TPA recovery with H ₂ SO ₄ [263].	25
2-11	Mechanism for PET acid hydrolysis, a: dissociation step, b: nucleophilic addition, c: hydrolysis step, d: deprotonation step, e: formation step [264-266].....	26
2-12	Mechanism for PET hydrolysis with H ₂ SO ₄ , proposed by Bryan Jr. et al. [296].	33
2-13	Mechanism for PET acid hydrolysis, a: dissociation step, b: first protonation step, c: water molecule attack step, d: second protonation step, e: formation step, proposed by Li et al. [297], reproduced from [58].	35

3-1	The ion-exchange reaction, converting PSSS (left) to PSSA (right).....	42
3-2	Poly (sodium 4-styrenesulfonate) (PSSS) (Left) and the synthesized PSSA (Right).....	43
3-3	Structures of aryl sulfonic acids, used for PET hydrolysis: a) P-toluene sulfonic acid (PTSA), b) 1, 5- Naphthalenedisulfonic acid (NDSA), and c) 2- Naphthalenesulfonic acid (NSA).	44
3-4	Synthesis reaction path for production of DBU-LA: a) DBU, b) LA, and c) DBU-LA.	45
3-5	Reaction path for production of DBU-SO ₄ : a) DBU, b) H ₂ SO ₄ , and c) DBU-SO ₄	46
3-6	Structures of a) oxalic acid (OA) and b) citric acid (CA).	48
3-7	Reaction path for production of DBU-OA: a) DBU, b) OA, and c) DBU-OA... ..	49
3-8	Reaction path for production of DBU-CA: a) DBU, b) CA, and c) DBU-CA.... ..	49
3-9	The acid hydrolysis process conducted in the lab, illustrated for PSSA.	52
3-10	The alkaline hydrolysis process conducted in the lab, illustrated for DBU-LA. 53	
4-1	Reaction temperature effect on the PET conversion (%) with 2 M solutions of (a) PSSA at 150°C (Δ), 140°C (□), and 130°C (○), and (b) H ₂ SO ₄ at 150°C (▲), 140°C (■), and 130°C (●).....	66
4-2	Reaction temperature effect on the TPA yield (%) for 2 M solutions of (a) PSSA at 150°C (Δ), 140°C (□), and 130°C (○), and (b) H ₂ SO ₄ at 150°C (▲), 140°C (■), and 130°C (●).	67
4-3	Shrinking-core model fitting to the results obtained with 2 M solutions of (a) PSSA (Δ), and (b) H ₂ SO ₄ (▲) at T _{reaction} =150°C.....	70

4-4	Arrhenius plots obtained from the hydrolysis of PET with 2 M solutions of (a) PSSA (Δ), and (b) H_2SO_4 (\blacktriangle).	71
4-5	PET conversions (%) obtained with (a) 1 M, (b) 2 M, and (c) 4 M solutions of PSSA (Δ) and H_2SO_4 (\blacktriangle) at $T_{\text{reaction}}= 150^\circ\text{C}$.	73
4-6	TPA yields (%) obtained with (a) 1 M, (b) 2 M, and (c) 4 M solutions of PSSA (Δ) and H_2SO_4 (\blacktriangle) at $T_{\text{reaction}}= 150^\circ\text{C}$.	74
4-7	Arrhenius plots obtained from the hydrolysis of ethyl acetate with (a) PSSA (Δ), and (b) H_2SO_4 (\blacktriangle).	76
4-8	(a-c) 0.5 M, 1 M, and 2 M solutions of PSSA on the PET surface, respectively, and (d-f) 0.5 M, 1 M, and 2 M solutions of H_2SO_4 on the PET surface, respectively.	78
4-9	Contact angle measurements obtained with different concentrations of PSSA (Δ) and H_2SO_4 (\blacktriangle) aqueous solutions on the PET surface.	79
4-10	Reutilization results obtained with a 2 M solution of PSSA: PET conversion (\blacksquare) and TPA yield (\square). Every reaction was run at 150°C for 14 h.	80
4-11	Titration results obtained from the recovered PSSA after every reaction cycle.	81
4-S1.	TGA analysis of fresh PSSA.	83
4-S2.	FTIR spectra of (a) commercial TPA and (b) recovered TPA.	85
4-S3.	$^1\text{H-NMR}$ spectra of (a) commercial TPA and (b) recovered TPA.	86
4-S4.	FTIR spectra of (a) fresh PSSA and (b) recycled PSSA.	87
4-S5.	$^1\text{H-NMR}$ spectra of recovered PSSA.	88
4-S6.	$^{13}\text{C-NMR}$ spectra of recovered PSSA.	88

4-S7.	PSSA recovery yield (% of mass recovered) after every reaction round (2 M solution of PSSA, 150 °C, and 14 h).	89
5-1	TGA analysis to determine water content of the as-purchased PTSA (...), 2-NSA (—), and 1,5-NDSA (---).	96
5-2	Structure of catalysts used for PET hydrolysis (a) PTSA, (b) 2-NSA, and (c) 1,5-NDSA.	97
5-3	Impact of time on PET conversion (%) / TPA yield (%) for PET hydrolysis with 2M solutions of PTSA (●/ ○), 2-NSA (▲/ Δ), and 1,5-NDSA (■/ □) at 150°C.....	100
5-4	Fit of shrinking core model to the kinetic data at 150°C for 2M catalyst solutions of PTSA (○, ...), 2-NSA (Δ, —) and 1,5-NDSA (□, ---).	102
5-5	Effect of catalyst concentration on TPA yield at $T_{\text{Reaction}} = 150^{\circ}\text{C}$ with (a) 1M, (b) 2M, and (c) 4M solutions of PTSA (○, ---), 2-NSA (Δ, ---) and 1,5-NDSA (□, —). The lines represent the fit of the shrinking core model.	103
5-6	Effect of Temperature on the TPA yield for 2M catalyst solutions with (a) PTSA, (b) 2-NSA, and (c) 1,5-NDSA at 130°C (□, ...), 140°C (Δ, —) and 150°C (○, ---). The lines represent the fit of the shrinking core model.	105
5-7	Application of Arrhenius equation to specific rate constants for the 2M catalyst solutions of PTSA (○, ...), 2-NSA (▲, —) and 1,5-NDSA (□, ---), PET hydrolysis....	107
5-8	Application of Arrhenius equation to reaction rate constants for the 0.5M catalyst solutions of PTSA (○, ...), 2-NSA (Δ, —) and 1,5-NDSA (□, ---) for ethyl acetate hydrolysis.....	109
5-9	Droplet shape of catalyst solutions on the PET films for PTSA: (a) 0.5M, (b) 1M, (c) 2M, (d) 4M; 2-NSA: (e) 0.5M, (f), 1M, (g) 2M, (h) 4M; 1,5-NDSA: (i) 0.5M, (j), 1M, (k) 2M, (l) 4M.	111
5-10	Contact angle values for the catalyst solutions, 0.25M to 4M, of PTSA (○), 2-NSA (Δ), 1,5-NDSA (□), and H_2SO_4 (x) [43] on the PET surface.....	112

5-11	Apparent reaction rate constant (K) dependence on Log P for PET hydrolysis with 2M catalyst concentrations of PTSA (●), 2-NSA (▲), 1,5-NDSA (■), and H ₂ SO ₄ (◆) at a reaction temperature of 150°C.....	114
5-12	Apparent reaction rate constant (K) dependence on Log D for PET hydrolysis with 2M catalyst concentrations of PTSA (●), 2-NSA (▲), 1,5-NDSA (■), and H ₂ SO ₄ (◆) at a reaction temperature of 150°C.....	115
5-S1	FTIR spectra for (a) commercial TPA and the TPA recovered from PET hydrolysis with catalyst solutions of (b) PTSA, (c) 2-NSA, and (d) 1,5-NDSA.....	119
5-S2	¹ H NMR spectra for (a) commercial TPA and the TPA recovered from PET hydrolysis with catalyst solutions of (b) PTSA, (c) 2-NSA, and (d) 1,5-NDSA.....	120
5-S3	Effect of catalyst concentration on PET conversion (%) at 150°C with (a) 1M, (b) 2M, and (c) 4M solutions of PTSA (○), 2-NSA (Δ) and 1,5-NDSA (□).	121
5-S4	Effect on the TPA yields for 2M catalyst solutions with (a) PTSA, (b) 2-NSA, and (c) 1,5-NDSA at 130°C (□), 140°C (Δ) and 150°C (○).	122
5-S5	Fit of shrinking core model to the kinetic data at 150°C for 1M catalyst solutions of PTSA (○, ...), 2-NSA (Δ, —) and 1,5-NDSA (□, ---).....	123
5-S6	Fit of shrinking core model to the kinetic data at 150°C for 4M catalyst solutions of PTSA (○, ...), 2-NSA (Δ, —) and 1,5-NDSA (□, ---).....	124
6-1	Fit of shrinking core model to the TPA yield kinetics data at T _R = 150°C for 1M (□, —), 2M (○, ---), and 4M (Δ, ...) solutions of DBU.	132
6-2	TPA yield kinetics data at T _R =150°C for 1M (□, —), 2M (○, ---), and 4M (Δ, ...) solutions of DBU. The lines illustrate the fit of shrinking core model.....	133
6-3	TPA yield kinetics data at T _R =150°C for (a) 1M, (b) 2M, and (c) 4M solutions of LA (□, —), OA (○, ---), and CA (Δ, ...).....	134

6-4	Effect of catalyst concentration on TPA yield at $T_R=150^\circ\text{C}$ for (a) 1M, (b) 2M, and (c) 4M solutions of DBU-LA (\square , —), DBU-OA (\circ , ---), and DBU-CA (Δ , ...). The lines illustrate the fit of shrinking core model.	136
6-5	Fit of shrinking core model to the TPA yield (%) kinetics data for 2M solutions of DBU at $T_R=130^\circ\text{C}$ (\square , —), $T_R=140^\circ\text{C}$ (\circ , ---), and $T_R=150^\circ\text{C}$ (Δ , ...).	139
6-6	TPA yield kinetics data for 2M solutions of DBU at $T_R=130^\circ\text{C}$ (\square , —), $T_R=140^\circ\text{C}$ (\circ , ---), and $T_R=150^\circ\text{C}$ (Δ , ...) solutions of DBU. The lines illustrate the fit of shrinking core model.....	140
6-7	Effect of reaction temperature on TPA yield at (a) $T_R=130^\circ\text{C}$, (b) $T_R=140^\circ\text{C}$, and (c) $T_R=150^\circ\text{C}$ for 2M solutions of LA (\square , —), OA (\circ , ---), and CA (Δ , ...). The lines illustrate the fit of shrinking core model.....	141
6-8	Effect of reaction temperature on TPA yield at (a) $T_R=130^\circ\text{C}$, (b) $T_R=140^\circ\text{C}$, and (c) $T_R=150^\circ\text{C}$ for 2M solutions of DBU-LA (\square , —), DBU-OA (\circ , ---), and DBU-CA (Δ , ...). The lines illustrate the fit of shrinking core model.....	142
6-9	Fitted lines of Arrhenius equation for 2M solutions of DBU (x, ---), LA (\square , ---), OA (\circ , ---), CA (Δ , ...), DBU-LA (\square , —), DBU-OA (\circ , —), DBU-CA (Δ , —).....	145
6-10	Evolution of the 0.25M solution of DBU droplet within the wetting process of the surface on the PET films at (a) $t=1$ s, (b) $t=3$ s, (c) $t=5$ s, (d) $t=7$ s, (e) $t=9$ s, (f) $t=11$ s, (g) $t=13$ s, (h) $t=15$ s, (i) $t=27$ s, (j) $t=39$ s, (k) $t=51$ s, (l) $t=63$ s, (m) $t=75$ s, (n) $t=87$ s, (o) $t=99$ s, (p) $t=111$ s.	147
6-11	The droplet shape of solutions of weak acids on the PET films for LA: (a) 0.25M, (b) 0.5M, (c) 1M, (d) 1M, (e) 4M; OA: (f) 0.25M, (g) 0.5M, (h) 1M; CA: (i) 0.25M, (j) 0.5M, (k) 1M, (l) 2M.	148
6-12	The droplet shape of solutions of DBU-acid ionic liquids on the PET films for DBU-LA: (a) 0.25M, (b) 0.5M, (c) 1M, (d) 1M, (e) 4M; DBU-OA: (f) 0.25M, (g) 0.5M, (h) 1M, (i) 2M, (j) 4M; DBU-CA: (k) 0.25M, (l) 0.5M, (m) 1M, (n) 1M, (o) 4M.....	148

6-13 The contact angle values as a function of the concentration of catalyst solution for LA (■), OA (●), CA (▲), DBU-LA (□), DBU-OA (○), and DBU-CA (Δ).....	149
7-1 Apparent reaction rate constants (K values) as the function of Log D for 2M solutions of catalysts H ₂ SO ₄ (X), PSSA (◇), PTSA (○), 2-NSA (○), 1,5-NDSA (○), LA (▲), OA (▲), CA (▲), DBU-LA (■), DBU-OA (■), and DBU-CA (■),.....	163
Reaction temperature = 150°C (Hydrolysis of PET in water) [43, 49].....	163
7-2 The SEM images of the surface of raw PET powder, a) agglomeration of smaller PET particles on the surface, b and c) the layer-by-layer structure of the PET surface.	164
7-3 The surface of unreacted PET powder, recovered after 3 hours reaction time for 2M catalyst solutions of a. H ₂ SO ₄ , b. PSSA, and c. DBU-LA.....	165
7-4 The observed patterns of degradation on the surface for unreacted PET powder for 2M solutions of catalysts a. H ₂ SO ₄ , b. PSSA, c. PTSA, and d. DBU-LA. The average TPA yield (20%) and TR = 150°C.	166
A-6-S1 TGA curves for DBU (—), H ₂ SO ₄ (—), LA (---), OA (...), and CA (— ●).	245
A-6-S2 TGA curves for DBU-SO ₄ (—), DBU-OA-equimolar (—), DBU-OA-titration (---), DBU-CA-equimolar (— ●), and DBU-CA-titration (...), synthesized in water.....	246
A-6-S3 TGA curves for DBU-SO ₄ (...), DBU-LA (---), DBU-OA (—), and DBU-CA (— ●), synthesized in organic solvents.....	247
A-6-S4 The hydroxyl (OH ⁻) concentration as a function of the concentration of DBU (O, ---), the dashed line is linear fitting; [OH ⁻] = 0.85 * [DBU], R ² = 0.9993.....	248
A-6-S5 The proton (H ⁺) concentration as a function of the concentrations of LA (O, ---), OA (O, ---), and CA (O, ---), the dashed lines are linear fitting; [H ⁺] _{LA} = 0.97 * [LA], R ² _{LA} = 0.9999; [H ⁺] _{OA} = 1.77 * [OA], R ² _{OA} = 0.9994; [H ⁺] _{CA} = 3.07 * [CA], R ² _{CA} = 0.9996.....	249

A-6-S6 Fit of shrinking core model to the TPA yield kinetic data at $T_R = 150^\circ\text{C}$ for (a) 1M, (b) 2M, and (c) 4M solutions of LA (\square , —), OA (\circ , ---), and CA (Δ , ...).	257
A-6-S7 Fit of shrinking core model to the TPA yield kinetic data at $T_R = 150^\circ\text{C}$ for (a) 1M, (b) 2M, and (c) 4M solutions of DBU-LA (\square , —), DBU-OA (\circ , ---), and DBU-CA (Δ , ...). The lines illustrate the fit of shrinking core model.	258
A-6-S8 PET conversion kinetics data at $T_R = 150^\circ\text{C}$ for 1M (\square), 2M (\circ), and 4M (Δ) solutions of DBU.	259
A-6-S9 PET conversion kinetics data at $T_R = 150^\circ\text{C}$ for (a) 1M, (b) 2M, and (c) 4M solutions of LA (\square), OA (\circ), and CA (Δ).	260
A-6-S10 Fit of shrinking core model to the TPA yield kinetic data, 2M solutions of LA (\square , —), OA (\circ , ---), and CA (Δ , ...) at (a) $T_R = 130^\circ\text{C}$ (b) $T_R = 140^\circ\text{C}$, and (c) $T_R = 150^\circ\text{C}$.	261
A-6-S11 Fit of shrinking core model to the TPA yield kinetic data for 2M solutions of DBU-LA (\square , —), DBU-OA (\circ , ---), and DBU-CA (Δ , ...) at (a) $T_R = 130^\circ\text{C}$ (b) $T_R = 140^\circ\text{C}$, and (c) $T_R = 150^\circ\text{C}$.	262
A-6-S12 PET conversion kinetics data for 2M solutions of DBU at $T_R = 130^\circ\text{C}$ (\square), $T_R = 140^\circ\text{C}$ (\circ), and $T_R = 150^\circ\text{C}$ (Δ) solutions of DBU.	263
A-6-S13 Effect of reaction temperature on PET conversion at (a) $T_R = 130^\circ\text{C}$, (b) $T_R = 140^\circ\text{C}$, and (c) $T_R = 150^\circ\text{C}$ for 2M solutions of LA (\square), OA (\circ), and CA (Δ).	264
B The chemical structures of catalysts a. sulfuric acid (H_2SO_4), b. lactic acid (LA), c. oxalic acid (OA), d. citric acid (CA), e. 1,8-Diazabicyclo (5.4.0) undec-7-ene (DBU),	
f. DBU- SO_4 , g. DBU-LA, h. DBU-OA, and i. DBU-CA.	267
C-1 The FTIR spectra for a. commercial TPA (—) [49] and recovered TPA samples from the hydrolysis of PET with 2M aqueous catalyst solutions of b. LA (—), c. OA (—), and d. CA (—), ($T_R = 150^\circ\text{C}$).	268

C-2 The FTIR spectra for a. commercial TPA (—) [49] and recovered TPA samples from the hydrolysis of PET with 2M aqueous catalyst solutions of b. DBU (—),.....	269
c. DBU-LA (—), d. DBU-OA (—), and e. DBU-CA (—), ($T_R = 150^\circ\text{C}$).	269
C-3 The FTIR spectra for a. DBU (—), b. DBU-SO ₄ synthesized in water (—),	270
and c. DBU-SO ₄ synthesized in organic solvent (—).	270
C-4 The FTIR spectra for a. DBU (—), b. lactic acid (LA) (—), and	271
c. synthesized DBU-LA (—).	271
C-5 The FTIR spectra for a. DBU (—), b. oxalic acid (OA) (—),	272
c. DBU-OA-equimolar synthesized in water (—),	272
d. DBU-OA-titration synthesized in water (—), and	272
e. DBU-OA synthesized in methanol (—).	272
C-6 The FTIR spectra for a. DBU (—), b. DBU-CA-equimolar synthesized in water (—), c. DBU-CA-titration synthesized in water (—), and d. DBU-CA synthesized in methanol (—).	273
D-1 The ¹ H NMR spectra of a. commercial TPA (—) [43, 49] and recovered TPA samples from the hydrolysis of PET with 2M aqueous catalyst solutions of b. LA (—), c. OA (—), and d. CA (—), ($T_R = 150^\circ\text{C}$).	275
D-2 The ¹ H NMR spectra of the recovered TPA samples from the hydrolysis of PET with 2M aqueous catalyst solutions of a. DBU (—) b. DBU-LA (—), c. DBU-OA (—), and d. DBU-CA (—), ($T_R = 150^\circ\text{C}$).	277
D-3 The ¹ H NMR spectra of a. DBU-SO ₄ synthesized in organic solvent (—) and	278

b. DBU-SO ₄ synthesized in water (—).....	278
D-4 The ¹ H NMR spectra of a. lactic acid (LA) (—) and.....	279
b. synthesized DBU-LA (—).....	279
D-5 The ¹ H NMR spectra of a. oxalic acid (OA) (—),.....	281
b. DBU-OA-equimolar synthesized in water (—), c. DBU-OA-titration synthesized in water (—), d. DBU-OA synthesized in methanol (—).....	281
D-6 The ¹ H NMR spectra of a. citric acid (CA) (—),.....	283
b. DBU-CA-equimolar synthesized in water (—), c. DBU-CA-titration synthesized in water (—), d. DBU-CA synthesized in methanol (—).....	283
E The TGA curves for DBU (...) and DBU-acid ionic liquids synthesized in methanol: DBU-LA (---), DBU-OA (—), and (DBU-CA (— •).....	284
F-1 The required time to achieve more than 90% TPA yield as a function of the catalyst concentration, 1M (—), 2M (---), 4M (...), aqueous solutions of LA, OA, and CA,.....	285
Reaction temperature = 150°C (Hydrolysis of PET in water) [43, 49].....	285
F-2 The required time to achieve more than 90% TPA yield as a function of the catalyst concentration, 1M (—), 2M (---), 4M (...), aqueous solutions of H ₂ SO ₄ , PSSA, (1,5-NDSA), 2-NSA, DBU-LA, DBU-OA, and DBU-CA,	286
Reaction temperature = 150°C (Hydrolysis of PET in water) [43, 49].....	286
F-3 The required time to achieve more than 90% TPA yield as a function of the reaction temperature, 130°C (—), 140°C (---), 150°C (...), 2M aqueous solutions of LA, OA, and CA,	287

Catalyst concentration = 2M (Hydrolysis of PET in water) [43, 49].....	287
F-4 The required time to achieve more than 90% TPA yield as a function of the reaction temperature, 130°C (—), 140°C (---), 150°C (...), 2M aqueous solutions of H ₂ SO ₄ , PSSA, (1,5-NDSA), 2-NSA, DBU-LA, DBU-OA, and DBU-CA,.....	288
Catalyst concentration = 2M (Hydrolysis of PET in water) [43, 49].....	288
G Apparent reaction rate constants (K values) as the function of Log P for 2M solutions of catalysts H ₂ SO ₄ (X), PSSA (◇), PTSA (○), 2-NSA (○), 1,5-NDSA (○), LA (▲), OA (▲), CA (▲), DBU-LA (■), DBU-OA (■), and DBU-CA (■),.....	290
Reaction temperature = 150°C (Hydrolysis of PET in water) [43, 49].....	290
H The apparent reaction rate constants as the function of the contact angle values for aqueous catalyst solutions of 2-NSA (●), PTSA (●), DBU-LA (●), and DBU-CA (●).	291
[43, 49].....	291

List of Abbreviations

3Bu6DPB	Tributylhexadecylphosphonium bromide
BHET	Bis (2-hydroxyethyl) terephthalate
BHETPA	Bis (2-hydroxyl-ethylene) terephthalamide
CA	Citric acid
¹² C-NMR	Carbon nuclear magnetic resonance spectroscopy
DBU	1,8-Diazabicyclo [5.4.0] undec-7-ene
DI	Deionized
DEHP	Di (2-ethylhexyl) phthalate
DMT	Dimethyl terephthalate
DP	Degree of polymerization
EG	Ethylene glycol
E	Equimolar
FTIR	Fourier-transform infrared spectroscopy
GVL	γ-valerolactone
¹ H-NMR	Proton nuclear magnetic resonance spectroscopy

IL	Ionic Liquid
LA	Lactic acid
MHET	Methyl-2-hydroxy ethylene terephthalate
MR	Mechanical recycling
MW	Molecular weight
NDSA	1, 5- Naphthalenedisulfonic acid
NSA	2- Naphthalenesulfonic acid
NMR	Nuclear magnetic resonance spectroscopy
OA	Oxalic acid
PET	Polyethylene terephthalate
PENTE	Pentaerythrytol
PSSA	Poly (4-styrene sulfonic acid)]
PSSS	Poly (sodium 4-styrenesulfonate)
PTA	Phase transfer agent
PTSA	P-toluene sulfonic acid
PVC	Polyvinyl chloride
RPET	Recycled polyethylene terephthalate
SEM	Scanning electron microscopy

TBD	1,5,7-triazabicyclo [4.4.0] dec-5-ene
TBAI	Tetra butyl ammonium iodide
TGA	Thermal gravimetric analysis
T	Titration
TPA	Terephthalic acid

List of Symbols

A	Pre-exponential factor
atm	Atmosphere
C	Catalyst concentration
oC	Degree centigrade
d	Day
Ea	Activation energy
g	Gram
Hz	Hertz
h	Hour
J	Joule
k	Kilo
Ka	Apparent reaction rate constant
ksp	Specific reaction rate constant
L	Liter
Log D	Logarithmic distribution coefficient
Log P	Logarithmic partition coefficient
M	Molar
MJ	Mega joule

m	Milli
$m_{PET,i}$	Initial mass of PET
$m_{PET,t}$	Mass of recovered PET after reaction time t
min	Minute
n	Nano
P	Pascal
P_R	Reaction pressure
pK _x	The acidity value for the x th proton
R	Universal gas constant
r_i	The average initial radius of PET particles
T	Absolute temperature
T_R	Reaction temperature
t	Reaction time
t_R	Reaction time
W	Watt
wt%.....	Weight percentage
ρ	Density
%	Weight percentage
[]	Aqueous concentration in molar

Preface

Plastics are consumed as packaging materials, textile fibers, automotive parts, and household utensils. This broad range of applications and the increase of market demand have caused an inevitable growth in the rate of plastic productions for the past four decades, which has estimated to be maintained for the next coming years. Recycling has been proposed as a strategic resolution to encounter with the generation of the plastic wastes. The main four types of recycling are classified as primary, mechanical, incineration, and chemical.

The primary recycling is a restrained method that is solely used in plastic production plants to recycle the plastic wastes, generated within the plants, and they have high-purity and near-to-zero contaminants. Comparatively, mechanical recycling can be applied to a larger spectrum of plastic wastes but may not be applicable to the mixture of different types of plastic wastes or the plastic wastes that are highly contaminated with other chemicals. Moreover, mechanical recycling may not be tried repeatedly for recycling of the same plastic waste, as the recycling sample, because it degrades the physical and chemical characteristics of the recycled plastic products for every recycling round. Incineration is usually applied when there's no way to separate the mixture of plastic wastes that are highly contaminated. It releases toxic gases of CO_x and NO_x with the residuals of ash. These gases are perceived as the main cause of the global warming and air pollution. Residual ashes are landfilled that may penetrate soil and water, threatening

the lives of species in these areas. Thus, chemical recycling is the only type of recycling that introduces more sustainable techniques.

Various techniques are proposed to chemically recycle plastic wastes. The three main techniques are glycolysis, methanolysis, and hydrolysis. Hydrolysis is the mere technique where an environmentally friendly solvent, i.e., water, is used to degrade plastic wastes. This dissertation focuses on hydrolysis of one major type of plastic wastes, polyethylene terephthalate (PET). PET is the main constituent of soft drink bottles, and it is also broadly used in packaging and textile industries. The factors that affect hydrolysis of PET are reaction conditions including reaction temperature and pressure, PET shape, PET size, catalyst type, catalyst concentration, and catalyst activity.

Hydrolysis suffers from harsh reaction conditions including high reaction temperature or high catalyst concentration and low rates of PET degradation. It is a heterogenous reaction that occurs on the surface of PET. The reaction products are terephthalic acid (TPA), the PET monomer, and ethylene glycol (EG). There are three types of hydrolysis, depending on the pH of catalyst-water solution, neutral, alkaline, and acid. This dissertation focuses on alkaline and acid hydrolysis since these two types of hydrolysis can provide milder reaction conditions for PET hydrolysis. Moreover, the focus is to study the wetting of the surface as one of the major effects on the rate of hydrolysis, explored and reported few in recycling literature. For this purpose, this study introduces the series of catalysts that can enhance the wetting of the surface of PET particles within the aqueous medium, causing an increase in the local concentration of hydroxyls (OH^-) and protons

(H⁺) for alkaline and acid hydrolysis, respectively. These catalysts can decompose PET at milder reaction conditions and higher degradation rates.

The catalyst concentration and the reaction temperature of hydrolysis of PET are explored in the aqueous solutions. The kinetics data of PET conversion (%) and TPA yield (%) are gathered and depicted to illustrate the progress of hydrolysis for PET particles. The reaction rate constants are determined by applying a shrinking core model to compare the activity of the tested catalysts quantitatively. The contact angle measurements are conducted to observe the catalyst concentration effect on the wetting of the surface with the aqueous solutions of the tested catalysts.

The dissertation is divided into four major parts. In the first part, a comprehensive review is conducted on PET recycling techniques with the focus on hydrolysis. In the second part, the synthesized poly (4-styrenesulfonic acid) is introduced as a recoverable and reusable catalyst for PET hydrolysis that can also increase the wetting of the surface of the PET particles in the aqueous reaction medium. The experimental kinetics data for PET conversion (%) and TPA yield (%) are compared with the ones obtained with sulfuric acid, the conventional catalyst used for acid hydrolysis of PET. For the third part of the dissertation, a series of aryl sulfonic catalysts are studied, which can increase the wetting of the surface and can propose milder reaction conditions for hydrolysis of PET. The last part focuses on the introduction of the 1,8-Diazabicyclo (5.4.0) undec-7-ene (DBU) as a super-basic catalyst that can degrade PET faster than the reported catalysts in literature for hydrolysis of PET. The DBU can wet the surface of PET particles completely, which is one of the factors of the DBU super activity. This trait of DBU is used to synthesize DBU-

acid ionic liquids with the weak acids to transform them to basic acids that can decompose PET considerably faster than their corresponding acids. Moreover, these ionic liquids are more thermally stable than DBU. This study features the enhancement of wetting of the surface of PET particles as a significant driving force to increase the rate of PET decomposition in hydrolysis reactions.

Chapter 1

Introduction

1.1 Overview

Polyethylene terephthalate (PET) recycling is a primary strategy to deal with the abundant plastic wastes that result from wide use of PET packaging. While various recycling techniques have been proposed to decrease the rate of PET waste production, recycling is far less than the PET waste production rate, and recycling has been slowly adapted [1-3]. Recycling is an open field for scientists to explore techniques to improve recycling process. There are three main recycling approaches: primary, secondary (mechanical), and tertiary (chemical) [4, 5]. Incineration and pyrolysis are also categorized as recycling approaches even though they will downcycle PET and may not be sustainable methods for plastic recycling [6-10].

Primary recycling [11, 12] focuses on high purity plastic wastes, which result from production of the plastic products. Recycling of this “in-plant” wastes is simply done by adding to the virgin material in the plastic production process. This approach is not applicable for plastic products which are used or contaminated with other wastes. Mechanical recycling (MR) [13, 14] is conducted by separating the used plastic products from the other types of wastes. MR includes sorting of the mixed waste into individual plastics, size reduction, and reprocessing via melt extrusion to produce plastic products [15]. The main drawback of this technique is that the recycled plastic degrades and loses

quality and mechanical properties with each subsequent mechanical recycling round [16, 17].

Tertiary (chemical) recycling has been studied as an approach to overcome the challenges of mechanical recycling [18]. The five major techniques in chemical recycling are: glycolysis, alcoholysis, aminolysis, ammonolysis, and hydrolysis [19-23]. Glycolysis is commonly used to depolymerize PET into bis (2-hydroxyethyl terephthalate), which can be repolymerized into pure PET. Glycolysis does not allow facile recovery of valuable comonomers. Hydrolysis can directly produce terephthalic acid (TPA) and ethylene glycol (EG) to recycle and polymerize into pure PET. There are three types of hydrolysis based upon catalyst used for reaction: acid, neutral, and alkaline [24, 25]. Neutral hydrolysis is usually conducted at very high reaction temperatures and pressures [26, 27]. Alkaline hydrolysis produces more wastes than acid hydrolysis due to the indirect production of the TPA [28, 29]. Acid hydrolysis directly produces TPA which can be recovered from unreacted polymers but has slower kinetics than alkaline hydrolysis. This slower kinetics require use of higher acid concentration or elevated temperatures to achieve reasonable conversions [30, 31]. This work develops catalysts with higher activity than the conventional catalysts used for hydrolysis of PET.

1.2 Hypothesis

PET hydrolysis occurs by the protons attacking the PET surface in a layer-by-layer process because of low water solubility of PET [32, 33]. So, the PET surface wetting can have an effective role in improving the reaction rate in hydrolysis of PET. The effect of catalyst hydrophobicity on the wetting and the reaction kinetics have been reported for

acid-catalyzed reactions, such as cellulose hydrolysis [34] or acetalization reactions [35], and for the enzymatic hydrolysis of esters [36]. The hypothesis of this work is that catalysts with hydrophobic regions will be more active than the conventional mineral acids due to the hydrophobic interactions with the PET particles in the aqueous reaction medium- results in higher local concentrations at the vicinity of the PET particles and consequently faster PET hydrolysis.

1.3 Research Objectives

PET hydrolysis occurs at the PET surface and therefore requires good surface wetting by the reaction media. The overall goal of this dissertation was to develop and characterize catalysts for acid or base hydrolysis of PET while targeting: (i) higher surface affinity to enhance the PET surface wetting by reaction media, (ii) increased catalytic activity, and (iii) recoverable catalysts. In acid hydrolysis, PET depolymerizes to TPA and EG in the presence of an acid catalyst. In the case of complete conversion of PET, the TPA is recovered by a filtration process [37, 38]. In alkaline hydrolysis, PET depolymerizes to the salted form of TPA and EG in the presence of a basic catalyst. In the case of complete conversion of PET, the TPA may be recovered through an acidification process where a strong acid is used to precipitate out the produced TPA. This will permit the recovery of TPA and can be readily extended to co-polyester waste streams [39, 40]. Following are the main objectives of this dissertation to investigate the PET hydrolysis:

1. Poly (4-styrene sulfonic acid) (PSSA): a recoverable and reusable acid catalyst for PET hydrolysis

Catalyst recovery and reusability are of considerable interest for PET depolymerization to reduce costs and improve sustainability of recycling processes [41, 42]. As the first part of this study, the aim was to introduce a recoverable and reusable catalyst for PET hydrolysis as alternative to mineral acid, H₂SO₄. In this regard, poly (4-styrene sulfonic acid) (PSSA) provided an opportunity to improve the surface activity combined with potential for facile recovery and recycling of the catalyst. The PET hydrolysis reactions were carried out at 130°C, 140°C, and 150°C in the ace pressure reactors where the reaction pressure didn't exceed 5 atm. The effect of PSSA concentration on PET hydrolysis was studied at active site concentrations from 1 to 4 molar [43]. These reaction conditions are comparatively lower than most of the reaction conditions applied for the PET degradation, reported in the literature. The reaction temperature and pressure could have a range of 100°C to 450°C and 1 atm to 26.5 atm, depending on the applied technique for hydrolysis [26, 44-46].

The results of PET conversion and TPA yield from PET hydrolysis with PSSA were compared with the results of PET hydrolysis with sulfuric acid, the conventional acid catalyst for PET hydrolysis. Ethyl acetate hydrolysis and surface wetting of the PSSA solutions on PET were explored to determine the effect of homogenous-heterogenous reaction system and the effect of hydrophobic moieties of catalyst on PET hydrolysis, respectively.

2. Aryl sulfonic acids: potentially higher catalyst activity than mineral acids for PET hydrolysis

Application of aryl and alkyl sulfonic acid molecules to hydrolyze cellulose indicate that catalysts with affinity for hydrophobic surfaces can exhibit sharp increases in activity relative to mineral acids (i.e., sulfuric acid and nitric acid) [34, 47, 48]. As the second part of this study, a series of acid catalysts with hydrophobic groups that target improved surface wetting of the PET were tested for PET hydrolysis. For this purpose, the selected catalysts were p-toluenesulfonic acid monohydrate (PTSA), 2-naphthalenesulfonic acid (2-NSA), and 1,5-naphthalenedisulfonic acid tetrahydrate (1,5-NDSA) [49].

The reactions were tested at 130°C, 140°C, and 150°C in the ace pressure reactors where the reaction pressure was not higher than 5 atm. Again, the effect of the reaction temperature and catalyst concentration on PET hydrolysis were explored. The kinetic results were compared with the kinetic results of PET hydrolysis with sulfuric acid. Also, the ethyl acetate hydrolysis and wetting studies of the catalyst solutions used for PET hydrolysis were explored [49].

3. 1,8-Diazabicyclo (5.4.0) undec-7-ene (DBU)-acid ionic liquids for PET hydrolysis

DBU has been reported as a super-basic and recyclable organo-catalyst for the efficient recycling of the polycarbonates [50]. It's also been used as a strong catalyst to depolymerize PET in a glycolysis technique [51, 52]. Weak acids are reported as catalysts for the hydrolysis of cellulose [53, 54], polyamide [55], starch [56], rice straw [57] and PET [58]. As the third part of the study, the focus was to synthesize ionic liquids (ILs) of

DBU with weak acids to increase the catalyst activity. This will also increase the thermal stability of weak acid catalysts when they are in the form of an ionic liquid (IL), meaning they may be applied at higher reaction temperatures for PET hydrolysis [59-62].

The selected acids for the third part of study were lactic acid, sulfuric acid, oxalic acid, and citric acid. First, the activity of these weak acids for PET hydrolysis was examined. Then, the ILs were prepared with DBU to explore the activity of the ILs for PET hydrolysis. The effect of solvent type, water or methanol, on the IL activity as a catalyst for hydrolysis of PET was studied. The reaction temperature and pressure for PET hydrolysis are the same as the ones described for the first two parts of the dissertation. The reaction temperature and catalyst concentration effects on PET hydrolysis along with wetting studies on prepared solutions for PET hydrolysis were explored.

1.4 Organization of the dissertation

Chapter 2 describes the current literature for PET recycling with a focus on hydrolysis as a potentially sustainable approach for PET recycling. **Chapter 3** discusses the materials used for the experiments of PET hydrolysis. It also describes the synthesis methods for catalyst preparation and the experimental methods to conduct the tests for PET hydrolysis, ethyl acetate hydrolysis, product characterizations, and wetting studies. **Chapter 4** discusses poly (4-styrene sulfonic acid) (PSSA) as a recoverable and reusable catalyst for PET hydrolysis. **Chapter 5** explores the effect of the hydrophobic group of aryl sulfonic acids on the activity of these catalysts for PET hydrolysis. **Chapter 6** studies the DBU-acid ionic liquids as the hydrolysis catalysts for PET depolymerization. **Chapter 7** includes the conclusions and the future work on PET depolymerization with hydrolysis.

Chapter 2

A review on recycling techniques of polyethylene terephthalate with the focus on hydrolysis

2.1 Abstract

Polyethylene terephthalate (PET) is among the most widely used polymers with two major areas of applications, textile and packaging industries. The main resource for PET production is fossil fuels with limited capacity. Additionally, many applications of PET are single use that transform into waste and have caused major ecosystem problems because of high volumes of plastic waste in environment. Recycling has been selected as an approach to address this challenge. The four major PET recycling techniques are mechanical, chemical, pyrolysis, and enzymatic. The mechanical, pyrolysis, and enzymatic recycling techniques have some capabilities to manage PET waste.

Chemical recycling is of interest for this work because it can expand options for recycling PET waste with potential for upcycling and addressing dirty waste streams. Several methods have been introduced and discussed in the literature to depolymerize PET into the monomers or associated oligomers. The five major chemical recycling techniques are glycolysis, alcoholysis, aminolysis, ammonolysis, and hydrolysis. This review describes PET depolymerization via each of these techniques and with an emphasis on hydrolysis as a method that avoids organic solvents.

Hydrolysis tolerates PET mixed wastes streams including copolymers. It avoids challenges attributed with using organic solvents in reaction systems. In addition, hydrolysis directly produces terephthalic acid (TPA) and ethylene glycol (EG), which are monomers used for commercial PET production. The chapter focuses on three forms of hydrolysis- alkaline, neutral, and acid by presenting background studies, issued patents, and recent trends on application of hydrolysis for PET depolymerization.

2.2 Introduction: Polyethylene terephthalate (PET) and the importance of recycling

Polyethylene terephthalate (PET) is a high-volume polyester that is widely used in the packaging and textile industries. This broad commercial use is due to the attractive physical and chemical properties of PET including high transparency, crystallization rate, high thermal stability, mechanical properties, and high oxygen barrier [30, 63, 64]. It is estimated that the PET market will have a global annual growth of 4.2% over the five-year period from 2019 to 2024, increasing to 11 billion dollars in a period time of 2019 to 2024 [65].

Figure 2-1 shows the two most used commercial processes for PET synthesis: (i) esterification of terephthalic acid (TPA) with ethylene glycol (EG) followed by polycondensation and (ii) transesterification of dimethyl terephthalate (DMT) with EG followed by polycondensation. The esterification reaction of TPA and EG is conducted at the average reaction temperature of 250°C and pressure of 400 kPa. For the transesterification reaction, DMT reacts with EG in the presence of a catalyst at an average reaction temperature of 180°C and pressure of 100 kPa. For both paths, the product for the

pre-polymerization step is bis (2-hydroxyethyl) terephthalate (BHET), which is polymerized further to the degree of polymerization (DP) of 30 [66, 67]. For the polymerization process, a polycondensation reaction occurs at the average reaction temperature of 280°C and pressure of 75 Pa to produce PET for fiber and sheet applications. While both processes produce high molecular weight PET, the esterification of TPA to BHET is the most used route as it does not require a catalyst and there are fewer side reactions. For higher MW of PET production, applicable for packaging productions, solid state polymerization of the product is used [68-70].

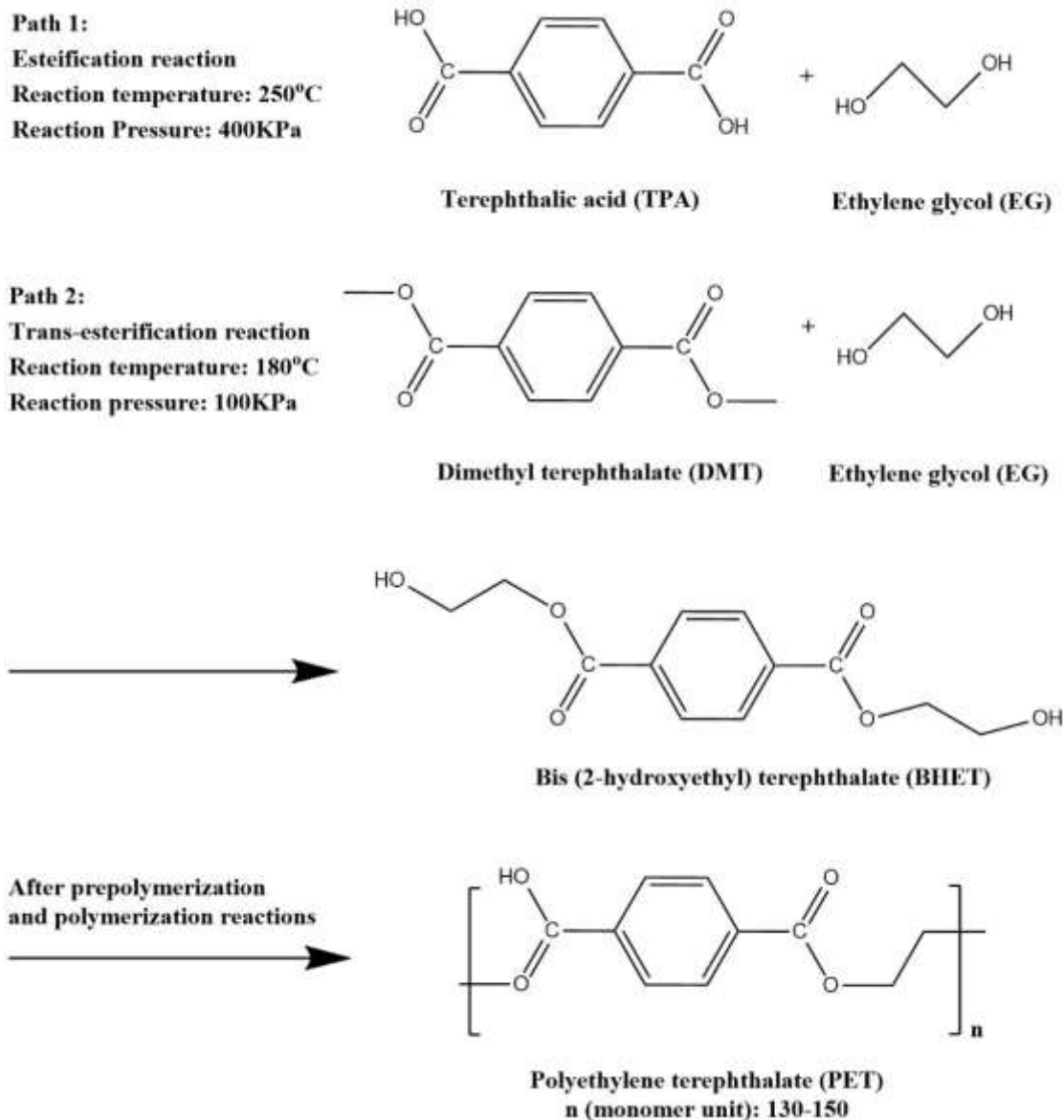


Figure 2-1: The two paths for the synthesis of PET.

Many PET products, such as water bottles, have short use lives, and become plastic wastes in the environment- causing threats to the environment [71-73]. Incineration and landfilling are two approaches that have been applied to address the volume of PET waste [38, 74]. Incineration is the direct combustion of PET waste to use the PET latent energy,

22.95 MJ.kg⁻¹, to produce energy [9, 75]. This process produces toxic gases including SO_x and NO_x and leaves ash as residual that is detrimental to the soil and water. However, incineration is inevitable when the PET waste is either too hazardous to be handled or too costly to be collected and separated from other wastes [76, 77].

Landfilling is a static method to collect the PET waste along with other wastes in a space on or under the soil [78]. This collected waste will gradually be displaced by penetrating within the soil and reaching to water resources. In this case, the waste can damage the ecosystem including the soil and water [79-81]. In addition, the feedstock to produce PET is typically from limited fossil fuel resources [82-85]. Due to the continual environmental legislations specially the reduction of carbon footprint and the protection of environment, there is a growing interest to reduce the use of these methods to address PET waste [86-88].

Therefore, two strategies have been proposed to address challenges of large volumes of PET waste: direct and indirect. In the direct strategy, recycling techniques are used to manage PET waste [89-91]. In the indirect strategy, biodegradable materials are used as a PET alternative to facilitate product degradability [92-94]. While replacing PET with biodegradable polymers is of interest, there are currently no polymers that can compete with PET in required thermal, mechanical and barrier properties needed for stringent packaging requirements [95, 96]. The direct strategy has been developed because of the need to handle current PET production volumes and subsequent produced PET waste [97, 98].

2.3 Direct strategy for PET waste management

The direct strategy encompasses a variety of techniques including primary recycling, mechanical recycling, and chemical recycling [99]. In primary recycling, the PET waste generated during the production process are recycled. This waste has a high purity and no contamination so it can readily go through the re-extrusion process for PET production [100-102]. This technique is applicable to a small portion of the PET waste and cannot be implemented for PET products which are used or contaminated with other wastes [103].

Mechanical recycling (MR) is the most used commercial method for recycling of PET from mixed plastic waste. MR requires sorting into individual plastics, washing, drying, size reduction, and melting to reproduce polymer pellets for further processing [104-106]. As PET waste has contaminants and other materials such as polymers and metals, the sorting facilities separate the PET from metal and other polymers using a variety of methods including by the density and the waste size. The PET waste is washed and dried to remove the contaminants and prepared for the size reduction process. In this phase, the waste is crushed with counter comb shredders to achieve uniformly small PET flakes that are appropriate for melting in the last step. The PET flake is reprocessed into pellets to produce recycled PET (RPET) for commercial use [13, 15, 107].

RPET pellets from mechanical recycling contain acetaldehyde and limonene, which are formed during reprocessing and can make RPET unsuitable for food and drink packaging [14, 17, 108]. Gas chromatography analysis of the RPET showed that the maximum level of acetaldehyde and limonene in these products can reach 86 mg.kg⁻¹ and

20 mg.kg⁻¹, respectively. However, if the mechanical recycling steps are implemented correctly, then it is estimated the level of the hazardous chemicals is less than 50 nanogram, making the recycled PET products safely applicable for food and water packaging [109, 110]. The main drawback of mechanical recycling is that the recycled plastic degrades, loses molecular weight and has decreased mechanical properties following reprocessing at elevated temperatures [11]. Solid state polymerization of the RPET pellets can be used to recover some molecular weight and improve properties [111-113]. Additionally, mechanical recycling does not allow recovery of high value co-monomers that are used to moderate PET properties.

2.4 Chemical recycling of PET

Chemical recycling of PET has been extensively studied as an alternative to traditional mechanical recycling [114-119]. In chemical recycling, the PET waste is converted, either by transformation to the monomer unit by solvolysis or by randomly scission of the chains by pyrolysis [120, 121]. In pyrolysis, the PET waste will go through extreme heating process under vacuum condition to produce a variety of hydrocarbons. In solvolysis, the PET waste is depolymerized in a solvent in the presence of a catalyst to produce monomers (i.e. TPA and EG), bis (2-Hydroxyethyl) terephthalate (BHET) or oligomers that can be used to synthesize PET or other polymers [122-125].

Pyrolysis is applied when the PET waste has high impurities including contaminants and other polymeric wastes and cannot be recycled using other methods. During pyrolysis, the PET waste is exposed to high reaction temperatures, from 370°C up to 700°C, in an oxygen free environment [126-128]. Pyrolysis occurs in an autoclave

reactor where the products are approximately 77% weight gas and 23% weight liquid oil. Half of the obtained liquid oil contains benzoic acid, which will not be a high-quality fuel due to its corrosive nature [129-132]. The applied catalysts for the pyrolysis process are reported to be FeOOH, ZSM-5, and metal oxides such as ZnO, MgO, TiO₂, etc. [8, 133]. The ZnO catalyst has been reported to particularly lead the pyrolysis reaction to decarboxylate benzoic acid and terephthalic acid (TPA), main pyrolysis products, to increase the amount of benzene in the liquid oil up to approximately 90% weight. This will increase the quality of the obtained fuel for subsequent processing for potential fuel applications [134-138]. Although pyrolysis is categorized as a method of chemical recycling of PET waste, it is downcycling the polymer PET value due to the thermal degradation that occurs during pyrolysis [139, 140].

Solvolysis can reintroduce PET without quality loss by depolymerizing PET waste into oligomers and monomers that can be used in direct polymerization of PET [141-144]. Solvolysis processes are designated based upon reactants/solvents used including glycolysis, alcoholysis, aminolysis, ammonolysis, and hydrolysis, as shown in **Figure 2-2** [145-147].

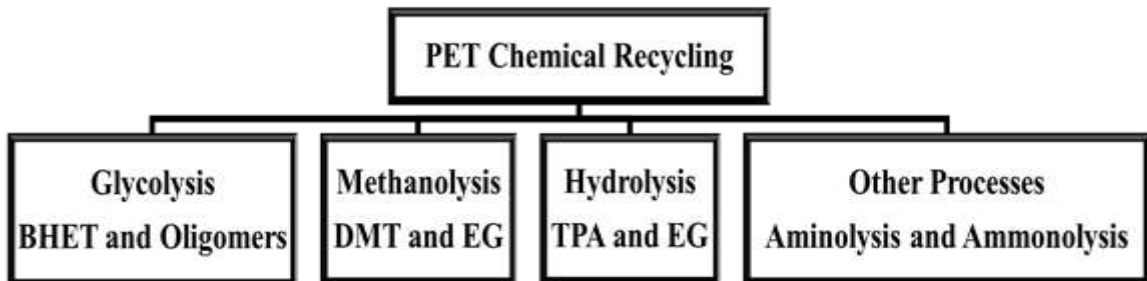


Figure 2-2: Schematic diagram of PET chemical recycling techniques.

PET glycolysis is the most widely studied process and has found commercial application [148-153]. Glycolysis was first patented in 1965, and the patenting for this technique was continued until 2020 [154-158] with commercial facilities in Europe and Japan [159]. Glycolysis depolymerizes the PET at temperatures from 110°C to 270°C and pressure range of 1 atm to 25 atm. The reaction medium can be ethylene glycol (EG), diethylene glycol, propylene glycol, or di-propylene glycol- with EG as the most widely used compound. As shown in **Figure 2-3**, the final product is bis(2-Hydroxyethyl) terephthalate (BHET) [31, 160]. PET glycolysis without a catalyst is a sluggish process where PET cannot completely depolymerize to BHET.

To resolve this challenge, various catalysts have been proposed including metal derivatives, zeolites, and ionic liquids where zinc acetate and magnesium acetate are the most significant ones [20, 161-164]. An advantage of glycolysis is its simplicity to produce high yields of BHET, which can be added to fresh BHET after a purification process, for synthesis of PET without the esterification step [165-167]. However, the drawbacks of the technique include the harmful effects of the reaction solvent to the environment and the need to separate the monomer from catalyst and EG [18, 168]. Glycolysis cannot tolerate low quality PET waste and may be limited in recovery of valuable comonomers [169-171].

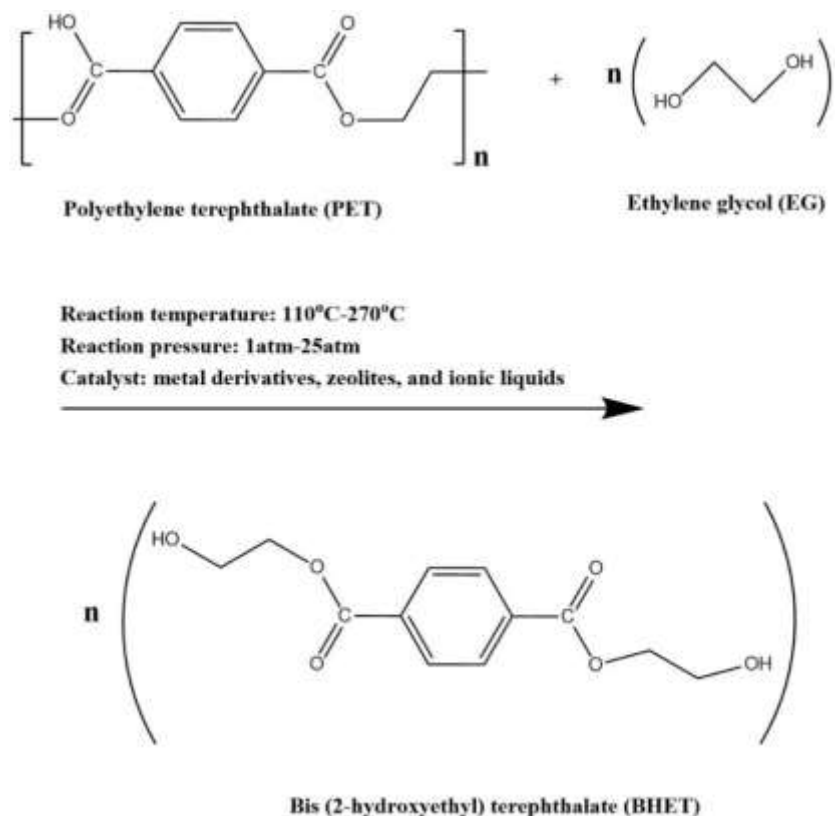


Figure 2-3: Glycolysis of PET.

Alcoholysis was firstly proposed in 1991 by Wang et. al. [172]. The reaction medium is an alcohol such as methanol, pentaerythrytol (PENTE), 1-butanol, 1-pentanol where the PET degradation occurs to produce corresponding esters of terephthalic acid and EG as the main products, as shown in **Figure 2-4** [173-176]. Among the reported reaction medium, methanol is of specific importance due to its abundance and low cost. In this case, dimethyl terephthalate (DMT) and EG are the products, as shown in **Figure 2-5** [23]. Heisenberg et al. introduced methanolysis for PET depolymerization in 1962 [177]. Methanol has been used in three phases for PET depolymerization- liquid, vapor, and supercritical [2, 178].

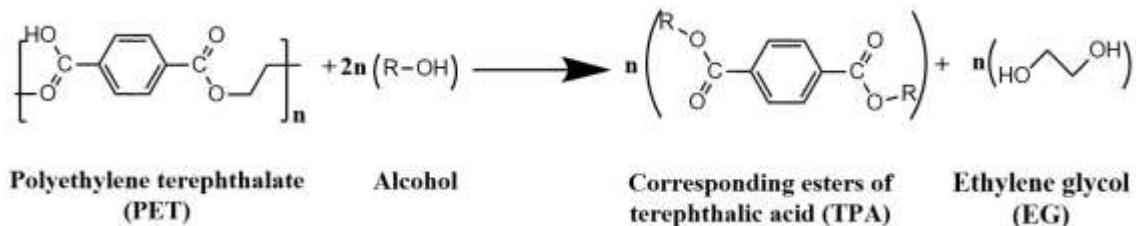


Figure 2-4: Alcoholysis of PET.

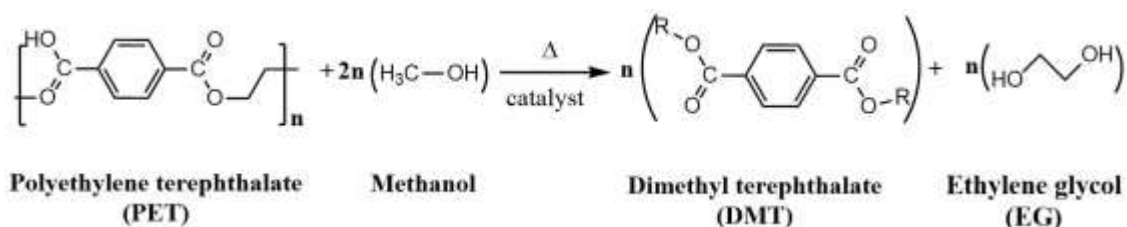


Figure 2-5: Methanolysis of PET.

Liquid phase methanolysis is conducted in the reaction temperature range of 160°C to 350°C. To increase the DMT yield to an average of 82% weight and to maintain the liquid state of the methanol, the reaction pressure increases to the range of 20 atm to 40 atm [179-181]. The applied catalysts are the metal acetates used for the transesterification. The produced DMT can be separated by crystallization and be further purified to reach an acceptable quality for PET production. However, these steps cause PET liquid methanolysis to be accounted as an expensive process [182, 183]. Additionally, it does not produce a direct replacement for TPA in commercial PET production.

Superheated vapor methanol and supercritical methanol are also reported in literature for PET methanolysis processes [19, 184]. In a comparative study, it was confirmed that PET depolymerizes faster in supercritical methanolysis. It has been reported that supercritical methanolysis can depolymerize PET in 30 minutes at 300°C temperature

and above 80 atm pressure [185-188]. However, the high pressure and temperature required increase the operating costs, making it unfavorable as a direct technique of PET depolymerization. The reaction products for supercritical methanolysis and vapor methanolysis are a mixture of BHET, DMT, and methyl-2-hydroxy ethylene terephthalate (MHET) where the DMT has a yield of 80% [189, 190]. Again, the separation of the DMT from the product mixture increases the associated costs for PET methanolysis. Nevertheless, methanolysis has been scaled up in the USA and Canada for PET decomposition due to the easy installation at PET production plants. [29, 191].

PET aminolysis [192-194] is conducted in primary amine solutions such as methylamine, ethylamine (EA), and allylamine, at a reaction temperature in the range of 20°C to 100°C and moderate pressures up to 20 atm. Catalysts such as metal acetates, glacial acetic acid, potassium sulfate, and 1,5,7-triazabicyclo [4.4.0] dec-5-ene (TBD) are used to increase the reaction rate [195-198]. The reaction products are the diamide of TPA and EG, as shown in **Figure 2-6**. Ethylamine has been used as the agent for PET aminolysis to produce the bi-functional monomer bis (2-hydroxyl-ethylene) terephthalamide (BHETPA). The BHETPA yield can reach as high as 91% and can be further processed to be used as a curing agent for epoxy resins [198-203].

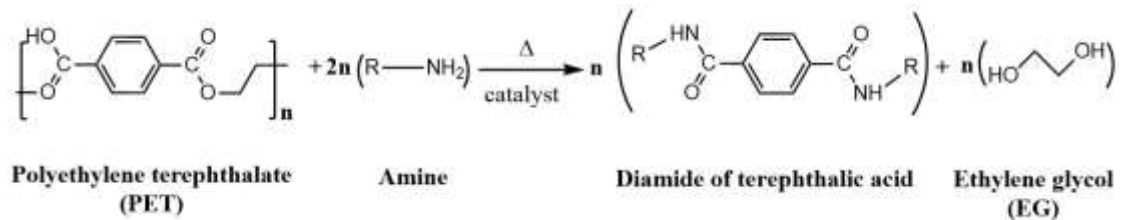


Figure 2-6: Aminolysis of PET.

PET ammonolysis [204-206] has been less studied in comparison to other PET chemical recycling techniques. In PET ammonolysis, ammonia (NH₃) is used as the reaction medium at a reaction temperature between 70°C to 180°C. As ammonolysis is notably slower than aminolysis, both a catalyst and high reaction pressures are required to increase the reaction rate [207, 208]. The applied catalysts are metal acetates to produce monomeric terephthalamide and EG, as shown in **Figure 2-7**. These products can be furtherly processed to produce value-added products such as p-lylenediamine or 1, 4-bis (amino-methyl) cyclohexane [209, 210].

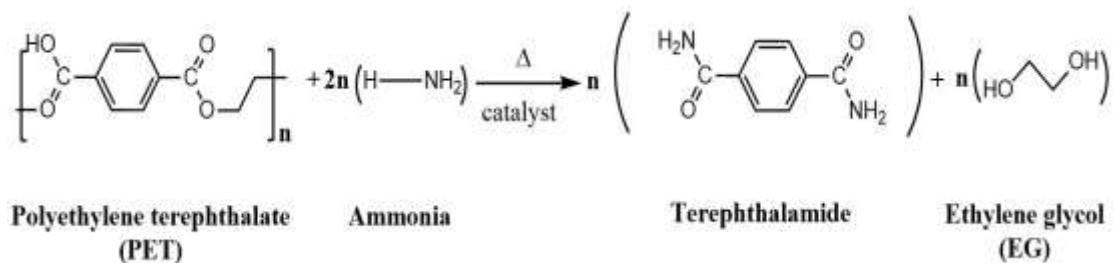


Figure 2-7: Ammonolysis of PET.

Both aminolysis and ammonolysis were explored to increase the PET depolymerization reaction rate because the amine group has higher activity than the hydroxyl groups in glycols and alcohols, which are applied in glycolysis and alcoholysis,

respectively. In addition, aminolysis and ammonolysis can depolymerize PET in less severe reaction conditions than methanolysis [211, 212]. However, both techniques have not been scaled up. This is due to the additional processes needed to be implemented on the PET aminolysis/ammonolysis products to produce value-added materials- applicable as plasticizers, curing agents for epoxy resins, and components for polyurethane production [213-216].

Each of the PET chemical recycling techniques discussed thus far has environmental concerns including the use of organic solvents and metal catalysts [18, 217-220]. Studies have been developed to recycle the catalysts for reuse or to apply eco-friendly (green) catalysts while the organic solvent application has remained as an issue [221-230]. PET hydrolysis, which is the depolymerization of PET in water, could be an answer to resolve the issue of application of organic solvents [231-235]. Despite that, current catalysts that are used for PET hydrolysis may damage the environment due to the toxicity and corrosiveness [236-239]. So, there is interest in catalysts that are recoverable and nontoxic for PET hydrolysis.

2.5 PET Hydrolysis

PET hydrolysis is divided into three categories, alkaline, neutral, and acid, depending on the pH of the applied catalyst in the aqueous reaction medium. As illustrated in **Figure 2-8** for acid hydrolysis, protons (H^+) attack PET surface and initiates the esterification reaction in hydrolysis. Hydrolysis is a heterogeneous reaction occurring at the surface of PET. Factors that affect the reaction rate are temperature, pressure, proton or

hydroxyl concentration, PET particle size, and the extent of surface wetting with the reaction medium [240-242].

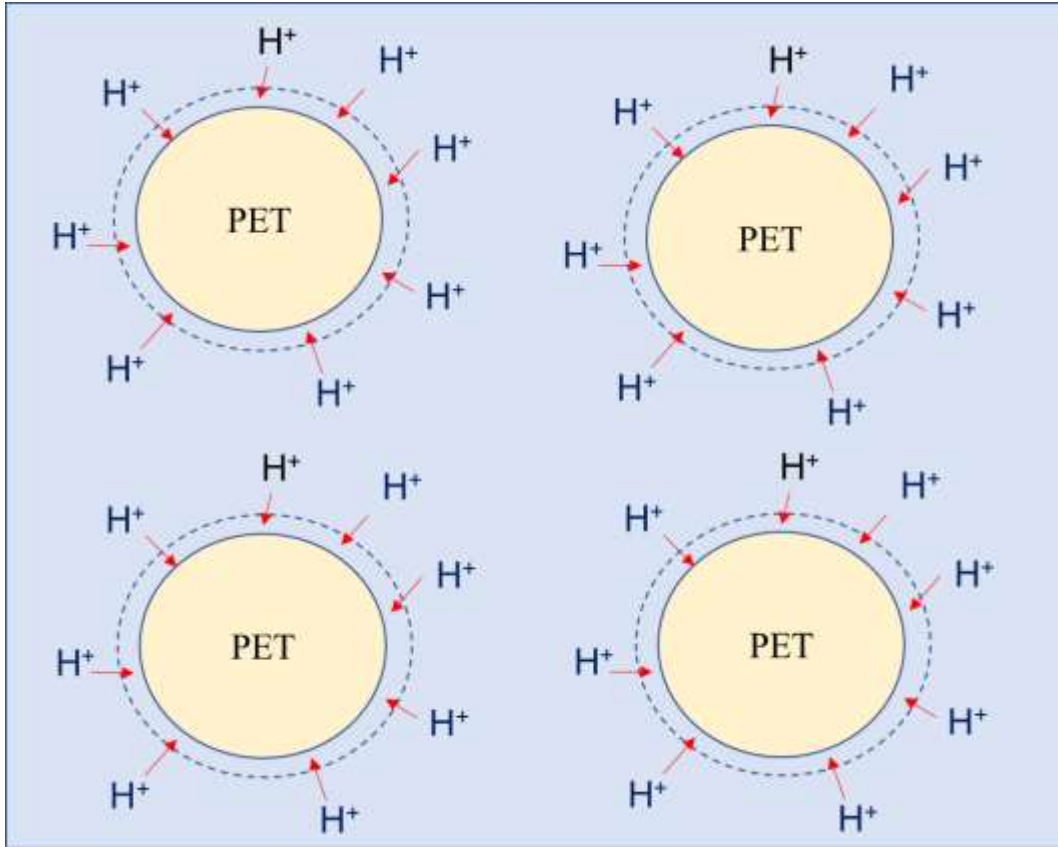


Figure 2-8: Schematic of PET particles distributed in a hydrolysis reaction medium.

2.5.1 Neutral hydrolysis

In neutral hydrolysis, PET depolymerizes in an excess of water or steam at a reaction temperature between 115°C to 420°C and pressures between 10 atm to 420 atm [243-245]. As shown in **Figure 2-9**, the products are TPA and EG. The TPA may be recovered from unreacted PET by acidification and filtration after hydrolysis. It was reported that when PET is in the molten state at temperatures higher 245°C, the reaction

proceeds faster [246, 247]. Campanelli et al. [248] found that when the weight ratio of water to PET was 5 to 1, complete PET depolymerization could be achieved in 2 hours at reaction temperature of 265°C. The kinetic and thermodynamic studies for PET neutral hydrolysis are given in the literature [26, 249]. For instance, Zope and Mishra [26] determined the activation energy and the frequency factor to be 9.58 kJ.mol⁻¹ and 2.9 × 10⁸ min⁻¹, respectively.

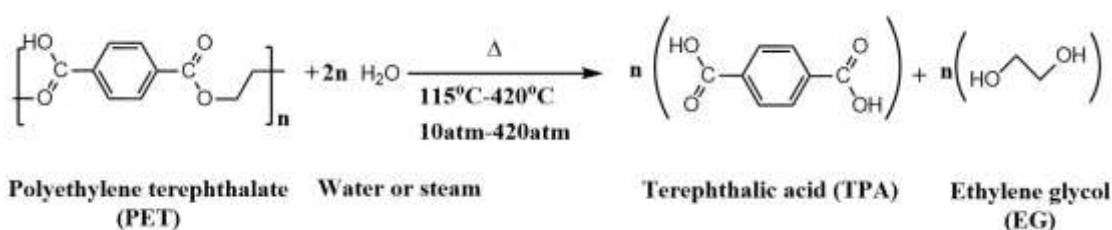


Figure 2-9: Neutral hydrolysis of PET to TPA and EG.

Neutral hydrolysis does not require organic solvents and catalysts, so this is a greener route for PET hydrolysis. However, neutral hydrolysis does not account for the mechanical impurities in PET waste, causing the produced TPA to have higher impurities than the produced TPA from alkaline hydrolysis. Therefore, a more intensive purification process is needed to purify the TPA [250, 251]. In addition, the operational costs are high in neutral hydrolysis due to the high reaction temperature and pressure required to achieve depolymerization in shorter times [19]. These are the two main reasons that no method under neutral hydrolysis technique has ever been patented or scaled up for PET recycling in high tonnages. However, some recent studies on PET neutral hydrolysis are reported, which are described in subsequent paragraphs.

Sato et al. [252] studied PET hydrolysis in liquid water at 300°C and under autogenous pressure. It was found only 10 minutes was needed for 1 gram of PET to convert completely to TPA in an excess amount of water (5 grams). In addition, a continuous hydrolysis process was simulated to depolymerize one ton of PET per day. It was concluded that by decreasing the water to PET molar ratio at the feed stream, the total energy needed to operate the PET hydrolysis in a continuous condition would decrease. The best condition was for the molar ratio of 16.7 (water to PET) with the total operation energy of 5,366 kWh.

Liu et al. [253] introduced zinc acetate as a catalyst for PET neutral hydrolysis. In the study, the PET with industrial grade was hydrolyzed in hot compressed water in an autoclave reactor within the reaction temperature and pressure range of 220°C to 280°C and 21 atm to 61 atm, respectively. The optimum reaction conditions occurred when the weight ratio of the catalyst to PET, reaction temperature, and pressure were 1.5%, 240°C, and 32 atm, respectively. In this case, the required reaction time for complete conversion of PET was 30 minutes. In addition, a fused silica capillary reactor was used to enable the study of the phase behavior of PET hydrolysis in the hot compressed water. The phase change data indicated the temperature of PET dissolution in the water to create a homogenous solution decreased with an increase in the zinc acetate amount in the solution.

Mancini et al. [254] proposed a two-stage method to increase the reaction rate of PET neutral hydrolysis. In the first stage, the PET flakes were treated by plasma at various conditions. Operating parameters including plasma composition (oxygen and air), power, pressure, and treatment time were investigated. This stage enhances the wettability of PET

surface by the reaction medium. The contact angle measurements indicated a value of 9.4 degree when the PET flakes were treated by plasma at optimum conditions. The optimum conditions were found when the PET flakes were treated by air plasma at power of 130 W, pressure of 6.67 Pa for 5 minutes. In the second stage, the PET flakes were ground to obtain the PET particles with an average diameter of 5 mm. The particles were hydrolyzed at the reaction temperature and pressure of 205°C and 16 atm, respectively. Complete PET conversion was obtained after 4 hours for treated samples and 60% of PET conversion was obtained in hydrolysis of base PET samples. This work shows a plasma treatment on PET surface facilitates the PET hydrolysis by increasing the PET surface wettability.

2.5.2 Alkaline hydrolysis

2.5.2.1 Background

In standard alkaline hydrolysis, PET waste reacts with a base catalyst in an aqueous medium. Alkaline hydrolysis is generally conducted using a metal oxide catalyst, such as sodium hydroxide and potassium hydroxide, with a concentration between 4% w/w to 20% w/w at an average reaction temperature of 225°C and a pressure of 17 atm [255-258]. Sodium hydroxide is a commonly used catalyst for alkaline hydrolysis of PET where the products are the sodium salt of TPA (TPA-Na_2^+) and EG [259-261]. The TPA is precipitated when a strong acid such as sulfuric acid and hydrochloric acid is applied to bring the solution pH to 2. The base catalyst is consumed during alkaline hydrolysis and the subsequent acidification process to recover the TPA [262]. The PET depolymerization steps for hydrolysis of PET with sodium hydroxide is shown in **Figure 2-10**.

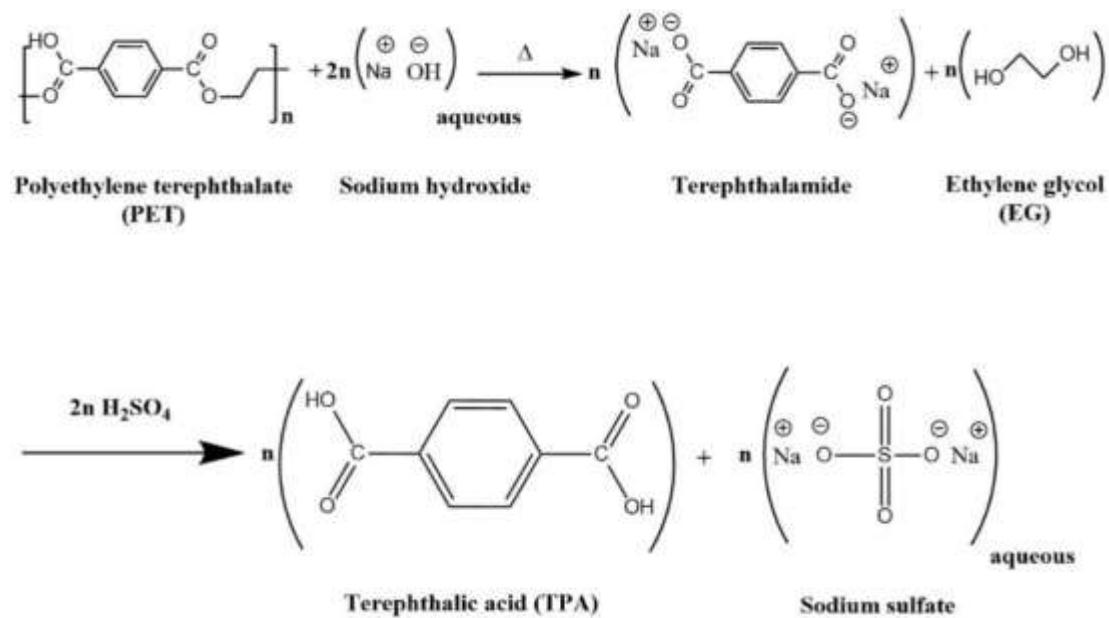


Figure 2-10: Alkaline hydrolysis of PET with NaOH, TPA recovery with H₂SO₄ [263].

The proposed mechanism for alkaline hydrolysis at the surface of the PET is illustrated in **Figure 2-11** [264-266]. In the dissociation step (**Figure 2-11. a**), the hydroxyl groups (OH⁻) are released from the catalyst in the aqueous solution. In the next step (nucleophilic addition), the hydroxyl anion attacks the carbon atom of the ester carbonyl group, forming a tetrahedral intermediate (**Figure 2-11. b**). Then, in the hydrolysis step, the attached ester to the tetrahedral intermediate (-OR') separates from the tetrahedral intermediate (**Figure 2-11. c**). Afterwards, the negative (-OR') group attacks the hydrogen bond of the hydroxyl group and separates the hydrogen to form the hydroxyl group (OH⁻) (**Figure 2-11. d**). This step is called the deprotonation of the carboxylic acid, which will eventually lead to the formation of the hydrolysis products, terephthalic acid and ethylene glycol (**Figure 2-11. e**).

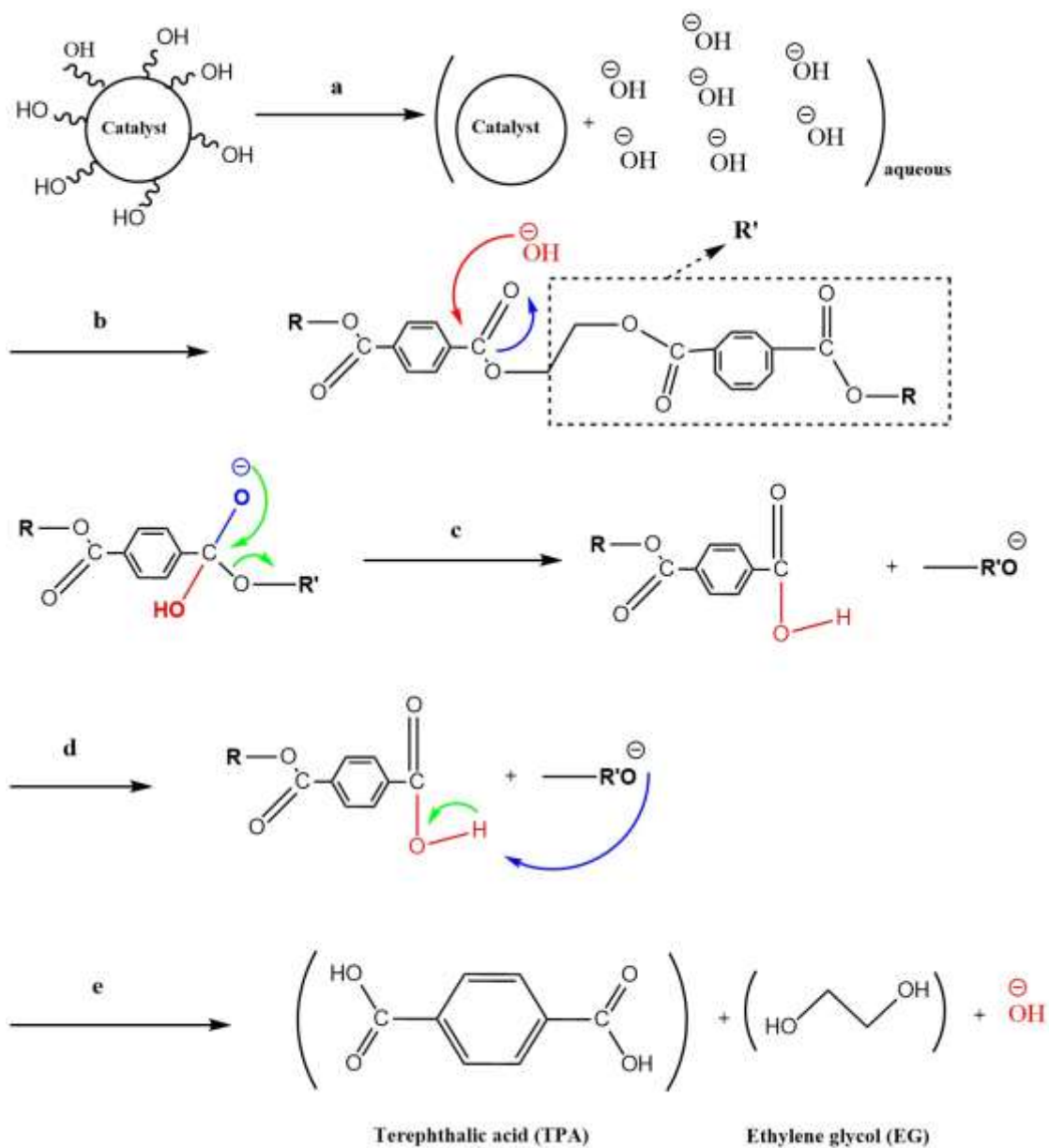


Figure 2-11: Mechanism for PET acid hydrolysis, a: dissociation step, b: nucleophilic addition, c: hydrolysis step, d: deprotonation step, e: formation step [264-266].

2.5.2.2 Issued patents for PET alkaline hydrolysis

Pitrat et al. [267] patented a PET alkaline hydrolysis method by applying 18% weight of sodium hydroxide in water. The most important finding was determining the maximum salting-out (precipitation of alkali sodium TPA) condition when the reaction temperature and time were 100°C and 2 hours, respectively.

In a later patent, Lazarus et. al [268] applied a 3.38% w/w NaOH to hydrolyze a blend of 70:30 w/w Nylon-6: PET at 230°C and 17 atm with a TPA yield of 97.4%. The latest patent is for Лакеев et. al [269] who reported the application of sodium hydroxide to produce TPA from PET. The reaction temperature range and pressure were 130°C to 150°C and 1 atm, respectively. They introduced Flotoreagent-oxal T-92, a mixture of polyhydric alcohols, as flotation reagent medium used during the alkaline process to dissolve the produced TPA accompanied by the addition of water. Then, the TPA was recovered using the acidification process described by Lazarus et. al [268]. Mishra et al. [270] and Karayannidis et al. [271] reported PET alkaline hydrolysis with the complete degradation of PET and high-yield production of TPA. They also studied the reaction kinetics of the PET hydrolysis.

2.5.2.3 Phase transfer agents as catalysts for PET alkaline hydrolysis

Kosmidis et al. [272] used trioctylmethylammonium bromide as a phase transfer agent in alkaline hydrolysis. The phase transfer agent (PTA) enhances the interactions between the basic catalyst and the PET surface in the reaction medium. Two features are specified for the PTA to function, possessing sufficient organic part to be lipophilic and

being small enough to avoid steric hinderance [272, 273]. A typical PTA structure consists of two cationic and anionic parts. It's found the cationic part can carry the scattered hydroxide anions to the PET surface, resulting in hydroxyl anions can more readily attack PET for depolymerization [274, 275].

This increased interaction allowed PET alkaline hydrolysis at milder reaction conditions with temperatures between 70°C to 95°C and atmospheric pressure. The produced TPA had high purity with a trace of 2% w/w isophthalic acid. Subsequently, other phase transfer agents including quaternary phosphonium, ammonium salts and tetra butyl ammonium iodide (TBAI) were reported for PET alkaline hydrolysis [273, 276-278]. For instance, tributylhexadecylphosphonium bromide (3Bu6DPB) was found to increase the reaction activity for PET alkaline hydrolysis, reducing the needed reaction time from 10 hours to 1.5 hours to achieve more than 90% PET conversion at 80°C in a Parr pressure reactor [276].

2.5.2.4 Alternative heating methods: microwave and ultrasound

The PET alkaline hydrolysis described in the previous sections used traditional heating methods. Microwave and ultrasound irradiation have been reported as alternative heating sources for PET alkaline hydrolysis [279]. Siddiqui et al. [280] reported complete degradation of PET in 30 minutes with 1.25M NaOH assisted with a phase transfer agent, at the reaction temperature of 180°C under the microwave irradiation. Paliwal and Mungray [281] conducted PET hydrolysis in 10% w/w sodium hydroxide assisted by tetrabutyl ammonium iodide (TBAI) as a phase transfer agent under the ultrasound irradiation. Complete PET depolymerization was achieved in 45 minutes at 90°C and 1 atm. Without

ultrasound irradiation, the required reaction time was 65 minutes at these reaction conditions. Microwave and ultrasound irradiation enhance the diffusion of water into the PET matrix by causing PET structural relaxation, resulting in higher reaction rates than those exhibited for traditional heating process alone [46].

2.5.2.5 PET alkaline hydrolysis: recent studies

Recent studies on PET alkaline hydrolysis have focused on the introduction of methods that can achieve more than 90% PET conversion in short reaction times, to recover and reuse the basic catalyst, or to depolymerize PET with higher impurities. Chen et al. [282] introduced a two-step process for PET alkaline hydrolysis. It was found the biomass-derived γ -valerolactone (GVL) can completely swell the PET flakes at 120°C for 1 hour. In addition, it was observed when the temperature was increased to 170°C, the PET dissolved completely in GVL in 2 minutes. So, for PET alkaline hydrolysis, the PET flakes were dissolved in the excess GVL as the first step. Then, the alkaline hydrolysis was conducted in a batch reactor. The hydrolysis performed at 90°C in the excess amount of sodium hydroxide (15 wt.%). The PET hydrolyzed completely in 8 minutes, and the produced sodium TPA was treated with the acidification process and subsequent recovery steps to determine the TPA yield. Afterward, the GVL, EG, water, and sodium chloride were separated by a distillation process.

Wang et al. [283] proposed a method with a pH-responsive catalyst to better the PET alkaline hydrolysis with sodium hydroxide. The catalyst is $[\text{C}_{16}\text{H}_{33}\text{N}(\text{CH}_3)_3]_3\text{PW}_{12}\text{O}_{40}$ (known as $(\text{CTA})_3\text{PW}$), which is also a phase transfer agent, and could be recycled and reused for PET hydrolysis up to 5 times. In the optimized reaction condition, PET

hydrolyzed completely within 5 hours in 4 wt.% of sodium hydroxide and 0.5 wt.% of (CTA)₃PW at 110°C. Without the catalyst, the PET conversion was only around 20%. So, the phase transfer catalyst in small amounts could increase the hydrolysis rate. The catalyst separated with the acidification process in a pH of 5 while the produced TPA could be precipitated out with further acidification in a pH of 2.

Ügdüler et al. [284] proposed the addition of ethanol (EtOH) to the sodium hydroxide solution to improve PET alkaline hydrolysis. The hydrolysis was done on PET flakes within the range size of 0.5 millimeter to 4 centimeters. The optimum reaction condition was found when the ratio of ethanol to water is 60:40 vol.% with 5 wt.% of sodium hydroxides in the solution. Then, the PET hydrolyzed completely in less than 20 minutes at 80°C. The study did not clarify why the addition of ethanol as a co-solvent could increase the alkaline hydrolysis rate significantly. However, it suggested the ethanol-water could be separated from the EG with a flashing process and be reused for PET hydrolysis.

Kumagai et al. [285] tried to hydrolyze PET fibers that were coated with polyvinyl chloride (PVC) in 1M sodium hydroxide aqueous solution. The coated PVC contained di(2-ethylhexyl) phthalate (DEHP) as a plasticizer and other additives such as titanium dioxide pigment. It was found the PET part of the fibers could be hydrolyzed completely in 2 hours at 180°C. At this condition, the PVC part was dechlorinated up to 22% while the leaching of the DEHP with the average of 61% was unavoidable. However, these simultaneous reactions did not affect the PET hydrolysis and the produced TPA. After the TPA was recovered with the acidification process, it was suggested that water, EG, and the partially

leached DHEP could be separated by distillation. The method shows the alkaline hydrolysis could be used to treat PET with higher impurities.

In conclusion, alkaline hydrolysis can be applied to treat PET waste with higher impurities. It was also reported the technique is more economical than methanolysis because the capital and operation costs are cheaper [19]. However, the needed acidification process to separate the TPA and the separation of the catalyst solution from the reaction medium are barriers that may limit the implementation of the technique for scaleup in chemically recycling PET waste [120, 278].

2.5.3 Acid hydrolysis

2.5.3.1 Background

Acid catalysts including mineral acids have been reported for PET hydrolysis where sulfuric acid is the most widely applied [120, 234, 286]. To avoid high reaction temperature and pressure, PET has been hydrolyzed in concentrated acid solutions with more than 90 wt.% of the acid [19]. As seen for neutral hydrolysis, the products are TPA solid and EG. The produced TPA is recovered with a crystallization process after a complete hydrolysis [31, 38, 287]. In the case of complete PET conversion, acid hydrolysis does not require the acidification process, which is an additional step for alkaline hydrolysis in TPA recovery. Note that the corrosiveness of the high concentration acidic solutions may cause earlier maintenance of the reaction systems.

Yoshioka et al. studied sulfuric acid and nitric acid for PET hydrolysis. Complete hydrolysis occurred in 5 hours in 7 M sulfuric acid at 150°C and atmospheric pressure

[288]. For nitric acid, complete hydrolysis was observed in 16 hours in 13 M nitric acid at 100°C [289]. In addition, kinetic studies confirmed the reaction temperature played a key role in the progress of PET hydrolysis. The reported activation energies for sulfuric acid and nitric acid were 88.7 kJ.mol⁻¹ and 101.3 kJ.mol⁻¹, respectively [288, 289].

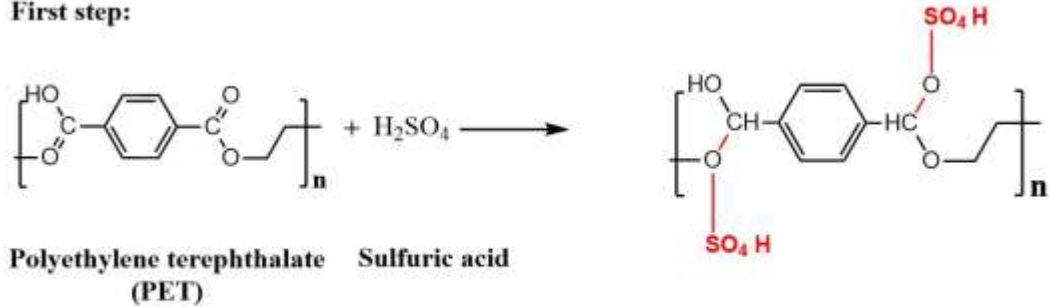
The reaction parameters that are important in PET hydrolysis using mineral acids include acid concentration, reaction temperature, pressure, PET shape, and PET size [290-294]. An increase in acid concentration and reaction temperature result in an increase in the rate of PET conversion. It was observed that a decrease in particle size will increase the rate of PET conversion due to the increase of surface area per volume and easier access to protons to react with the PET surface. Santos and Mendes [295] tried three different reaction media for PET acid hydrolysis- concentrated sulfuric acid, concentrated sulfuric acid along with iodine as a co-catalyst, and fumigant sulfuric acid. For all cases, the hydrolysis reaction occurred at 87.5°C for 2 hours. There were no side reactions, and complete PET conversion was achieved only with the concentrated sulfuric acid.

2.5.3.2 Issued patents for PET acid hydrolysis

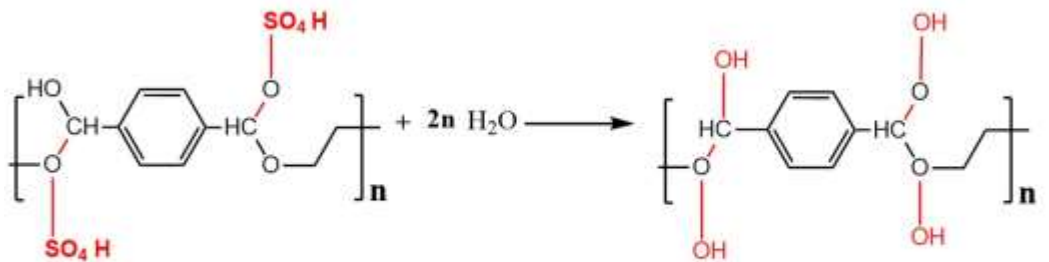
Bryan Jr. et al. [296] published the first patent on PET acid hydrolysis using sulfuric acid with at least 87 wt.% concentration at temperatures from 60°C to 93°C and ambient pressure. Complete PET conversion was observed in about 4 minutes when the acid concentration was 95 wt.% at an average temperature of 75°C. In addition, the mechanism shown in **Figure 2-12** was proposed for acid hydrolysis. In the first step, sulfuric acid reacts with the double bond oxygen of the ester linkage within the PET chain. In the second step, water addition reproduces sulfuric acid in the reaction medium and substitutes hydroxyl

groups within the chain. In the last step, the carbon bonds with two hydroxyl groups are chemically unstable and are swiftly split into TPA and EG.

First step:



Second step:



Third step: unstable condition

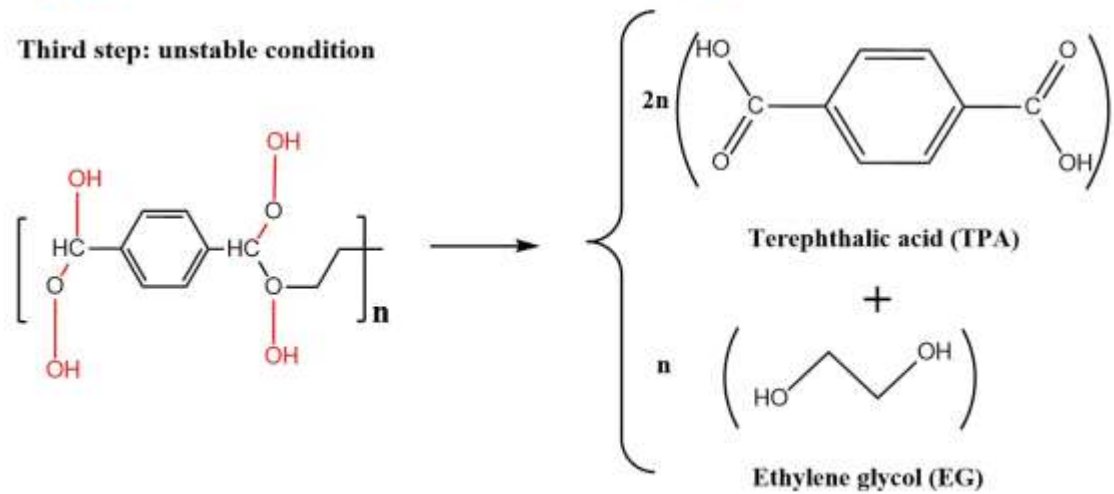


Figure 2-12: Mechanism for PET hydrolysis with H_2SO_4 , proposed by Bryan Jr. et al.

[296].

The mechanism proposed by Bryan Jr. et al. [296] may not be extended to other acid catalysts. So, a comprehensive mechanism for acid hydrolysis, shown in **Figure 2-13**, was recently proposed by Li et al. [297]. First, the hydrogen protons dissociate from the catalyst into the aqueous phase (**Figure 2-13. a**). Second, the proton randomly strikes the carbon atom of the ester carbonyl group (**Figure 2-13. b**). Here, the oxygen atom of the carbonyl group changes into a secondary hydroxyl group. Third, the oxygen atom of water attacks the protonated carbon atom of the ester carbonyl group (**Figure 2-13. c**). At the same time, the hydrogen proton of water integrates with the oxygen atom of the ester bond, making it protonated as the result of the effect of hydrogen bond (**Figure 2-13. d**). The ester bond is unstable and is swiftly broken to form terminal carboxyl group and hydroxyl group (**Figure 2-13. e**). Simultaneously, the hydrogen proton separates from the carbonyl oxygen and returns to the water environment for the next strike.

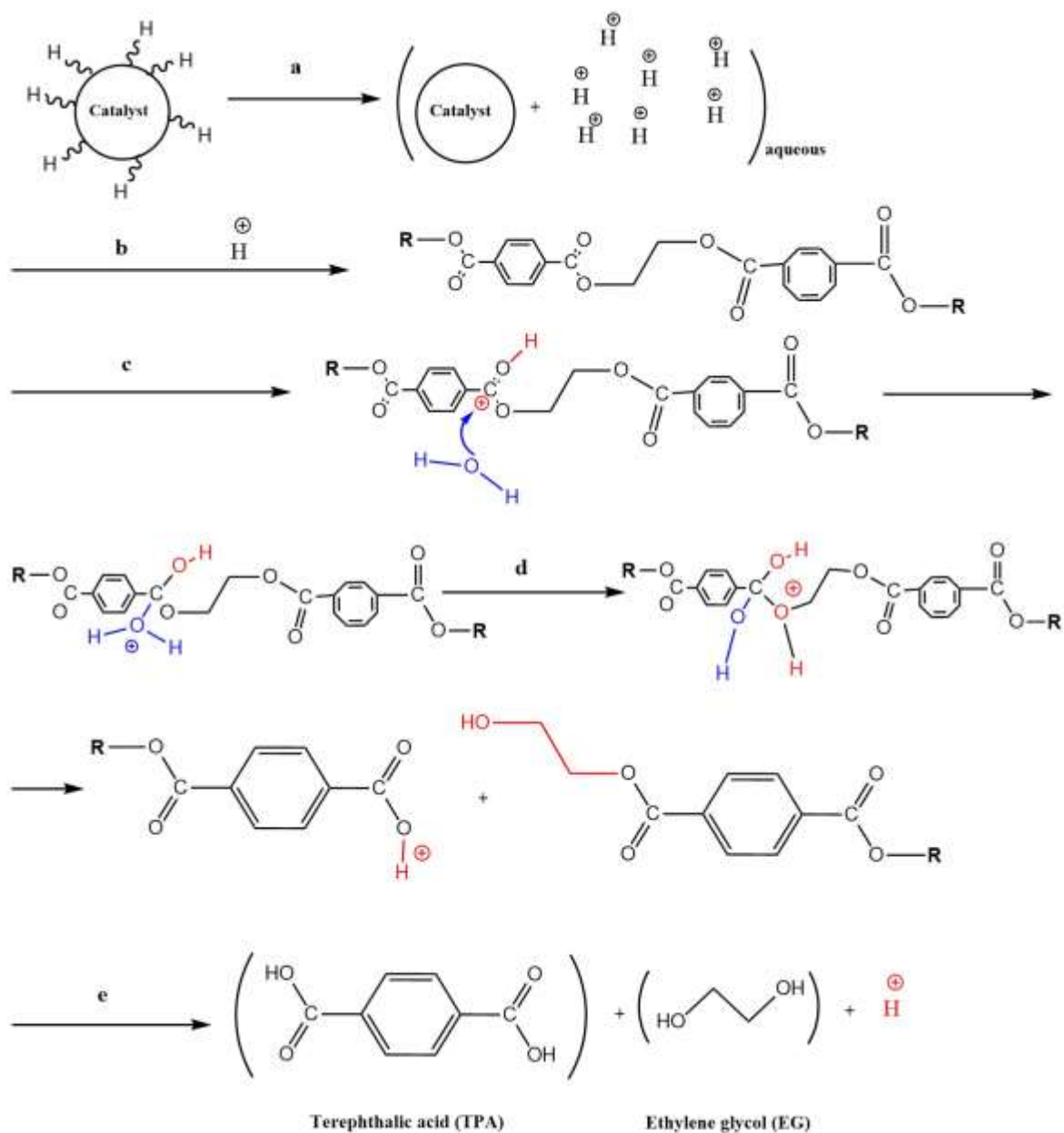


Figure 2-13: Mechanism for PET acid hydrolysis, a: dissociation step, b: first protonation step, c: water molecule attack step, d: second protonation step, e: formation step, proposed by Li et al. [297], reproduced from [58].

Pusztaszeri [298] patented a method that could economically and industrially hydrolyze PET waste in concentrated sulfuric acid solution at room temperature and

atmospheric pressure. Complete PET hydrolysis was achieved in 30 minutes with volume ratio of acid to water of at least 6 to 1. Four types of PET waste were considered as the feed for hydrolysis including silver-bearing films, regular films, textiles, and bottles. The invention revolves around a technique to produce the TPA of 99% purity. After hydrolysis, the solid material in the solution was filtered and mixed in an alkali solution to dissolve the produced TPA. The second filtration separated the TPA from the remaining impurities. Finally, the TPA was precipitated by bringing the pH solution within the range of 0 to 3. The filtrates from the first and second filtrations were neutralized and disposed.

These two patents were from 1970s and 1980s, and no patent has been issued since then for PET acid hydrolysis. There are possibly two major reasons for that. First, PET acid hydrolysis requires a highly concentrated mineral acid solution to convert PET completely in a short time with ambient conditions. This high acid concentration is corrosive which limits the selection of the reactor for hydrolysis. Second, substantial volumes of acid and EG in water are produced during the reaction, which require a costly distillation process to separate acid from EG [107, 120, 278]. However, studies on methods to improve PET acid hydrolysis technique have been pursued due to the promising features including use of aqueous solvent and the direct production of TPA.

2.5.3.3 Enzymes as catalysts for PET acid hydrolysis

The application of enzymes as acid catalysts to depolymerize PET has been studied to introduce greener methods for acid hydrolysis of PET [299, 300]. These enzymes are classified as carboxylic acid hydrolases including cutinases [301, 302], lipases [303, 304], serine esterases [305, 306] and carboxylesterases [307, 308]. With enzymatic catalysts,

PET hydrolysis is performed at the average reaction temperature of 45°C and atmospheric pressure, producing TPA and EG. Complete PET conversion generally takes days or weeks, depending on the enzyme activity [309, 310]. Thus, this approach may not be suitable for PET degradation in recycling plants. However, enzyme application for PET hydrolysis might be applied for degradation of the PET wastes that are piled up on static stations such as landfills [227, 311-313].

2.5.3.4 PET acid hydrolysis: recent studies

Ohmura et al. [314] introduced modified silica gels with phosphoric acid as solid catalysts for PET hydrolysis in water. The catalyst was prepared by mixing silica gels and phosphoric acid at a molar ratio of 1 to 3 for 24 hours at room temperature and pressure. The mixture was dried for 12 hours in an oven at 100°C to obtain the solid catalyst. In this study, the reaction heating source was microwave irradiation where the effect of microwave power on hydrolysis rate was explored. It was observed that an increase in power will increase the hydrolysis rate. The optimum reaction condition was with the power of 200W and the weight ratio of 6:2:1 for the catalyst: PET: water. Approximately 5 minutes was required to achieve more than 90% TPA yield under these conditions. The study did not discuss recovery and reuse of the solid catalyst after hydrolysis. However, it was suggested that an increase in the catalyst amount and use of the microwave heating can increase the PET conversion rate and save energy, respectively.

In another study, ZSM-5-based zeolites were investigated as solid acid catalysts for PET hydrolysis [315]. The catalyst structure has both Brønsted and Lewis acidic sites that contribute to PET hydrolysis. ZSM-5-based catalysts were prepared by changing the ratio

of Al to Si of the zeolite framework to explore the effect of the acidic type on PET hydrolysis. It was found that Brønsted acidic site had a greater contribution to PET hydrolysis. So, the best catalyst was determined to be $\text{H}^+@\text{ZSM-5-25}$, which had the highest acidic concentration (1.25 mmol.g^{-1}) where the Brønsted acidic site amount was dominant. The PET hydrolysis tests were conducted with 0.1 g PET granules and 0.05 g catalyst in an excess amount of 12 g water inside a 30 mL glass reactor. More than 90% TPA yield was achieved within 40 minutes with the microwave irradiation as the heating source and reaction temperature of 121°C . In addition, the $\text{H}^+@\text{ZSM-5-25}$ was readily separated after PET hydrolysis with filtration. After drying, the catalyst exhibited retention of the acidic active sites, and it was reused for PET hydrolysis up to 6 times, without losing activity. Under microwave heating, the kinetic reaction study indicated the $\text{H}^+@\text{ZSM-5-25}$ has an activation energy of 1.2 kJ.mol^{-1} , which is about 19-fold smaller than the activation energy of PET hydrolysis in the catalyst-free condition ($19.46 \text{ kJ.mol}^{-1}$). As observed, the recoverability and reusability of the catalyst could improve sustainable methods for acid hydrolysis of PET.

Another recently introduced method to improve acid hydrolysis was to examine the ability of TPA, the PET monomer, to act as a solid catalyst for PET hydrolysis [58]. This study found that 0.1 g.mL^{-1} of TPA in water (0.6M TPA) with a weight ratio of 1:8 for PET: water is the optimum reaction condition to achieve more than 90% TPA in 3 hours at reaction temperature of 220°C and in a pressure-tight reactor. After hydrolysis, the produced TPA was recovered and reused as the catalyst up to eight reaction cycles, determined that the TPA yield had an average value of 94.5%. In addition, the produced

TPA had a high purity of 99%, like commercial TPA. The method was claimed to be a green and low-cost technology for PET acid hydrolysis.

2.6. Conclusions

A broad array of methods and techniques have been introduced for recycling of PET. The general challenges of PET chemical recycling include method scaleup, method cost, organic solvent handling, and recoverability/reusability of the catalysts. Chemical recycling is regarded as the key approach to recycle PET without downcycling the polymer. Solvolysis methods, including glycolysis, methanolysis, and hydrolysis, depolymerize PET into compounds that can be used in synthesis of PET.

Aqueous hydrolysis avoids the use of organic solvents as the reaction medium for PET depolymerization. Aqueous hydrolysis could have three forms of alkaline, neutral, and acid, depending on the applied catalyst and the pH of the aqueous reaction medium. Alkaline hydrolysis consumes the catalyst in PET hydrolysis, and the TPA recovery process will not permit to recover the basic catalyst. So, the technique is not categorized as a catalytic reaction. Neutral hydrolysis is proposed as a green path for PET depolymerization as the reaction occurs simply in water or steam. Despite that, the severe reaction conditions including high temperature, pressure, and highly resistant reactor, have caused the technique to be considered too costly as a commercialized method for recycling of PET.

Aqueous acid hydrolysis has recently been of interest to academia and industry due to the feasibility of running PET hydrolysis at milder reaction conditions. In addition, the recent studies have focus on applying the catalysts with higher functionalities including

better PET surface wetting within the aqueous form, catalyst recoverability, and catalyst reusability. Aqueous acid hydrolysis may provide greener methods for sustainable depolymerization of PET. However, it's needed to do the method scaleup and relevant cost estimates to propose a potential green path for PET depolymerization in marketing scale.

This dissertation focused on an increase of wetting of PET particles within the aqueous reaction medium with different catalysts. The increase in wetting was expected to cause the increase of the local concentration of the catalyst within the vicinity of PET particles in the reaction medium, resulting in higher rate of the hydrolysis. For this purpose, these catalysts are either selected or synthesized by accounting for having structural affinity to the PET particles.

Chapter 3

Materials and Methods

3.1 Materials

Poly (sodium 4-styrenesulfonate) (PSSS) with an average molecular weight of 70 kDa, p-toluene sulfonic acid monohydrate, 1, 5- Naphthalenedisulfonic acid tetrahydrate, 2- Naphthalenesulfonic acid, terephthalic acid (TPA), ammonium hydroxide solution (30-33% NH₃ in H₂O), ether, ethyl acetate, acetonitrile, [1,8-diazabicyclo (5.4.0) undec-7-ene] (DBU), oxalic acid (OA), lactic acid (LA), citric acid (CA), methanol, methyl sulfoxide-d₆, chloroform, and deuterium oxide were all purchased from Sigma-Aldrich. Sulfuric acid (Certified ACS plus) was purchased from Fisher Scientific. Amberlyst®-15 was purchased from Alfa Aesar and was ground to a fine powder for the ion-exchange of PSSS to the protonated form (PSSA). PET pellets were provided by Alpek Company. They were ground and sieved into a powder with the diameter size range of 250µm to 354µm.

3.2 Experimental Methods

3.2.1 Synthesis of poly (4-styrene sulfonic acid) (PSSA) catalyst

As shown in **Figure 3-1**, the sodium form of the polystyrene sulfonate, [poly (sodium 4-styrenesulfonate)] (PSSS), was converted to the protonated form, [poly (4-styrene sulfonic acid)] (PSSA), using a well-established ion exchange-reaction method [316]. Briefly, 10 mL of PSSA (25 wt%) solution was added to 12 g of grounded

Amberlyst®-15 and 50 mL deionized water, under stirring condition. The reaction completed after 12 h at room temperature and 1 atmosphere pressure. Then, the mixture was filtered to separate the PSSA/water solution from the Amberlyst®-15. The solution was dried for 24 h at 60°C to recover the PSSA films. These films were crushed into smaller pieces and were furtherly dried at 60°C to obtain PSSA in powder form with minimum water amount [2].

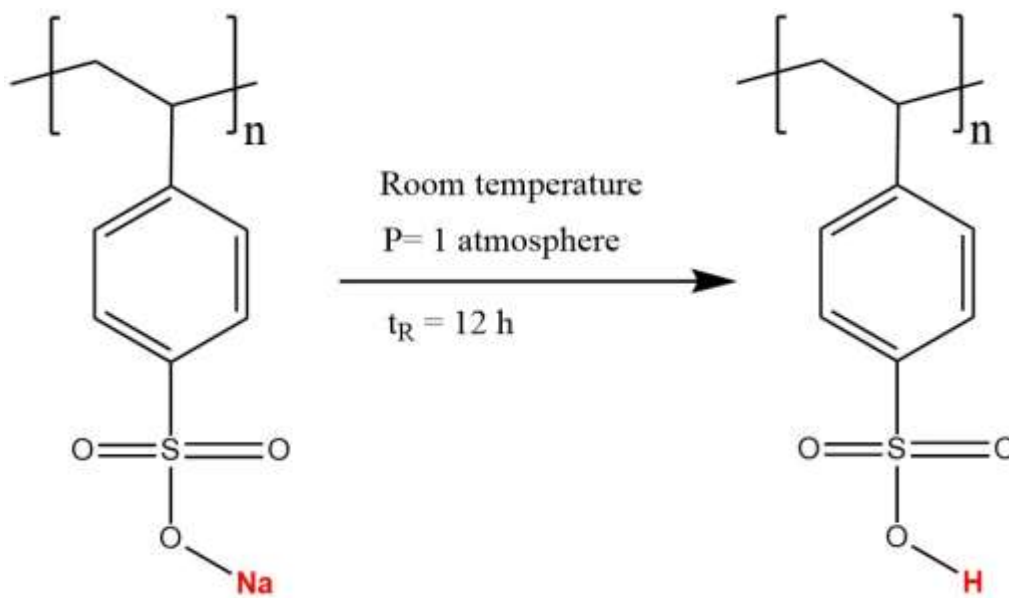


Figure 3-1: The ion-exchange reaction, converting PSSS (left) to PSSA (right).

For a complete ion-exchange, there would be 5.4 mmol protons per gram of PSSA. The titration results, after conducting the ion-exchange reaction, indicated that the recovered PSSA has 4.7 mmol protons per gram of PSSA, 87 percent ion-exchange completion. The white powder of the sodium form of polymer before ion-exchange reaction is illustrated in **Figure 3-2 (Left)**. The brown powder of the PSSA after the ion-

exchange reaction is illustrated in **Figure 3-2 (Right)**. This color change is another indication that the ion-exchange reaction was successful [43, 316].



Figure 3-2: Poly (sodium 4-styrenesulfonate) (PSSS) (Left) and the synthesized PSSA (Right).

3.2.2 Aryl sulfonic acids as catalysts for PET hydrolysis

P-toluene sulfonic acid (PTSA), 1, 5- Naphthalenedisulfonic acid (NDSA), and 2-Naphthalenesulfonic acid (NSA) were selected as catalysts to investigate the impact of surface affinity and wetting on PET hydrolysis reaction. The moisture content of each catalyst was determined by thermal gravimetric analysis (TGA), which was used to determine required mass of catalyst to prepare an aqueous catalyst solution with concentrations of 1 M, 2 M, and 4 M. These solutions were used for PET hydrolysis. The structures of the stated aryl sulfonic acids are shown in **Figure 3-3**.

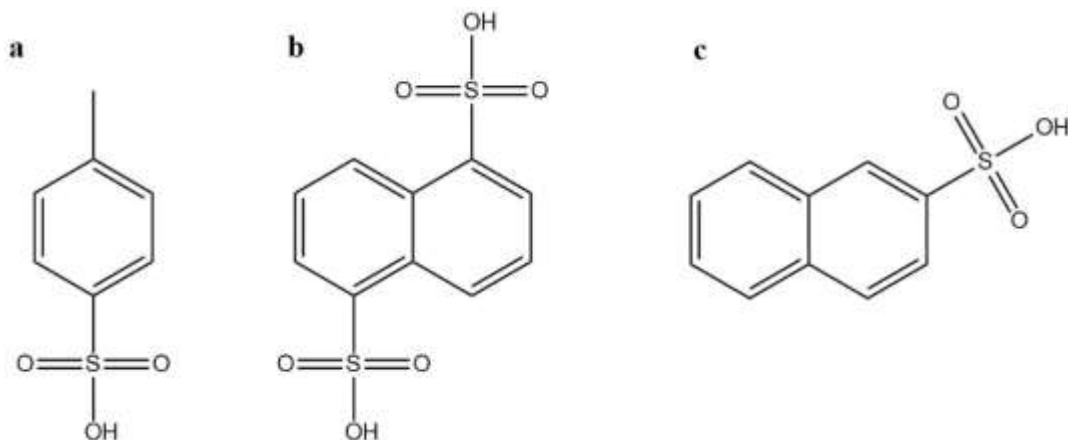


Figure 3-3: Structures of aryl sulfonic acids, used for PET hydrolysis: a) P-toluene sulfonic acid (PTSA), b) 1, 5- Naphthalenedisulfonic acid (NDSA), and c) 2- Naphthalenesulfonic acid (NSA).

3.2.3 Synthesis of DBU-LA catalyst

The DBU-LA catalysts were synthesized using a method reported in the literature [317]. [1,8-diazabicyclo (5.4.0) undec-7-ene] (DBU) (40.00 mmol, 6.09 g, 5.97 mL) was charged into a 100 mL round-bottom flask, equipped with a magnetic stirrer, and surrounded with water-ice to maintain a temperature between 0-5°C at the reaction pressure of 1 atmosphere. Then, an equimolar amount of lactic acid (LA) (40.00 mmol, 3.60 g, 2.98 mL) was added dropwise to the flask. Afterwards, the flask was left under stirring conditions for 4 hours at room temperature to ensure that the neutralization reaction was completed. The mixture was placed into an oven under vacuum with the temperature of 60°C overnight [317]. This helped in removal of any excess water. The obtained compound is the DBU-LA ionic liquid with the yellow-pale color. **Figure 3-4** illustrates the synthesis process of DBU-LA.

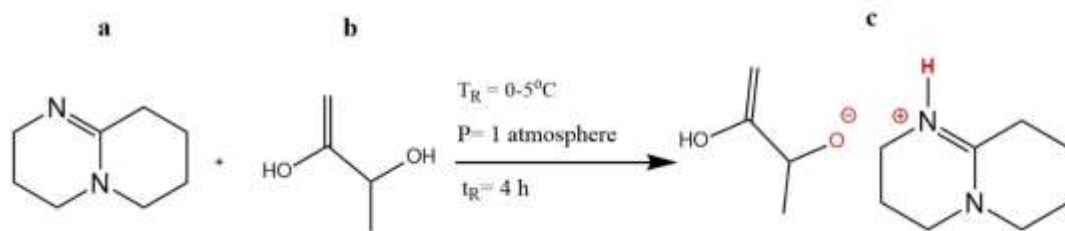


Figure 3-4: Synthesis reaction path for production of DBU-LA: a) DBU, b) LA, and c) DBU-LA.

3.2.4 Synthesis of DBU sulfate (DBU-SO₄) catalyst

3.2.4.1 Synthesis in acetonitrile as the solvent

The DBU-SO₄ was synthesized in acetonitrile as a solvent using method described in the literature [318]. [1,8-diazabicyclo (5.4.0) undec-7-ene] (DBU) (40.00 mmol, 6.09 g, 5.97 mL) was charged into a 100 mL round-bottom flask, equipped with a magnetic stirrer, and surrounded with water-ice to maintain a temperature between 0-5°C. Since H₂SO₄ is a strong acid, acetonitrile (12 mL) was added to the flask to reduce the reaction rate of the neutralization process between DBU and H₂SO₄. Afterwards, an equimolar of H₂SO₄ (40 mmol, 3.92 g, 2.14 mL) was added dropwise under the stirring condition. After adding H₂SO₄, the stirring condition was maintained for 4 hours at room temperature. Then, the mixture was washed repeatedly with ether (3 x 10 mL) to remove non-ionic and oily residues. After that, the mixture was placed in an oven for 12 hours under vacuum condition at 60°C to remove ether residues [318]. The obtained compound was DBU-SO₄ ionic liquid with the yellow-pale color.

3.2.4.2 Synthesis in water as the solvent

A method was developed to synthesize DBU-SO₄ in water as the reaction solvent to avoid use of organic solvents. In this case, DBU (40.00 mmol, 6.09 g, 5.97 mL) was charged into a 100 mL round-bottom flask, with the same reaction conditions stated for synthesis of DBU-SO₄ in acetonitrile as the solvent. Then, an equimolar amount of H₂SO₄ (40.00 mmol, 2.14 mL) which was diluted with water with the volume ratio of 1 (H₂SO₄) to 5 (water), was added dropwise to the flask under stirring condition. The stirring condition was maintained for 4 hours. Afterwards, the solution was placed in an oven under the vacuum condition for 12 hours at the temperature of 60°C. This process removed all the excess water of the solution, and the recovered compound was the DBU-SO₄, a yellow-pale color liquid [317, 318].

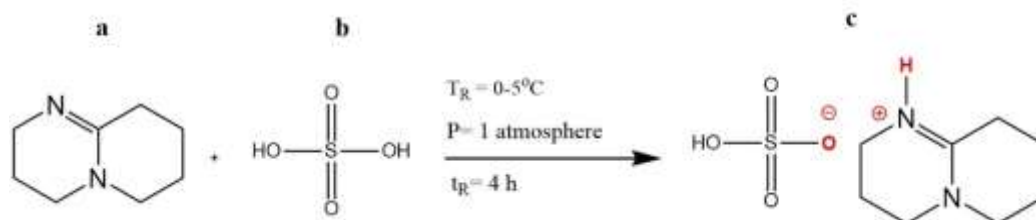


Figure 3-5: Reaction path for production of DBU-SO₄: a) DBU, b) H₂SO₄, and c) DBU-SO₄.

3.2.5 Syntheses of DBU-OA and DBU-CA catalysts

3.2.5.1 Synthesis in water as the solvent

Two synthesis methods were tried to prepare DBU-OA and DBU-CA ionic liquids in water as the reaction solvent. In the first method, equimolar amounts of the DBU and

OA or CA were reacted in water. In the second method, the acid-base titration results were considered to determine the concentration of released hydroxyls (OH^-) of DBU and the concentration of released protons (H^+) of OA or CA. The number of hydroxyls (OH^-) and protons (H^+) must be equal. So, the needed amounts of DBU and OA or CA to neutralize in the water medium were calculated and used for preparation of DBU-OA and DBU-CA ionic liquids.

For the equimolar synthesis method, [1,8-diazabicyclo (5.4.0) undec-7-ene] (DBU) (40.00 mmol, 6.09 g, 5.97 mL) was added into a 100 mL round-bottom flask, equipped with a magnetic stirrer. Then, OA (40.00 mmol, 3.60 g, 1.90 mL) (for preparation of DBU-OA) or CA (40.00 mmol, 7.68 g, 4.63 mL) (for preparation of DBU-CA) was dissolved in excess amount of water in a 60 mL beaker. Then, the aqueous OA or CA solution was added dropwise to the DBU flask, and the mixing was maintained for 4 h. To remove the excess water, the mixture was placed in an oven under vacuum condition at temperature of 60°C overnight. The recovered compound is DBU-OA or DBU-CA as the ionic liquid.

For the titration synthesis method, the synthesis process was the same as the equimolar synthesis method except the amounts of OA or CA were different, determined by the titration results. So, the applied amount of DBU was (40.00 mmol, 6.09 g, 5.97 mL). The applied amounts of OA (for preparation of DBU-OA) and CA (for preparation of DBU-CA) were (22.22 mmol, 2.00 g, 1.06 mL) and (12.90 mmol, 2.48 g, 1.49 mL), respectively.

3.2.5.2 Synthesis in methanol as the solvent

Figure 3-6 shows the structures of oxalic acid (OA) and citric acid (CA). The number of carboxylic acid functional group are two and three for OA and CA, respectively. It was assumed the protons are released from all the carboxylic acid groups and they react with the amine groups of DBU in methanol. This assumption was confirmed by FTIR and NMR analyses on the synthesized DBU-OA and DBU-CA. So, molar ratios of 1 (DBU) to 2 (OA) and 1 (DBU) to 3 (CA) were used to prepare DBU-OA and DBU-CA, respectively, in methanol as the solvent [317, 319, 320].

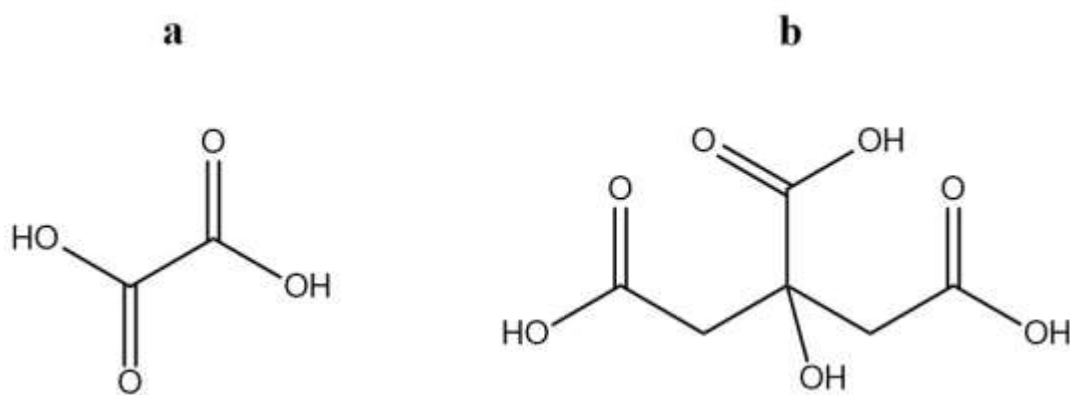


Figure 3-6: Structures of a) oxalic acid (OA) and b) citric acid (CA).

The synthesis process to prepare DBU-OA and DBU-CA in methanol is the same as the synthesis process to prepare DBU-OA and DBU-CA in water, except the methanol was used as the solvent and the amounts of OA and CA were determined by considering the number of carboxylic acid functional groups. The applied amount of DBU was (40.00 mmol, 6.09 g, 5.97 mL). The applied amounts of OA (for preparation of DBU-OA) and CA (for preparation of DBU-CA) were (20.00 mmol, 3.05 g, 2.99 mL) and (13.33 mmol,

2.03 g, 1.99 mL), respectively. **Figure 3-7** and **Figure 3-8** illustrate the reaction paths for preparation of DBU-OA and DBU-CA, respectively.

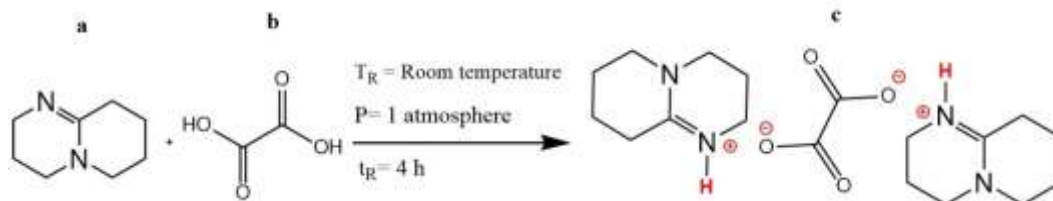


Figure 3-7: Reaction path for production of DBU-OA: a) DBU, b) OA, and c) DBU-OA.

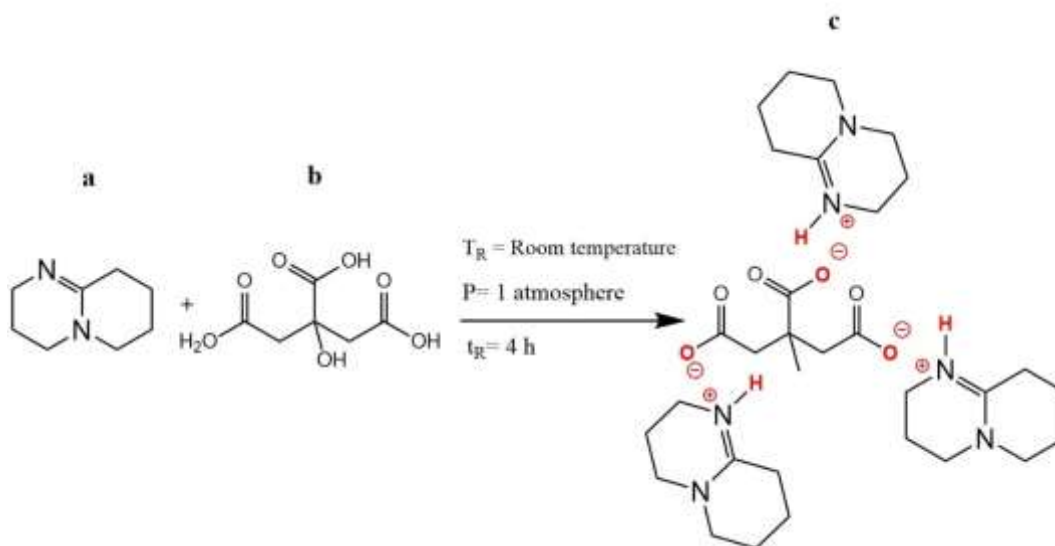


Figure 3-8: Reaction path for production of DBU-CA: a) DBU, b) CA, and c) DBU-CA.

3.2.6 Titration measurements

Acid-base titration [321] was conducted to determine the proton concentration and hydroxyl concentration of the catalysts, used to do the kinetic studies on PET hydrolysis. In titration tests, 5 mL solutions of the catalysts were prepared in deionized water with the catalyst concentration range of 0.125 M to 4 M. The solution was titrated against a 0.01 N

NaOH solution, which is standardized with potassium acid phthalate. Phenolphthalein was used as the indicator to specify the endpoint. Every titration was done three times to assure the reproducibility and validity of the results.

3.2.7 pH tape strips

The pH tape strips were used to estimate the acidity of synthesized DBU-acid ionic liquids [322, 323]. This is an alternative technique to the titration measurement method since the synthesized DBU-acid ionic liquids have too low concentrations of proton (H^+) and hydroxyl (OH^-) to use phenolphthalein as an indicator to determine the endpoint. The DBU-acid catalyst solutions were prepared within the range of 0.125 M to 4M. Then, the pH strips were used to estimate the concentrations of proton (H^+) and hydroxyl (OH^-) of the DBU-acid catalyst solutions.

3.2.8 Contact angle measurements

The contact angle measurements were conducted for the aqueous solutions of the catalysts used for PET hydrolysis [43, 49]. The tested catalyst concentrations were within the range of 0.125M to 4M. The testes were done at room temperature and pressure. For a typical test, a droplet of the catalyst solution was placed on a PET film, affixed to a flat glass substrate. The PET films used for these tests had an average thickness of 0.35 mm and were prepared in a HAAKE Rheomex Brabender single screw extruder. The droplet contact angle was measured by using a Keyence VHX-600 digital microscope. The microscope was equipped with a camera in reflection mode along with full coaxial light on the stage. For each catalyst solution with certain concentration, the test was repeated at least six times by positioning new droplets on new PET films.

3.2.9 Ethyl acetate hydrolysis reactions

The hydrolysis of ethyl acetate was examined to understand the homogeneity effect on the catalyst activity. For this purpose, 5 mL of 5 wt.% ethyl acetate was added to 5 mL of 0.5M catalyst aqueous solution in a 15-mL ace pressure reactor, equipped with a magnetic stirrer. Then, the reactor was immersed into a stirring bath oil and the hydrolysis was conducted for 1-hour reaction time. The tested reaction temperatures were within the range of 40°C to 70°C. The extent of the reaction was determined by titration. To determine the amount of product (i.e., acetic acid), 2 mL of the reaction solution was titrated against 0.1 N sodium hydroxide (NaOH), standardized with potassium hydrogen phthalate. The calculated proton (H^+) amount is the total amount, which was subtracted from the proton (H^+) amount of catalyst to determine the amount of produced acetic acid. This was used then to do calculations to determine the reaction rate constants and the activation energy values [43, 49].

3.2.10 PET hydrolysis reactions

The PET resins were ground and sieved to collect the PET powders in the diameter size range of 250 μm to 354 μm . In a hydrolysis reaction, 0.2 grams of the PET powder was placed in a 15-mL Ace pressure reactor, equipped with a magnetic stirrer, where 10 mL aqueous catalyst solutions were prepared with 1, 2, and 4 molarities. The reactor was immersed completely in a preheated oil bath with the temperatures of 130°C, 140°C, and 150°C, equipped with a magnetic stirrer. The hydrolysis reactions were repeated three times to find the average and the standard deviation for the reaction kinetic data. After a

hydrolysis reaction, the reactor was immersed in a cold-water vessel while rinsing with a cold water to quench the reaction process.

For acid hydrolysis, the unreacted PET along with any produced TPA was separated by passing the reaction mixture through a Whatman-5 filter paper with a pore size of 55 mm. The catalyst could be recovered by evaporating the filtrate solution. In the next step, the TPA and the unreacted PET were mixed with 20 mL of the 5M ammonium hydroxide solution to form a soluble sodium salt of the TPA [290]. The unreacted PET was separated by filtration from the ammonium hydroxide solution. To recover the TPA, a 2M H_2SO_4 solution was added to the filtrate to reduce the pH of the filtrate to 2. Finally, a third filtration process was conducted to collect the precipitated TPA powder. The described process for acid hydrolysis is illustrated in **Figure 3-9**.

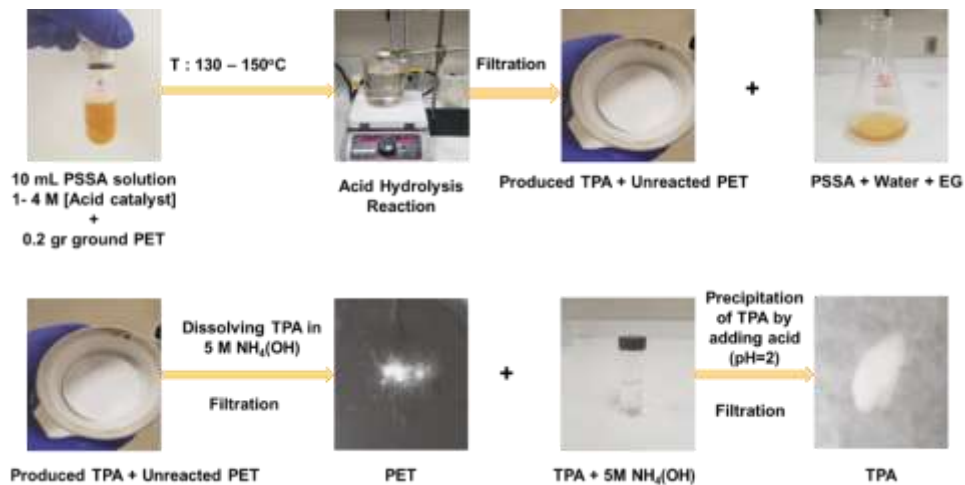


Figure 3-9: The acid hydrolysis process conducted in the lab, illustrated for PSSA.

For alkaline hydrolysis, the produced TPA was dissolved in the hydrolysis solution. The unreacted PET was separated by filtration from the solution, using a Whatman-5 filter paper with a pore size of 55 mm. Then, a 2M H₂SO₄ solution was added to the filtrate to reduce the pH of the filtrate to 2. This will result in precipitation of the produced TPA from the hydrolysis solution. Afterward, a second filtration was done to collect the precipitated TPA powder [276, 284, 324]. The described process for alkaline hydrolysis is illustrated in **Figure 3-10**.

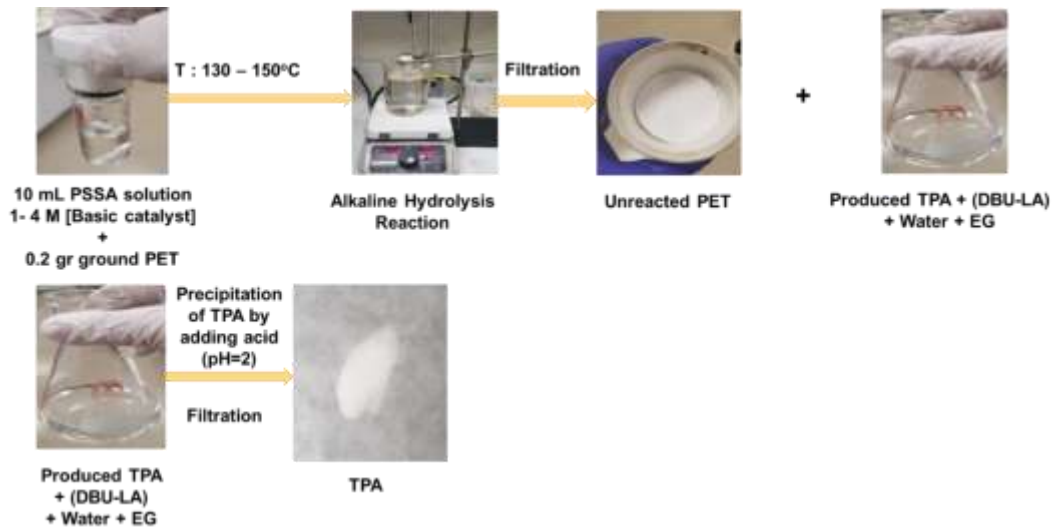


Figure 3-10: The alkaline hydrolysis process conducted in the lab, illustrated for DBU-LA.

In both cases (i.e., acid hydrolysis and alkaline hydrolysis), the recovered unreacted PET and the produced TPA powder were dried in a vacuum oven at 70°C for 4 hours for subsequent analyses. The PET conversion (%) and the TPA yield were determined as reported in the literature [21, 288, 290].

3.3 Thermal Characterization

TA instruments' Q50 Thermogravimetric analyzer was applied to determine the water content of the catalysts. This information was used for preparation of catalyst solutions with different molarities. In a typical TGA test, 20-30 mg of the sample was heated from room temperature to 800°C at a heating rate of 2°C.min⁻¹ under nitrogen environment, helping to avoid oxidative degradation [43, 316, 325]. Each TGA test was repeated at least three times on each catalyst for accurate measurements.

3.4 Structural Characterization

3.4.1 Fourier Transform-Infrared Spectroscopy (FTIR)

Fourier transform infrared spectroscopy (FTIR) was used to confirm the structure of the synthesized catalysts, produced TPA, and commercial TPA. The samples were mixed with KBr to form pellets to be analyzed in the transmission mode in the range of 400 cm⁻¹ to 4000 cm⁻¹ with the bench setup. The system (FTS-4000) was set to average the IR spectra with 128 scans. Characteristic peaks that correspond to the vibrations and functional groups of the material structure were specified using the literature [326, 327].

3.4.2 Nuclear Magnetic Resonance Spectroscopy (NMR)

The proton nuclear magnetic resonance spectroscopy (¹H-NMR) and carbon nuclear magnetic resonance spectroscopy (¹²C-NMR) were used to study the structure of the synthesized catalysts, produced TPA, and recovered TPA [328, 329]. The NMR spectra were recorded in a Bruker Avance III spectrometer at 600 MHz. The produced TPA

samples were dissolved in methyl sulfoxide-d₆. The samples of PSSA and the DBU-acid ionic liquids were dissolved in deuterium dioxide (D₂O).

3.4.3 Scanning Electron Microscopy (SEM)

A Hitachi S-4800 high resolution scanning electron microscope (SEM) was used to study the surface morphology of the unreacted PET samples [330-332]. These unreacted PET samples were recovered following PET hydrolysis with catalyst solutions.

Chapter 4

Poly (4-Styrenesulfonic Acid): A Recoverable and Reusable Catalyst for Acid Hydrolysis of Polyethylene Terephthalate

This chapter is reproduced from an article published in Polymer Journal, Elsevier ¹.

Hossein Abedsoltan^{*,2}, Ibeh S. Omodolor^{*}, Ana C. Alba-Rubio^{*,3}, and Maria R. Coleman^{*,3}.

“Poly (4-Styrenesulfonic Acid): A Recoverable and Reusable Catalyst for Acid Hydrolysis of Polyethylene Terephthalate”, Polymer 2021, 222, 123620.

* Department of Chemical Engineering, The University of Toledo, Toledo, OH 43606, United States.

¹ Reprinted with the permission of Polymer Journal, Elsevier.

² First Author

³ Corresponding Authors: ana.albarubio@utoledo.edu & maria.coleman6@utoledo.edu

4.1 Highlights

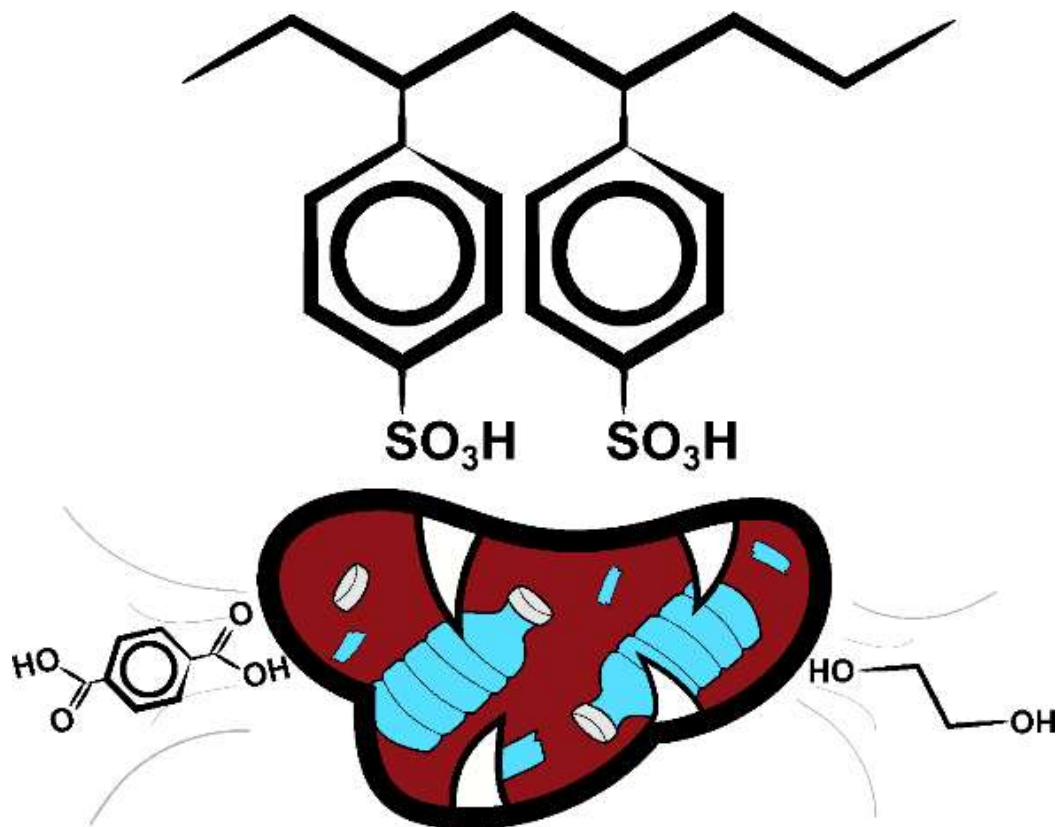
- A recoverable, reusable catalyst, poly (styrene sulfonic acid) (PSSA) was investigated as a catalysis of acid hydrolysis of poly (ethylene terephthalate) (PET).
- The PSSA exhibited lower slightly higher activity for hydrolysis of PET than the homogeneous H₂SO₄, but less active for hydrolysis of ethyl acetate.
- The increase in activity of the PSSA relative to H₂SO₄ was attributed to the adsorption affinity for hydrophobic PET surfaces which would increase local concentration.
- The PSSA was recoverable and exhibited no loss in activity following five repeat cycles for PET hydrolysis.

4.2 Abstract

Poly (4-styrenesulfonic acid) (PSSA) was used as a recoverable acid catalyst for the hydrolysis of polyethylene terephthalate (PET) to terephthalic acid (TPA) and ethylene glycol (EG). The effect of catalyst concentration, time, and temperature on the depolymerization of PET and yield of TPA were determined with PSSA and H₂SO₄. The PSSA system exhibited faster hydrolysis kinetics than H₂SO₄ with a shorter induction period than those often observed for acid hydrolysis of PET. The activation energies for the hydrolysis of PET were 24.6 kJ·mol⁻¹ and 29.1 kJ·mol⁻¹ for 2 M PSSA and 2 M H₂SO₄, respectively. The hydrophobic backbone of PSSA improves surface wetting of the catalyst solution at the PET interface, resulting in a higher localized concentration of protons. Contact angle measurements indicated better surface wetting of PET films by the aqueous solutions of PSSA than H₂SO₄ at equal concentrations. Additionally, the reutilization and

titration results indicated that PSSA maintained the activity after reuse for five reaction cycles.

4.3 Graphical abstract



4.4 Keywords

Recycling, Hydrolysis, Sustainability, Polyesters, PET, TPA, Acid catalysis, PSSA

4.5 Introduction

Polyethylene terephthalate (PET) is a semi-crystalline, colorless polyester with excellent thermal and mechanical properties that is readily processed into films, fibers, and bottles [333]. Because of these unique properties, PET has found broad applications, including food and beverage packaging and in textiles. The annual growth rate for the global PET market is estimated to be around 4.2% over the five-year period from 2019 to 2024, increasing from 40 billion US dollars in 2019 to 51 billion US dollars in 2024 [334]. While PET is the most recycled polymer by volume, the recycle rate for PET in the US is less than 30% [335]. The broad use of PET combined with a low recycle rate results in accumulation of high volumes of waste PET in landfills and the environment [336-341].

While most of the commercial recycling of PET is through mechanical recycling, this method requires clean polymer streams and can lead to degradation in properties, thus, limiting the volume of recycled PET incorporated into the process streams [342, 343]. Chemical recycling can be used to depolymerize the polymer and produce monomers or upgraded molecules for broad industrial applications [344-346]. A variety of processes have been explored for chemical recycling of PET including glycolysis, methanolysis, and hydrolysis [347-356]. Hydrolysis produces terephthalic acid (TPA) and ethylene glycol (EG) that can be directly polymerized to virgin PET. Alkaline hydrolysis has been reported in presence of base catalysts, such as sodium hydroxide and potassium hydroxide in aqueous solutions [357, 358] and non-aqueous systems [359-361]. In contrast, neutral hydrolysis typically takes place in water or steam under pressure and at high temperatures, in the range of 200°C to 450°C [362-364].

Acid hydrolysis is a well-established process in which the reactions occur at moderate temperatures but require high acid concentrations and long reaction times [365-369]. The important factors that determine the extent of PET conversion and TPA yield are PET particle size, catalyst type and concentration, reaction temperature, and reaction time. For example, Yoshioka *et al.* [370] converted more than 90% of PET using a 7 M sulfuric acid (H₂SO₄) aqueous solution at 150°C for 5 h. A modified shrinking-core model was developed to describe the kinetics of the reaction [371]. Nitric acid [372] and hydrochloric acid [373, 374] have also been reported as other acid catalysts for PET recycling. The main drawback of acid hydrolysis is the use of high molarity acid solutions that require costly equipment to avoid corrosion and a subsequent neutralization step after reaction.

Since hydrolysis occurs at the PET surface, wetting by the catalyst solution and adsorption of the catalyst may be important in determining the reaction kinetics [370-372]. For example, Amarasekara *et al.* demonstrated that the reaction kinetics for acid hydrolysis at the surface of cellulose increased for alkyl sulfonic acid. The reaction rate constant correlated well with the distribution coefficients of these alkyl sulfonic acid catalyst between octanol and water [375]. Poly (4-styrenesulfonic acid) (PSSA) is a soluble catalyst that combines the rapid kinetics of H₂SO₄ with ease of recovery and reuse. PSSA has been used in different reactions for biomass conversion, including biodiesel synthesis, xylose dehydration to furfural, hydroxymethylfurfural production from fructose, and the selective oxidation of furfural with H₂O₂ to C₄ diacids [376-379]. In addition, PSSA in aqueous medium has been shown to adsorb on hydrophobic surfaces (e.g., alumina) [380-383].

Here, we report the use of PSSA as a recoverable acid catalyst for the hydrolysis of PET along with a comparison with H₂SO₄. Specifically, we have studied the impact of the reaction temperature, catalyst concentration, and reaction time on PET conversion and TPA yield. PSSA exhibited increased hydrolysis kinetics relative to H₂SO₄ over the full range of conditions investigated. This improvement was attributed to increased surface wetting by the PSSA solutions combined with the adsorption of PSSA on the PET surface, which would increase the local concentration of Brønsted acid sites (H⁺) for hydrolysis.

4.6 Experimental

4.6.1 Materials

Poly (sodium 4-styrenesulfonate) (PSSS) with an average molecular weight of 70 kDa, terephthalic acid (TPA), ammonium hydroxide solution (30-33% NH₃ in H₂O), methyl sulfoxide-d₆, and deuterium oxide were all purchased from Sigma-Aldrich. Sulfuric acid (Certified ACS plus) was purchased from Fisher Scientific. Amberlyst[®]-15 was purchased from Alfa Aesar and was ground to a fine powder for the ion-exchange of PSSS to PSSA. PET pellets were generously donated by Alpek and were grounded and sieved to a powder in the diameter size range of 250 μm to 354 μm.

4.6.2 PSSA catalyst synthesis

PSSS was converted into the protonated form by ion exchange using a sulfonic resin, as reported elsewhere [376]. Briefly, 100 mL of PSSA (25 wt%) solution was added to the mixture of 120 g of grounded Amberlyst[®]-15 and 500 mL of DI water. Then, it was stirred at room temperature overnight. After ion exchange, the mixture was filtered to

separate the resin from the solution, and the PSSA solution was dried at 60°C to recover the PSSA. The recovered PSSA films were cut into small pieces and dried for another 6 h at 60°C to minimize the water content. Thermogravimetric analysis (TGA) of the recovered PSSA indicated that the synthesized PSSA had 4.2% water (**Figure 4-S1 in the Supplementary Material**). A complete ion exchange would generate a PSSA containing 5.4 mmol H⁺/g. As the titration results showed an acidity of 4.7 mmol H⁺/g, this indicated 87% completion of the ion exchange.

4.6.3 Titration measurements

Acid-base titration was performed to determine the proton concentration on PSSA. In a typical titration test, around 20 mg of PSSA was dissolved in 10 mL DI water. The solution was titrated against a 0.01 N NaOH solution standardized with potassium acid phthalate. To determine the end point, phenolphthalein was used as the indicator. Each titration was repeated three times.

4.6.4 PET hydrolysis reactions

For the PET hydrolysis reactions, 0.2 g of PET powder was placed in a 15-mL Ace pressure reactor equipped with a magnetic stirrer and 10 mL of 1, 2 or 4 M PSSA aqueous solutions. The solutions were prepared by dissolving PSSA in DI water at temperatures up to 50°C. The reactor was immersed in a preheated oil bath at 130, 140, and 150°C. The same reaction conditions were used for 1, 2, and 4 M H₂SO₄ solutions in order to maintain constant concentrations of catalyst. Every reaction time was an independent measurement and was repeated three times.

After a predefined time, the reaction was quenched by submerging the reactor in a cold-water bath, and the unreacted PET and TPA powders were recovered by filtration. The TPA product was separated from unreacted PET by dissolving the mixture in a 5 M NH_4OH solution [365]. The recovered TPA was compared with commercial TPA by Fourier-transform infrared spectroscopy (FTIR) and proton nuclear magnetic resonance (^1H NMR) analyses (**Figure 4-S2 and Figure 4-S3 in the Supplementary Material**). After that, PSSA was recovered for further uses by evaporating the filtrate solution. The recovered PSSA was washed several times with an excess of water to ensure the removal of EG and dried to remove water that would affect the mass of catalyst.

The PET conversion (%) was determined by **Equation 4-1**:

$$PET \text{ Conversion } (\%) = \left(\frac{m_{PET,i} - m_{PET,f}}{m_{PET,i}} \right) \cdot 100 \quad (4-1)$$

where $m_{PET,i}$ is the initial mass of PET (0.2 g), and $m_{PET,f}$ is the final mass of dried PET.

The molar yield of TPA (TPA yield (%)) was determined by **Equation 4-2**:

$$TPA \text{ Yield } (\%) = \left(\frac{m_{TPA}}{m_{PET,i}} \right) \left(\frac{MW_{PET}}{MW_{TPA}} \right) \cdot 100 \quad (4-2)$$

where m_{TPA} , MW_{PET} , and MW_{TPA} represent the mass of recovered TPA, molecular weight of PET ($192.2 \text{ g}\cdot\text{mol}^{-1}$), and molecular weight of TPA ($166.1 \text{ g}\cdot\text{mol}^{-1}$), respectively.

4.6.5 Characterization of recovered PSSA and TPA

FTIR and ^1H NMR were used to compare the structure of the recovered TPA with that of commercial TPA. Also, the as-synthesized PSSA and the recovered PSSA were

analyzed by FTIR, ^1H NMR, and ^{13}C NMR for structural comparison. For FTIR, the samples were mixed with KBr, pressed into thin pellets and analyzed in a Varian Excalibur Series FTIR spectrometer with microscope transmission mode in the range of 400 to 4000 cm^{-1} . ^1H NMR spectra were recorded in a Bruker Avance III spectrometer at 600 MHz. To do so, the TPA samples were dissolved in methyl sulfoxide- d_6 and the PSSA samples were dissolved in deuterium oxide.

4.6.6 Contact angle measurements

Contact angle measurements [384] were used to determine the relative wetting of the surface of PET films by PSSA and H_2SO_4 aqueous solutions with concentrations from 0.125 to 2 M at room temperature. PET films of 0.35 mm average thickness were processed in a HAAKE Rheomex Brabender single screw extruder for this study. The contact angle was measured using a Keyence VHX-600 digital microscope equipped with a camera in the reflection mode with a full-coaxial light stage. For a typical test, a droplet of PSSA or H_2SO_4 solution was placed on a PET film affixed to a flat glass substrate. An image of the droplet on the PET surface was captured to determine the contact angle. Each test was repeated at least six times by placing new droplets on a new film.

4.6.7 Ethyl acetate hydrolysis (Model System)

Briefly, 5 mL of a 5 wt% ethyl acetate solution was transferred to a 15-mL Ace pressure reactor followed by the addition of 5 mL of a 0.5 M H_2SO_4 solution. Then, the reactor was immersed in a silicon oil bath stirred at 600 rpm. Because of how fast the hydrolysis process occurs, the reaction was carried out for 1 h at temperatures ranging from 40 $^\circ\text{C}$ to 70 $^\circ\text{C}$. Upon completion, the reactor was immersed in crushed ice to stop the

reaction. To determine the extent of the reaction (production of acetic acid) and the activation energy, 2 mL of the reaction sample was titrated against a 0.1 N NaOH solution standardized with potassium hydrogen phthalate, and the H^+ content of the catalyst was subtracted from the total. For the sake of comparison, similar reactions were conducted using 5 mL of PSSA solutions with the same H^+ content as the H_2SO_4 solutions. To do so, it was taken into account that a 0.5 M H_2SO_4 solution dissociates mostly as H^+ and HSO_4^- (instead of 2H^+ and SO_4^{2-}) [385]. Finally, the activation energies of the hydrolysis of ethyl acetate with PSSA and H_2SO_4 were determined and compared.

4.7 Results and Discussion

4.7.1 Temperature effect on the reaction kinetics

As PSSA has been shown to be thermally stable at temperatures equal to or lower than 150°C , this work focused on studying the hydrolysis kinetics of PET at temperatures between 130°C and 150°C [379, 386-388]. **Figure 4-1** and **Figure 4-2** show the effect of the temperature on the reaction kinetics in terms of PET conversion and TPA yield obtained with 2 M solutions of PSSA and H_2SO_4 , respectively. Note that each point was an independent PET hydrolysis experiment and was run in triplicate, with the error bars indicating the standard deviation. The PET conversions and TPA yields follow similar trends for all systems studied. It should also be noted that the TPA yield was slightly lower than the PET conversion, particularly at lower conversion, likely due to the loss of TPA during the product recovery phase. Therefore, the TPA yield was used in fitting modeling to provide a conservative value for the rate constant for these systems.

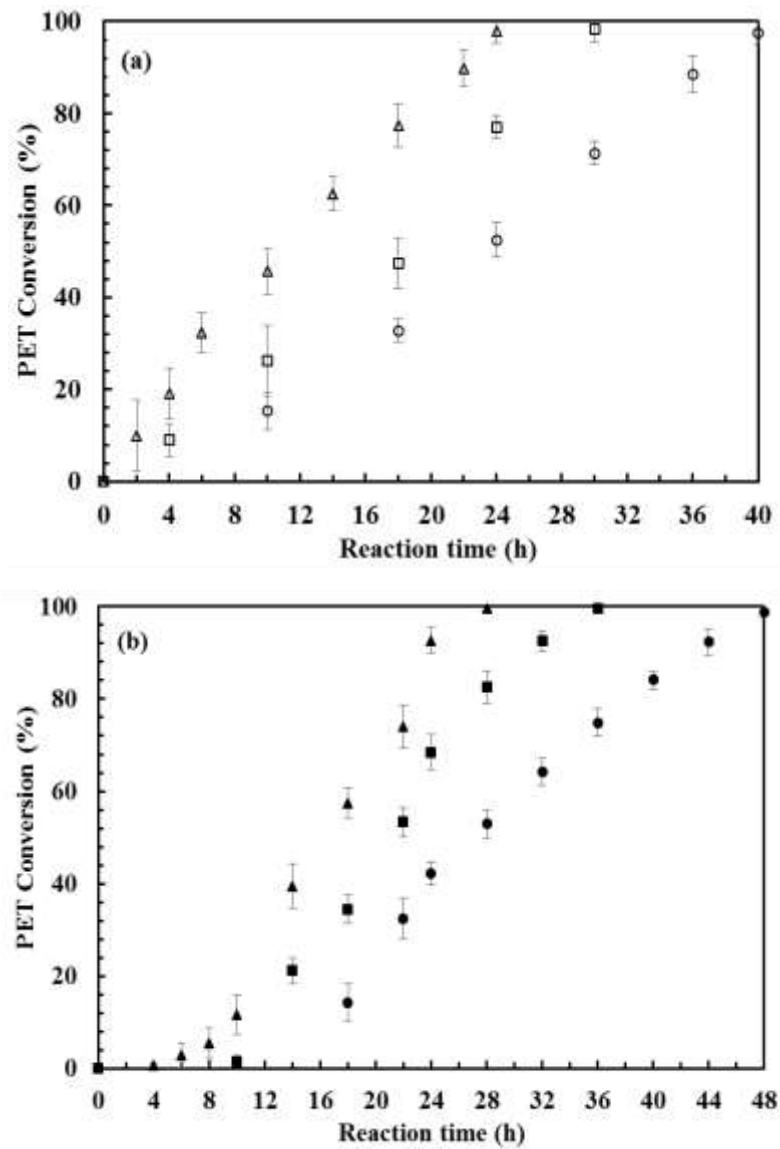


Figure 4-1: Reaction temperature effect on the PET conversion (%) with 2 M solutions of (a) PSSA at 150°C (Δ), 140°C (□), and 130°C (○), and (b) H₂SO₄ at 150°C (▲), 140°C (■), and 130°C (●).

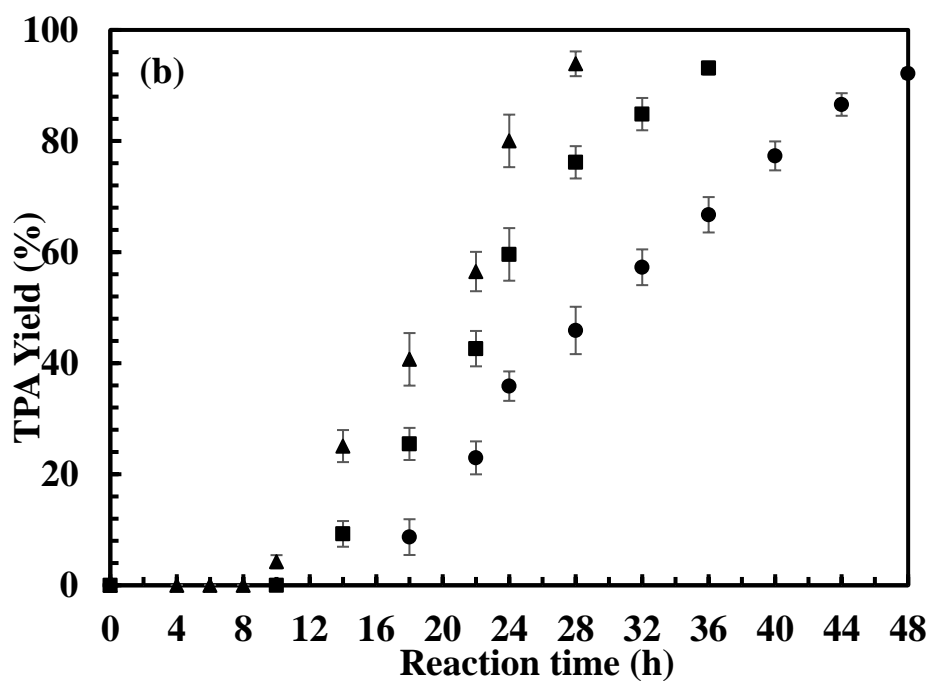
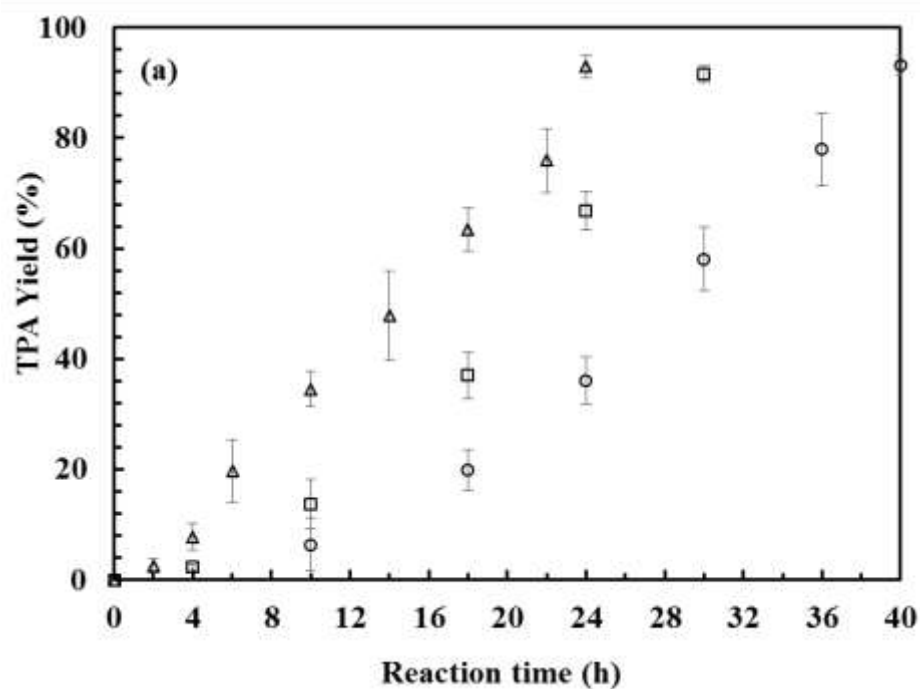


Figure 4-2: Reaction temperature effect on the TPA yield (%) for 2 M solutions of (a) PSSA at 150°C (Δ), 140°C (□), and 130°C (○), and (b) H₂SO₄ at 150°C (▲), 140°C (■), and 130°C (●).

As shown in **Figure 4-1b**, a significant induction period was observed for this reaction when using H₂SO₄ as the catalyst for all temperatures studied. This induction time has been attributed in the literature to the formation of cracks in the PET surface by the acid catalyst that facilitates access to the interior of the PET particles [365, 370, 371]. The induction time was much shorter for the 2 M PSSA solution and decreased with increasing reaction temperature for both catalysts. As expected, there was a decrease in the reaction rate with decreasing reaction temperature for both catalysts.

The shrinking-core model, reported by Mancini *et al.* [365], was applied to determine the rate constants and activation energies with PSSA and H₂SO₄ catalysts. In this model, it was assumed that the TPA produced during the hydrolysis reaction did not deposit on the PET surface because of continuous stirring during the reaction [365, 370, 371]. The final equation for the TPA yield as a function of the reaction time (t), density of spherical PET particles (ρ_{PET}), catalyst concentration ($[H^+]$), and the rate constant per unit surface area (k) is:

$$(1 - [TPA Yield]_{induction})^{\left(\frac{1}{3}\right)} - (1 - [TPA Yield]_t)^{\left(\frac{1}{3}\right)} = \left(\frac{k \cdot [H^+]}{\rho_{PET} \cdot r_i}\right)(t - t_{induction}) \quad (4-3)$$

Where $[TPA Yield]_{induction}$ and $t_{induction}$ are the amount of recovered TPA at the induction time and the required time to reach the linear part of the TPA yield vs t plot, respectively. $\left(\frac{k \cdot [H^+]}{\rho_{PET} \cdot r_i}\right)$ is the apparent reaction rate constant (time⁻¹ units), also denoted as K, with k as the specific reaction rate constant, $[H^+]$ as the catalyst concentration (H⁺), ρ_{PET} as the density of PET, and r_i indicating the initial size (radius) of the PET particles. The induction time was used to allow for better comparison between systems with broad

differences in onset of PET degradation. **Equation 4-3** was used together with TPA yield data in **Figure 4-2** to calculate the apparent reaction rate constant (K) with PSSA and H₂SO₄ catalysts at each reaction temperature. Then, the specific rate constants (k) were calculated from the apparent rate constants using the density of PET (1.38 g/cm³) and an average radius of 0.015 cm for the PET particles. **Table 4-1** presents the k values obtained from the hydrolysis reaction with 2 M solutions of PSSA and H₂SO₄. For all cases, the k values obtained with PSSA were slightly higher than those with H₂SO₄, indicating the higher activity of PSSA. The Arrhenius equation (**Equation 4-4**) was used to determine the activation energies with PSSA and H₂SO₄.

$$\ln(k) = \ln(k_0) - \frac{E_a}{RT} \quad (4-4)$$

Where k is the specific reaction rate constant, k₀ is the pre-exponential factor, E_a is the activation energy, R is the universal gas constant, and T is the reaction temperature. **Figure 4-3** shows the fit of the model to the data from the hydrolysis reactions at 150°C with 2 M solutions of PSSA and H₂SO₄. **Figure 4-4** shows the Arrhenius plots obtained with 2 M PSSA and 2 M H₂SO₄ as catalysts. The activation energies obtained with PSSA and H₂SO₄ were 24.6 kJ·mol⁻¹ and 29.1 kJ·mol⁻¹, respectively. Activation energies for PET acid hydrolysis have been reported in the range between 57 kJ·mol⁻¹ with aqueous solutions of phosphoric and sulfuric acid to 101 kJ·mol⁻¹ for aqueous solutions of hydrochloric acid and nitric acid [366, 372, 389]. The lower activation energies here obtained may be due to the continuous stirring of the reaction systems during the hydrolysis of PET. The slightly lower activation energy obtained with PSSA is consistent with the increased activity relative to H₂SO₄.

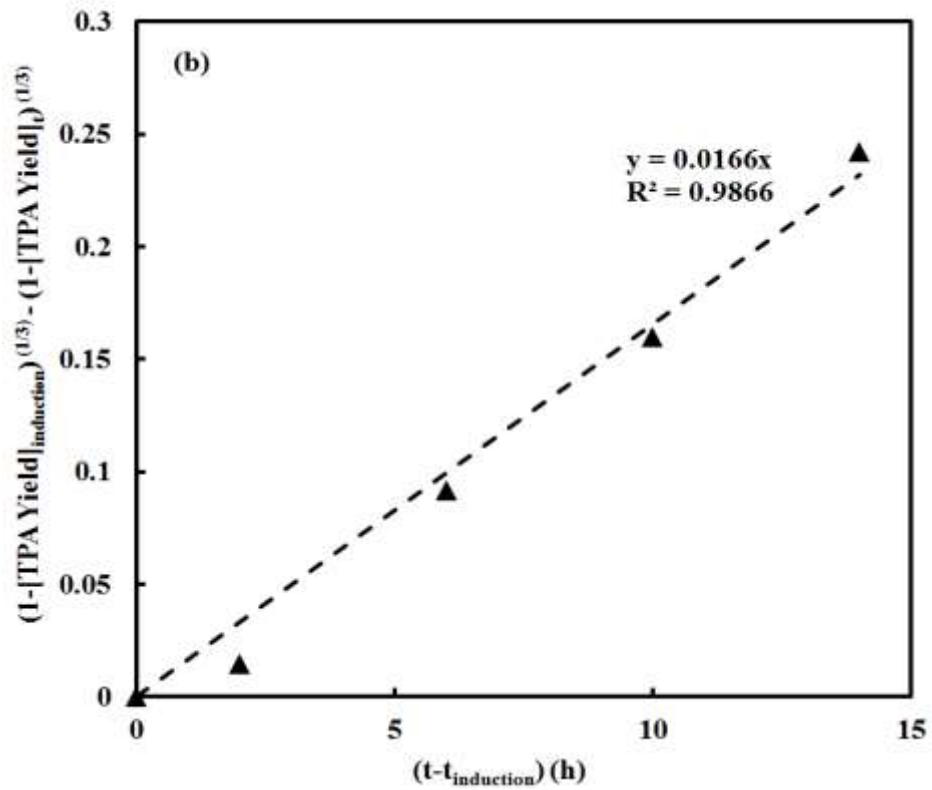
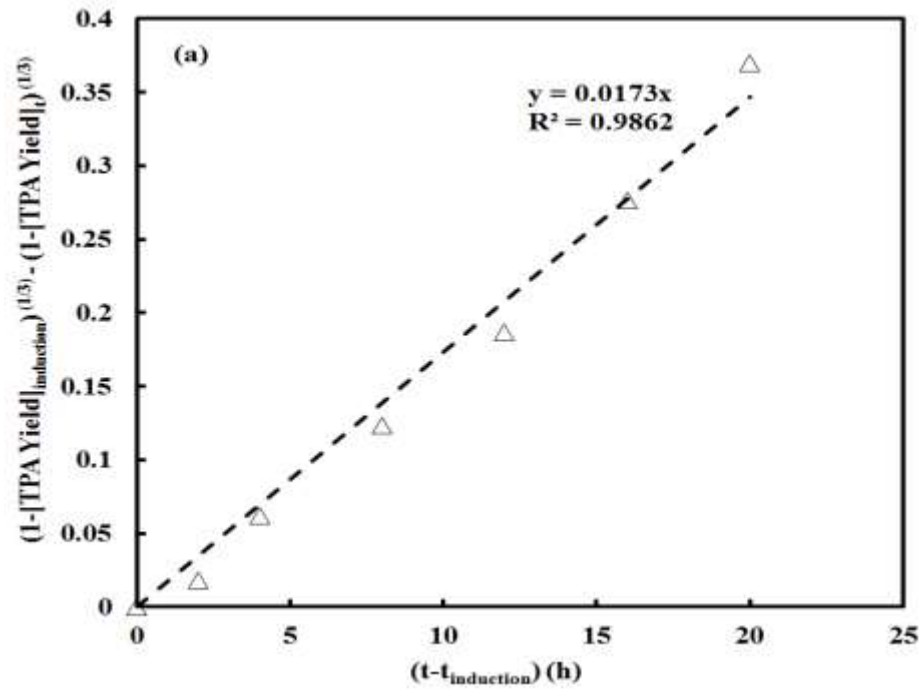


Figure 4-3: Shrinking-core model fitting to the results obtained with 2 M solutions of (a)

PSSA (Δ), and (b) H_2SO_4 (\blacktriangle) at $T_{\text{reaction}}=150^\circ\text{C}$.

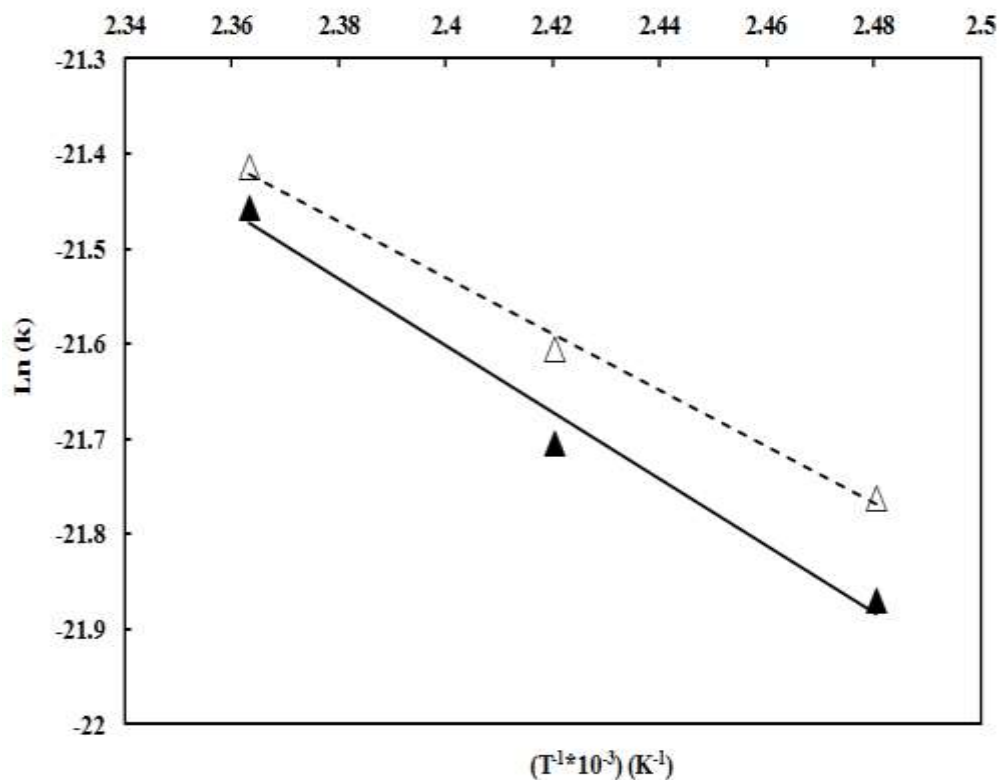


Figure 4-4: Arrhenius plots obtained from the hydrolysis of PET with 2 M solutions of (a) PSSA (Δ), and (b) H_2SO_4 (\blacktriangle).

Table 4-1: Specific reaction rate constants (k) obtained with 2 M aqueous solutions of PSSA and H_2SO_4 as a function of the reaction temperature.

	2 M PSSA	2 M H_2SO_4
T ($^{\circ}\text{C}$)	$k \text{ (kg}_{\text{PET}} \cdot \text{m} \cdot (\text{mol H}^+)^{-1} \cdot \text{s}^{-1}) \cdot (10^{10})$	$k \text{ (kg}_{\text{PET}} \cdot \text{m} \cdot (\text{mol H}^+)^{-1} \cdot \text{s}^{-1}) \cdot (10^{10})$
150	5.01	4.80
140	4.14	3.75
130	3.54	3.18

4.7.2 Catalyst concentration effect on acid hydrolysis reaction

Figure 4-5 and **Figure 4-6** show the PET conversions and TPA yields obtained with different catalyst concentrations at 150°C. As seen in these figures, PET hydrolyzed more rapidly when using PSSA solutions than with H₂SO₄ for all catalyst concentrations studied. As expected, there was an increase in the reaction rate at higher catalyst concentration along with a decrease in the induction time for PET depolymerization. When using 1 M, 2 M, and 4 M solutions of PSSA, more than 90% PET conversion and TPA yield were achieved in 30, 24, and 16 h, respectively, while it took 36, and 28, and 18 h when using the same concentration of H₂SO₄. The difference in time required to achieve a specific conversion was primarily due to the longer induction times when using H₂SO₄ particularly at lower concentrations. **Table 4-2** shows the apparent rate constant obtained by using the shrinking-core model at the reaction temperature of 150°C. As expected, the apparent rate constants (K) were higher for higher catalyst concentrations, being these similar for the two catalysts studied.

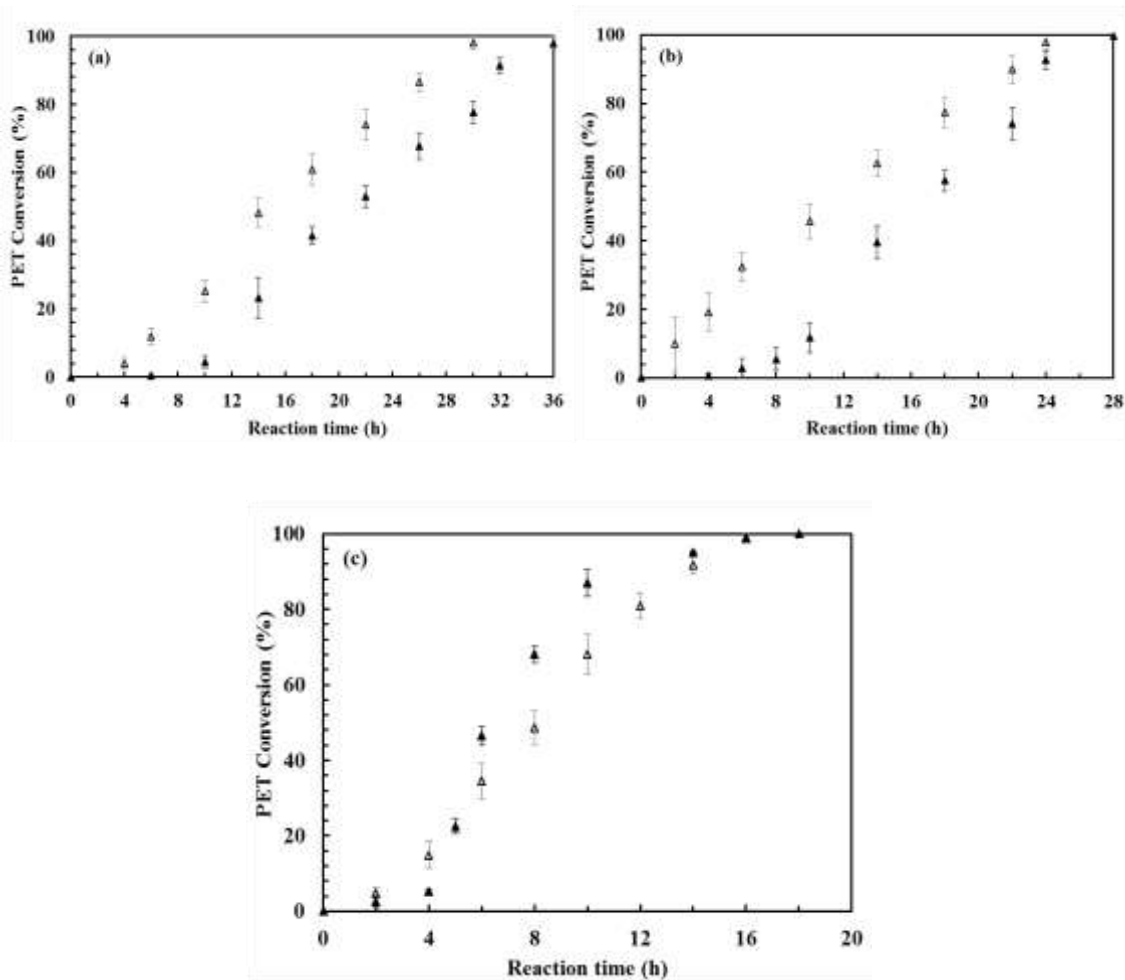


Figure 4-5: PET conversions (%) obtained with (a) 1 M, (b) 2 M, and (c) 4 M solutions of PSSA (Δ) and H_2SO_4 (\blacktriangle) at $T_{\text{reaction}} = 150^\circ C$.

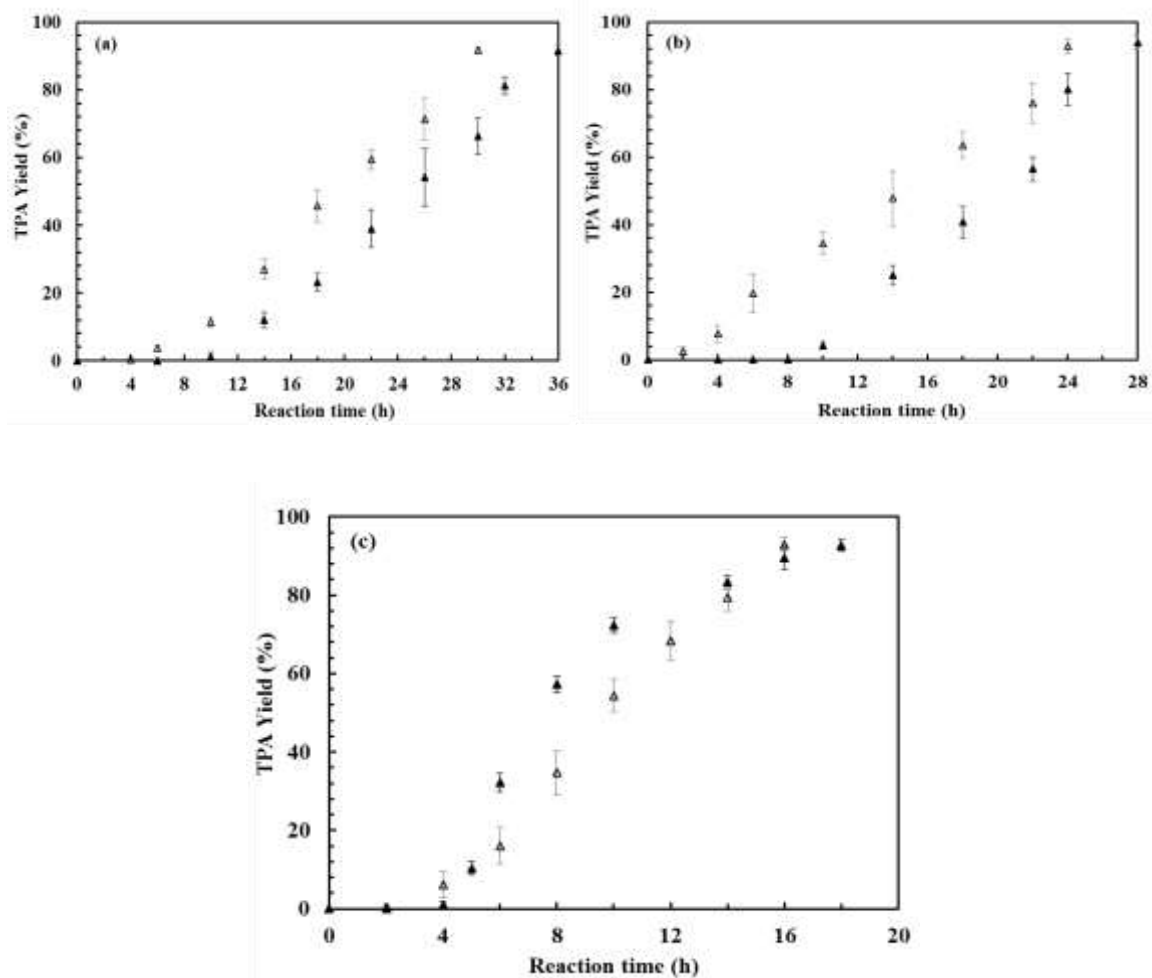


Figure 4-6: TPA yields (%) obtained with (a) 1 M, (b) 2 M, and (c) 4 M solutions of PSSA (Δ) and H₂SO₄ (\blacktriangle) at T_{reaction}= 150°C.

Table 4-2: Apparent reaction rate constants (K) vs catalyst concentration (H^+), based on the shrinking-core model and TPA recovery with PSSA and H_2SO_4 catalysts at $T_{\text{reaction}}=150^\circ\text{C}$.

$T_{\text{reaction}}= 150^\circ\text{C}$	PSSA	H_2SO_4
Catalyst Concentration (M)	K (h^{-1}) $\cdot(10^2)$	K (h^{-1}) $\cdot(10^2)$
1	1.52	1.38
2	1.73	1.66
4	3.66	3.72

4.7.3 Hydrolysis of ethyl acetate (Model System)

Figure 4-7 shows the Arrhenius plot obtained for the hydrolysis of ethyl acetate when using 0.5 M H_2SO_4 and 0.5 M PSSA as catalysts. As can be seen in **Figure 4-7**, the activation energy obtained with H_2SO_4 ($39.6 \text{ kJ}\cdot\text{mol}^{-1}$) was considerably lower than that with PSSA ($53.8 \text{ kJ}\cdot\text{mol}^{-1}$), which shows a faster hydrolysis rate in the presence of H_2SO_4 . These results are consistent with those in the literature, in which the activation energies for the hydrolysis of ethyl acetate range between $30\text{-}70 \text{ kJ}\cdot\text{mol}^{-1}$ [390-392]. As H_2SO_4 is a mineral acid, all protons are readily available for the hydrolysis of ethyl acetate. In contrast, due to the nature of PSSA, there might be some active sites not exposed to the reactants, thereby reducing the catalytic activity. A similar performance was reported in the literature for the acid-catalyzed methanolysis of tributyrin, in which the authors used H_2SO_4 , PSSA, and solid sulfonic resins, and concluded that the activity of PSSA was lower than that of a pure homogeneous catalyst (H_2SO_4) but higher than that of heterogeneous catalysts

(sulfonic resins), being this attributed to the accessibility of the reactants to the Brønsted acid sites [376]. Even when H₂SO₄ showed to be more active than PSSA in the hydrolysis of ethyl acetate, the opposite was observed in the case of the hydrolysis of PET (**Figure 4-4** and **Figure 4-7**), which might indicate the occurrence of an additional important mechanism at the PET surface. Interestingly, while **Figure 4-7** shows that the activity of PSSA and H₂SO₄ in the hydrolysis of ethyl acetate are closer at lower temperatures (130°C), this behavior was reversed in the case of the hydrolysis of PET, with the activities becoming closer at higher temperatures (150°C). It is hypothesized that as the temperature increases, the solubility of PSSA in water decreases, thus increasing the interaction of PSSA with the surface of PET and improving the hydrolysis rate.

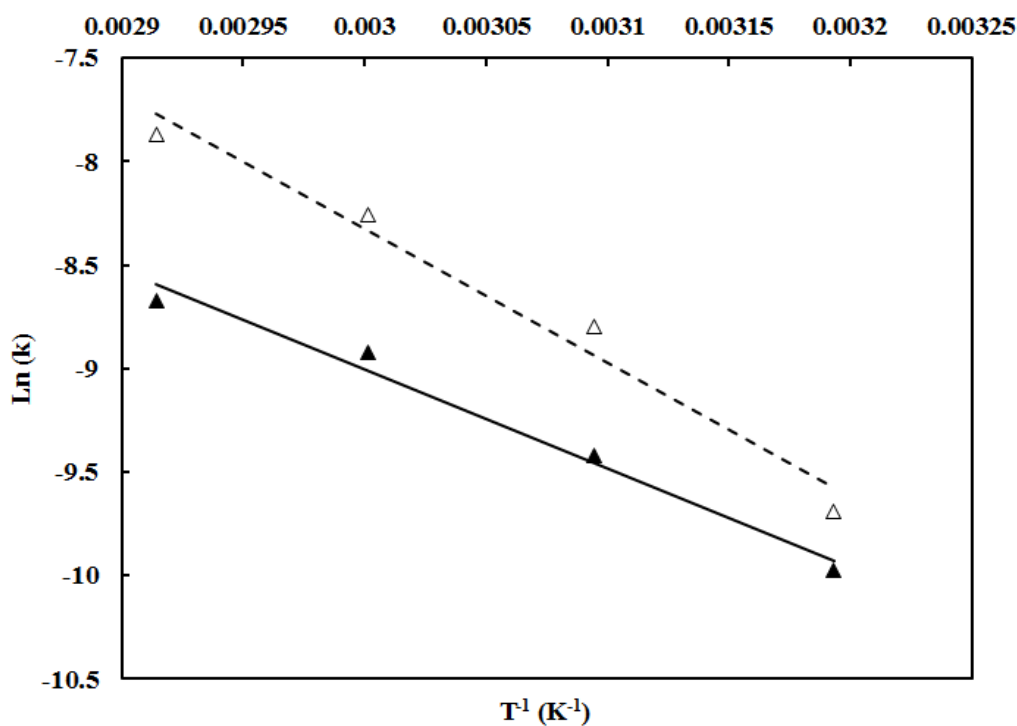


Figure 4-7: Arrhenius plots obtained from the hydrolysis of ethyl acetate with (a) PSSA (Δ), and (b) H₂SO₄ (\blacktriangle).

4.7.4 Mechanism for the acid hydrolysis of PET

In the acid hydrolysis of PET, protons (Brønsted acid sites) attack the polymer chains on the surface of the PET particles, resulting in a layer-by-layer reaction with no reaction occurring in the aqueous media. Since this reaction occurs at the polymer surface, any hydrophobic interactions between the catalyst and the PET particles could affect the reaction rate. The importance of hydrophobic interactions has been reported in the literature for acid-catalyzed reactions, such as the hydrolysis of cellulose [375] or acetalization reactions [393, 394], and for the enzymatic hydrolysis of esters [395, 396]. Specifically, these studies found that increasing the interaction of the catalyst with the surface resulted in an increased reaction rate.

To our knowledge, this is the first study that focuses on the hydrophobicity effect on the hydrolysis of PET using a recoverable acid catalyst. As noted above, PSSA exhibited a higher activity for the hydrolysis of PET than H₂SO₄, particularly at higher concentrations. This difference can be attributed to a combination of improved surface wetting of PET by PSSA and the adsorption of PSSA onto the PET surface. Contact angle measurements with PSSA and H₂SO₄ aqueous solutions on the PET surface were used to evaluate the interaction between PSSA and the hydrophobic surface [397]. **Figure 4-8** shows images of droplets of 0.5 M, 1 M, and 2 M aqueous solutions of PSSA and H₂SO₄ on the surface of PET films.

As seen in **Figure 4-8**, the droplets of PSSA solutions exhibited greater wetting of the PET surface than the H₂SO₄ solutions, particularly at higher concentrations. This is consistent with literature reports on PSSS wetting an alumina surface due to the

hydrophobic nature of the polystyrene backbone and improvements in the configurational entropy of PSSS that drives the surface adsorption [398]. This adsorption is dependent upon the nature of the surface, the concentration of PSSA, and the configuration of PSSA in solution. Additionally, this will lead into a higher effective local concentration of Brønsted acid sites in the vicinity of the PET surface relative to H_2SO_4 at a given solution concentration. The increased wetting by PSSA solutions is reflected in a decrease in the contact angle with increasing concentrations, as shown in **Figure 4-9**. While the contact angle for H_2SO_4 solutions with different concentrations ranged between 78 and 86 degrees, the contact angles with PSSA solutions were considerably lower, particularly at higher molarities.

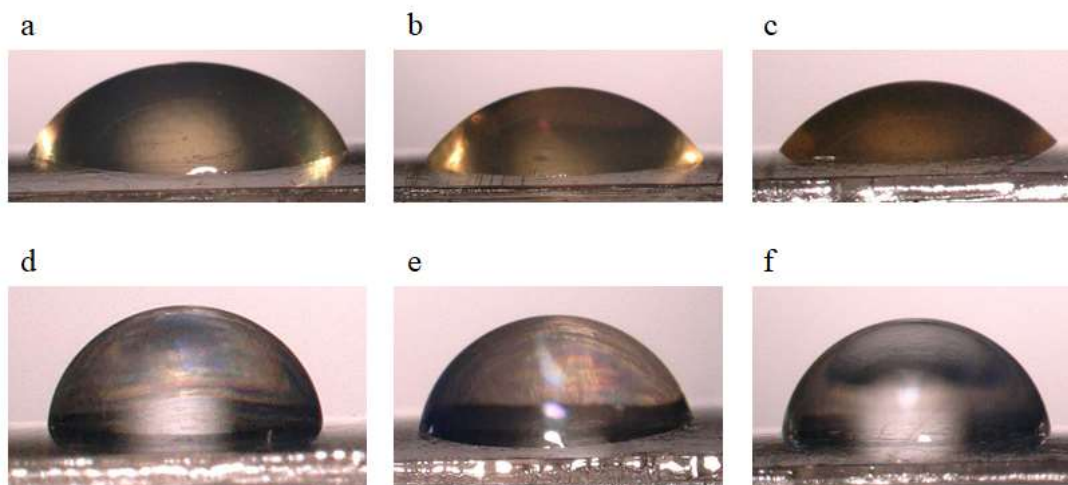


Figure 4-8: (a-c) 0.5 M, 1 M, and 2 M solutions of PSSA on the PET surface, respectively, and (d-f) 0.5 M, 1 M, and 2 M solutions of H_2SO_4 on the PET surface, respectively.

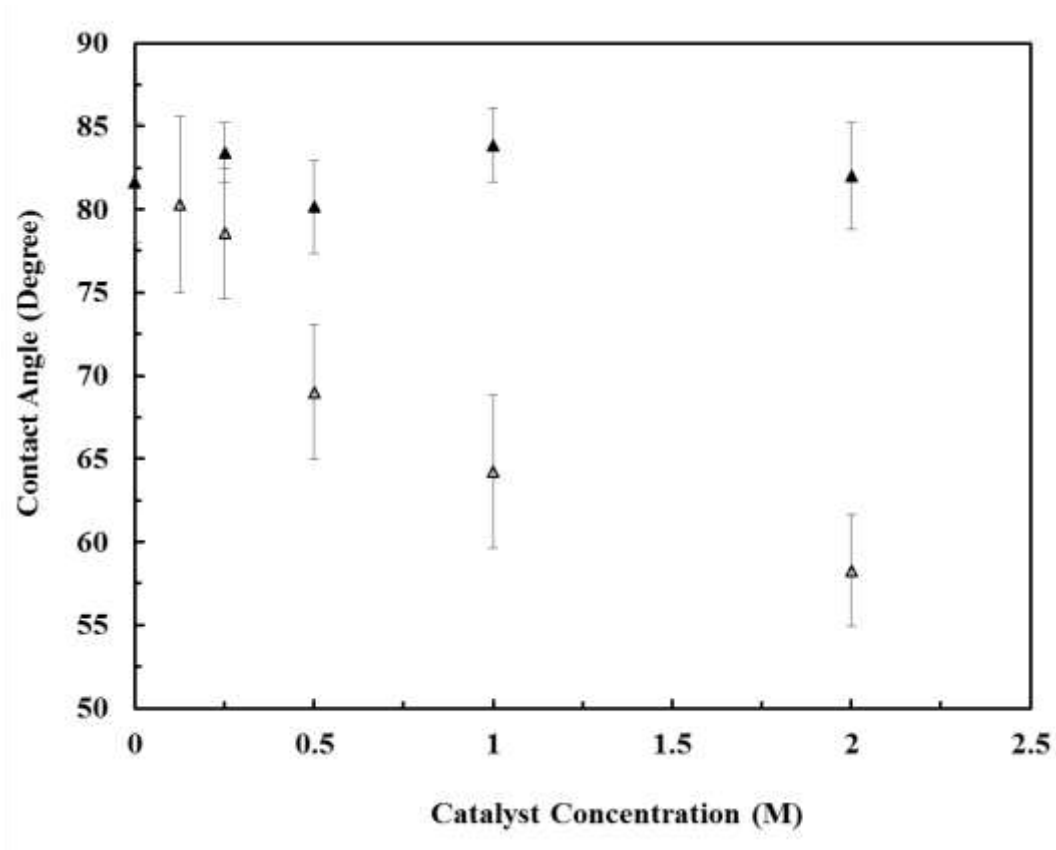


Figure 4-9: Contact angle measurements obtained with different concentrations of PSSA (Δ) and H₂SO₄ (▲) aqueous solutions on the PET surface.

4.7.5 Reutilization experiments with PSSA catalyst

PSSA was recovered by evaporation from the filtrate after 14 h of reaction at 150°C with a 2 M solution of PSSA to examine its reusability for acid hydrolysis of PET. Interestingly, the structure of the PSSA catalyst showed to be constant after five catalytic cycles (Figure 4-S4 to Figure 4-S6 in the Supplementary Material). Figure 4-10 presents the reutilization results obtained after five cycles with a 2 M solution of PSSA catalyst at 150°C for 14 h, including PET conversions and the TPA yields. As can be seen in Figure 4-10, the PSSA maintained its activity during five cycles without significant loss

of activity. **Figure 4-S7** shows the PSSA recovery yield (% of mass recovered) after every reaction round, which was close to 100% in all cases. Additionally, the acidity of the recovered PSSA was evaluated after every cycle by titration with a 0.01 N NaOH solution. The titration results (**Figure 4-11**) confirmed that PSSA maintained the number of Brønsted acid sites after every reaction cycle.

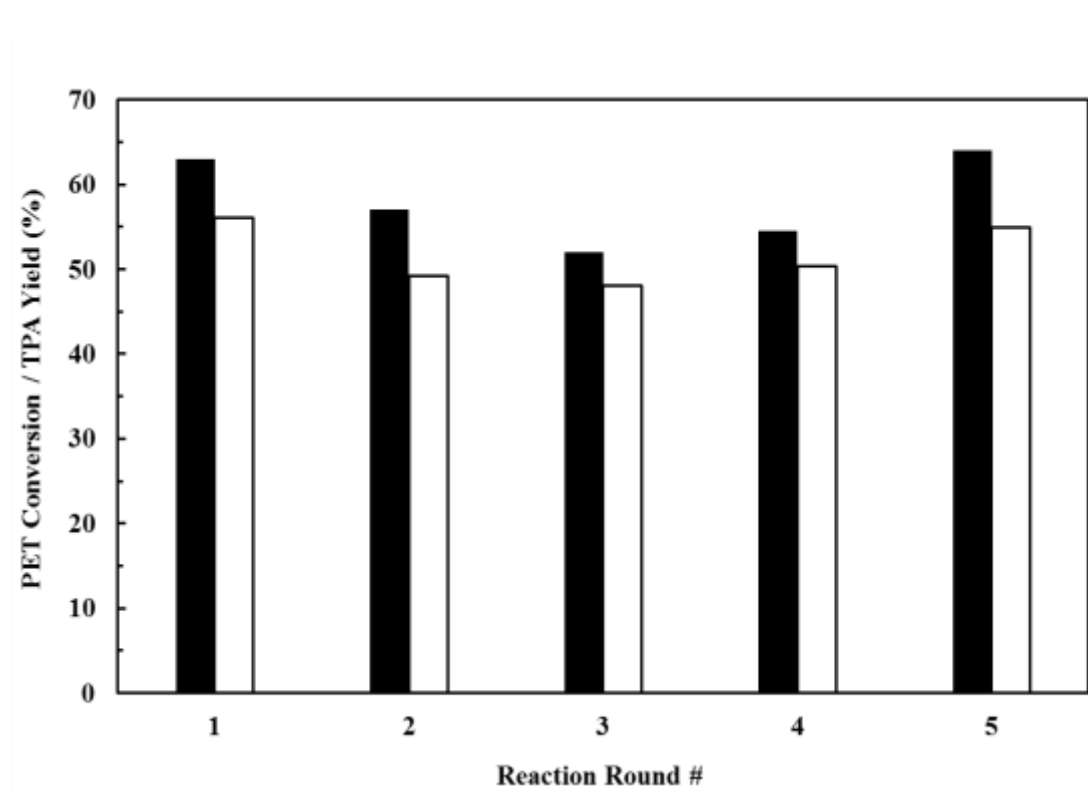


Figure 4-10: Reutilization results obtained with a 2 M solution of PSSA: PET conversion (■) and TPA yield (□). Every reaction was run at 150°C for 14 h.

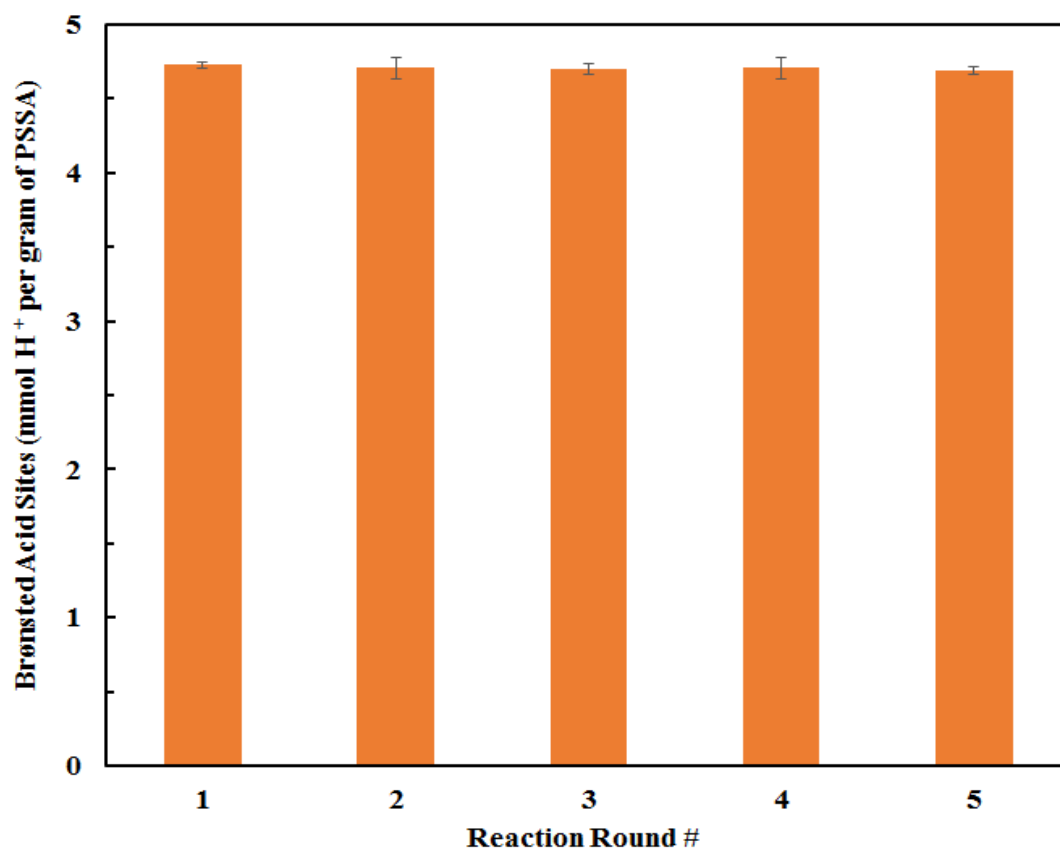


Figure 4-11: Titration results obtained from the recovered PSSA after every reaction cycle.

4.8 Conclusions

Poly (4-styrenesulfonic acid) (PSSA) was investigated as a reusable and recoverable catalyst for the acid hydrolysis of PET. The catalytic activity of PSSA was compared with that of a conventional mineral acid catalyst (H₂SO₄) for the depolymerization of PET. The PSSA systems exhibited much shorter induction times and slightly higher activity than H₂SO₄ at similar reaction conditions.

The shrinking-core model provided a good fit to the kinetics data and allowed the determination of the specific reaction rate constants and the activation energies. While hydrolysis studies of a small model molecule (ethyl acetate) showed a lower activation energy with H₂SO₄ (39.6 *vs* 53.8 kJ·mol⁻¹ with PSSA), PSSA was more active (24.6 kJ·mol⁻¹) than H₂SO₄ (29.1 kJ·mol⁻¹) in the hydrolysis of PET

The increased reaction rate and the reduction of the induction time with PSSA was attributed to improved surface wetting combined with adsorption of PSSA on PET surface because of the hydrophobic region of PSSA. This improved wetting was confirmed by contact angle measurements of PSSA and H₂SO₄ aqueous solutions on PET surfaces. While the contact angle of the H₂SO₄ solutions remained constant and near the value for water, there was a decrease in the contact angle for PSSA solutions with increasing concentrations. These lower contact angles with the PSSA solutions are consistent with reports in the literature and are attributed to the hydrophobic nature of the polystyrene backbone with improved interaction with PET particles. This should lead into a higher local concentration of acid sites near the PET surface, and consequently, higher activity in the hydrolysis reaction. Further, the reutilization and titration results confirmed that PSSA is a reusable and recoverable catalyst, which is another advantage from an environmental point of view with respect to H₂SO₄.

4.9 Acknowledgements

The authors would like to acknowledge Alpek for providing the PET pellets for this study. The authors are also thankful to the Polymer Institute and the Polyester and Barrier Consortium at the University of Toledo for providing the PET films for contact angle

measurements and support for this project, respectively. We are also grateful to Dr. Yong-Wah Kim from the Instrumentation Center at the University of Toledo for his help recording the ^1H NMR spectra and to G. Alba for the design of the graphical abstract.

4.10 Supplementary Material

4.10.1 Water content in the as-synthesized (Fresh) PSSA

Thermogravimetric analysis (**Figure 4-S1**) shows the amount of water in the fresh PSSA.

The amount of water was determined by the first loss of weight and showed to be of 4.2%.

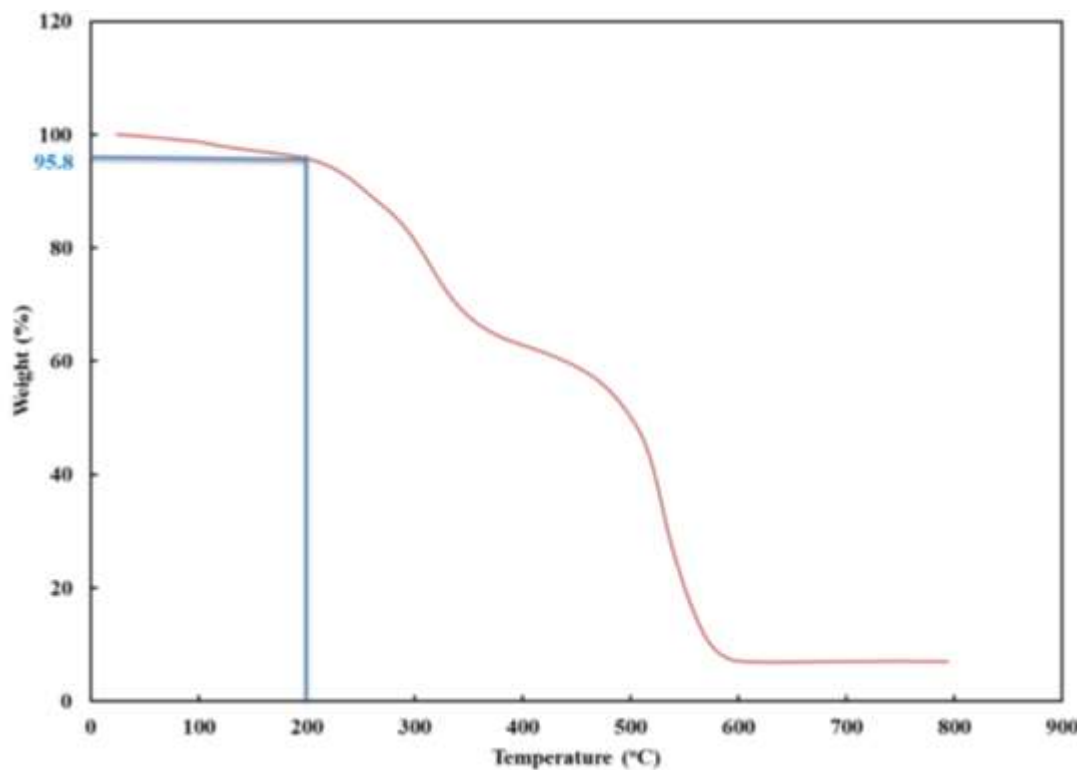


Figure 4-S1. TGA analysis of fresh PSSA.

4.10.2 Confirmation of TPA structure

FTIR and ^1H NMR analyses of the recovered TPA were compared with the commercial TPA to confirm the recovered TPA purity. As it can be seen in **Figure 4-S2**, the characteristic bands in the FTIR spectra for recovered and commercial TPA are similar. Aromatic ring, carbonyl group, and carboxylic group characteristic bands are observable at 1574-1425, 1685, and 2500-3000 cm^{-1} , respectively. **Figure 4-S3** shows the ^1H NMR spectra obtained with commercial TPA and TPA recovered from the PET hydrolysis with PSSA as the catalyst. Both spectra look very similar. The 8-ppm peak relates to the hydrogen in the aromatic ring, and the band close to 13 ppm is assigned to the hydroxyl groups of the carboxylic acid in the TPA structure. The short peak at 2.5 ppm corresponds to the reference solvent, methyl sulfoxide- d_6 . Therefore, the structure of the recovered TPA was confirmed by FTIR and ^1H NMR and there is no evidence of PET or PET oligomer in the TPA product.

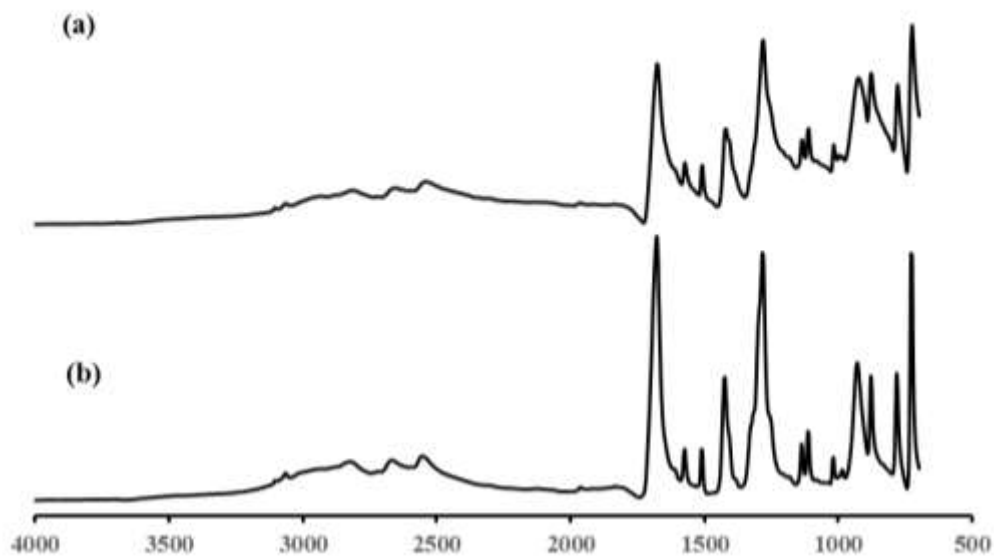
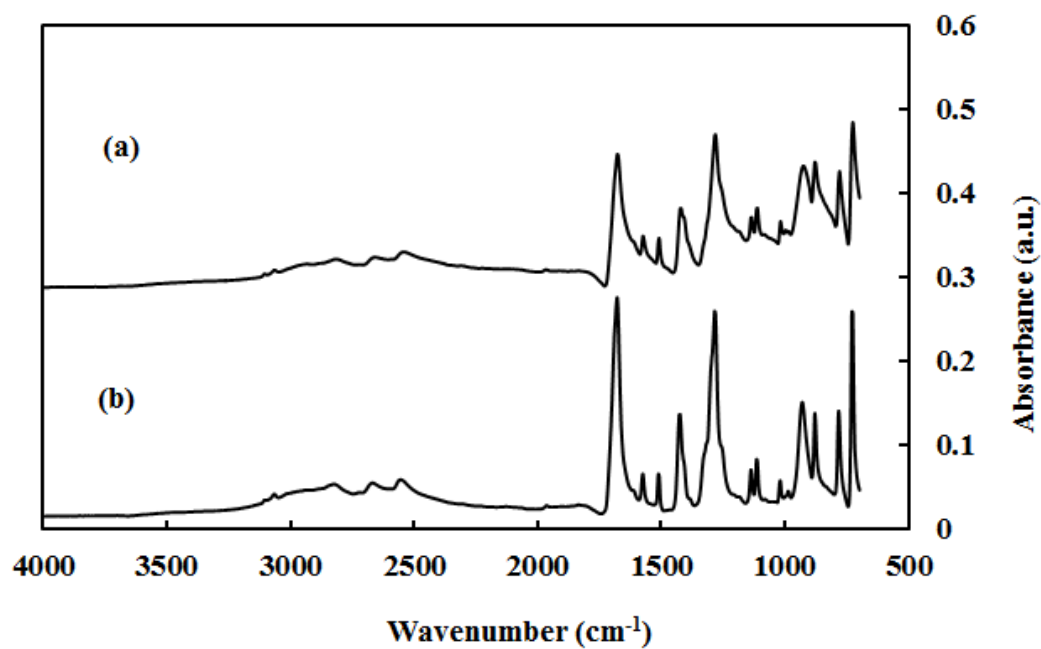


Figure 4-S2. FTIR spectra of (a) commercial TPA and (b) recovered TPA.

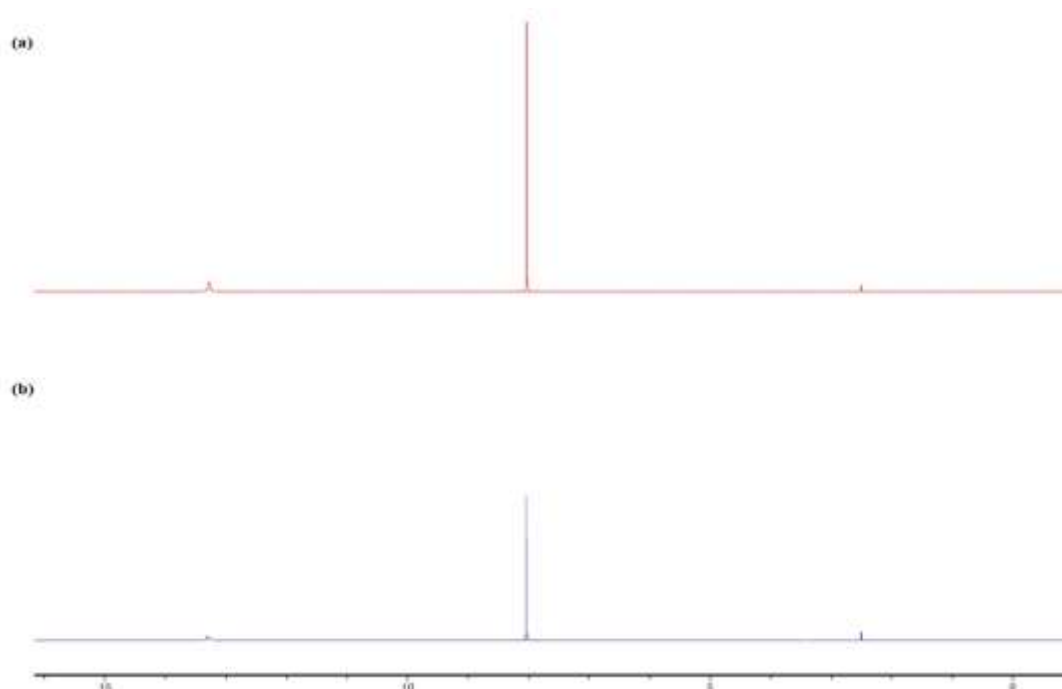


Figure 4-S3. ^1H -NMR spectra of (a) commercial TPA and (b) recovered TPA.

4.10.3 Confirmation of PSSA structure

Figure 4-S4 shows the FTIR spectra obtained with fresh PSSA and recovered PSSA. The sharp band at 1001 cm^{-1} refers to the aromatic ring in-plane deformation. Other major bands at 773 , 1350 , and 1597 cm^{-1} are associated to the carbon-hydrogen single bond wagging, oxygen-sulfur-oxygen double bond in $-\text{SO}_3\text{H}$, and carbon-carbon single bond in the aromatic ring, respectively [399-402]. **Figure 4-S5** and **Figure 4-S6** show the ^1H -NMR and ^{13}C -NMR spectra of recovered PSSA, respectively. For ^1H -NMR, the featured peaks at 1.36 (signal A), 6.56 (signal B), 7.05 (signal C), and 7.47 (signal D) ppm were previously reported in the literature for PSSA [376]. For ^{13}C -NMR, the featured peaks at 40 (signal A), 130 (signal B), 140 (signal C) and 150 (signal D) ppm were also previously reported in the literature for PSSA [376, 399]. Thus, both ^1H -NMR and ^{13}C -NMR spectra confirmed

that there were not significant changes in the structure of PSSA during the hydrolysis of PET.

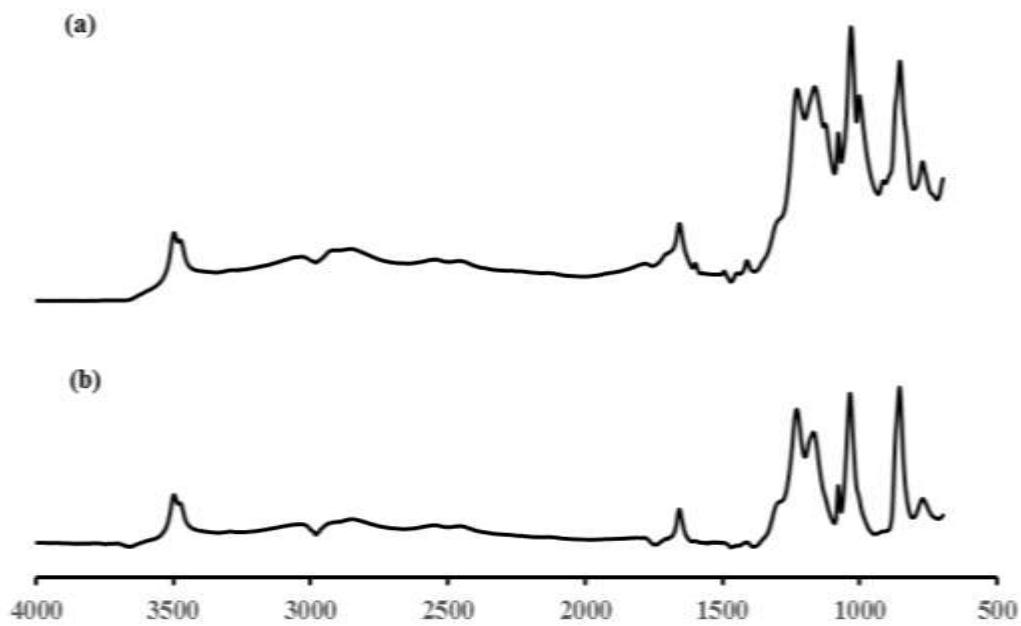
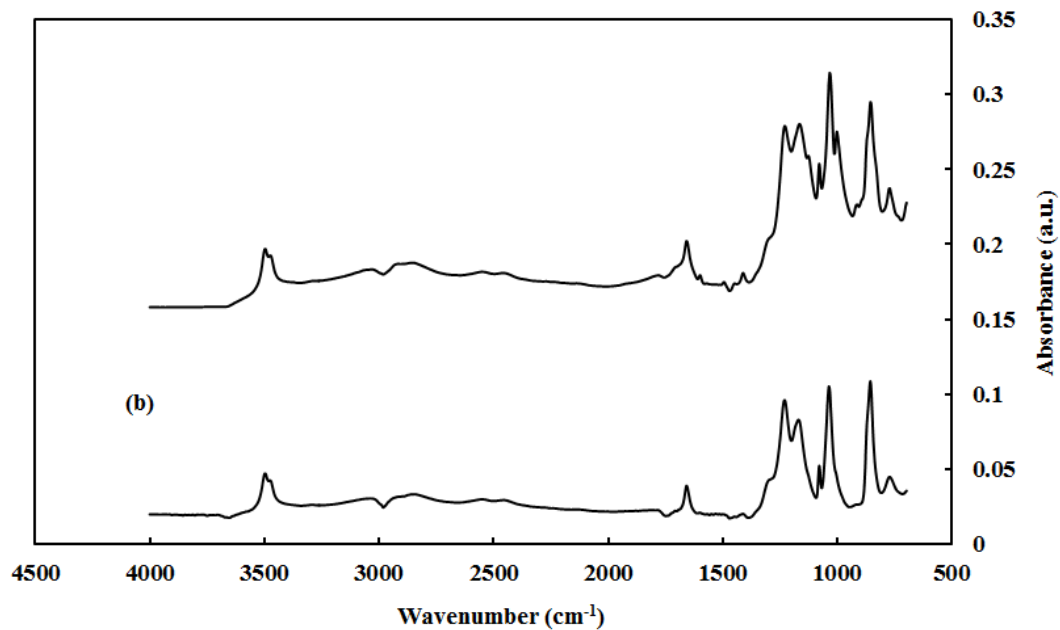


Figure 4-S4. FTIR spectra of (a) fresh PSSA and (b) recycled PSSA.

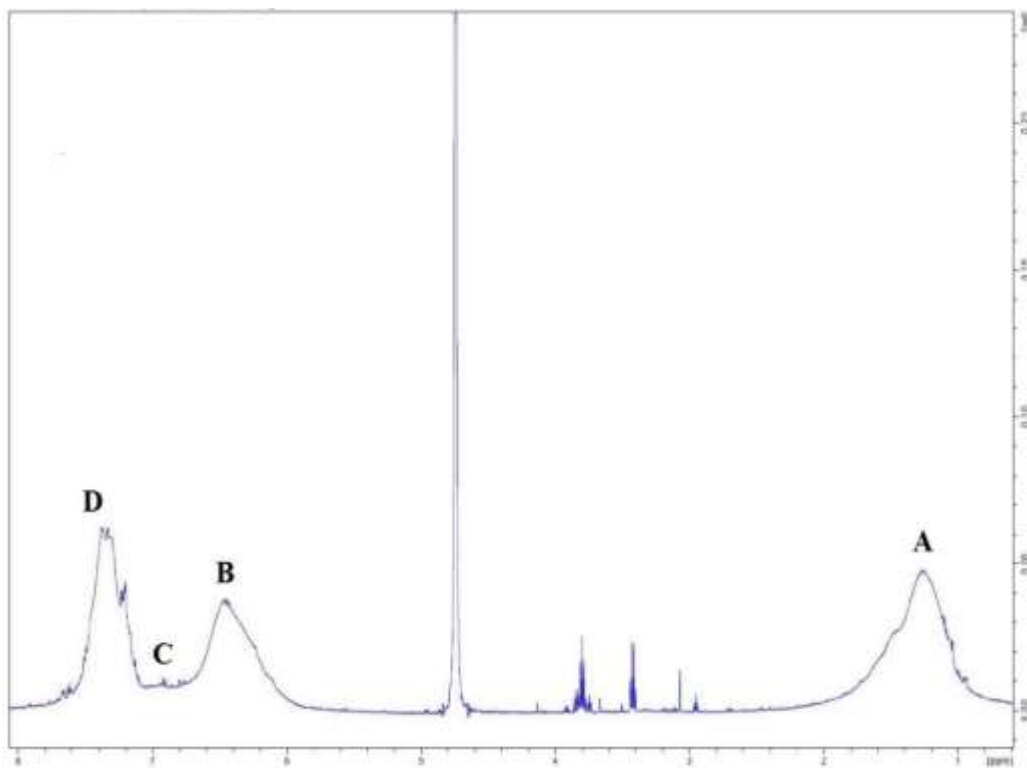


Figure 4-S5. ^1H -NMR spectra of recovered PSSA.

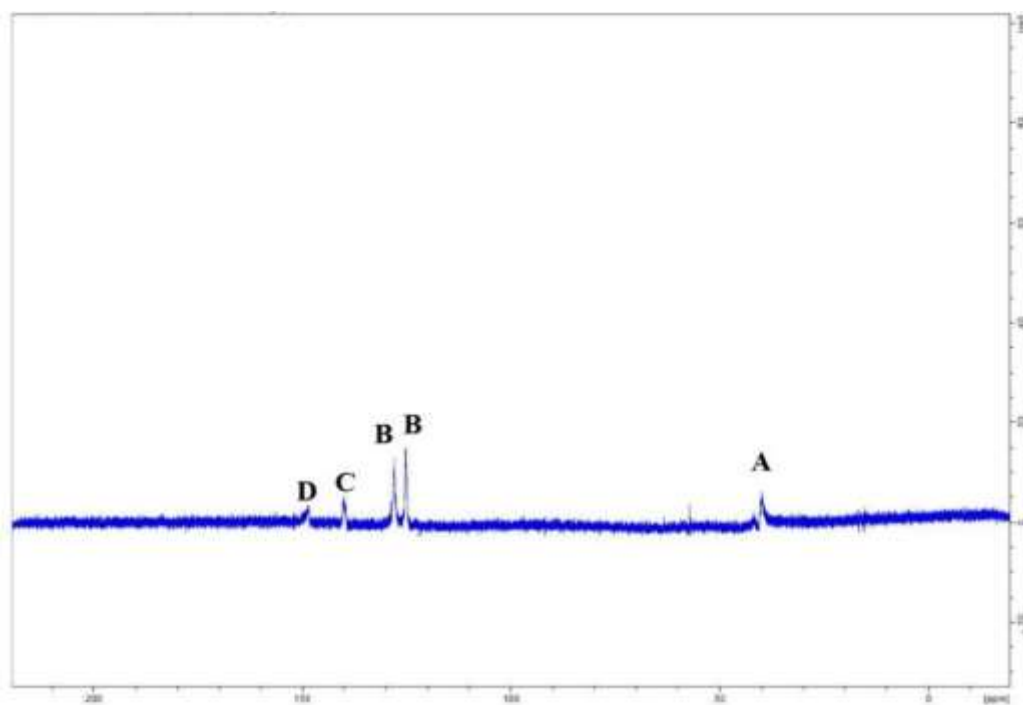


Figure 4-S6. ^{13}C -NMR spectra of recovered PSSA.

4.10.4 PSSA recovery yield

After conducting the hydrolysis of PET with 2 M PSSA solution at 150 °C for 14 h, PSSA, unreacted PET, and produced TPA were recovered as described in the main document. **Figure 4-S7** shows the high yield of PSSA recovered after five catalytic cycles, being this always close to 100%. As small samples of PSSA were taken after every reaction to run for titration, in order to keep the same reaction conditions, the mass of PET and DI water were adjusted to accommodate the slight drop of PSSA mass (due to handling + sample for titration).

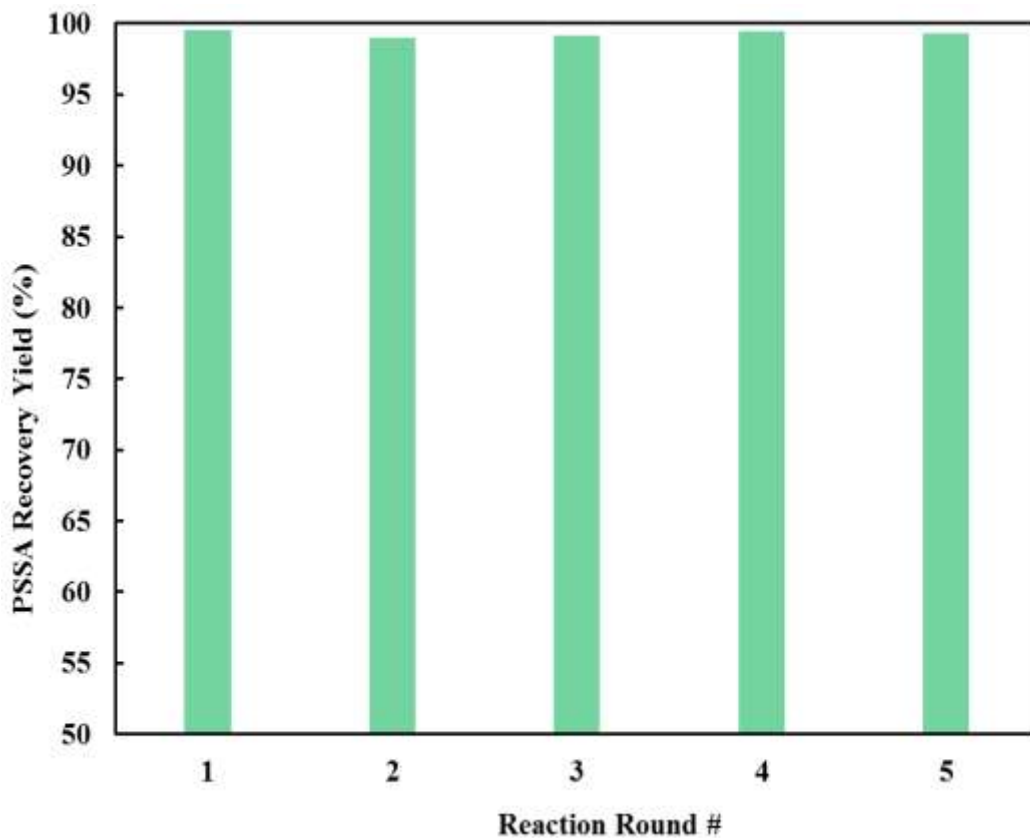


Figure 4-S7. PSSA recovery yield (% of mass recovered) after every reaction round (2 M solution of PSSA, 150 °C, and 14 h).

Chapter 5

Aryl sulfonic acid catalysts: Effect of pendant group structure on activity in hydrolysis of polyethylene terephthalate (PET)

This chapter is reproduced from an article published in Journal of Applied Polymer Science, Wiley ¹.

Hossein Abedsoltan^{*, 2} and Maria R. Coleman^{*, **, 3}.

“Aryl sulfonic acid catalysts: Effect of pendant group structure on activity in hydrolysis of polyethylene terephthalate (PET)”, Journal of Applied Polymer Science 2022, e52451.

* Department of Chemical Engineering, The University of Toledo, Toledo, OH, 43606, United States.

**Polymer Institute, University of Toledo, Toledo, OH, 43606, United States.

¹ Reprinted with the permission of Journal of Applied Polymer Science, Wiley.

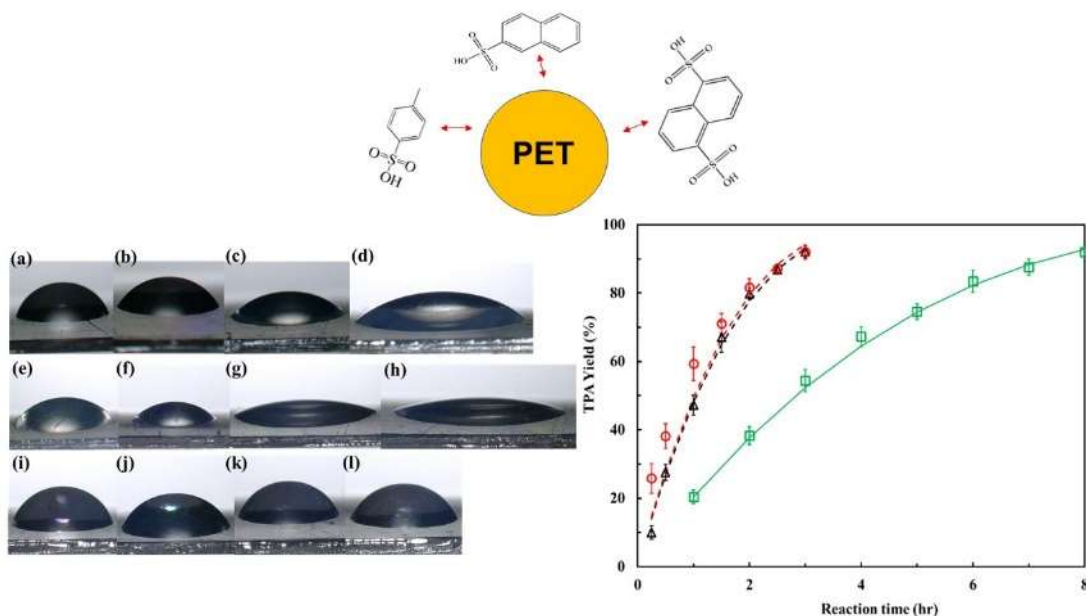
² First Author

³ Corresponding Author

5.1 Abstract

A series of aryl sulfonic acids were tested as catalysts for acid hydrolysis occurring at the surface of poly(ethylene) terephthalate (PET) particles. Specifically, p-toluenesulfonic acid monohydrate (PTSA), 2-naphthalenesulfonic acid (2-NSA), and 1,5-naphthalenedisulfonic acid tetrahydrate (1,5-NDSA) were chosen to provide sulfonic acid active groups and varying hydrophobic functionality. The effect of catalyst concentration and reaction temperature on PET hydrolysis rate were studied. The aryl sulfonic acid catalysts exhibited much higher rates of PET hydrolysis than the mineral acid, H₂SO₄. At 150°C and 4M catalyst, the time required to achieve more than 90% TPA yield was 3, 3, and 8 h, and 18 h for (PTSA), (2-NSA), (1,5-NDSA), and H₂SO₄, respectively. Ethyl acetate hydrolysis was performed as a model reaction to probe the activity of the catalysts in homogenous reactions to compare with the heterogenous hydrolysis reaction occurring at the PET surface. The higher catalytic activities for PET hydrolysis of the PTSA, 2-NSA and 1,5-NDSA than H₂SO₄ was attributed to improved wetting by the reaction media and affinity of the aryl sulfonic acid catalysts for the PET surface.

5.2 Graphical abstract



5.3 Study description

The wide use of poly (ethylene terephthalate) (PET) for single use packaging and textiles has led to a need for broader recycling methods. Chemically depolymerizing waste PET into base monomers is an attractive alternative to traditional mechanical recycling. This paper focuses on the effect of catalyst structure on acid hydrolysis of the PET surface. Catalysts with hydrophobic pendant groups exhibited an affinity for the PET flake surface and improved depolymerization kinetics.

5.4 Keywords

Catalysts, degradation, kinetics, polyesters, recycling, wetting

5.5 Introduction

Polyethylene terephthalate (PET) is among the most widely used polymers due to its unique thermal-physical properties [90, 403, 404]. High transparency, high barrier and excellent mechanical-chemical properties make PET an important feedstock in the packaging and textile industries [405-410]. PET is the main constituent of water bottles, blister packs, and ready-meal packages [279, 411, 412]. Most PET products have short lifetimes, which has resulted in fast accumulation of PET waste [413-416]. There are many challenges to managing PET wastes, including a very slow bio-degradation rate in the environment resulting in direct and indirect threats to species health and food chains [417-420]. PET is primarily produced from fossil fuels which have been recently used with more constraints due to the regulations implemented to battle global climate change [421-427]. The two primary reasons for the importance of PET recycling are reduction of PET waste and need for fossil fuels [428-430].

Chemical recycling leads to the production of prepolymers, oligomers, and monomers, which can be used as a feedstock for PET synthesis [19, 184, 212, 303, 431-437]. Of particular interest to this study, PET hydrolysis produces the monomers, terephthalic acid (TPA) and ethylene glycol (EG) [292, 438-443]. Alkaline hydrolysis processes are implemented at relatively mild reaction conditions, reaction temperature and reaction pressure range 200-250°C and 1-5 atm, respectively [271, 273, 324, 444]. The applied catalysts are mineral bases, reported both in aqueous and non-aqueous reaction mediums with maximum concentrations of 20 wt.% [257, 258, 280, 445]. Similarly, acid hydrolysis processes are applied with mild reaction conditions, but with high catalyst concentrations of the mineral acids, such as H₂SO₄ and HCl [58, 289, 291, 297, 446-448].

Hydrolysis is a heterogenous reaction occurring at the PET surface and is dependent upon the concentration of water and catalyst at the surfaces [43]. The relatively low activity of acid catalysts in these heterogenous reactions require long reaction times and high catalytic concentrations to achieve desired PET conversion [19]. Recent work with alkaline hydrolysis demonstrated that a sharp increase in alkaline hydrolysis rate was observed in the presence of phase transfer catalysts that have high affinity for PET surface [273, 276, 281].

Acid catalysts with hydrophobic functionality have been shown to increase the rate of hydrolysis at polymer surfaces relative to mineral acids [276, 281, 303, 449]. In a recent paper, Abedsoltan et.al. demonstrated that surface wetting and hydrophobicity of the catalyst can affect the rate of PET hydrolysis with poly(styrene sulfonic acid) (PSSA) and H₂SO₄ [43]. Amarasekara et al. [34] demonstrated hydrophobicity effects to classify the higher activities of the aryl sulfonic acids relative to H₂SO₄ for cellulose hydrolysis. Aryl sulfonic acids are thermally stable and have high acidity due to the accessible protons released in the reaction media, are efficient catalysts for cellulose hydrolysis [450-453].

In this work, aryl sulfonic acids with hydrophobic functionality were used as catalysts for PET hydrolysis. The effect of reaction temperature and catalyst concentration on PET hydrolysis was studied. The shrinking core model was applied to determine the reaction rate constants and the activation energies for each catalyst [43, 290, 454]. PET hydrolysis is a heterogenous reaction at the particle surface, therefore, the catalysts were tested in model homogenous hydrolysis of ethyl acetate to determine catalyst activity. The extent of PET surface wetting and the interactions between the catalyst and PET surface were explored to explain the differences in the activities of the catalysts for PET hydrolysis.

5.6 Experimental section

5.6.1. Materials

P-toluenesulfonic acid monohydrate (ACS reagent $\geq 98.5\%$) (PTSA), 2-naphthalenesulfonic acid (technical grade:70%) (2-NSA), 1,5-naphthalenedisulfonic acid tetrahydrate (97%) (1,5-NDSA), ethyl acetate (ACS reagent $\geq 99.5\%$), methyl sulfoxide-d₆, and ammonium hydroxide solution (30-33% NH₃ in water) were purchased from Sigma-Aldrich. PET pellets were provided by Alpek Polyester. The pellets were ground and sieved within the particle size range of 250-354 μm . The water content of the PTSA, 2-NSA, and 1,5-NDSA were determined from the initial weight loss by thermal gravimetric analysis (TGA) (**Figure 5-1**). The TGA analysis was performed on a TA instruments Q50 thermogravimetric analyzer under a nitrogen environment with a ramp rate of 2 $^{\circ}\text{C}\cdot\text{min}^{-1}$. Specifically, the water fraction was 15.4, 10.7, and 20.0 wt.% for PTSA, 2-NSA, and 1,5-NDSA, respectively. These values were used to determine the mass of catalysts required for the 1M, 2M and 4M catalyst solution preparations.

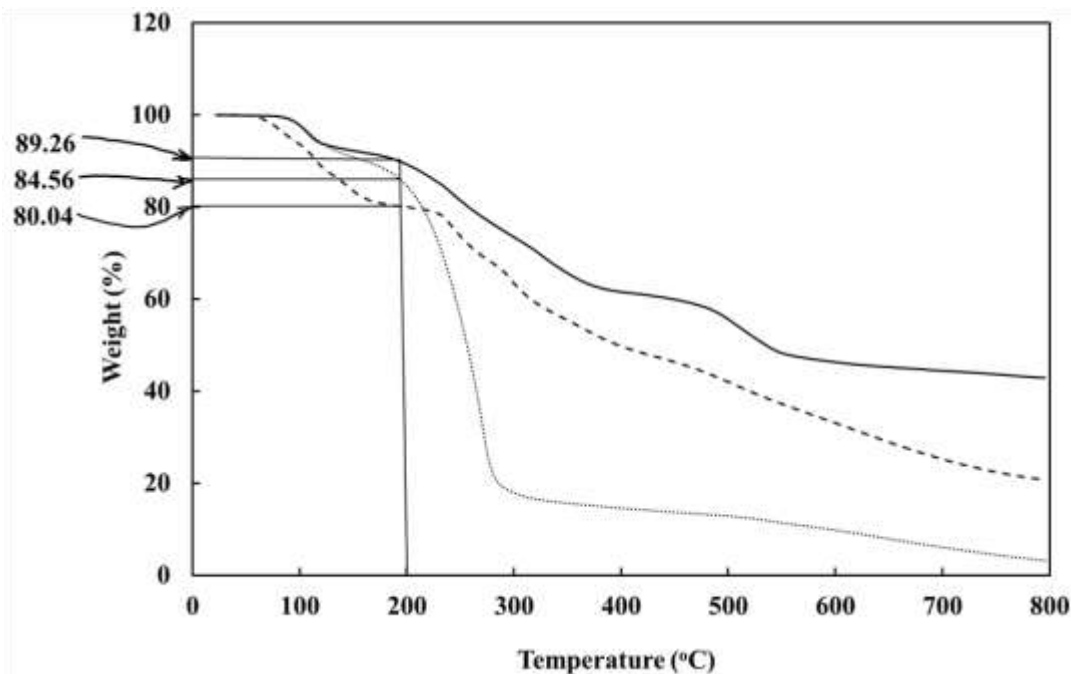


Figure 5-1: TGA analysis to determine water content of the as-purchased PTSA (...), 2-NSA (—), and 1,5-NDSA (---).

5.6.2 PET hydrolysis

PET hydrolysis was conducted in a 15-mL ACE pressure reactor equipped with a magnetic stirrer [43]. For each reaction, 0.2 g of PET along with the 10 mL of 1M, 2M, and 4M catalyst solutions were added to the reactor, heated and stirred. A series of aryl sulfonic acid catalysts with hydrophobic functionality, as shown in **Figure 5-2**, were used to moderate the interactions with the PET and the surface wetting by the reaction media. The reactor was immersed in a hot-oil bath equipped with a magnetic stirrer to maintain a fixed reaction temperature during PET hydrolysis. At the desired reaction time, the reactor was immersed in a cold-water bath to quench the hydrolysis reaction. The produced TPA and the unreacted PET powders were separated from the reaction solution by filtration.

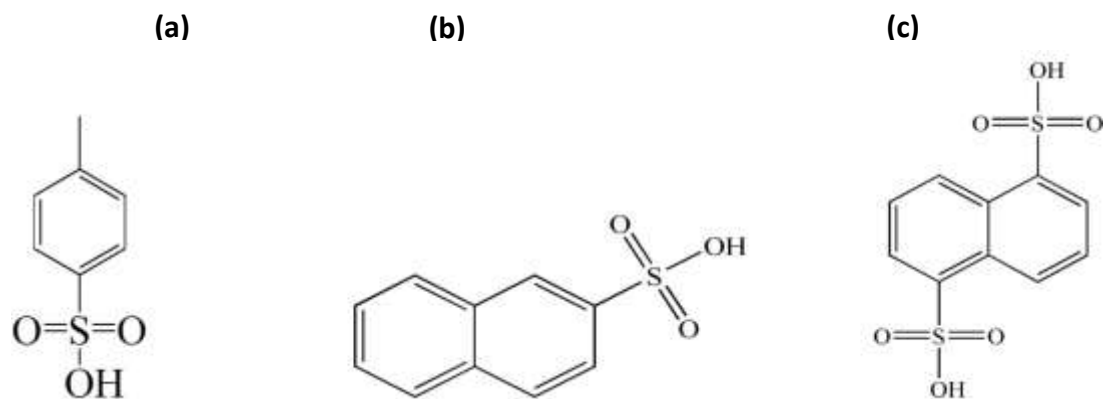


Figure 5-2: Structure of catalysts used for PET hydrolysis (a) PTSA, (b) 2-NSA, and (c) 1,5-NDSA.

The TPA was separated and recovered from the unreacted PET by dissolution in 5M ammonium hydroxide solution and precipitating with pH change, respectively, as described in detail elsewhere [43, 290]. Ammonium hydroxide solution was added to the solids filtered from reaction to dissolve the TPA. After filtration to recover unreacted PET, the pH of the ammonium hydroxide solution was decreased to 2 by addition of 2M H₂SO₄ solution to precipitate the TPA. The precipitated TPA was filtered and washed with excess water. The recovered unreacted PET and TPA were dried overnight at room temperature and 6 h at 70°C.

The PET conversion (%) and the TPA yield (%) were calculated using **Equations 5-1 and 5-2** [43, 290]:

$$PET \text{ conversion } (\%) = \left(\frac{m_{PET,i} - m_{PET,t}}{m_{PET,i}} \right) * 100 \quad (5-1)$$

$$TPA \text{ Yield } (\%) = \frac{MW_{PET}}{MW_{TPA}} * \frac{m_{TPA,t}}{m_{PET,i}} * 100 \quad (5-2)$$

Where $m_{PET,i}$, $m_{PET,t}$, $m_{TPA,t}$, MW_{PET} , and MW_{TPA} are the initial mass of PET, mass of recovered PET after the reaction time t, mass of recovered TPA after the reaction time t, PET molecular weight, and TPA molecular weight, respectively.

5.6.3 Ethyl acetate hydrolysis

For ethyl acetate hydrolysis, 5mL of a 0.5M catalyst solution was prepared and mixed with 5mL of 5 wt.% ethyl acetate in a 15-mL ACE pressure reactor equipped with a magnetic stirrer [43]. The reactor was immersed in a hot-bath oil equipped with a stirrer to maintain a fixed reaction temperature. Since ethyl acetate hydrolysis is a rapid reaction, the constant temperature hydrolysis tests were conducted for 1 h at temperatures in the range of 40-70°C. After a defined time, the reactor was immersed in a cold water/crushed ice-bath (0-5°C) to quench the hydrolysis process. The extent of ethyl acetate conversion to acetic acid was determined by titration. A 5mL sample of the reaction solution was titrated against 0.1N NaOH solutions, standardized with potassium hydrogen phthalate, to determine the total H⁺ content. The catalyst H⁺ content was subtracted from the total H⁺ to determine the amount of acetic acid produced. Afterwards, the reaction rate constants and the activation energies were calculated and compared [43, 455].

5.6.4 Contact angle measurements

Contact angle measurements [43, 456] were performed to determine the surface wetting of the PET films with each catalyst solutions at concentrations from 0.25M to 4M. The tests were performed at room temperature on the PET films with the average thickness of 0.35 mm. The films were processed on a HAAKE Rheomex Brabender single screw extruder. In a typical contact angle test, a droplet of the catalyst solution was positioned on

the PET film that was attached to a flat-glass substrate. The image of the droplet on the PET surface was captured by a Keyence VHX-600 digital microscope armed with a camera in reflection mode with a full-coaxial light stage. The image was analyzed to determine the contact angle value [43]. Each test was repeated at least 6 times with new droplets on the PET film surface.

5.6.5 Recovered TPA characterization

FTIR and ^1H NMR analyses were performed to confirm the structure of the TPA recovered following PET hydrolysis. For the FTIR analysis, samples were prepared by forming thin pellets of TPA mixed with KBr. The pellets were analyzed by a Varian Excalibur Series FTIR spectrometer equipped with a microscope using transmission mode in frequencies of $400\text{--}4000\text{ cm}^{-1}$. For the ^1H NMR analysis, the samples were prepared by dissolving the TPA in methyl sulfoxide- D_6 and the spectra were obtained using a Bruker Avance III spectrometer at 600 MHz. The TPA structure was confirmed with FTIR and ^1H NMR analysis and compared to the commercial TPA as discussed in **Figures 5-S1 and 5-S2, Section 1, Supporting Information**.

5.7. Results and Discussion

5.7.1 Shrinking core model for PET hydrolysis

The impact of structure of the aryl-sulfonic acid catalysts on the kinetics of PET conversion and TPA yield was investigated at 2M catalyst concentration and 150°C (**Figure 5-3**). For all the studied catalysts, the TPA yields were slightly lower than the PET conversions. This may be due to losses in TPA powder during the downstream processing

steps. It was noted that in all cases the TPA yield was within 10 % of the PET conversion and followed similar trends.

The TPA yield has been used in the literature to apply reaction kinetic models and determine the reaction rate constants and activation energies [43, 290, 457]. Similarly, results will be reported in terms of the TPA yields in this paper. PET conversion (%) for all reaction conditions are given in the **Figures 5-S3 and 5-S4, Sections 2 and 3, Supporting Information.**

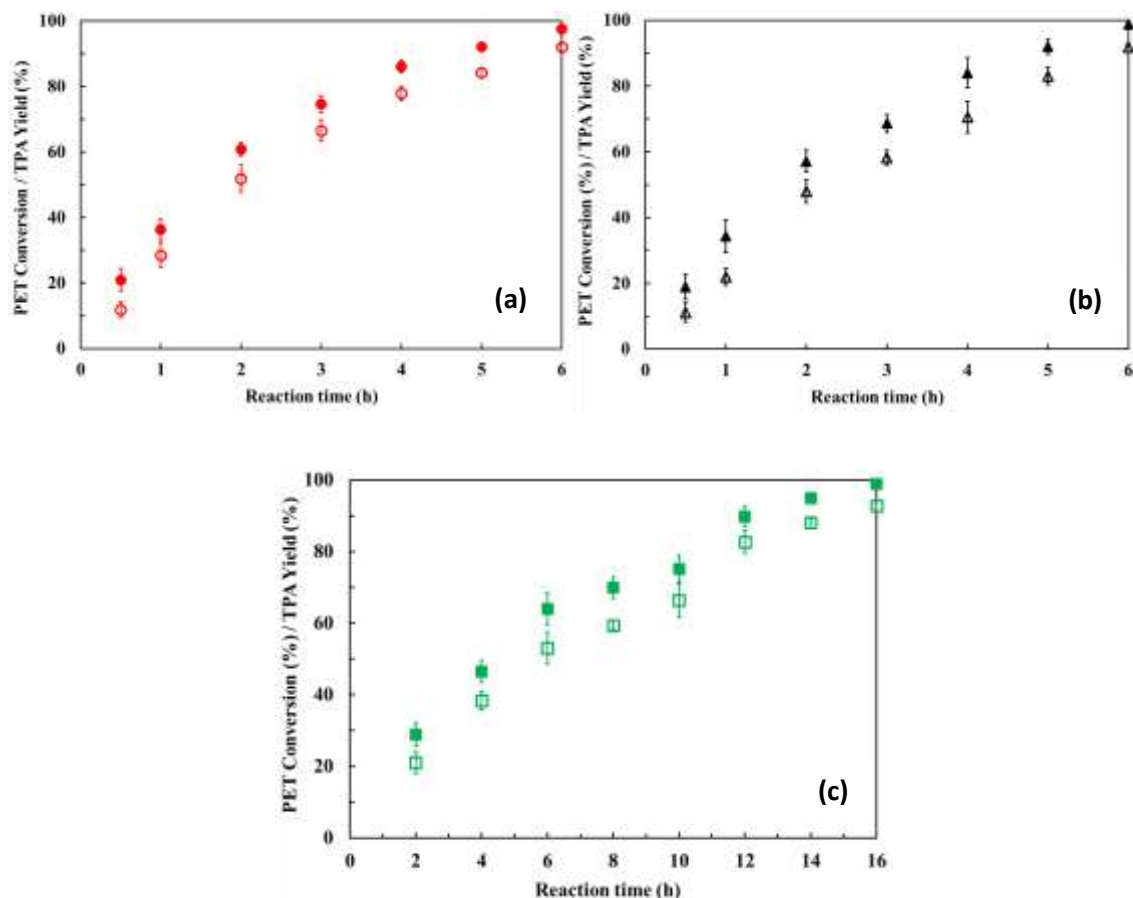


Figure 5-3: Impact of time on PET conversion (%) / TPA yield (%) for PET hydrolysis with 2M solutions of PTSA (●/○), 2-NSA (▲/△), and 1,5-NDSA (■/□) at 150°C.

A shrinking core model applicability to the description of the reaction kinetic data for PET hydrolysis has been described in the literature [43, 290, 454]. The shrinking-core model describes the surface reaction at the liquid-solid interface with the solid reactant shrinking as the reaction progresses. A key assumption for the model, as applied to PET hydrolysis, is that the solid products do not deposit on the solid surface [454]. The shrinking core model was applied to calculate apparent (K_a) and specific (k_{sp}) reaction rate constants of the PET hydrolysis with H₂SO₄ solutions [43, 290, 454]. The expression relating the TPA yield to the specific reaction rate constant is given in **Equation 5-3** [43, 290, 454]:

$$1 - (1 - [TPA Yield]_t)^{0.33} = \frac{k_{sp}C}{\rho_{PET}r_i} (t) = K_a t \quad (5-3)$$

Where the $[TPA Yield]_t$, C , ρ_{PET} , and r_i are the TPA yield at a reaction time t , catalyst concentration, PET density, and the average initial radius of PET particles, respectively. The apparent reaction rate constant (K_a) is defined as $\frac{kC}{\rho_{PET}r_i}$ with units of inverse time. As shown in **Figure 5-4**, the shrinking core model provided a good fit ($R^2 = 0.99$) to the kinetic data for the 2M catalyst solutions and will be used to process kinetic data throughout this paper. Moreover, the model fitting and the level of fit for 1M and 4M catalyst solutions are respectively given in **Figures 5-S5 and 5-S6, Section 4, Supporting Information**.

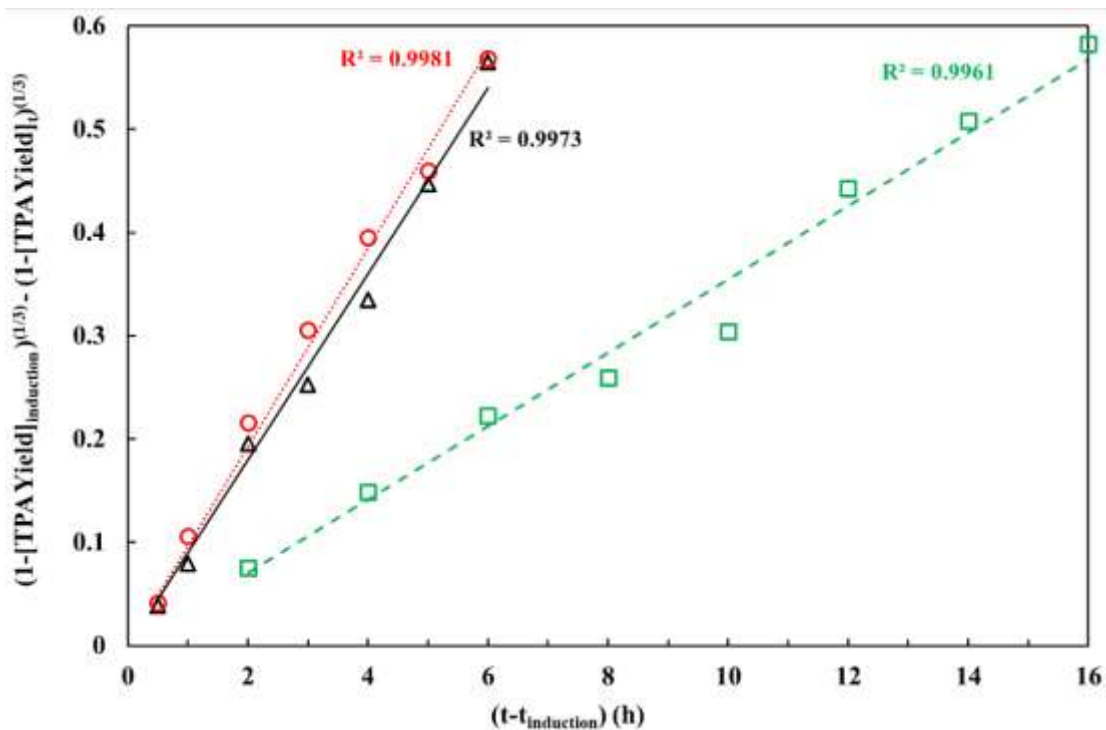


Figure 5-4: Fit of shrinking core model to the kinetic data at 150°C for 2M catalyst solutions of PTSA (○, ...), 2-NSA (△, —) and 1,5-NDSA (□, ---).

5.7.3 Effect of catalyst concentration the TPA yield

The effect of catalyst structure on the hydrolysis kinetics was monitored at 150°C and 1M, 2M, and 4M catalyst. TPA yield dependance on the reaction time for each catalyst is shown in **Figure 5-5**. The standard deviation for three repeats of the tests for each point is indicated by error bars. As expected, an increase in the catalyst concentration resulted in decreases in the reaction time required to depolymerize PET.

For the 4M PTSA and 2-NSA solutions, the time required to achieve more than 90% TPA yield was 3 hours, while 8 hours was required for the 1,5-NDSA. These reaction times are considerably lower than the 18 hours required for the 4M H₂SO₄ solutions [43]. No induction time was seen in the kinetic data as was previously reported in the literature

for H₂SO₄ [43, 290, 458]. The PTSA and 2-NSA showed similar activity while the 1,5-NDSA was a less active catalyst for PET hydrolysis. Similar outcomes were observed by Amarasekara et. al. for hydrolysis of cellulose using aryl sulfonic acid catalysts [34].

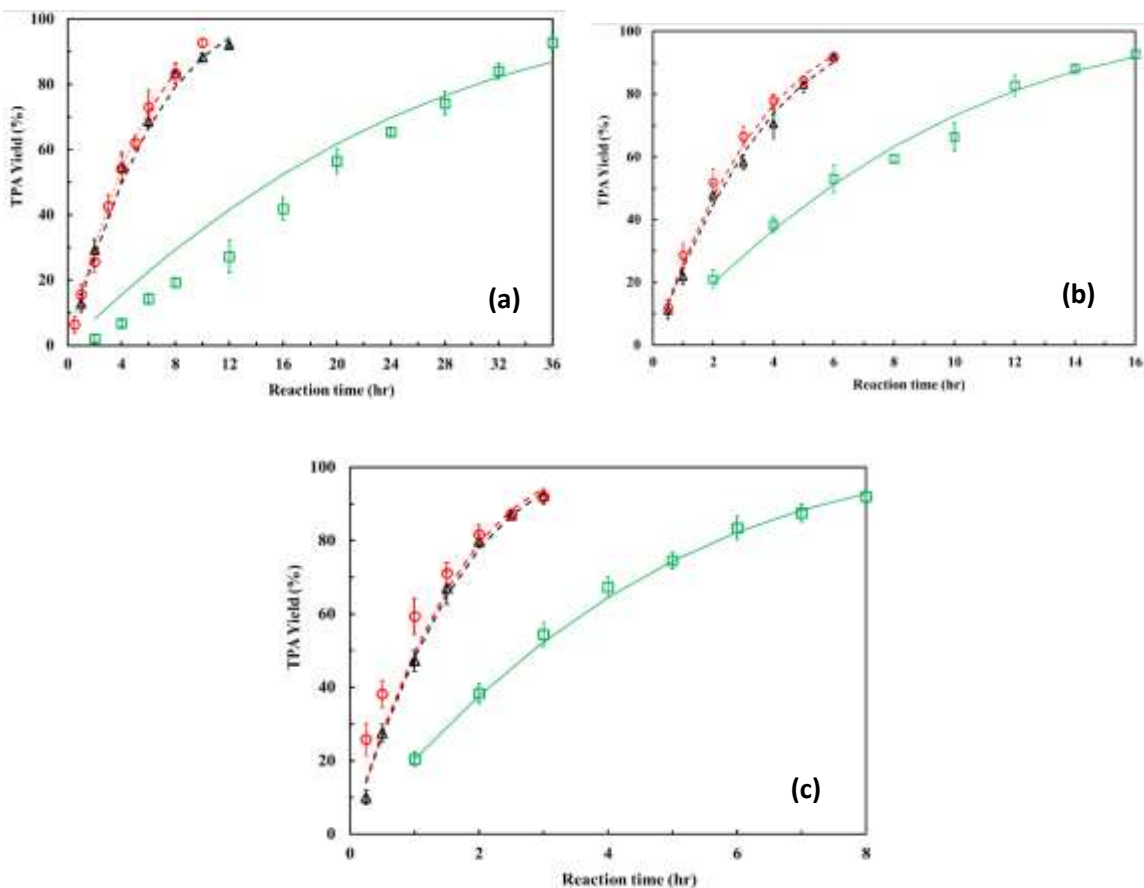


Figure 5-5: Effect of catalyst concentration on TPA yield at $T_{\text{Reaction}} = 150^{\circ}\text{C}$ with (a) 1M, (b) 2M, and (c) 4M solutions of PTSA (\circ , ---), 2-NSA (Δ , ---) and 1,5-NDSA (\square , —).

The lines represent the fit of the shrinking core model.

As discussed in detail in the previous section, the shrinking-core model was applied to kinetic TPA yield data to determine the apparent rate constants. The K_a values for the 1M, 2M and 4M aryl sulfonic acid catalysts at 150°C are presented in **Table 5-1**. The apparent rate constant for H₂SO₄ previously reported by Coleman and coworkers is

provided for comparison [43]. The PTSA and 2-NSA have similar K_a values which were higher than the K_a value for 1,5-NDSA. All the aryl sulfonic acid catalysts exhibited greater activity and larger K_a than the sulfuric acid. The lines in **Figure 5-5** were generated using the shrinking-core model fit using the K_a to demonstrate the model fit to the experimental data.

Table 5-1: Apparent reaction rate constants (K_a values) as a function of the catalyst concentration for PET hydrolysis at $T_{\text{Reaction}} = 150^\circ\text{C}$.

$T_{\text{Reaction}} =$ 150°C	PTSA	2-NSA	1,5-NDSA	H ₂ SO ₄ [43]
Catalyst concentration (M)	K_a (h ⁻¹). (10 ²)	K_a (h ⁻¹). (10 ²)	K_a (h ⁻¹). (10 ²)	K_a (h ⁻¹). (10 ²)
1	5.72	5.12	1.46	1.38
2	9.61	9.00	3.55	1.66
4	20.48	19.69	7.30	3.72

5.7.4 Effect of reaction temperature on the TPA yield

The hydrolysis kinetics for the 2M catalyst solution at temperatures of 130°C, 140°C, and 150°C is shown in **Figure 5-6**. As expected, the rate of hydrolysis increased with temperature increase. At 150°C, more than 90% TPA yield was achieved in 6 h for PTSA and 2-NSA and in 16 h for 1,5-NDSA. These reaction times are much shorter than

the reported times for similar reaction systems and conditions for 2M H₂SO₄ solutions, 28 h [43].

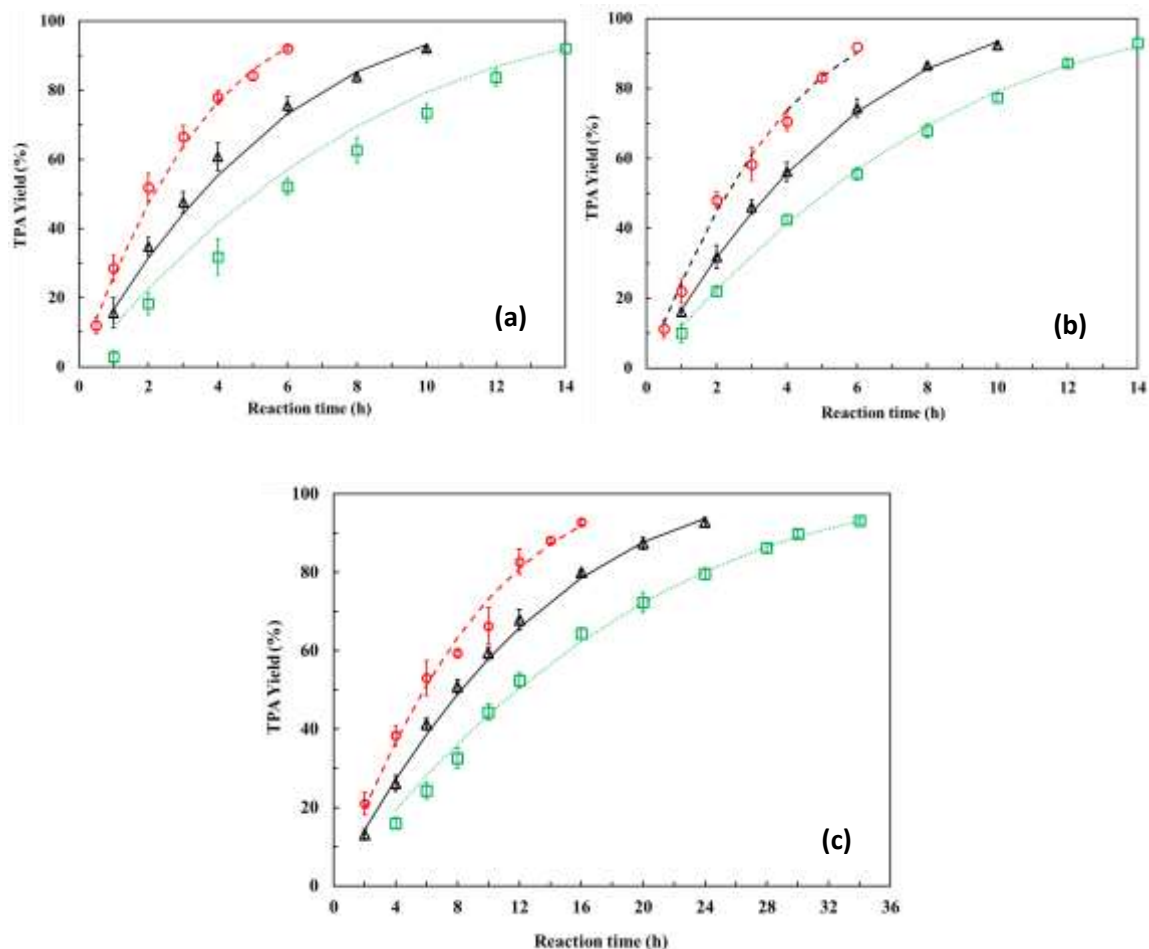


Figure 5-6: Effect of Temperature on the TPA yield for 2M catalyst solutions with (a) PTSA, (b) 2-NSA, and (c) 1,5-NDSA at 130°C (□, ...), 140°C (Δ, —) and 150°C (○, ---).

The lines represent the fit of the shrinking core model.

The shrinking-core model [43, 290, 454] was applied to determine the specific reaction rates constants as a function of temperature. The rate constants for 2M catalyst solutions at 130°C, 140°C, and 150°C are shown in **Table 5-2**. PTSA and 2-NSA have similar activity and 1,5-NDSA is the least active catalyst studied. These aryl sulfonic acids

exhibited considerably higher activities than reported mineral acid catalysts [43, 289, 290, 458]. For example, the K_a for PTSA is around 6 times greater than H_2SO_4 at 2M and 150°C. These K_a values from the shrinking-core model were used to estimate the TPA yields and to fit to the experimental data in **Figure 5-6**.

Table 5-2: Apparent reaction rate constants (K) for the 2M catalyst solutions as function of reaction temperature for PET hydrolysis.

T_R	PTSA	2-NSA	1,5-NDSA	H_2SO_4 [43]
(°C)	$K_a (h^{-1}).(10^2)$	$K_a (h^{-1}).(10^2)$	$K_a (h^{-1}).(10^2)$	$K_a (h^{-1}).(10^2)$
130	4.10	4.08	1.74	1.10
140	5.91	5.94	2.51	1.30
150	9.61	9.00	3.55	1.66

The Arrhenius equation [43, 290] was used to determine the apparent activation energies for the 2M catalyst solutions over the full temperature range studied. As shown in **Figure 5-7**, the Arrhenius equation provided a good fit of the rate data and allowed determination of the activation energy. The pre-exponential factor values are 0.08, 0.02, and 0.002 [$kg\ PET.m.(mol\ catalyst)^{-1}\ s^{-1}$] for PTSA, 2-NSA, and 1,5-NDSA, respectively. The apparent activation energies are 60.3 $kJ.mol^{-1}$, 56.1 $kJ.mol^{-1}$, and 50.6 $kJ.mol^{-1}$ for PET hydrolysis with 2M aqueous catalyst solutions of PTSA, 2-NSA, and 1,5-NDSA, respectively. These activation energy for aryl sulfonic acids are higher than the reported values for 2M aqueous solutions of H_2SO_4 (29.1 $kJ.mol^{-1}$) [43].

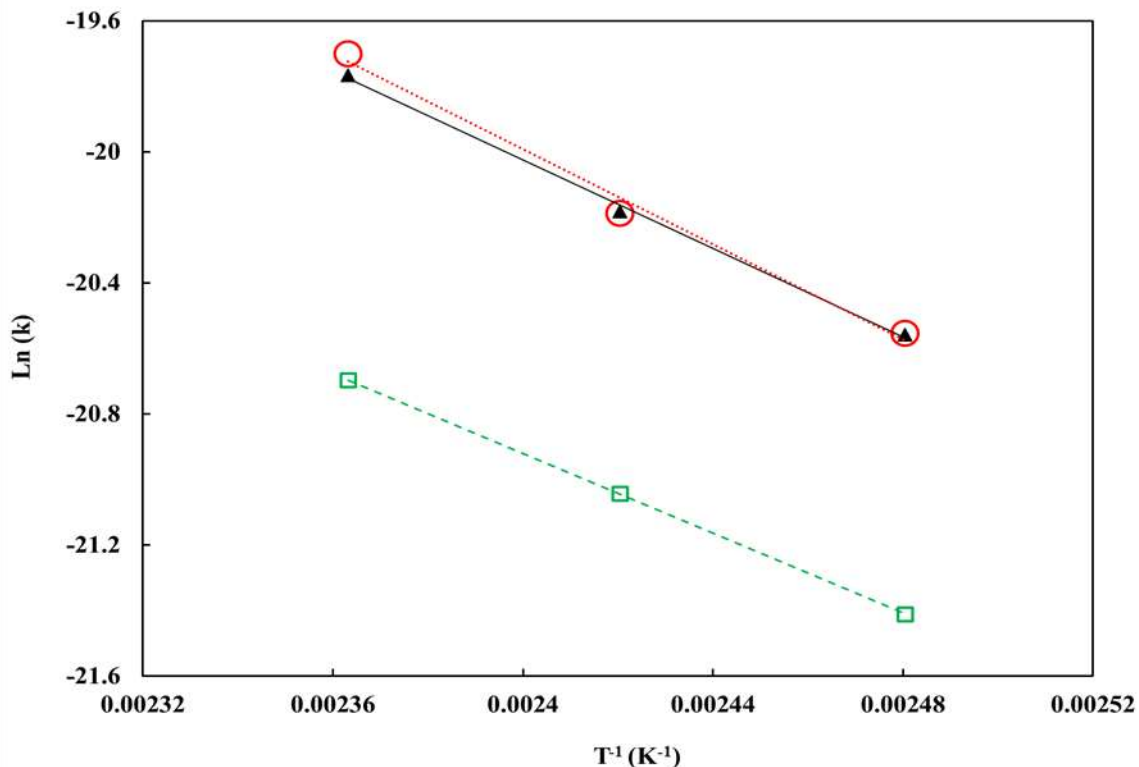


Figure 5-7: Application of Arrhenius equation to specific rate constants for the 2M catalyst solutions of PTSA (O, ...), 2-NSA (\blacktriangle , —) and 1,5-NDSA (\square , ---), PET hydrolysis.

A similar result was obtained for the aqueous hydrolysis of cellulose with aryl sulfonic acids and sulfuric acid as the catalysts [34]. This may be due to the positive heat of sorption, which has an additive effect on the apparent activation energy values. This was determined in the microscopic analysis of the adsorption of sulfur molecules on the calcite surface [459]. As discussed in detail below, the impact of catalyst structure and concentration on the interaction of the reaction media with the PET surface were studied using contact angle measurements and analysis of catalyst dissociation between octanol/water solutions [34, 43].

5.7.5 Ethyl acetate hydrolysis, homogeneity effect on the reaction rate and activation energy

PET hydrolysis is a heterogeneous reaction occurring at the PET surface and requires wetting of the PET surface by the aqueous reaction media. Ethyl acetate hydrolysis was studied using the aryl sulfonic acids from PET hydrolysis to eliminate the effect of surface wetting. The hydrolysis tests were done with similar reaction system but at lower catalyst concentrations, 0.5M, and reaction temperatures, 40-70°C, due to the rapid ethyl acetate hydrolysis. The apparent reaction rate constants (K values) for the tested reaction temperatures are presented in **Table 5-3**.

Table 5-3: Apparent reaction rate constants (K values) for the ethyl acetate hydrolysis with 0.5M PTSA, 2-NSA, and 1,5-NDSA solutions [43].

T _R	PTSA	2-NSA	1,5-NDSA	H ₂ SO ₄ [43]
(°C)	K _a (h ⁻¹). (10 ²)	K _a (h ⁻¹). (10 ²)	K _a (h ⁻¹). (10 ²)	K _a (h ⁻¹). (10 ²)
40	12.24	20.66	16.02	16.34
50	23.90	35.93	27.11	28.69
60	39.24	48.60	43.92	48.96
70	55.44	69.48	62.28	66.24

The calculated K_a values were fit to Arrhenius equation to determine the apparent activation energies, as shown in **Figures 5-8** [43]. The pre-exponential factor values are 1185, 45, and 296 [kg ethyl acetate.m.(mol catalyst)⁻¹.s⁻¹] for PTSA, 2-NSA, and 1,5-NDSA, respectively. The activation energies were 45.1 kJ.mol⁻¹, 35.2 kJ.mol⁻¹, and 40.8

$\text{kJ}\cdot\text{mol}^{-1}$ for PTSA, 2-NSA, and 1,5-NDSA solutions, respectively. These values are within the similar range of reported activation energies for ethyl acetate hydrolysis, $30\text{-}70\text{ kJ}\cdot\text{mol}^{-1}$ [43, 391, 455, 460]. Moreover, these values are within the range of the activation energy values reported for ethyl acetate hydrolysis by H_2SO_4 aqueous solutions at the same reaction system and reaction conditions, reported $39.6\text{ kJ}\cdot\text{mol}^{-1}$ [43]. So, the catalysts have similar activities and activation energies as found for hydrolysis in a homogenous reaction medium.

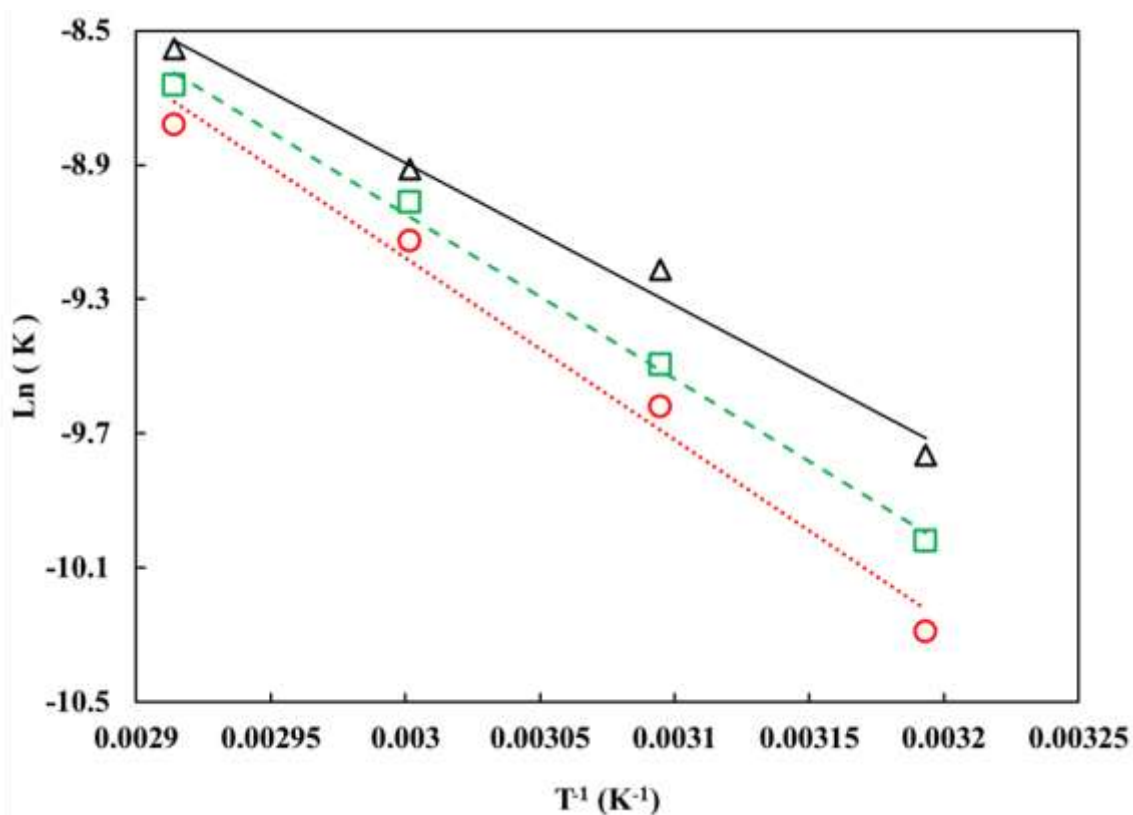


Figure 5-8: Application of Arrhenius equation to reaction rate constants for the 0.5M catalyst solutions of PTSA (\circ , ...), 2-NSA (Δ , —) and 1,5-NDSA (\square , ---) for ethyl acetate hydrolysis.

5.7.6 Wetting studies of catalyst solutions on the PET surface

PET hydrolysis involves chain scission by the protons attacking ester groups at the polymer surface, and formation of the smaller polymer chains. As hydrolysis progresses terephthalic acid (TPA) and ethylene glycol (EG) are produced. Factors affecting rate of hydrolysis include reaction temperature, PET particle shape and size, catalyst structure, and catalyst concentration. These factors have been explored extensively for a variety of hydrolysis reactions [43, 289, 290, 458]. Another factor that can impact PET hydrolysis, which has not been extensively addressed in the literature [43, 316], is the extent of the PET surface wetting by the reaction solution. In an earlier study by Coleman and coworkers, the higher activity of polystyrene sulfonate catalyst relative to H₂SO₄ for PET hydrolysis was attributed to greater surface wetting and adsorption of PSSA on the PET surface [43]. Similarly, the enhanced activity of aryl sulfonic acid groups for cellulose hydrolysis was attributed to affinity of the catalyst for the cellulose surface [34, 316].

In this work, the contact angle of the catalyst solutions on a PET film were measured to check the extent of wetting. The concentrations, ranged from 0.25M to 4M, were used for the PET hydrolysis. The captured images of the catalyst solution droplets, within the range of 0.5M to 4M positioned on the PET films, are presented in **Figure 5-9**. For PTSA (**Figure 5-9. a-d**) and 2-NSA (**Figure 5-9. e-h**) solutions, as the catalyst concentration increases the droplet spread on the PET surface increases. For 1,5-NDSA solutions (**Figure 5-9. i-l**), same as reported for droplets of H₂SO₄ solutions on PET surface [43], an increase in catalyst concentration had a negligible effect on the extent of wetting of the PET surface.

The contact angle values were determined to quantify the extent of wetting. The contact angle for the catalyst solutions within the range of 0.25M to 4M are presented in **Figure 5-10**. The contact angle values of the PTSA, and 2-NSA solutions decreased as the concentration increased. For 1,5-NDSA, the contact angle values maintained an average value of 80 degrees, which is close to the average value of 82 degrees, reported for H₂SO₄ solutions [43]. For both cases, the interactions of the catalyst solutions is not as extensive, that is less effective PET surface wetting was observed [43].

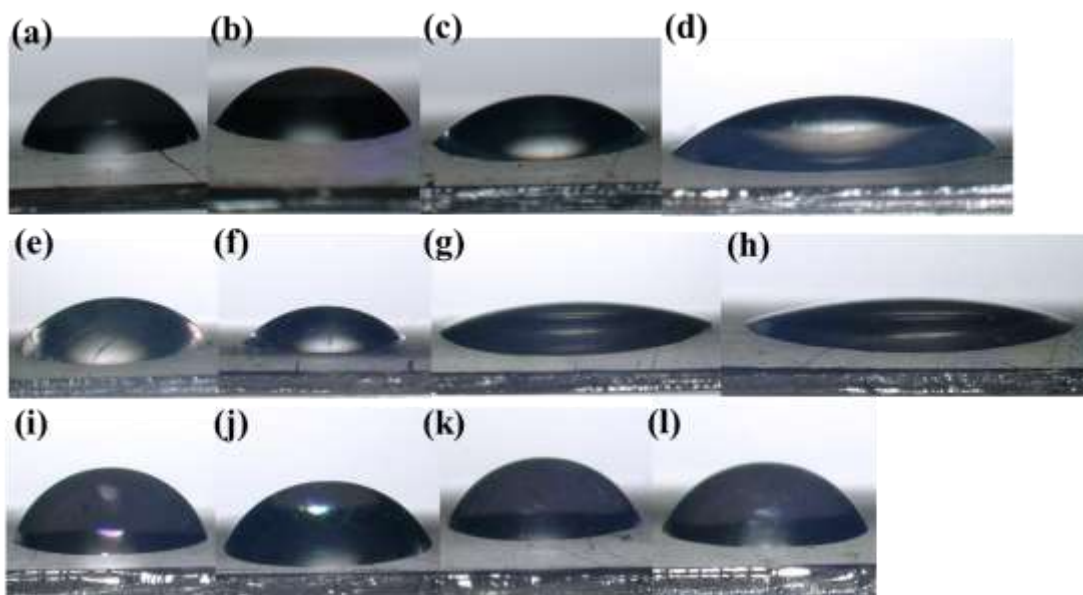


Figure 5-9: Droplet shape of catalyst solutions on the PET films for PTSA: (a) 0.5M, (b) 1M, (c) 2M, (d) 4M; 2-NSA: (e) 0.5M, (f), 1M, (g) 2M, (h) 4M; 1,5-NDSA: (i) 0.5M, (j), 1M, (k) 2M, (l) 4M.

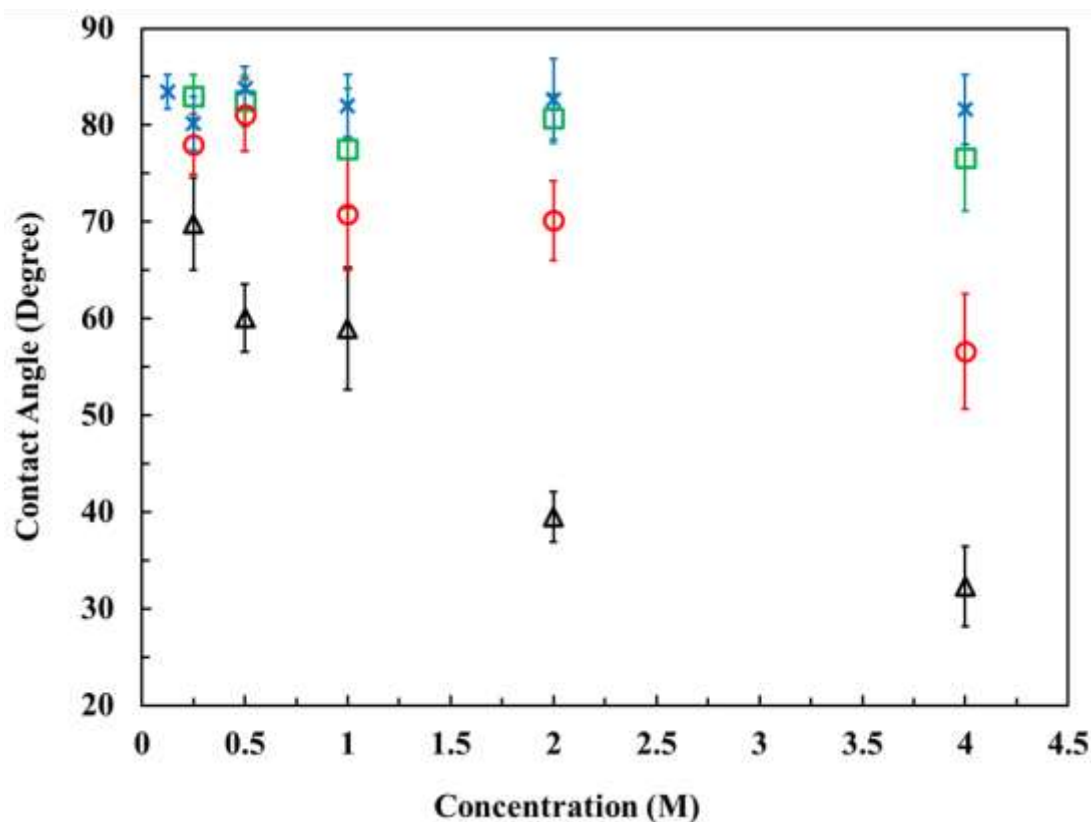


Figure 5-10: Contact angle values for the catalyst solutions, 0.25M to 4M, of PTSA (○), 2-NSA (Δ), 1,5-NDSA (□), and H₂SO₄ (x) [43] on the PET surface.

5.7.7 Octanol/water distribution coefficients of the catalysts

Earlier reports indicate that catalysts with hydrophobic moieties exhibit higher activity for acid hydrolysis of solid surfaces including PET hydrolysis with poly(styrene sulfonic acid) (PSSA) [43], and cellulose hydrolysis using aryl sulfonic acids [34]. Hydrophobicity of the catalyst was proposed as an contributing factor in determining effectiveness of catalysts for acid hydrolysis at the cellulose surface [34]. Similarly, the importance of hydrophobicity of small molecules on PET hydrolysis with equal catalyst concentrations is considered in this work. The method reported by Amarasekara et. al., which compared octanol/water distribution with the catalyst activity for cellulose

hydrolysis, was adopted in this work [34]. In this work, the logarithmic partition coefficient (Log P) and logarithmic distribution coefficient (Log D) were determined for the catalysts used for PET hydrolysis using method outlined in the literature [461].

The Log P describes the concentration ratio of un-ionized catalyst compound in octanol and water solution while the Log D is the ratio of the sum of both ionized and un-ionized catalyst compound in each phase [34]. ChemAxonTM software was used to determine the Log P and Log D values for the tested catalysts in this work as well as H₂SO₄ reported for PET hydrolysis [34, 43, 335]. The first order apparent reaction rate constants dependence on the Log P and the Log D values are shown in **Figure 5-11** and **Figure 5-12**, respectively. The catalysts with higher hydrophobicity (i.e., higher log P and log D) exhibit higher activities for PET hydrolysis. As was reported for the cellulose system, the Log D provided a better correlation with kinetics of the PET hydrolysis [34].

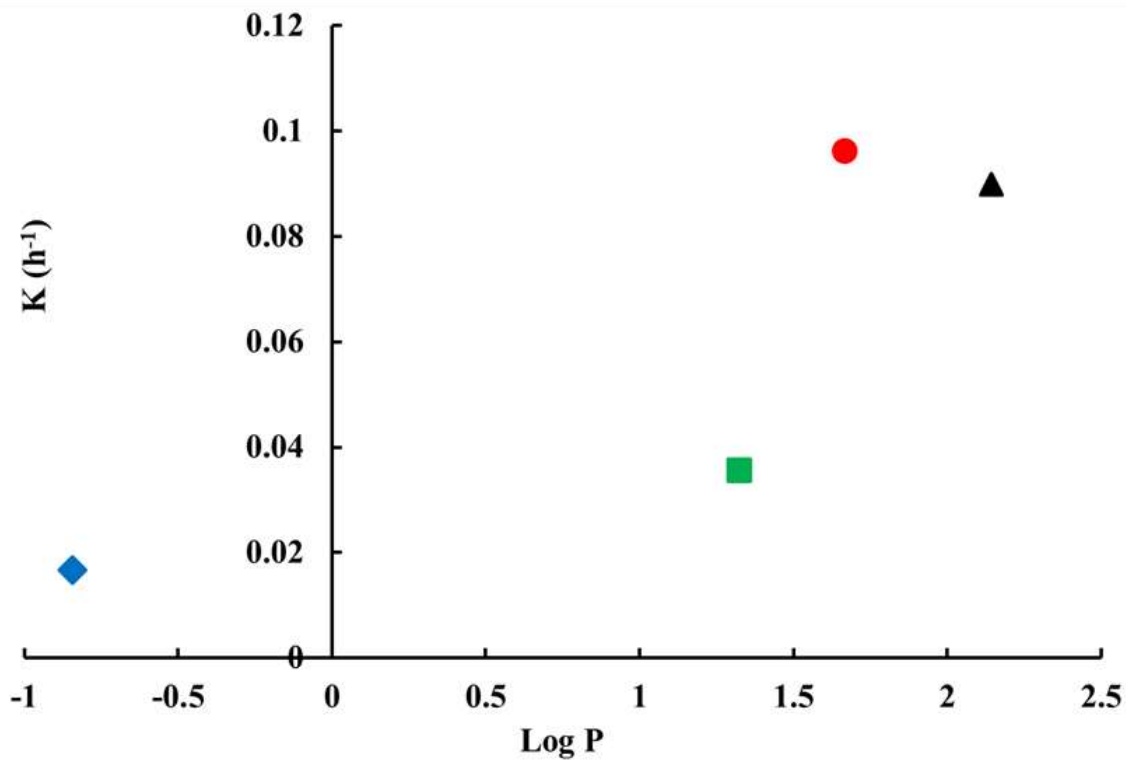


Figure 5-11: Apparent reaction rate constant (K) dependence on Log P for PET hydrolysis with 2M catalyst concentrations of PTSA (●), 2-NSA (▲), 1,5-NDSA (■), and H₂SO₄ (◆) at a reaction temperature of 150°C.

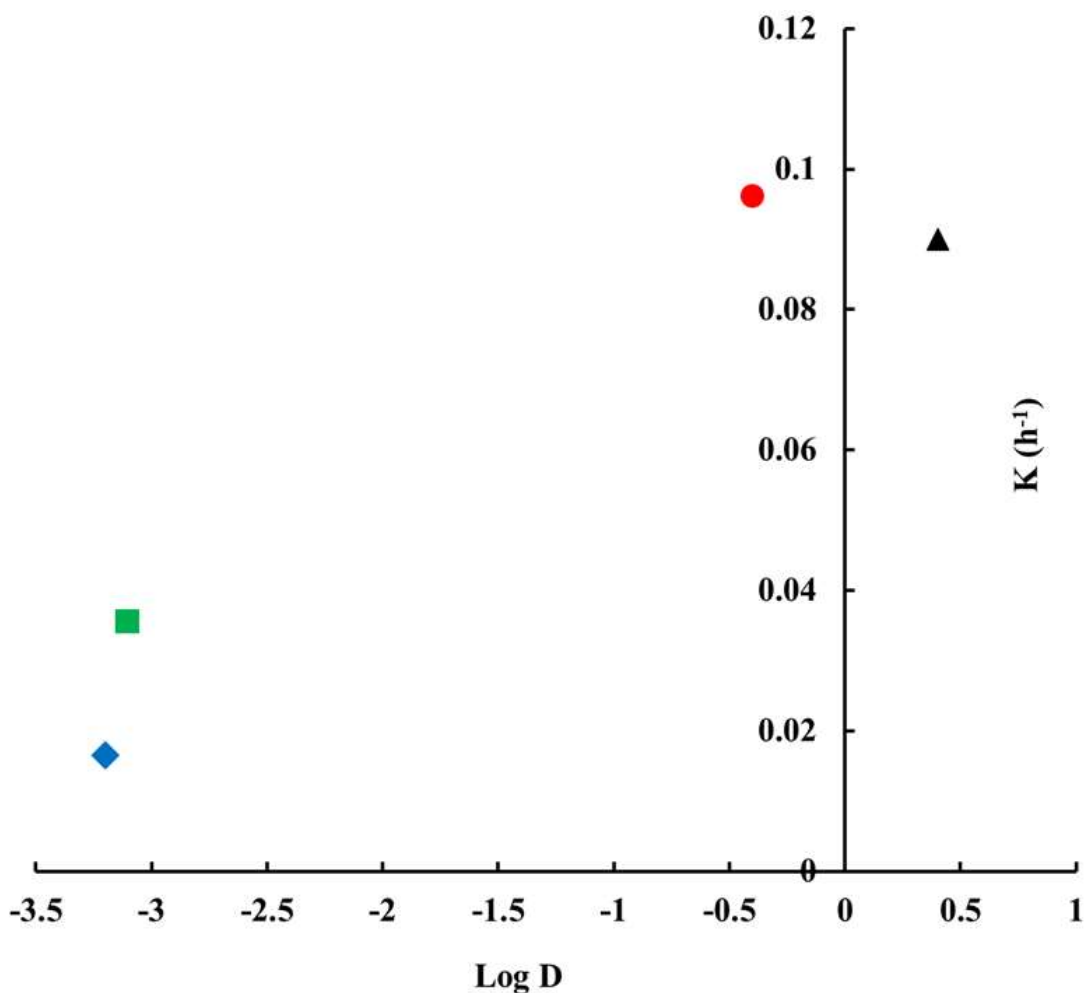


Figure 5-12: Apparent reaction rate constant (K) dependence on Log D for PET hydrolysis with 2M catalyst concentrations of PTSA (●), 2-NSA (▲), 1,5-NDSA (■), and H₂SO₄ (◆) at a reaction temperature of 150°C.

The reaction conditions required to achieve more than 90% TPA yield for PET hydrolysis reported for several acid catalysts are presented in **Table 5-4**. The reaction temperature, T_R , pressure, P_R , and reaction time, t_R , are listed for each system. PTSA and 2-NSA are considerably more active catalysts than the mineral acid, H₂SO₄, at the same reaction conditions [290, 458]. Note that the reaction conditions, specifically catalyst

concentration, reaction pressure and reaction temperature, are considerably milder than required for mineral acids [43, 289, 438, 462].

Table 5-4: Reported reaction conditions to achieve more than 90% TPA yield for PET acid hydrolysis.

Catalyst type	Catalyst Concentration (M)	PET _{avg.} size (μm)	T _R (°C)	P _R (atm)	t _R (h)	Ref.
HNO ₃	13	90.5	100	1	18	[289]
H ₂ SO ₄	4	302	150	~ 5	18	[43]
PSSA	4	302	150	~ 5	16	[43]
H ₂ SO ₄	7.5	595	135	1	6	[290]
H ₂ SO ₄	7	200	150	N/R	5	[458]
PTSA	4	302	150	~ 5	3	This Paper
2-NDS	4	302	150	~ 5	3	This Paper
NDSA	4	302	150	~ 5	8	This Paper

5.8 Conclusions

Aryl sulfonic acid catalysts for the PET hydrolysis with catalyst concentration between 1M and 4M and temperatures between 130°C and 150°C were explored in this work. The aryl sulfonic acid catalysts were more active catalysts for hydrolysis of PET than mineral acid, H₂SO₄. At 4M and 150°C, the time required to achieve more than 90% TPA yields were 6 h, 6 h, and 16 h for PTSA, 2-NSA, 1,5-NDSA, respectively, compared

to 18 hours for H₂SO₄ at similar conditions. The PTSA and 2-NSA were the most active acid catalysts tested in this study.

The shrinking-core model was applied to determine the reaction rate constants for PET hydrolysis. The apparent activation energy values were calculated to be 60.3 kJ.mol⁻¹, 56.1 kJ.mol⁻¹, and 50.6 kJ.mol⁻¹ for PTSA, 2-NSA, and 1,5-NDSA. The homogeneity effect was explored by testing the ethyl acetate hydrolysis with the same aryl sulfonic acids used for PET hydrolysis. The determined activation energy values were 45.1 kJ.mol⁻¹, 35.2 kJ.mol⁻¹, and 40.8 kJ.mol⁻¹ for PTSA, 2-NSA, and 1,5-NDSA solutions, respectively. This showed that in homogeneous reaction medium, these acids have similar activities, same as reported for ethyl acetate hydrolysis for H₂SO₄ [43, 391, 455, 460]. While the enthalpy of adsorption was not determined, the higher activity of these catalysts was evidenced by PET surface wetting [43] and determination of octanol/water partition coefficients [34]. Contact angle measurements revealed better wetting of the PET surface, which has a positive effect on higher efficiency of these catalysts for PET hydrolysis. Graphs of reaction rate constants dependence on the Log P and the Log D values confirmed the hydrophobicity effect as another inducing factor, which improved the efficiency of these catalysts for PET hydrolysis- similar to what's reported for cellulose hydrolysis with aryl sulfonic acids [34].

5.9 Acknowledgements

The authors would like to acknowledge Alpek Polyester for providing the PET pellets for this study. The authors are also thankful to the Polymer Institute of the University of Toledo for providing the PET films and support for this project.

5.10 Supporting Information

5.10.1 Confirmation of the structure of recovered terephthalic acid (TPA)

FTIR and ^1H NMR analyses were done on the recovered TPA from the PET hydrolyses with the tested catalyst solutions. **Figure 5-S1** shows the spectra for commercial TPA (**Figure 5-S1.a**) and the recovered TPA from PET hydrolysis with catalysts, PTSA (**Figure S1.b**), 2-NSA (**Figure 5-S1.c**), and 1,5-NDSA (**Figure 5-S1.d**). The characteristic bands for the recovered TPA are similar to commercial polymer. Characteristic bands at $2500\text{-}3000\text{ cm}^{-1}$, 1685 cm^{-1} , and $1574\text{-}1425\text{ cm}^{-1}$ which are attributed to the carboxylic group, carbonyl group, and aromatic ring, respectively, are present in the spectra of the recovered TPAs. **Figure 5-S2** shows the ^1H NMR spectra for the commercial TPA (**Figure 5-S2.a**) and the recovered TPA from the PET hydrolysis within the reaction solutions of PTSA (**Figure 5-S2.b**), 2-NSA (**Figure 5-S2.c**), and 1,5-NDSA (**Figure 5-S2.d**). The spectra for the recovered TPAs are comparatively analogous to the commercial TPA spectrum. The short band at 2.5 ppm and close to the 13 ppm relates to the reference solvent (methyl sulfoxide- d_6) and the hydroxyl groups of the carboxylic acid in the TPA structure. The peak at 8 ppm corresponds to the hydrogen of the aromatic ring in the TPA structure. Thus, the structures of the recovered TPA were the same as the commercial TPA structure.

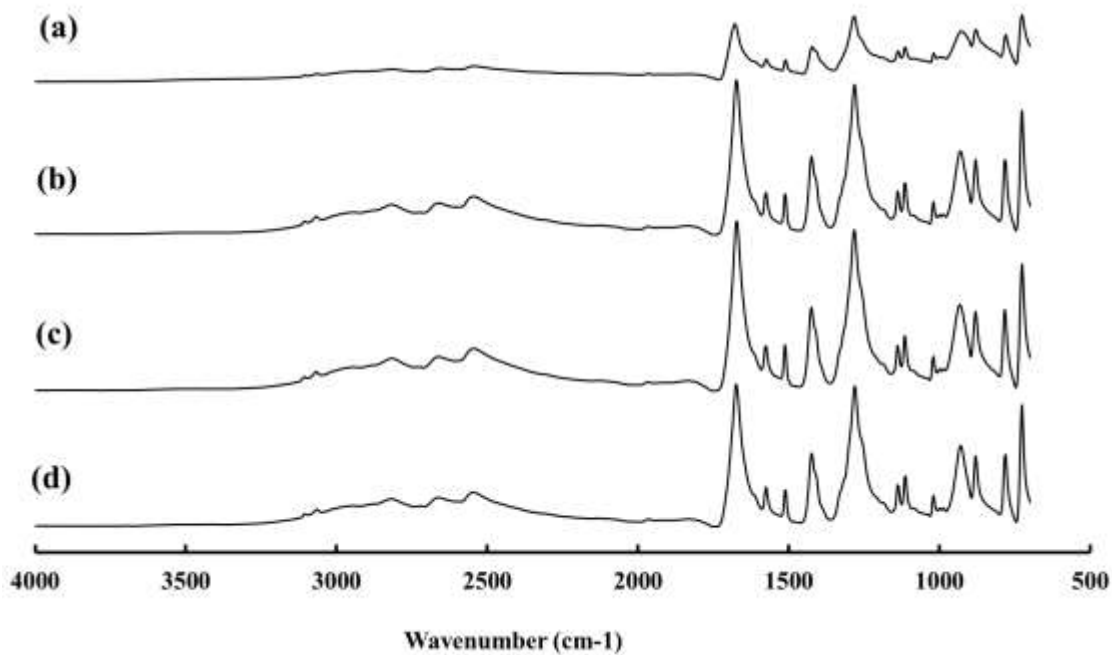


Figure 5-S1: FTIR spectra for (a) commercial TPA and the TPA recovered from PET hydrolysis with catalyst solutions of (b) PTSA, (c) 2-NSA, and (d) 1,5-NDSA.

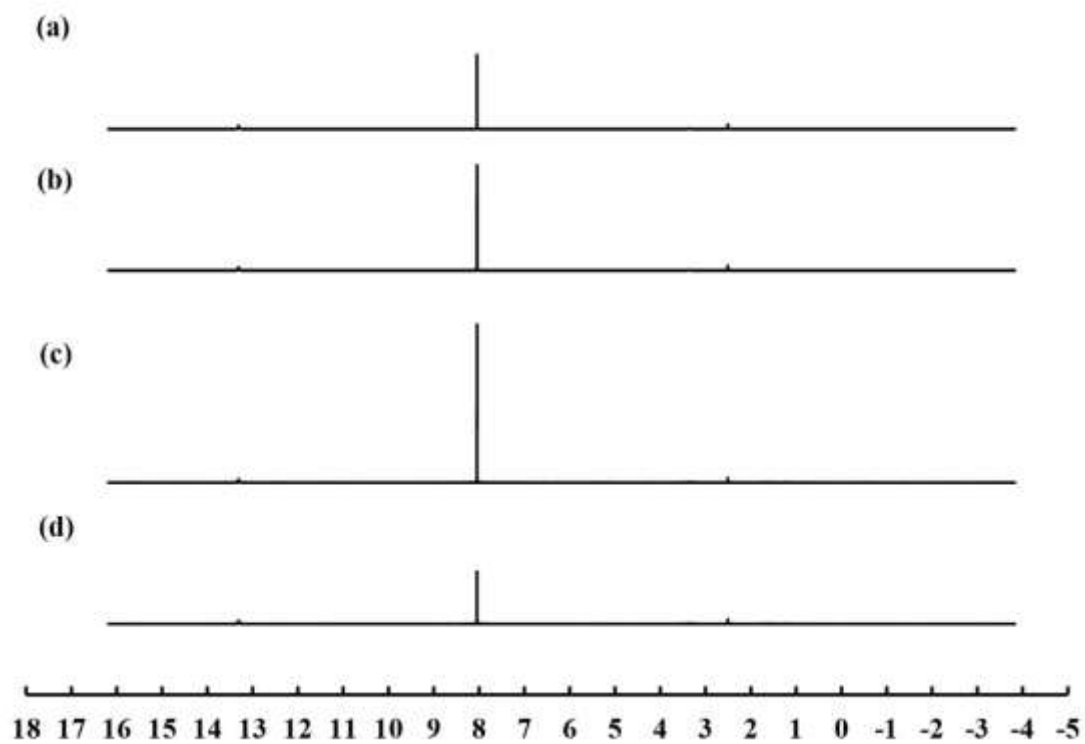


Figure 5-S2: ^1H NMR spectra for (a) commercial TPA and the TPA recovered from PET hydrolysis with catalyst solutions of (b) PTSA, (c) 2-NSA, and (d) 1,5-NDSA.

5.10.2 Effect of catalyst concentration on PET conversions (%)

Figure 5-S3 shows effect of concentration on PET conversion (%) results for PET hydrolysis with catalyst solutions of PTSA, 2-NSA, and 1,5-NDSA. The catalyst concentration was within the range of 1M to 4M with a reaction temperature of 150°C. The PET conversion (%) results are consistent with the TPA yield (%) results discussed in the manuscript. The PTSA and 2-NSA are the most active catalysts and 1,5-NDSA is the least active catalyst for PET hydrolysis.

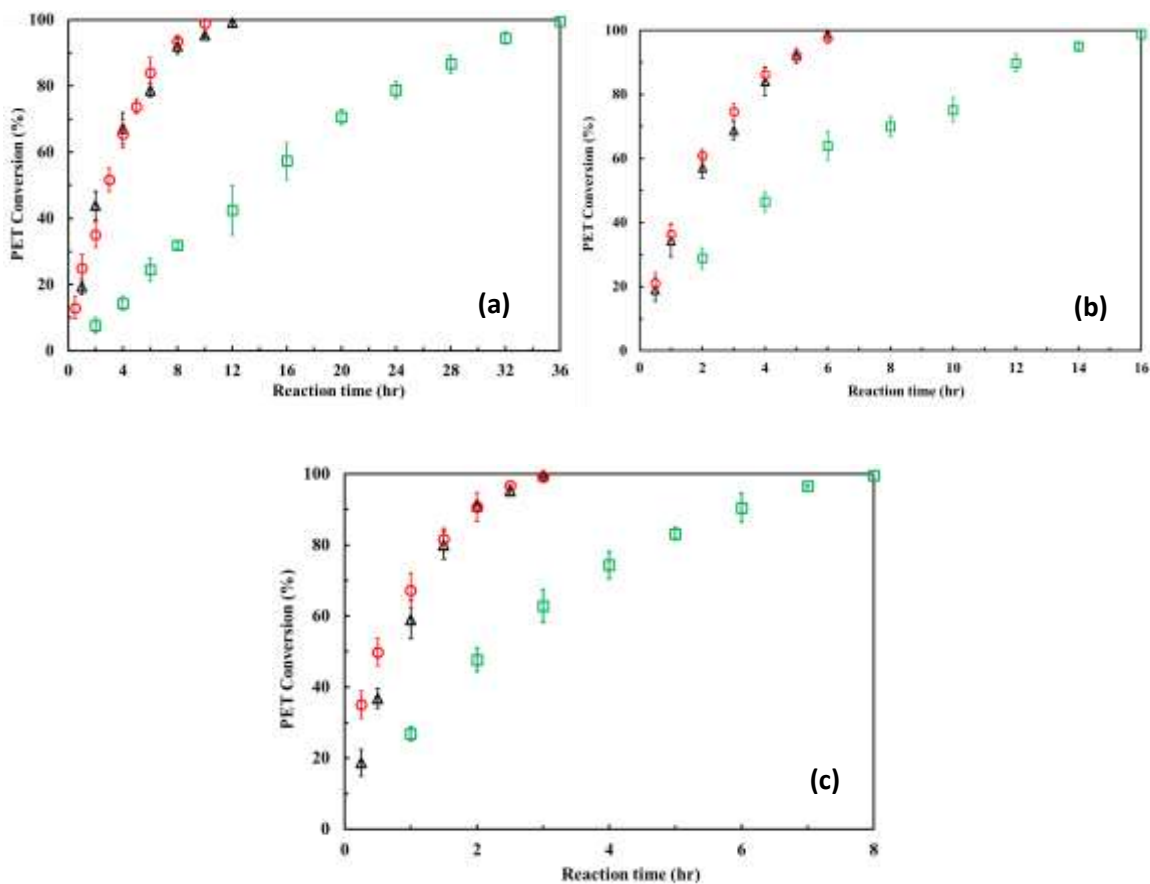


Figure 5-S3: Effect of catalyst concentration on PET conversion (%) at 150°C with (a) 1M, (b) 2M, and (c) 4M solutions of PTSA (○), 2-NSA (Δ) and 1,5-NDSA (□).

5.10.3 Reaction temperature effect on PET conversions (%), PET hydrolysis

Figure 5-S4 shows the effect of reaction temperature on PET conversion (%) for PET hydrolysis with 2M catalyst solutions of PTSA, 2-NSA, and 1,5-NDSA at 130°C, 140°C, and 150°C. The results are consistent with the TPA yield (%) results, the PET conversion (%) results reaffirm the reaction temperature increase will result in the faster PET hydrolysis.

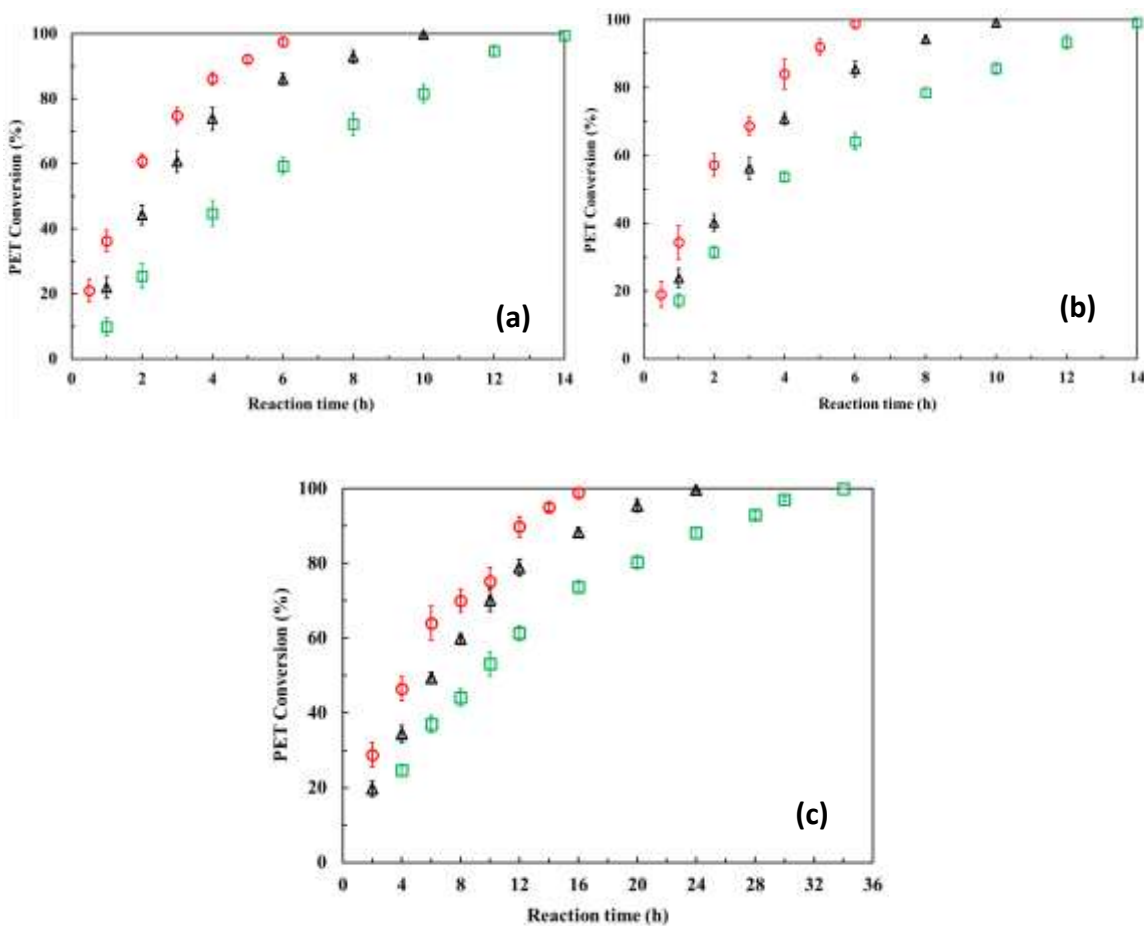


Figure 5-S4: Effect on the TPA yields for 2M catalyst solutions with (a) PTSA, (b) 2-NSA, and (c) 1,5-NDSA at 130°C (□), 140°C (Δ) and 150°C (○).

5.10.4 Fitting the shrinking core model to PET hydrolysis kinetic data

The shrinking core model was fitted to the TPA yields, obtained from PET hydrolysis with 1M and 4M catalyst solutions at the reaction temperature of 150°C, are presented in **Figure 5-S5** and **Figure 5-S6**, respectively. As shown, the level of model fit is good ($R^2 = 0.99$) for both cases of 1M and 4M catalysts solutions, used for PET hydrolysis.

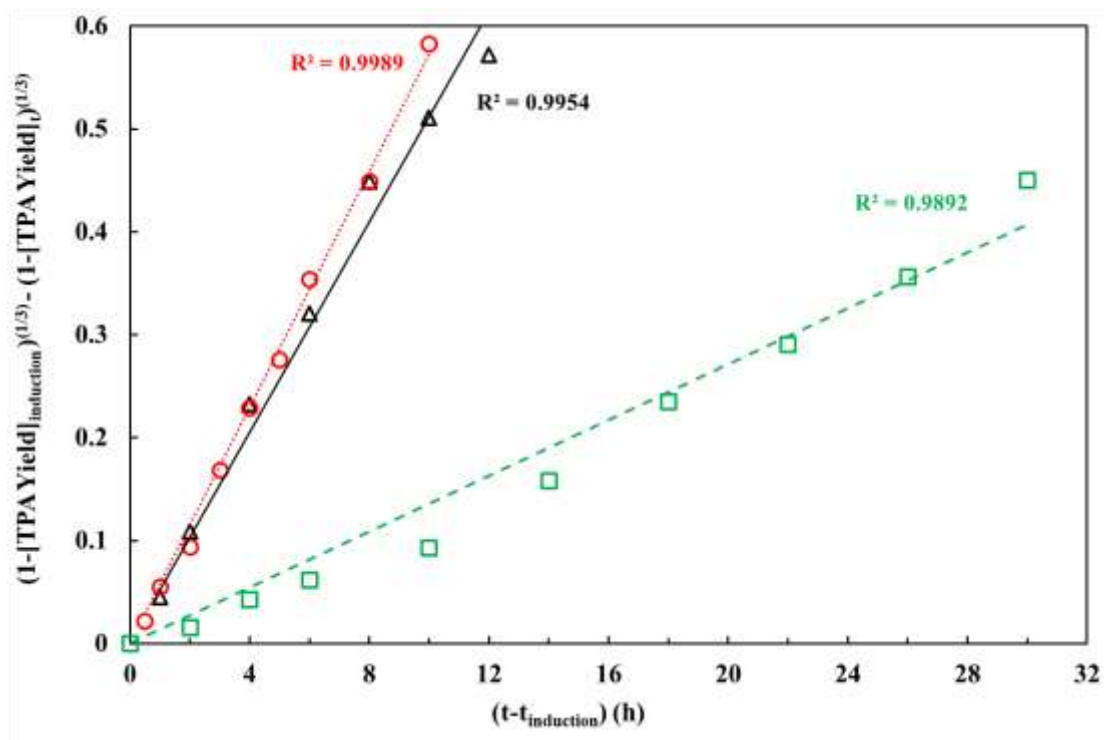


Figure 5-S5: Fit of shrinking core model to the kinetic data at 150°C for 1M catalyst solutions of PTSA (\circ , \dots), 2-NSA (Δ , —) and 1,5-NDSA (\square , ---).

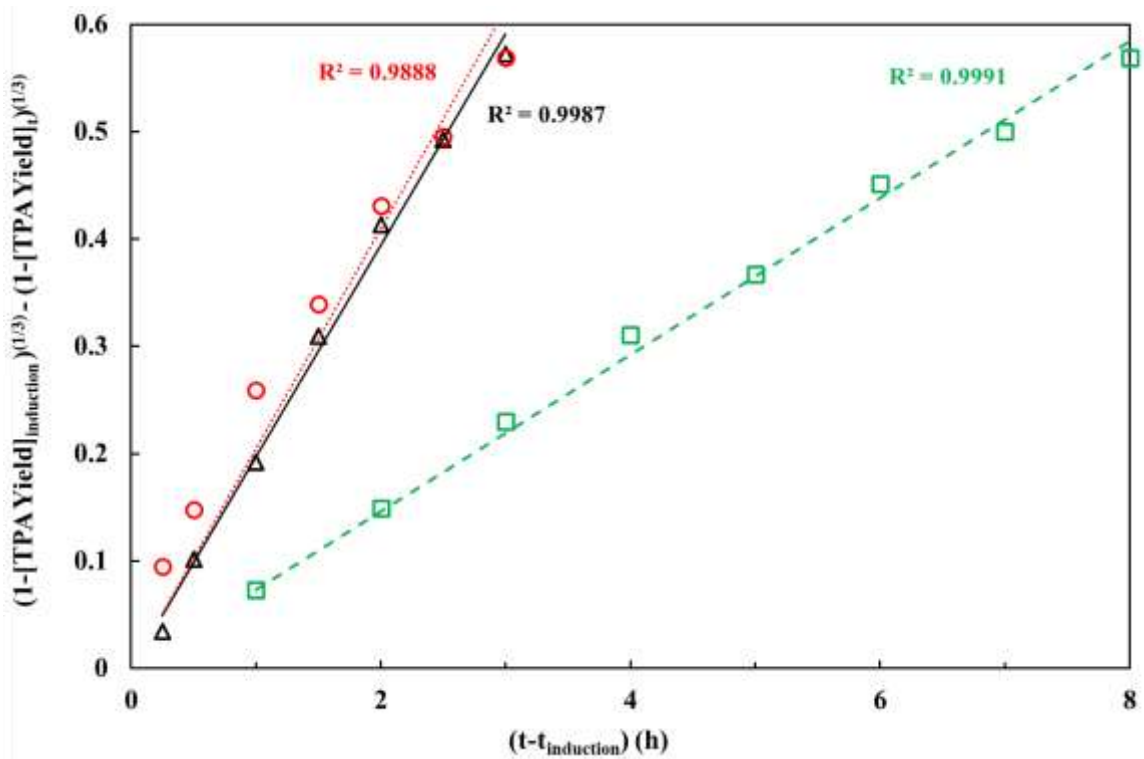


Figure 5-S6: Fit of shrinking core model to the kinetic data at 150°C for 4M catalyst solutions of PTSA (○, ...), 2-NSA (△, —) and 1,5-NDSA (□, ---).

Chapter 6

DBU-acid ionic liquids: transformation of weak acids to basic ionic liquids as more thermally stable and higher active catalysts for PET hydrolysis

6.1. Abstract

Acids may apply as catalysts for polyethylene terephthalate (PET) hydrolysis. However, the needed reaction time to achieve more than 90% TPA yield is generally longer than basic catalysts, specifically for weak acids and mineral acids. The 1,8-diazabicyclo [5.4.0] undec-7-ene (DBU) has been reported as a super basic catalyst for a fast hydrolysis of polycarbonates. In this work, DBU was tested for hydrolysis of PET, but was found it has a lower thermal stability than acid catalysts. So, the DBU-acid ionic liquids (ILs) were synthesized to obtain catalysts with higher thermal stability (than DBU) and activity (than their corresponding acids). The selected acids were sulfuric acid (H₂SO₄), Lactic acid (LA), Oxalic acid (OA), and citric acid (CA). These ionic liquids were characterized with the FTIR and NMR analyses to confirm the synthesized structure. The gathered kinetics data for hydrolysis of PET confirmed the ILs are more active than their corresponding acids and less active than DBU, but more thermally stable than DBU. This was furtherly confirmed by calculations of the reaction rate constants by applying a shrinking-core model.

This study shows DBU can considerably better acid catalysts by transforming them to the ILs.

6.2. Introduction

Polyethylene terephthalate (PET) is the main material used in bottles for packaging soft drinks and drinking water [98, 463]. It's also broadly used in textile and automotive industries for productions of fibers and automotive parts, respectively [464-466]. As these industry sectors have extended to fulfill the market needs, the production rate of PET has increased [467, 468]. The resources for PET production, which are mainly fossil fuels, are limited and may not support long term PET production [469, 470]. In addition, many PET products have short lifetimes and are piled up as PET wastes rapidly [471, 472]. So, managing these wastes is necessary to maintain a clean environment and may also provide an alternative resource for reproduction of PET products [37, 473]. For this purpose, recycling is proposed as an approach to manage PET wastes [116, 178, 474].

Among the reported recycling techniques, chemical recycling has recently received considerable attention because it can address complex PET waste streams and provide purified monomers for reuse in PET synthesis [115, 475-477]. The three major techniques of chemical recycling are glycolysis, methanolysis, and hydrolysis where glycolysis is the most studied one in literature [478-484]. Aside from the techniques, which are named based on the solvent type used for recycling of PET, the role of catalyst type on the rate of recycling is significant [485-487]. Extensive studies are reported for the catalysts that have been used for recycling of PET [18, 89, 117, 488-491]. Ionic liquids are a recent category of the catalysts that have gained attention due to high thermal stability and recoverability, especially for glycolysis of PET [161, 492-497].

There are few studies exploring ionic liquids for hydrolysis of PET [242, 497, 498]. This study has focus on hydrolysis of PET powder with a group of ionic liquids that are synthesized with 1,8-Diazabicyclo [5.4.0] undec-7-ene (DBU) as the coupling agent. The DBU was selected as it has exhibited great results for decomposing of polycarbonate [499, 500]. This study explored the possibility of transforming weak acids to DBU-weak acid ionic liquids that possess higher activity than weak acids as catalysts for hydrolysis of PET and higher thermal stability than DBU. Lactic acid (LA), oxalic acid (OA), and citric acid (CA) were chosen. In addition, the effects of catalyst concentration and reaction temperature on the rate of hydrolysis were studied.

6.3. Results and Discussion

6.3.1 The acidity of the individual components for hydrolysis of PET

The acidity value (pK_x) represents the capability of a component to release the proton (H^+) where x denotes the number and the order of the proton that releases in an aqueous solution, illustrated in **Table 6-1** for compounds used in this study [501, 502]. The H_2SO_4 and DBU are the strongest acid and base, respectively. LA, OA, and CA can be categorized as weak acids [503-505]. The selected acids were coupled with DBU, as a strong base, to form DBU-acid ionic liquids. The catalyst activity of the synthesized ionic liquids was compared with their corresponding acids.

Table 6-1: The acidity (pK_x) values of the tested components as catalysts for hydrolysis of PET. The values are based on dissociation in water at 25°C [501, 502].

Component	pK_1	pK_2	pK_3
DBU	13.5 ± 1.5	—	—
H ₂ SO ₄	-2.73	1.92	—
LA	3.86	—	—
OA	1.27	4.27	—
CA	3.13	4.76	6.40

6.3.2 TGA of the catalysts used for hydrolysis of PET

Thermogravimetric analysis (TGA) studies were conducted on the catalysts used for hydrolysis of PET including individual components DBU, LA, OA, and CA; DBU-acid ionic liquids synthesized in water; and DBU-acid ionic liquids synthesized in organic solvents. The TGA curves were gathered to determine the water content of the catalysts. This information was used in preparation of the solutions of catalysts with certain concentrations. The TGA curves are illustrated in **Figure 6-S1, Figure 6-S2, and Figure 6-S3 of Supporting Information**. The amount of water in these catalysts at room temperature, in weight percentage, are given in **Table 6-2**. W denotes the ionic liquids that were synthesized in water, either with equimolar (E) or titration (T) ratio of the DBU and

the acid. Moreover, the TGA curves showed the DBU-acid ionic liquids are thermally more stable than the DBU, which has complete decomposition at temperature of 200°C (**Figure 6-S1**).

Table 6-2: The water content of the catalysts, determined by TGA curves.

Catalyst	Water Content (wt.%)
DBU	6.33
H ₂ SO ₄	4.65
LA	6.86
OA	3.44
CA	7.96
DBU-SO ₄ -W	4.72
DBU-OA-E-W	5.20
DBU-OA-T-W	8.67
DBU-CA-E-W	4.21
DBU-CA-T-W	4.75
DBU-SO ₄	5.49
DBU-LA	3.01
DBU-OA	7.69
DBU-CA	3.34

6.3.3 Preliminary results for TPA yield (%) for 2M solutions of ionic liquids

The synthesized DBU-acid ionic liquids were tested for hydrolysis of PET when the catalyst solution, reaction temperature (T_R), and reaction time (t_R) were 2M, 150°C, and

10 hours, respectively. The TPA yield (%) for these reaction conditions are shown in **Table 6-3**. As observed, the DBU-acid ionic liquids that were synthesized in water didn't have sufficient activity to hydrolyze PET. So, the TPA yield (%) was zero. However, the DBU-acid ionic liquids that were prepared in organic solvent (methanol), except for DBU-SO₄ (acetonitrile as solvent), were comparatively more active and produced TPA in considerable amounts. For the DBU-OA and DBU-CA, the hydrolysis was completed within 10 hours.

Table 6-3: TPA yield (%) for 2M solutions of DBU-acid ionic liquids for hydrolysis of PET at T_R= 150°C and t_R= 10 hours.

Catalyst	TPA yield (%)
DBU-SO ₄ -W	0
DBU-OA-E-W	0
DBU-OA-T-W	0
DBU-CA-E-W	0
DBU-CA-T-W	0
DBU-SO ₄	0
DBU-LA	36
DBU-OA	90
DBU-CA	92

The titration graphs, proton or hydroxyl concentration versus catalyst concentration, for individual components are shown in **Figure 6-S4** and **Figure 6-S5** of the **Supporting Information**. The error bars indicate the three-time repetitions of the titration tests to show the reproducibility. As noted in **Figure 6-S4** and **Figure 6-S5**, the

correlation between the proton or hydroxyl concentration and catalyst concentration is linear for individual components.

Titration of the DBU-acid ionic liquids were conducted by using pH strip tapes. The results are shown in **Table 6-S1** through **Table 6-S8** in **Supporting Information**. As noted, the DBU-acid ionic liquids that were synthesized in water are weak acids with the pH values within the range of 1 to 7. Conversely, the DBU-acid ionic liquids that were synthesized in an organic solvent, except for DBU-SO₄, are weak bases with the pH values within the range of 7 to 10. The DBU-SO₄ is the same as the one prepared in water with respect to the pH values and the catalyst activity for hydrolysis of PET. The DBU-acid ionic liquids that were active for hydrolysis of PET are DBU-LA, DBU-OA, and DBU-CA produced using organic solvent. Therefore, the rest of the work was focused on study of these catalysts produced in organic solvent and comparison of activity of ionic liquids with the corresponding acids for hydrolysis of PET.

6.3.4 Effect of catalyst concentration hydrolysis kinetics at 150°C

6.3.4.1 Shrinking core model to fit the kinetics data of TPA yield

(%)

The shrinking core model was shown to fit the experimental data for acid hydrolysis of PET in chapters 4 and 5. This model was applied to the kinetic data for PET hydrolysis with catalyst solutions of 1M, 2M, and 4M at the series of different reaction times for the reaction temperature of 150°C. For instance, the fitted lines for the kinetics data gathered for PET hydrolysis in DBU solutions are illustrated in **Figure 6-1**. For the other tested catalysts, the fitting of shrinking-core model to the kinetics data of TPA yield (%) are

illustrated in **Figure 6-S6** and **Figure 6-S6** in **Supporting Information**. The model provided a good fit for all catalysts studied and was used to determine the rate constants reported in this chapter. Additionally, the shrinking core model was used to fit the data for all kinetic studies described below and are included in each of the graphs.

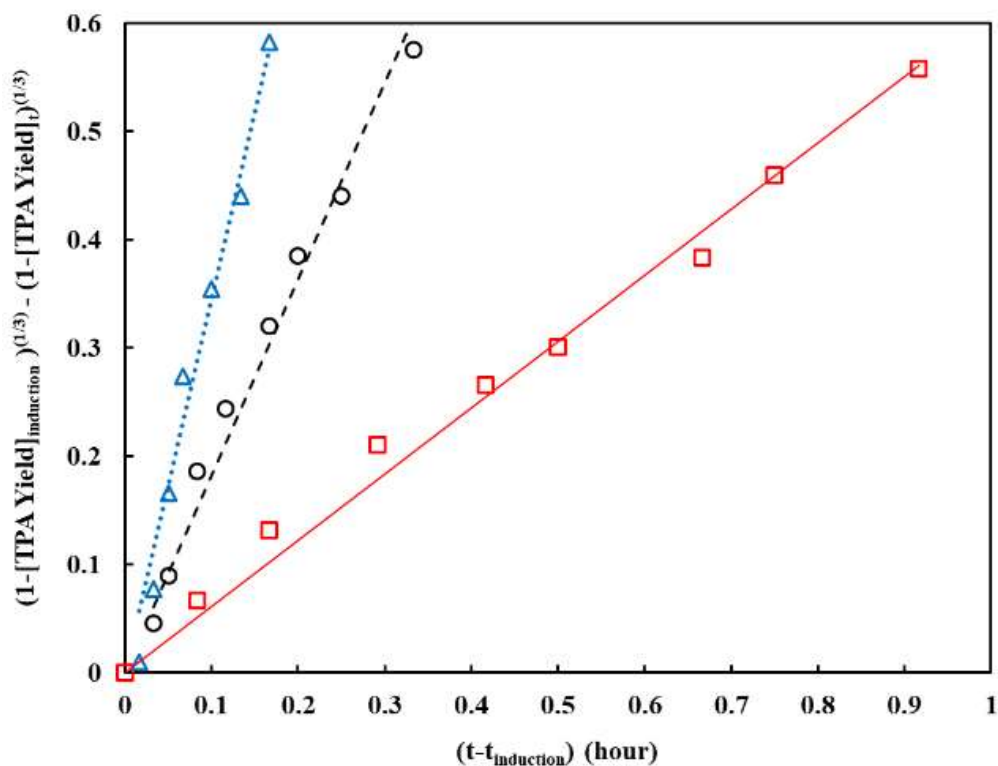


Figure 6-1: Fit of shrinking core model to the TPA yield kinetics data at $T_R = 150^\circ\text{C}$ for 1M (□, —), 2M (○, ---), and 4M (△, ...) solutions of DBU.

6.3.4.2 Comparison of catalytic activity DBU and organic acids at 150°C

The individual components of the DBU based ionic liquids were tested as catalysts for PET hydrolysis to set a baseline for comparison with the ionic liquids. The kinetics data in terms of TPA yield (%) in DBU solutions of 1M, 2M, and 4M at reaction temperature

of 150°C are given in **Figure 6-2**. The fitted lines to the kinetics data of TPA yield (%) were produced using the constants from the shrinking core model. The reaction times required to achieve more than 90% TPA yield (%) are 60 minutes, 20 minutes, and 10 minutes, for 1M, 2M, and 4M solutions of DBU. DBU was a highly active catalyst for hydrolysis of PET which is consistent with results from literature for hydrolysis of polycarbonate [499]. The primary challenge with DBU is that it is not easily recovered and limited thermal stability. The PET conversion (%) kinetics data are illustrated in **Figure 6-S8 of Supporting Information**.

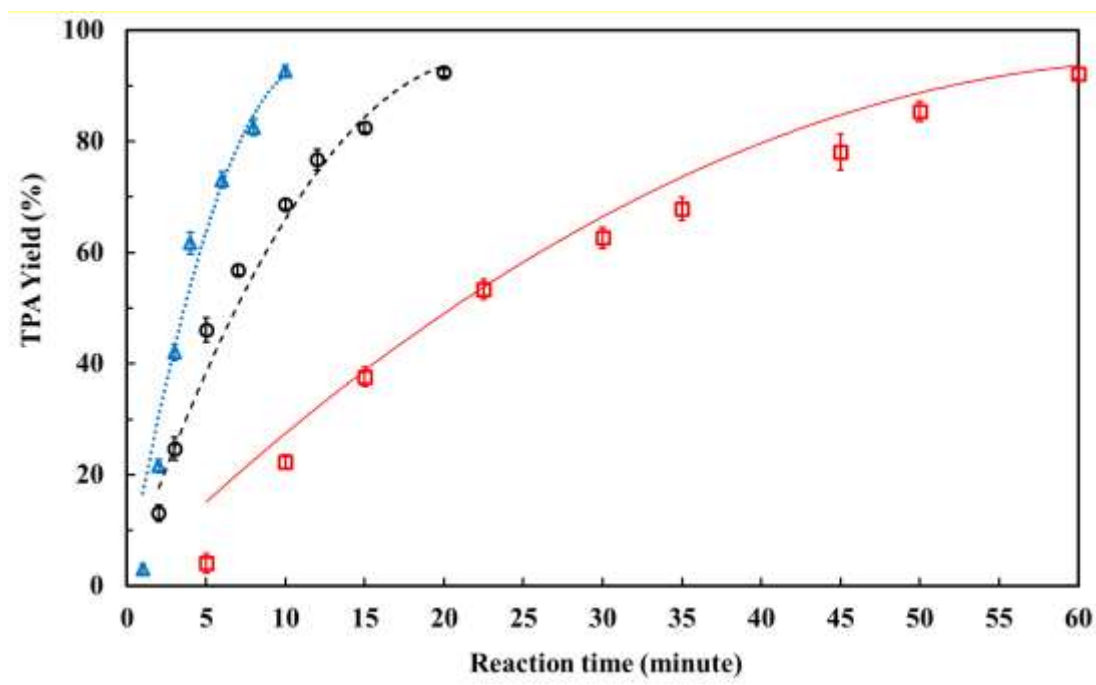


Figure 6-2: TPA yield kinetics data at $T_R=150^\circ\text{C}$ for 1M (\square , —), 2M (\circ , ---), and 4M (Δ , ...) solutions of DBU. The lines illustrate the fit of shrinking core model.

The kinetics data of TPA yield (%) for 1M, 2M, and 4M solutions of LA, OA, and CA are shown in **Figure 6-3 (a)**, **Figure 6-3 (b)**, and **Figure 6-3 (c)**, respectively. The fitted lines were obtained from applying the shrinking core model. As expected, an increase

in catalyst concentration leads to a decrease in the reaction time needed to achieve more than 90% TPA yield (%). For the case of 4M catalyst solutions, the needed reaction times for more than 90% TPA recovery are 12 days, 5 days, and 3 days for LA, OA, and CA, respectively. The CA solutions are more active than the LA and OA solutions since more protons (H^+) are released in CA solutions, causing more attacks occurring to the surface of PET particles with protons (H^+). This results in a higher activity of the catalyst for PET hydrolysis. The same scenario is repeated regarding the higher activity of the OA solutions than the LA solutions. Note that in all cases these weak acids are poor catalysts for PET hydrolysis. The kinetics data of the PET conversion (%) graphs are illustrated in **Figure 6-S9 of Supporting Information**.

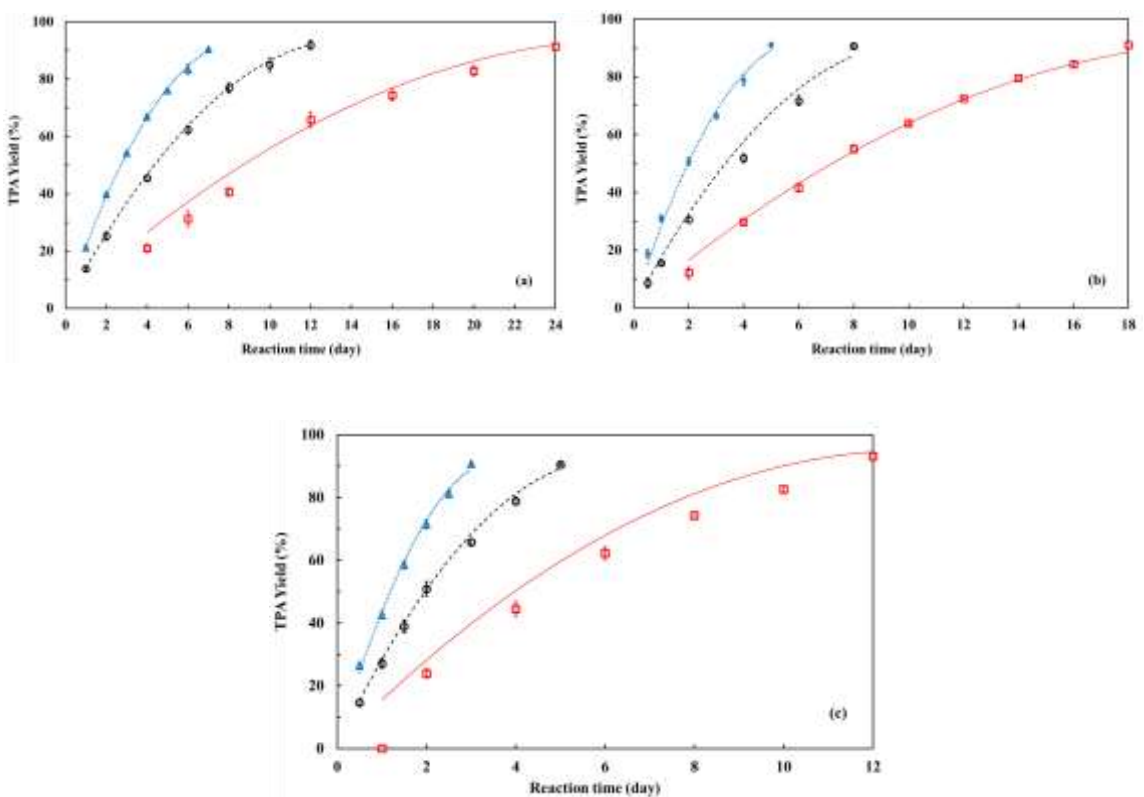


Figure 6-3: TPA yield kinetics data at $T_R=150^{\circ}C$ for (a) 1M, (b) 2M, and (c) 4M solutions of LA (\square , $—$), OA (\circ , $---$), and CA (Δ , \dots).

6.3.4.3 Catalytic activity of DBU-acid ionic liquids at 150°C

The kinetic data of TPA yield (%) for the solutions of DBU-acid ionic liquids are shown in **Figure 6-4**. The kinetics data of TPA yield (%) for 1M, 2M, and 4M aqueous catalyst solutions are shown respectively in **Figure 6-4 (a)**, **Figure 6-4 (b)**, and **Figure 6-4 (c)**. Again, as expected, an increase of catalyst concentration would decrease the reaction time needed to achieve more than 90% TPA yield (%).

The DBU-CA was more active than the DBU-OA and the DBU-OA is more active than the DBU-LA. For the case of 4M catalyst solutions, the required reaction times to achieve more than 90% TPA yield are 12 hours, 4 hours, and 1 hour. Similar results were seen for the lower catalyst concentrations. The DBU forms a complex with each of the carboxylic acid groups present in the weak acid structure. The DBU-CA has three active sites compared to two for the DBU-OA and one for the DBU-LA. Therefore, at a concentration of 1 M catalyst, the concentration of active sites would be 3 M for DBU-CA, 2 M for DBU-OA and 1 M for DBU-LA. The time to achieve 90% TPA yield at 4 M active site concentration for DBU-OA (2 M solution) and DBU-LA (4 M solution) were 7 and 12 hours, respectively. The 1 M DBU-CA system, which is equivalent to 3 M active groups, took 8 hours to achieve more than 90% TPA yield. Therefore, the increased activity of the DBU-OA cannot be solely attributed to the difference in concentration of active groups.

Additionally, the increased activity may be attributed to the number of amidine-benzene ring groups in the catalyst structure, which is 3, 2, and 1 for the DBU-CA, the DBU-OA, and the DBU-LA, respectively. The amidine-benzene group may improve affinity of the catalyst solution to the PET surface. This phenomenon was also observed

for PET hydrolysis [49] and cellulose hydrolysis [34] with aryl sulfonic acids as discussed in Chapter 5. Better wetting of the PET surface results in higher local concentration of the protons (H^+) in the case of acid hydrolysis and higher local concentration of the hydroxyls (OH^-) in the case of alkaline hydrolysis. Eventually, this higher localized number of protons or hydroxyls will increase the probability of the attack to the surface of PET particles, leading to higher activity of the catalyst solution [233, 242, 255, 506].

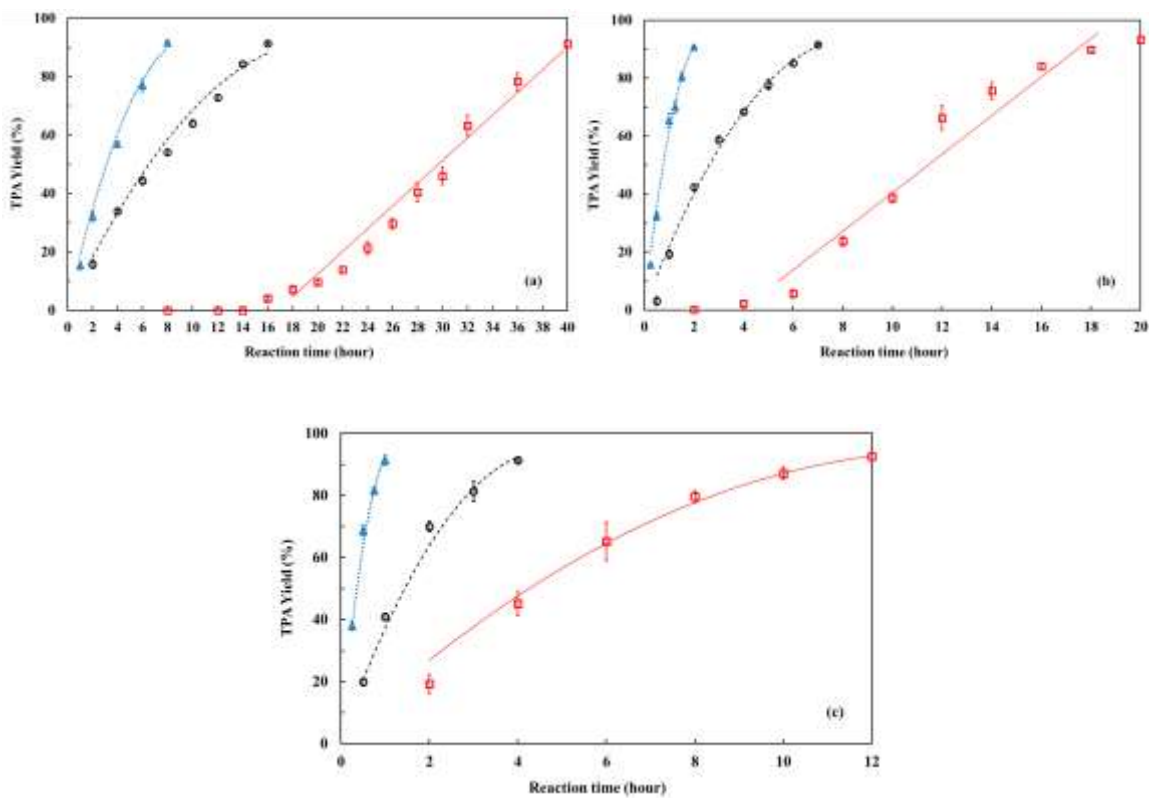


Figure 6-4: Effect of catalyst concentration on TPA yield at $T_R=150^\circ C$ for (a) 1M, (b) 2M, and (c) 4M solutions of DBU-LA (\square , —), DBU-OA (\circ , ---), and DBU-CA (Δ , ...).

The lines illustrate the fit of shrinking core model.

6.3.4.4 Comparison of times to achieve 90% TPA at 150°C

The reaction times (t_R) required to achieve more than 90% TPA yield (%) for PET hydrolysis at 150 °C are summarized in **Table 6-4**. The tested catalyst solutions had 1M, 2M, and 4M concentrations. This needed reaction time has the broad range, starting from 10 minutes for 4M DBU solution to 24 days for 1M LA solution. As presented, the weak acids are considerably less active than their corresponding DBU-acid ionic liquids for PET hydrolysis. This shows that the synthesis of DBU-acid ionic liquids will help the increase of the catalyst activity enormously for PET hydrolysis.

Table 6-4: Reaction time needed to achieve more than 90% TPA yield at $T_R=150^\circ\text{C}$.

Catalyst type	Concentration (M)		
	1M	2M	4M
Reaction time (t_R)			
DBU	60 minutes	20 minutes	10 minutes
LA	24 days	18 days	12 days
OA	12 days	8 days	5 days
CA	7 days	5 days	3 days
DBU-LA	40 hours	20 hours	12 hours
DBU-OA	16 hours	7 hours	4 hours
DBU-CA	8 hours	2 hours	1 hour

6.3.4.5 Reaction rate constants for catalysts studied at 150°C

The shrinking core model was applied to determine the apparent reaction rate constants (K_a values) for all tested catalysts (see **Table 6-5**). DBU solutions have the highest K_a values consistent with the presented kinetics data for TPA yield (%) and PET conversion (%). The acids of LA, OA, and CA were the least active catalysts, respectively. The DBU-acid ionic liquids were in the middle between DBU and the acids, but considerably have higher K_a values than their corresponding acids. The specific reaction rate constants (k_{sp} values) were calculated from the K_a values versus the catalyst concentration and are reported in **Table 6-S9** of the **Supporting information**. The k_{sp} values indicate the DBU as the highest active catalyst and confirms the DBU-acid ionic liquids as the considerably more active catalysts than their corresponding acids.

Table 6-5: Apparent reaction rate constants (K_a) as a function of the catalyst concentration for PET hydrolysis at 150°C.

Cat.	DBU	LA	OA	CA	DBU-LA	DBU-OA	DBU-CA
Con. (M)	* K_a (h ⁻¹)	* K_a (h ⁻¹)	* K_a (h ⁻¹)	* K_a (h ⁻¹)	* K_a (h ⁻¹)	* K_a (h ⁻¹)	* K_a (h ⁻¹)
1	61.21	0.10	0.20	0.32	1.21	3.19	6.69
2	181.75	0.12	0.26	0.42	3.07	7.97	27.53
4	345.47	0.22	0.44	0.73	4.9	14.47	57.54

* K_a values are multiplied by 100.

6.3.5 Effect of reaction temperature on TPA yield (%), 2M catalyst solutions

6.3.5.1 Shrinking core model to fit the kinetics data of TPA yield (%)

The effect reaction temperatures were 130°C, 140°C, and 150°C. The shrinking core model was used to fit the gathered kinetic data for TPA yield (%) in PET hydrolyses with 2M solutions of the catalysts. For DBU, the model fitted lines to the TPA yield (%) kinetics data are illustrated in **Figure 6-5**. For the other tested catalysts, the model fitted lines are brought in **Figure 6-S10** and **Figure 6-S11**.

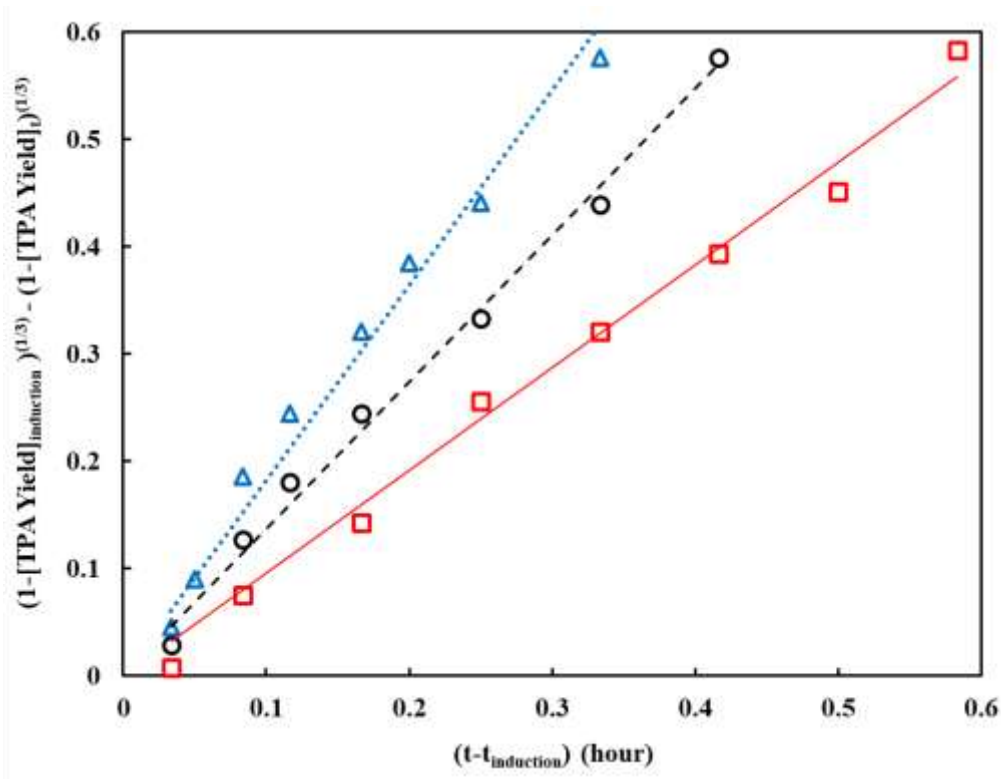


Figure 6-5: Fit of shrinking core model to the TPA yield (%) kinetics data for 2M solutions of DBU at $T_R= 130^\circ\text{C}$ (\square , —), $T_R= 140^\circ\text{C}$ (\circ , ---), and $T_R= 150^\circ\text{C}$ (Δ , ...).

6.3.5.2. Reaction kinetics for 2 M DBU and acid solutions

The 2M solutions of the DBU, LA, OA, and CA were tested as catalysts for PET hydrolysis at 130°C, 140°C, and 150°C were considered to observe the reaction temperature effect on the rate of hydrolysis. The TPA yield (%) for PET hydrolysis in 2M solutions of DBU are depicted in **Figure 6-6**. The lines were obtained by applying the shrinking core model to the kinetic data. As expected, the fastest hydrolysis to achieve more than 90% TPA yield was occurred at reaction temperature of 150°C in 20 minutes. The kinetics data of the TPA yield (%) for PET hydrolysis in the 2M solutions of LA, OA, and CA are illustrated in **Figure 6-7**. The kinetics data of PET conversion (%) for DBU and other individual components are illustrated in **Figure 6-S12** and **Figure 6-S13** of **Supporting Information**, respectively.

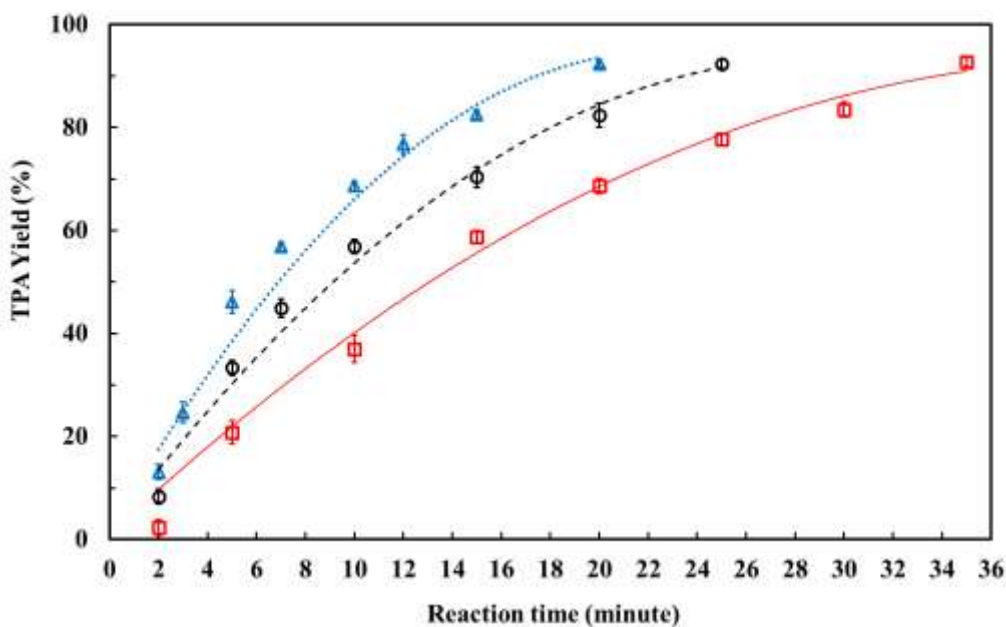


Figure 6-6: TPA yield kinetics data for 2M solutions of DBU at $T_R=130^\circ\text{C}$ (\square , —), $T_R=140^\circ\text{C}$ (\circ , ---), and $T_R=150^\circ\text{C}$ (Δ , ...) solutions of DBU. The lines illustrate the fit of shrinking core model.

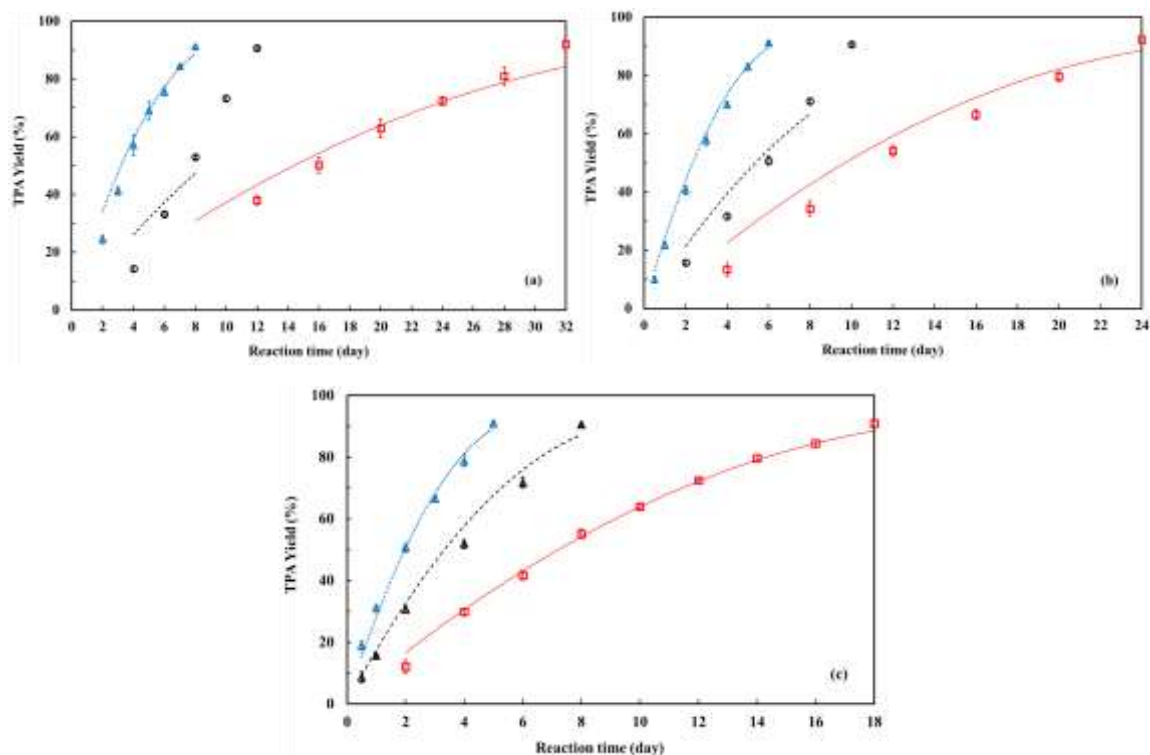


Figure 6-7: Effect of reaction temperature on TPA yield at (a) $T_R=130^\circ\text{C}$, (b) $T_R=140^\circ\text{C}$, and (c) $T_R=150^\circ\text{C}$ for 2M solutions of LA (\square , —), OA (\circ , ---), and CA (Δ , ...). The lines illustrate the fit of shrinking core model.

6.3.5.3. Reaction kinetics for 2 M DBU-acid ionic liquids

The TPA yield (%) for the 2M solutions of the DBU-acid ionic liquids are illustrated in **Figure 6-8**. The kinetics data of TPA yield for the reaction temperatures of 130°C , 140°C , and 150°C are shown in **Figure 6-8 (a)**, **Figure 6-8 (b)**, and **Figure 6-8 (c)**, respectively. As expected, an increase in the reaction temperature resulted in an increase in the rate of hydrolysis for PET particles. While the rate of reaction increased with increasing temperature for DBU-LA, there was still a significant incubation time prior to onset of the reaction.

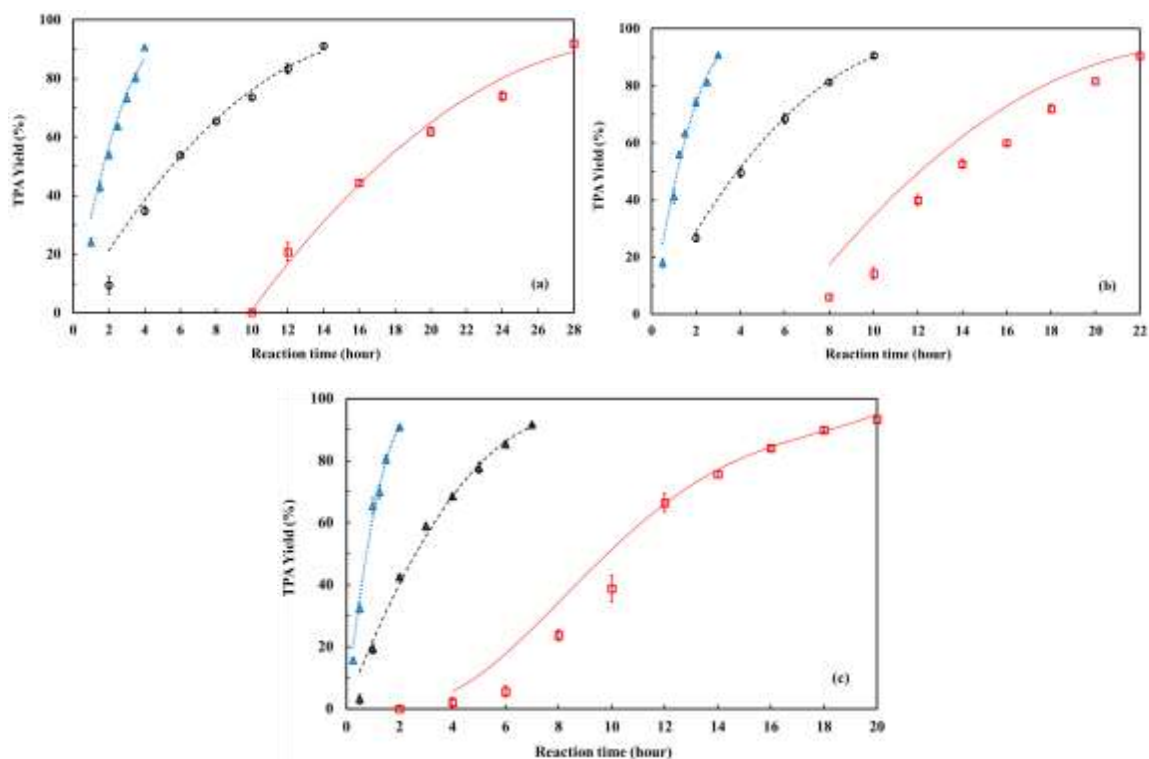


Figure 6-8: Effect of reaction temperature on TPA yield at (a) $T_R=130^\circ\text{C}$, (b) $T_R=140^\circ\text{C}$, and (c) $T_R=150^\circ\text{C}$ for 2M solutions of DBU-LA (\square , —), DBU-OA (\circ , ---), and DBU-CA (Δ , ...). The lines illustrate the fit of shrinking core model.

6.3.5.4. Time to achieve 90% TPA yield for 2 M solutions of catalysts

The reaction times required to achieve more than 90% TPA yield (%) for the 2M solutions are summarized in **Table 6-6**. The reaction temperature of 150°C had the highest effect on the increase of the rate for PET hydrolysis. The DBU is the most active catalyst while the DBU-acid ionic liquids are considerably more active catalysts than their corresponding acids.

Table 6-6: Reaction time needed to achieve more than 90% TPA yield for 2M catalyst solutions at reaction temperature of 130°C, 140°C and 150°C.

2M Catalyst Solutions	Reaction temperature (°C)		
	130	140	150
Reaction time (t_R)			
DBU	35 minutes	25 minutes	20 minutes
LA	32 days	24 days	18 days
OA	12 days	10 days	8 days
CA	8 days	6 days	5 days
DBU-LA	28 hours	22 hours	20 hours
DBU-OA	14 hours	10 hours	7 hours
DBU-CA	4 hours	3 hours	2 hours

6.3.5.5 Reaction rate constants at 2 M catalyst solution

The shrinking core model was used to determine the apparent reaction rate constants (K_a values) of the 2M catalysts solutions for PET hydrolysis, as shown in **Table 6-7**. The K_a values are consistent with the kinetics data for the TPA yield (%), illustrated in **Figure 6-6**, **Figure 6-7**, and **Figure 6-8**. The DBU has the highest K_a values as the most active catalyst while the LA has the least value of K_a as the least active catalyst. The DBU-acid ionic liquids have K_a values considerably higher than their corresponding acid catalysts. Same scenario is valid for the specific reaction rate constants (k_{sp} values) that are brought in **Table 6-S10** of the **Supporting Information**.

Table 6-7: Apparent reaction rate constant (K_a values) as a function of the reaction temperature for 2M catalyst solutions for PET hydrolysis.

2M Catalyst Solution	DBU $*K_a$ (h ⁻¹)	LA $*K_a$ (h ⁻¹)	OA $*K_a$ (h ⁻¹)	CA $*K_a$ (h ⁻¹)	DBU-LA $*K_a$ (h ⁻¹)	DBU-OA $*K_a$ (h ⁻¹)	DBU-CA $*K_a$ (h ⁻¹)
130	95.71	0.06	0.10	0.27	2.92	3.77	12.26
140	136.83	0.09	0.16	0.37	3.64	5.37	17.93
150	181.80	0.12	0.26	0.44	4.05	7.97	27.53

** K_a values are multiplied by 100.*

6.3.5.6 Activation energy for 2M solutions of catalysts

The logarithmic form of the Arrhenius equation (**Equation 6-1**) was used to calculate the values of apparent activation energy (E_a) for PET hydrolysis with 2M solutions of the catalysts [285, 290].

$$\ln(k_{sp}) = \ln A - \frac{E_a}{RT} \quad (6-1)$$

Where the terms k_{sp} , A , E_a , R , and T are specific reaction rate constant, pre-exponential factor, activation energy, universal gas constant, and absolute reaction temperature. The fitted lines to the k_{sp} values as a function of the absolute reaction temperature for hydrolysis of PET with 2M solutions of the catalysts are illustrated in **Figure 6-9**. The activation energy shown in **Table 6-8**, are in the range of 23 KJ.mol⁻¹ to 68 KJ.mol⁻¹. The range corresponds with some of the reported activation energy values of the catalysts used for the degradation of PET [49, 238, 283, 315].

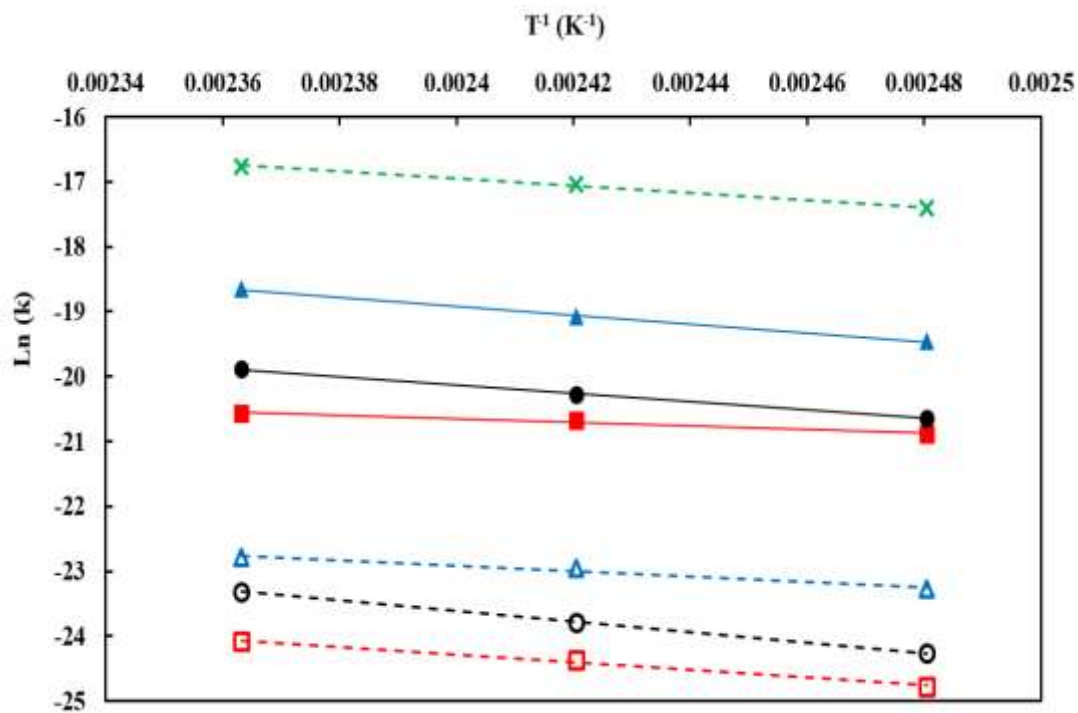


Figure 6-9: Fitted lines of Arrhenius equation for 2M solutions of DBU (x, ---), LA (□, ---), OA (○, ---), CA (Δ, ...), DBU-LA (□, ---), DBU-OA (○, ---), DBU-CA (Δ, ---).

Table 6-8: activation energies for 2M solutions of the tested catalysts for PET hydrolysis.

Catalyst type	E_a (KJ.mol ⁻¹)
DBU	45.5
LA	49.2
OA	67.7
CA	34.7
DBU-LA	23.3
DBU-OA	53.1
DBU-CA	57.3

6.3.6 Wetting studies of the tested catalysts for hydrolysis of PET

The wetting studies were conducted by measuring the contact angle value that is formed by a droplet of the solution of catalyst on the surface of PET film. A range of catalyst concentration were tested, as reported in literature, to explore the effect of catalyst concentration on contact angle value, and subsequently on the extent of surface wetting [507-509].

For DBU solutions, it was observed that the droplets wetted the surface completely. For instance, the evolution of a droplet of 0.25 M DBU solution on the PET films is illustrated in **Figure 6-10**. As shown, the droplet wetted the surface completely. After one second that the droplet was placed on the surface, it rapidly formed an oval shape that extended completely throughout the surface within next six second. Then, the droplet moved forward and reached the surface edges. This could be one of the reasons that DBU is super active catalyst in hydrolysis of PET, as witnessed by the presented kinetics data of PET conversion (%) and TPA yield (%).

The droplets of solutions of LA, OA, and CA on PET surface are illustrated in **Figure 6-11**. As shown, for solutions of the weak acids, the shape of the droplets didn't change tangibly with respect to the acid concentration. The droplets of solutions of DBU-acid ionic liquids are illustrated in **Figure 6-12**. With an increase in catalyst concentration, the droplet stretches further on the surface, indicating better wetting of the surface by catalyst solution. This is consistent with surface wetting with the aryl sulfonic acids with hydrophobic pendant groups as catalysts for hydrolysis of PET discussed in Chapter 5 [49].

The contact angle values for these catalysts as a function of catalyst concentration are shown in **Figure 6-13**. As observed, solutions of weak acids are quite independent of the catalyst concentration and maintains a constantly average values between 76 and 78 °. For DBU-acid ionic liquids, the contact angle values decrease with the increase of catalyst concentration, consistent with what's observed regarding the extension of droplet on the surface. The contact angle values for DBU-acid ionic liquids were within the approximate range of 50- 65 degrees, indicating the better wetting of surface compared to the acids.

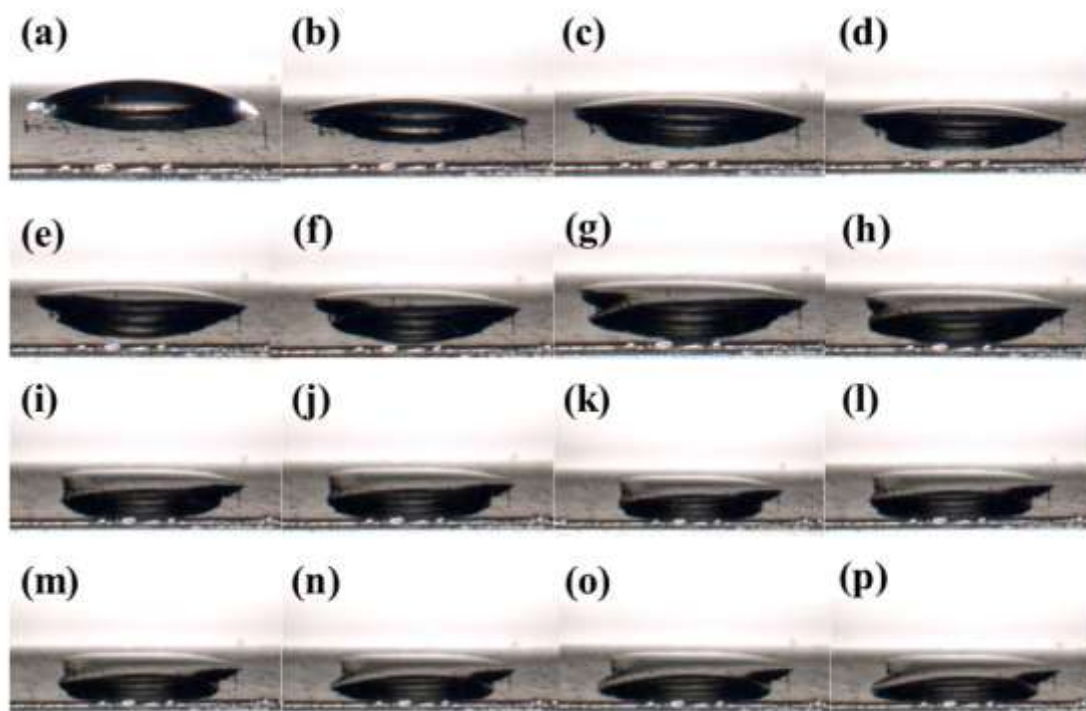


Figure 6-10: Evolution of the 0.25M solution of DBU droplet within the wetting process of the surface on the PET films at (a) $t = 1$ s, (b) $t = 3$ s, (c) $t = 5$ s, (d) $t = 7$ s, (e) $t = 9$ s, (f) $t = 11$ s, (g) $t = 13$ s, (h) $t = 15$ s, (i) $t = 27$ s, (j) $t = 39$ s, (k) $t = 51$ s, (l) $t = 63$ s, (m) $t = 75$ s, (n) $t = 87$ s, (o) $t = 99$ s, (p) $t = 111$ s.

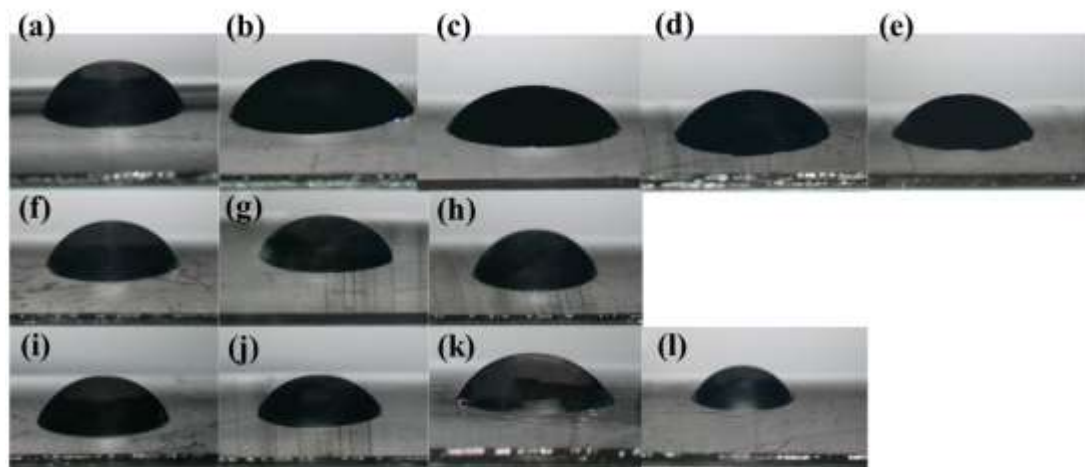


Figure 6-11: The droplet shape of solutions of weak acids on the PET films for LA: (a) 0.25M, (b) 0.5M, (c) 1M, (d) 1M, (e) 4M; OA: (f) 0.25M, (g) 0.5M, (h) 1M; CA: (i) 0.25M, (j) 0.5M, (k) 1M, (l) 2M.

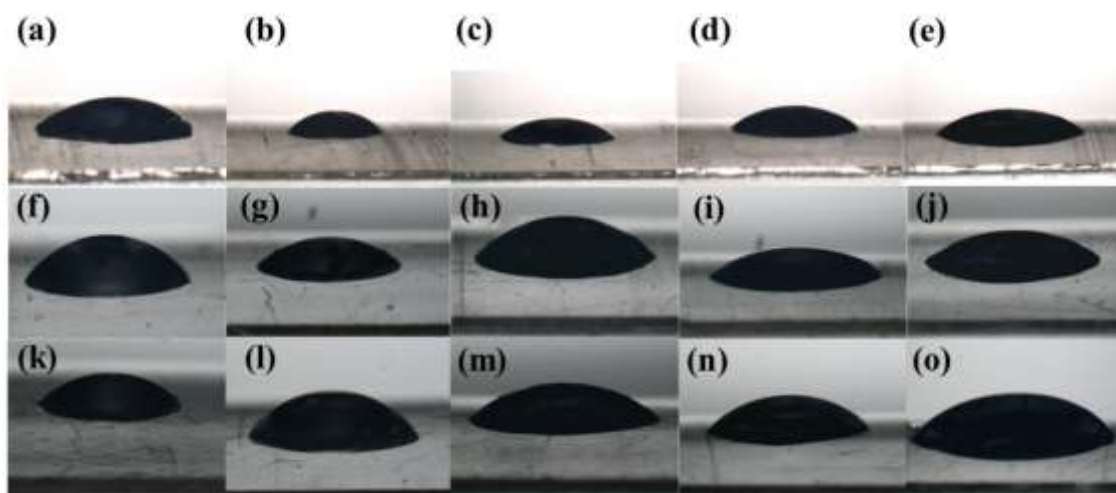


Figure 6-12: The droplet shape of solutions of DBU-acid ionic liquids on the PET films for DBU-LA: (a) 0.25M, (b) 0.5M, (c) 1M, (d) 1M, (e) 4M; DBU-OA: (f) 0.25M, (g) 0.5M, (h) 1M, (i) 2M, (j) 4M; DBU-CA: (k) 0.25M, (l) 0.5M, (m) 1M, (n) 1M, (o) 4M.

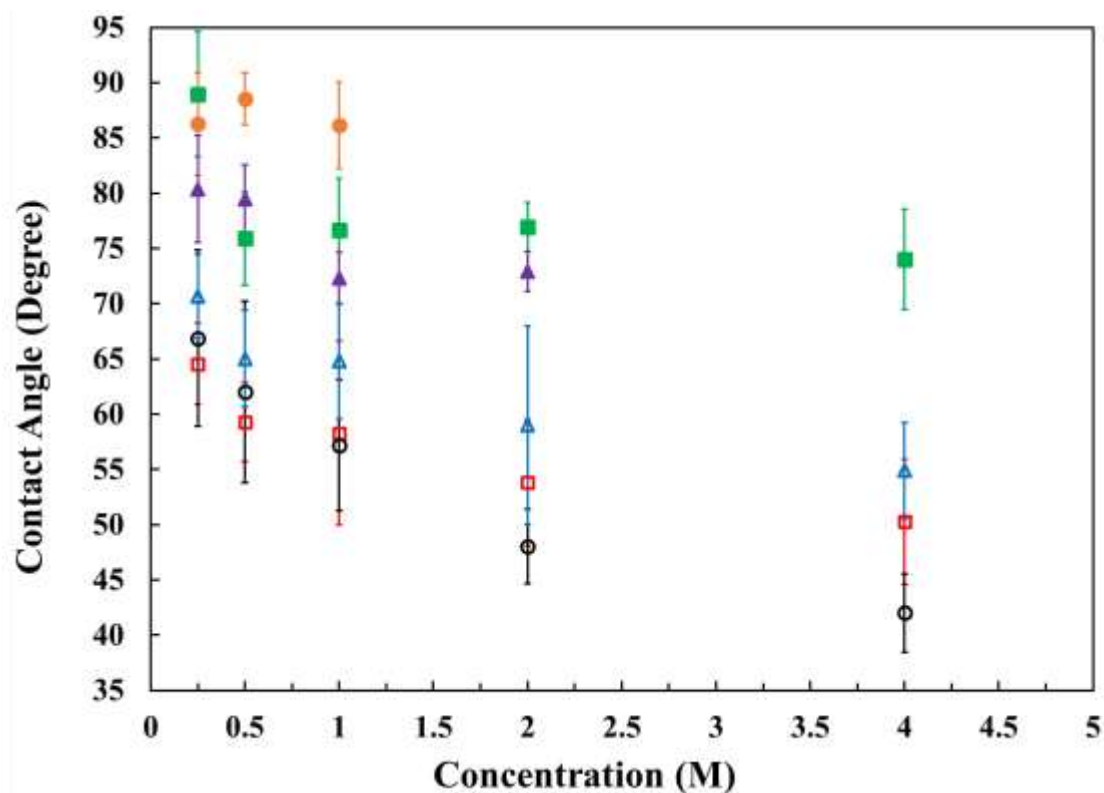


Figure 6-13: The contact angle values as a function of the concentration of catalyst solution for LA (■), OA (●), CA (▲), DBU-LA (□), DBU-OA (○), and DBU-CA (△).

6.4 Comparison with ionic liquids reported as catalysts for hydrolysis of PET

The DBU-acid catalysts that were introduced in this work are compared with the reported ionic liquids that were used for hydrolysis of PET in **Table 6-9**. As noted, the DBU-acid ionic liquids presented in this work may hydrolyze PET milder reaction conditions than the ones reported in literature [242, 498, 510].

Table 6-9: Comparison of this study with the reported ionic liquids as catalysts for hydrolysis of PET.

Catalyst type	Concentration (M)	PET shape/ size_(avg.) (µm)	T_R¹ (°C)	P_R² (atm)	t_R³ (hour)	TPA yield (%)	Ref.
[Hexanemim][HSO ₄]	2	Particle/ NR	185	N/R	3	79	[510]
1-(3-propylsulfonic)-3-methylimidazolium chloride	1	Powder/ NR	210	N/R	24	94	[242]
[bmim]Cl	NR	Pellets / NR	170	1	7	0	[498]
DBU	1	Powder/ 302	150	~5	1	91	This study
DBU-LA	4	Powder / 302	150	~5	20	90	This study
DBU-OA	4	Powder / 302	150	~5	4	92	This study
DBU-CA	2	Powder / 302	150	~5	2	91	This study

DBU-CA	4	Powder / 302	150	~5	1	91	This study
--------	---	--------------	-----	----	---	----	---------------

¹ T_R: reaction temperature, ² P_R: reaction pressure, ³ t_R: reaction time

6.5 Conclusions

This study introduced DBU-acid ionic liquids as catalysts for hydrolysis of PET. The solvent used during formation of the DBU-acid ionic liquids had an effect on the acidity of the synthesized DBU-acid ionic liquids as shown by titration studies. Methanol was the solvent where DBU-acid ionic liquids were synthesized as bases and were considerably more active than the DBU-acid ionic liquids synthesized in water as the solvent. In addition, the DBU-acid ionic liquids synthesized in methanol were thermally more stable than DBU and were considerably more active than their corresponding acids that were coupled with DBU in the synthesis of ionic liquids.

The shrinking core model could be used to fit the experimental kinetics data gathered for TPA yields (%) of hydrolysis tests. This is consistent with the reaction occurring at the PET surface of the particles and the reports in literature [148, 511-514]. The reaction rate constants reflect the higher values for DBU-acid ionic liquids synthesized in methanol in comparison with their corresponding acids, i.e., LA, OA, and CA. The wetting studies of the tested catalysts revealed that DBU-acid ionic liquids wetted the surface of PET films more than their corresponding acids, consistent with what was obtained for the kinetics data. Moreover, the proposed DBU-acid ionic liquids in this work were compared with the ionic liquids reported for hydrolysis of PET, indicating the higher activity of these catalysts comparatively in milder reaction conditions.

Chapter 7

Conclusions and Future Work

7.1. Conclusions

7.1.1 Overall outcomes for hydrolysis of PET with presented catalysts

Hydrolysis is one of the primary techniques for chemically recycling PET wastes [42, 515, 516]. In hydrolysis, a catalyst is added to an aqueous solution to increase the rate of PET decomposition [27, 240]. As a heterogenous reaction, the rate of hydrolysis can be controlled by many factors including reaction conditions, sample shape and size, catalyst type, and catalyst concentration. The impact of these factors has been explored extensively in the literature [255, 462, 517-520]. However, the extent of wetting of the surface of PET particles with catalyst solutions as an approach to increase the rate of hydrolysis has been explored in less detail [43, 49, 233, 521]. This study introduced a series of catalysts that were designed to increase the wetting of the surface by the reaction media for PET particles and/or increase activity of catalyst. The goal was to allow operation at milder reaction conditions or shorter time than reported for PET hydrolysis [49, 290, 291, 518]. The effect of catalyst concentration (1M, 2M, and 4M) and the reaction temperature (130°C, 140°C, and 150°C) for 2M catalyst solutions on the rate of hydrolysis reactions for recycling of PET particles were explored.

In the first part of the dissertation [43], hydrolysis kinetics studies revealed that poly (4-styrenesulfonic acid) (PSSA) was a more active catalyst than sulfuric acid (H_2SO_4), the conventional mineral acid catalyst applied for hydrolysis of PET. It was also observed the induction times experienced in the kinetics data of PET hydrolysis with H_2SO_4 were shorter for PET hydrolysis with PSSA. This was attributed to the better wetting of the surface of the PET particles with PSSA solutions than H_2SO_4 solutions.

PSSA has a hydrophobic aliphatic backbone that can interact with PET and hydrophilic aryl sulfonic acid pendant groups. The PSSA can act as a surfactant in aqueous solution to modify the surface wetting of the PET particles during hydrolysis [43, 316, 522]. This leads to higher local concentration of the acid sites near PET particles, which can result in higher activity of the catalyst. Contact angle measurements confirmed better wetting of the surface with the PSSA solutions, which was consistent with the improved reaction kinetics for hydrolysis of PET with PSSA relative to H_2SO_4 . The shrinking core model was applied to fit kinetic data of TPA yield (%) to determine the reaction rate constants of the PSSA and H_2SO_4 [290, 292, 523]. It was noted that the model could be applied to fit the experimental data, specifically for data after the induction time portion. The apparent activation energies were $24.6 \text{ kJ}\cdot\text{mol}^{-1}$ and $29.1 \text{ kJ}\cdot\text{mol}^{-1}$ for 2M catalyst solutions of PSSA and H_2SO_4 , respectively [43].

To study the impact of catalyst on hydrolysis in homogenous solution, ethyl acetate was hydrolyzed in water with PSSA and H_2SO_4 [524, 525]. The activation energies for hydrolysis of ethyl acetate were $53.8 \text{ kJ}\cdot\text{mol}^{-1}$ and $39.6 \text{ kJ}\cdot\text{mol}^{-1}$ for 0.5M solutions of PSSA and H_2SO_4 , respectively. This higher activation energy of PSSA may have been due to lower accessibility to the exposed acid sites of PSSA in a homogenous reaction, which may

come from its considerable bigger size than H_2SO_4 [43]. Moreover, reutilization and titration results proved PSSA was a recoverable and reusable catalyst for PET hydrolysis (up to 5 cycles), consistent with literature report about the recoverability and reusability of this polymer [316]. So, hydrolysis with PSSA as the catalyst may introduce a sustainable method for PET recycling.

In the second part of the dissertation [49], a series of aryl sulfonic acids were proposed as the higher activity catalysts than mineral acid for hydrolysis of PET. For this purpose, p-toluenesulfonic acid monohydrate (PTSA), 2-naphthalenesulfonic acid(2-NSA), and 1,5-naphthalenedisulfonic acid tetrahydrate (1,5-NDSA) were selected. The selected catalysts were considered for hydrolysis of PET from the reported work on the high effectiveness of these catalysts for hydrolysis of cellulose due to the hydrophobic structure they possess [34, 526]. Catalyst concentration of 1M, 2M, and 4M at 150°C and reaction kinetics with 2 M catalyst at 130°C, 140°C and 150°C were explored for hydrolysis of PET. As expected, an increase in catalyst concentration or reaction temperature resulted in an increase in the rate of hydrolysis- consistent with the reports on hydrolysis of PET in the literature [29, 235, 288, 289, 527, 528]. For 4M catalyst solutions at 150°C, the required reaction time to achieve more than 90% TPA yield was 6 hours, 6 hours, and 16 hours for PTSA, 2-NSA, and 1,5-NDSA, respectively, less than the acid catalysts reported for hydrolysis of PET [120, 288-290, 517].

A higher activity of these catalysts relative to mineral acids was reported in literature for the hydrolysis of cellulose [34]. This is due to the hydrophobic structure of aryl sulfonic acids, which improves interaction of these catalysts with the surface of the PET particles as similar hydrophobic regions existed in the structure of PET [49]. The

contact angle measurements confirmed better wetting of the surface of PET with solutions of these catalysts relative to the mineral acids such as H₂SO₄. In addition, the water/octanol partition and distribution coefficients were estimated for these catalysts as indication of relative affinity for the PET surface. The apparent reaction rate constant values, determined for the case of 2M catalyst solutions at the reaction temperature of 150°C, had a first order dependence on the logarithmic values of water/octanol partition and distribution coefficients [49]. This is consistent with reports in literature for the cellulose system and is an indication of the hydrophobicity effect on the increase of the rate of hydrolysis for PET particles [34].

The Arrhenius equation was successfully applied to determine the apparent activation energies for the tested catalysts. These values were 60.3 kJ.mol⁻¹, 56.1 kJ.mol⁻¹, and 50.6 kJ.mol⁻¹ for PTSA, 2-NSA, and 1,5-NDSA, respectively [49]. The hydrolysis of ethyl acetate in 0.5M solutions of the catalysts used for hydrolysis of PET to compare heterogenous and homogenous hydrolysis reactions [43]. The calculated values were 45.1 kJ.mol⁻¹, 35.2 kJ.mol⁻¹, and 40.8 kJ.mol⁻¹ for PTSA, 2-NSA, and 1,5-NDSA, respectively [49]. The activation energy values of hydrolysis of ethyl acetate were lower than the ones for the hydrolysis of PET. This is consistent with literature reports for the activation energies of homogenous and heterogenous reactions [529-532]. The reason is that the hydrolysis of PET is a heterogenous reaction, occurring on the surface of the particles while the hydrolysis of ethyl acetate is a homogenous reaction where the acid sites have easier accessibility to react with the ethyl acetate molecules. This was also confirmed with the reaction rate constants calculated for hydrolysis of PET and ethyl acetate. It was noted the

values of reaction rate constant are considerably larger for hydrolysis of ethyl acetate than the ones for hydrolysis of PET.

In the third part of the dissertation, the focus was to synthesize ionic liquids as catalysts for hydrolysis of PET. The intension was not only to produce more thermally stable catalysts, but also to enhance the activity of acids [61, 533-535]. The selected acids for this study were sulfuric acid (H_2SO_4), lactic acid (LA), oxalic acid (OA), and citric acid (CA). The coupling compound used to synthesize the ionic liquids was 1,8-Diazabicyclo (5.4.0) undec-7-ene (DBU). DBU was previously applied as a super basic catalyst for hydrolysis of polycarbonates [499]. To examine that for the case of hydrolysis of PET, DBU was directly tested as a catalyst. The gathered kinetics data confirmed DBU is the most active catalyst in this study for hydrolysis of PET. The reason that DBU was selected as the coupling compound for the synthesis of ionic liquids is that it has very high activity as a catalyst and hydrophobic regions that may form interactive attractions to the surface of PET particles [499, 536-539]. In addition, the goal is to synthesize DBU-acid ionic liquids that will possess higher thermal stability than DBU.

The synthesized ionic liquids were DBU- SO_4 , DBU-LA, DBU-OA, and DBU-CA. The DBU- SO_4 and DBU-LA were synthesized as stated in literature [540-542]. A new synthesis method was proposed for synthesis of DBU- SO_4 where no additional chemical was applied and the DBU- SO_4 could be synthesized in water. For both cases, the DBU- SO_4 was a weak acid with low catalyst activity for hydrolysis of PET. The pH tape strip testing revealed that DBU-LA was a basic catalyst. For synthesis of DBU-OA and DBU-CA, there was no synthesis path in literature. So, synthesis methods were explored with two solvents considered for the syntheses: water and methanol.

For water as the solvent, two scenarios were considered to determine relative concentration of the DBU and acids, equimolar and titration. In the equimolar scenario, the molar ratio of 1 to 1 of the DBU and OA (or CA) were used to synthesize DBU-OA or DBU-CA. In the titration scenario, the concentration of hydroxyl (OH^-) for DBU and the concentration of proton (H^+) for OA or CA were determined by titration and considered for the synthesis of DBU-OA or DBU-CA. For both scenarios, the synthesized DBU-OA and DBU-CA were weak acids with low catalyst activity for hydrolysis of PET. For methanol as the solvent, the number of carboxylic groups in the structures of OA and CA were considered, which is 2 and 3, respectively. So, the DBU-OA and DBU-CA were synthesized with the molar proportion of 2 to 1 and 3 to 1 for DBU to OA and DBU to CA, respectively. The pH tape strip testing revealed the DBU-OA and DBU-CA synthesized in methanol were basic catalysts. This may be attributed to the solvent type and the relative amounts of DBU and acid (OA or CA).

The synthesized basic ionic liquids, DBU-LA, DBU-OA (prepared in methanol), and DBU-CA (prepared in methanol) were studied as catalysts for hydrolysis of PET. For comparison, the corresponding acids of LA, OA, and CA were studied for hydrolysis of PET. The effects of catalyst concentration (1M, 2M, and 4M) and temperature (130°C, 140°C, and 150°C) were explored for hydrolysis of PET. The DBU-acid ionic liquids were significantly more active than their corresponding acids for hydrolysis of PET but less active than DBU. For instance, for the case of 2M catalyst concentration and the reaction temperature of 150°C, the times required to achieve more than 90% TPA yield were 0.33, 20, 7, and 2 hours for DBU, DBU-LA, DBU-OA, and DBU-CA, respectively. However,

for the same reaction conditions, the required reaction times to achieve more than 90% TPA yield were 432, 192, and 120 hours for LA, OA, and CA, respectively.

Wetting studies were conducted by measuring the contact angle for the aqueous catalyst solutions at various concentrations on PET films. It was observed that the solutions of DBU wetted the surface completely. It was also observed that the solutions of the DBU-acid ionic liquids wetted the surface better than the solutions of their corresponding acids. These observations are all consistent with the hydrolysis kinetics data and calculated reaction rate constants for hydrolysis of PET with DBU, DBU-acid ionic liquids, and their corresponding acids. The Arrhenius equation was successfully applied to calculate the reaction rate constants and activation energies. For the case of 4M catalyst solution, DBU was ranked as the highest active catalysts with K_a of 345.47 h^{-1} . Then, the DBU-acid ionic liquids possess higher activity, with the K_a values of 57.54, 14.47, and 4.90 for DBU-CA, DBU-OA, and DBU-LA, respectively. The weak acids were the last group of the catalysts regarding the catalyst activity with K_a values of 0.73, 0.44, and 0.22 h^{-1} for CA, OA, and LA, respectively. The calculated activation energies were within the range of 34 to 68 KJ.mol^{-1} for the 2M solutions of DBU, LA, OA, CA, DBU-LA, DBU-OA, and DBU-CA, within the rational range reported for activation energy values for catalysts used for hydrolysis of PET [43, 49, 238, 315].

7.1.2 Comparison of catalysts used for hydrolysis of PET

Three main criteria were selected for a comprehensive comparison of the catalysts tested in this study. These criteria are explained as follow:

1. The required reaction time to achieve more than 90% TPA yield

As noted, an increase in catalyst concentration or reaction temperature will increase the rate of hydrolysis of PET, consistent with the relevant reported studies on PET degradation [284, 543, 544]. So, the highest values for catalyst concentration and reaction temperature tested in this work were selected as the best reaction conditions, i.e., 4M catalyst in water and 150°C. In addition, the reaction pressure was ~5 atmosphere and the tested PET samples were in powder form with the average size of 302 μm . The required reaction time to achieve more than 90% TPA yield for the catalysts studied are presented in **Table 7-1**. Moreover, the catalysts are ranked based on the activity for hydrolysis of PET in water. Among the tested catalysts, DBU and LA are the most and the least active catalysts for hydrolysis of PET [43, 49].

Table 7-1: The required reaction time to achieve more than 90% TPA yield, 4M catalyst concentration, $T_R = 150^\circ\text{C}$ (Hydrolysis of PET in water).

Rank (#)	Catalyst type	Reaction time (t_R) (hour)	Specific reaction rate constant (k_{sp})*	References
1	DBU	0.17	5730	—
2	DBU-CA	1	970	—
3	PTSA	3	280	[49]
4	2-NSA	3	260	[49]
5	DBU-OA	4	210	—
6	1,5- NDSA	8	103	[49]
7	DBU-LA	12	69	—
8	H_2SO_4	16	48	[43, 49]
9	PSSA	18	51	[43, 49]
10	CA	72	7.98	—
11	OA	120	4.7	—
12	LA	288	2.4	—

$$*[\mathbf{k}_{sp}] = [\mathbf{kg\ PET. m. (mol\ catalyst)^{-1}. s^{-1}}] * 10^{11}$$

2. Octanol/water distribution coefficient values

The octanol/water system is reported as a medium to understand the distribution of a compound within the two phases of water and octanol when the compound is comprised of ionized and unionized parts [545-548]. This method was applied to elaborate the catalyst activity by considering the hydrophobic effect of the catalyst structure on hydrolysis of cellulose [34]. This is illustrated by the depiction of values of apparent reaction rate constants as the function of Log D. D is the distribution coefficient, which is the ratio of the summation of ionized and unionized parts in each phase [549-551]. The method was adopted and used to determine the values of Log D for tested catalysts. An online software,

ChemAxonTM, was used for calculations [335]. The graph of apparent reaction rate constants as the function of Log D is shown for 2M solutions of tested catalysts in **Figure 7-1**. The Log D values for H₂SO₄ and aryl sulfonic acids were taken from our reported paper in literature [49]. The values of apparent reaction rate constant (K_a) are for a reaction temperature of 150°C.

The tested catalysts can be divided into distinguishable categories that account for the activity of functional groups and the hydrophobicity effect that exhibit based on structure. These categories are illustrated with oval shapes to classify the catalysts. Weak acids, aryl sulfonic acids, and DBU-acid ionic liquids are the main groups while H_sSO₄ and PSSA may not be fitted in these groups due to the tangible difference in structure. In addition, the Log D graph indicates that every catalyst group exhibits a first-order dependency of the reaction rate constant to the Log D, illustrated with fitted lines in **Figure 7-1**. In addition, it's observed as the value for Log D increases, the reaction rate constant will increase, within every catalyst group, indicating the importance of catalyst tendency to distribute on the surface (hydrophobicity) is a significant factor on effecting the reaction rate. Same result was also reported for the correlation between the Log D values and the apparent reaction rate constants of aryl sulfonic acids in hydrolysis of cellulose [34].

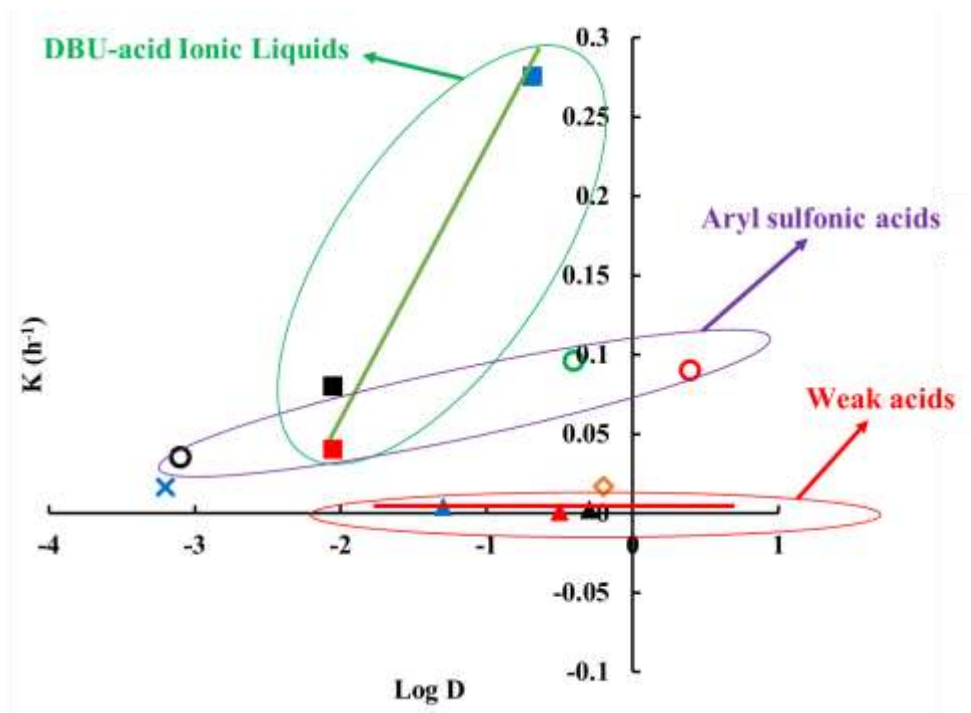


Figure 7-1: Apparent reaction rate constants (K values) as the function of $\text{Log } D$ for 2M solutions of catalysts H_2SO_4 (X), PSSA (\diamond), PTSA (\circ), 2-NSA (\circ), 1,5-NDSA (\circ), LA (\blacktriangle), OA (\blacktriangle), CA (\blacktriangle), DBU-LA (\blacksquare), DBU-OA (\blacksquare), and DBU-CA (\blacksquare),

Reaction temperature = 150°C (Hydrolysis of PET in water) [43, 49].

3. Observation of SEM images of the raw and unreacted PET particles

As the hydrolysis of PET is a reaction occurring on the surface of PET [27, 120], SEM images were taken from the surface of PET to better understand the process and impact on the surface structure. First, the SEM images were taken from the surface of raw PET powder to observe the configuration of the surface before any changes. These images are illustrated in **Figure 7-2**. As observed, there are agglomerated sites on the surface of PET or may be surface roughness, as shown in **Figure 7-2 a**. Also, the PET surface is

comprised of different micro-scale sizes of the layers that are integrated to form the surface (Figure 7-2 b, Figure 7-2 c, and Figure 7-2 d).

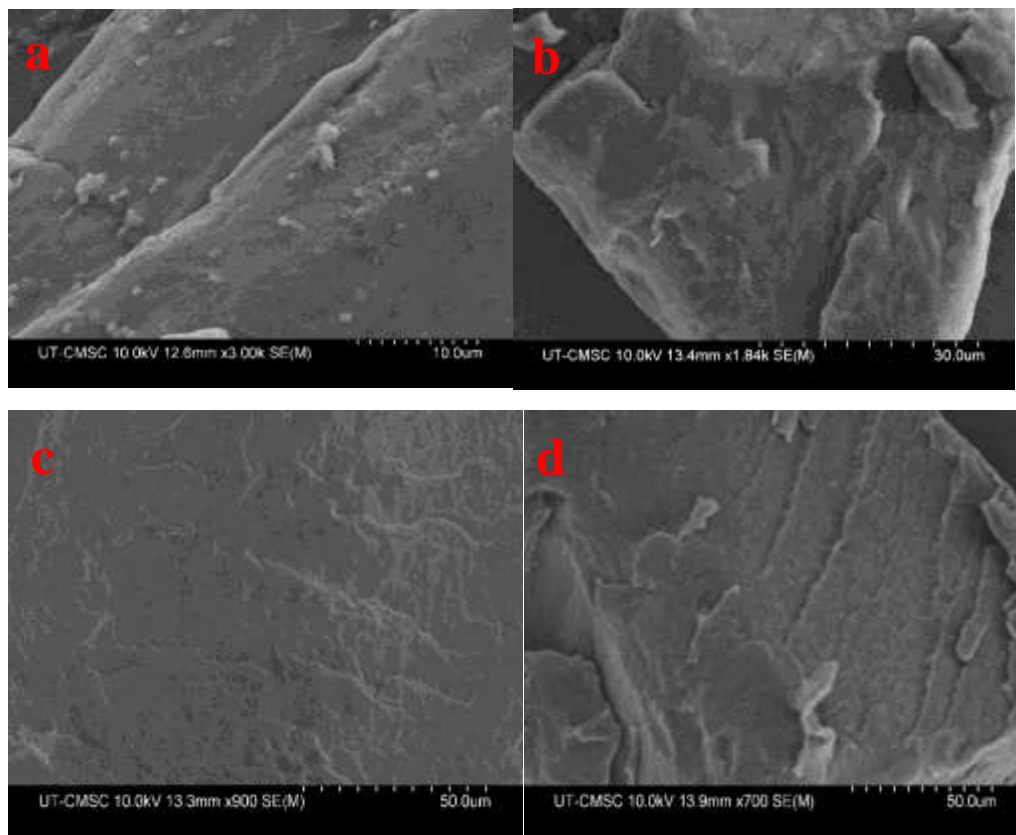


Figure 7-2: The SEM images of the surface of raw PET powder, a) agglomeration of smaller PET particles on the surface, b and c) the layer-by-layer structure of the PET surface.

For the catalysts that had considerable induction times in the kinetics data of PET conversion (%) and TPA yield (%), the SEM images were captured from the surfaces of unreacted PET powder for the reaction time that was within the induction time region. These catalysts were H_2SO_4 , PSSA, and DBU-LA. As illustrated in **Figure 7-3**, no tangible changes occur to the surface and the surface may maintain its uniform stability in the structure.

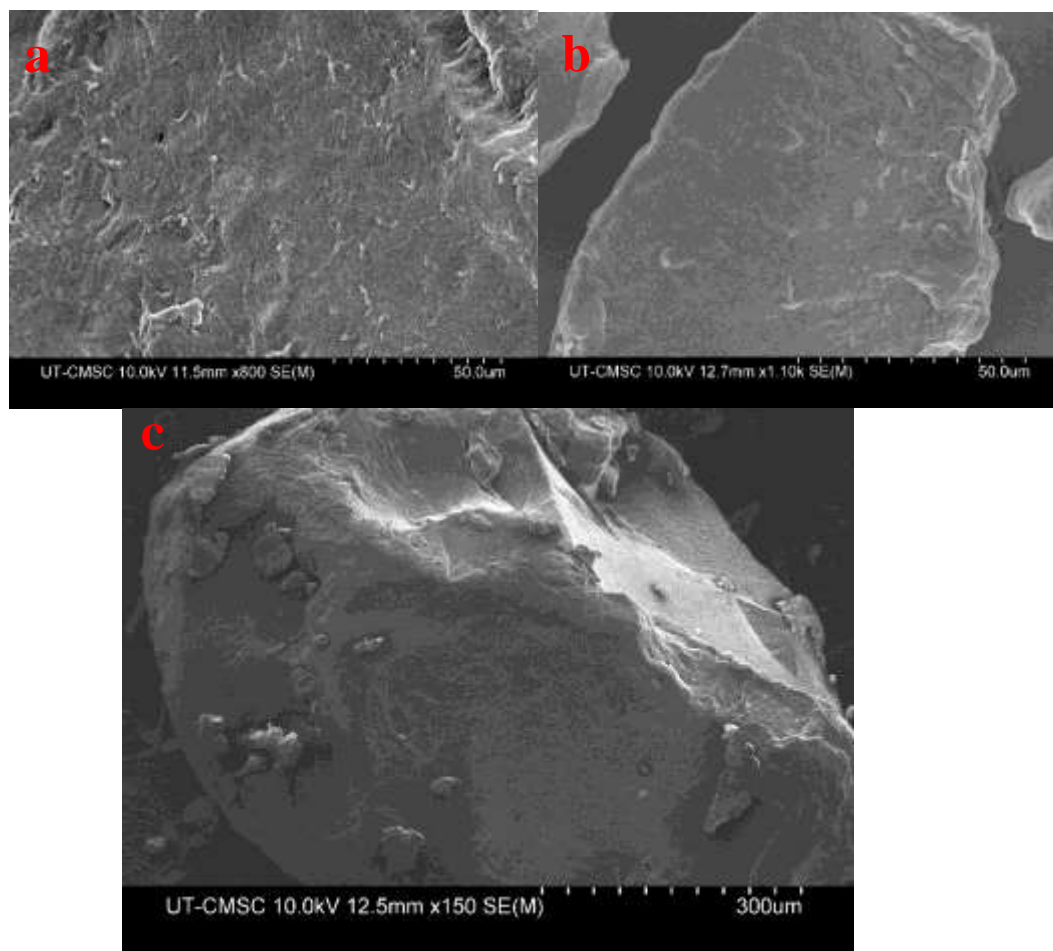


Figure 7-3: The surface of unreacted PET powder, recovered after 3 hours reaction time for 2M catalyst solutions of a. H_2SO_4 , b. PSSA, and c. DBU-LA.

Moreover, SEM images were taken of the surface of PET particles recovered from the hydrolysis solutions for reactions with TPA yield (%) had an average of 20%. There are reported studies that observed changes on the surface of PET during hydrolysis to explain the induction times observed in kinetics data [288, 289, 458]. It's reported that there are cracks occurring on the surface of PET in hydrolysis which increase the surface area for reactions and improve the reaction rate. As shown in **Figure 7-4**, SEM images indicate that etching of the PET surface with the solutions of catalysts, reflected with

scratches observed on the surface. More importantly, pores and cracks were formed on the PET surface, which eventually resulted in the breakage of the PET particles.

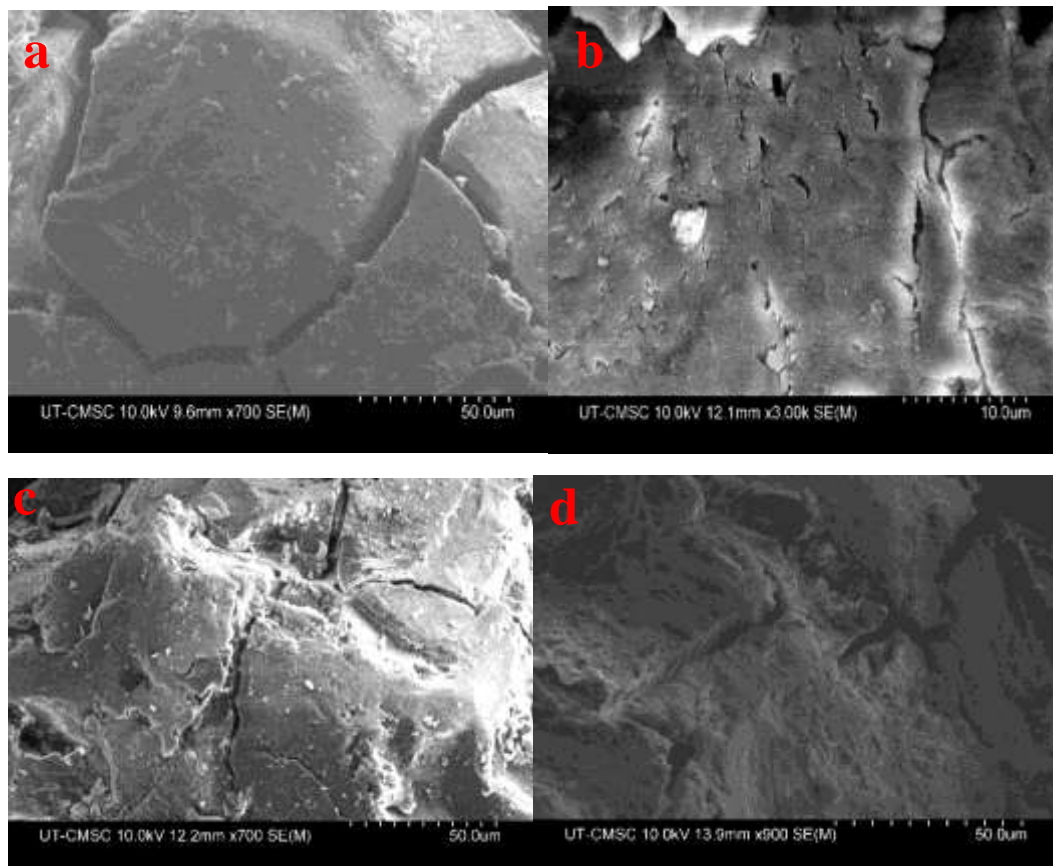


Figure 7-4: The observed patterns of degradation on the surface for unreacted PET powder for 2M solutions of catalysts a. H₂SO₄, b. PSSA, c. PTSA, and d. DBU-LA.

The average TPA yield (20%) and TR = 150°C.

In conclusion, this study presented catalysts in aqueous solutions that were targeted to better the wetting of the surface of PET particles. The shrinking core model was fitted well to the gathered kinetics data of TPA yield (%), specifically to the region where there's no induction time. Contact angle measurements of the catalysts solutions on PET films revealed that better wetting of the surface with the catalysts improved activity for hydrolysis of PET. The literature has few reports on addressing the extent of the wetting

of the surface of PET as a significant factor that can enhance the rate of hydrolysis of PET. This work extended this topic and paved the way for future studies to focus on the design of the catalysts that not only possess high amounts of acid sites (number of protons) or basic sites (number of hydroxyls), but more importantly can form interactive attractions with the surface of PET in the reaction medium to better the wetting and increase the rate of hydrolysis.

7.2. Future work

The following recommendations are provided to address the other aspects that were not within the scope of this study, but they are important as future explorations to further the understanding on the hydrolysis of PET.

1. Develop methods to calculate the energy share of the steps of hydrolysis of PET

As described, hydrolysis of PET is a surface reaction type where the catalysts adsorb to the surface and after the reaction they desorb from the surface. Aside from the apparent activation energy calculations, as a future work, it's necessary to develop practical methods to calculate the enthalpies of adsorption, reaction, and desorption to clarify the energy share of the steps of hydrolysis of PET.

2. Study on the evolution of the surface of PET particles during hydrolysis

A study on the evolution on the surface of PET during hydrolysis at different reaction times can provide insights on how the hydrolysis is performed in micro or nano size scales. This study may be deepened by monitoring the etching occurs on surface and how the scratches and cracks evolve as the reaction proceeds with time. Another fascinating work could be to monitor how the pores are formed and augmented on the

surface of PET with time and to find meaningful correlation between the catalyst activity and this phenomenon.

3. Study on calculations of partition coefficient and distribution coefficient values

In this work, the octanol/water system was considered to mimic the PET/aqueous catalyst solution system. Then, the reaction rate constants that were determined for hydrolysis of PET in the tested catalyst solutions were correlated to the Log P and Log D values determined for these catalysts in the octanol/water system. A more accurate approach will be a study on how to determine the values of partition coefficients and distribution coefficients of catalyst solutions directly for the PET/catalyst solution system.

4. Scaling up the application of proposed catalysts for hydrolysis of PET

This work was conducted in a laboratory and the hydrolysis testes were done in a 15-mL ace pressure reactor where the amount of PET sample was 0.2 grams and the catalyst solution was 10 mL, tested at the concentrations of 1M, 2M, and 4M. So, a study on the feasibility of scaling up the amounts may help to understand the value of these catalysts for PET hydrolysis from the industrial aspect. As the first step, it's needed to simulate the process in Aspen Plus and estimate the costs for recycling of PET wastes in tonnages with the proposed catalysts in aqueous solutions. Then, the cost results should be compared with the costs of the current industrial catalysts used for chemically recycling of PET to understand whether the proposed catalysts are competitive from the cost aspect. Another step could be to analyze the sustainability of the recycling method with these catalysts.

References

1. Gere, D. and T. Czigany, *Future trends of plastic bottle recycling: Compatibilization of PET and PLA*. Polymer Testing, 2020. **81**: p. 106160.
2. Pudack, C., M. Stepanski, and P. Fässler, *PET Recycling—Contributions of crystallization to sustainability*. Chemie Ingenieur Technik, 2020. **92**(4): p. 452-458.
3. Zimmermann, W., *Biocatalytic recycling of polyethylene terephthalate plastic*. Philosophical Transactions of the Royal Society A, 2020. **378**(2176): p. 20190273.
4. Shen, L. and E. Worrell, *Plastic recycling*, in *Handbook of recycling*. 2014, Elsevier. p. 179-190.
5. Goodship, V., *Plastic recycling*. Science progress, 2007. **90**(4): p. 245-268.
6. Luedemann, L., A. Felber, and M. Golder, *Development of a recycling process for textiles made from PET, and proof of its environmental preference with life cycle assessment*. International Journal of Technology Management, 2022. **88**(2-4): p. 134-154.
7. Li, C., et al., *Effects of volatiles on properties of char during sequential pyrolysis of PET and cellulose*. Renewable Energy, 2022. **189**: p. 139-151.
8. Liu, Y., et al., *Microwave pyrolysis of polyethylene terephthalate (PET) plastic bottle sheets for energy recovery*. Journal of Analytical and Applied Pyrolysis, 2022. **161**: p. 105414.

9. Shen, M., et al., *Can incineration completely eliminate plastic wastes? An investigation of microplastics and heavy metals in the bottom ash and fly ash from an incineration plant*. *Science of The Total Environment*, 2021. **779**: p. 146528.
10. Kajiwara, N., et al., *Destruction of decabromodiphenyl ether during incineration of plastic television housing waste at commercial-scale industrial waste incineration plants*. *Journal of Environmental Chemical Engineering*, 2021. **9**(2): p. 105172.
11. Hopewell, J., R. Dvorak, and E. Kosior, *Plastics recycling: challenges and opportunities*. *Philosophical Transactions of the Royal Society B: Biological Sciences*, 2009. **364**(1526): p. 2115-2126.
12. Chen, Y. and S. Selvinsimpson, *Current Trends, Challenges, and Opportunities for Plastic Recycling*. *Plastic and Microplastic in the Environment: Management and Health Risks*, 2022: p. 205-221.
13. Vollmer, I., et al., *Beyond mechanical recycling: Giving new life to plastic waste*. *Angewandte Chemie International Edition*, 2020. **59**(36): p. 15402-15423.
14. Ragaert, K., L. Delva, and K. Van Geem, *Mechanical and chemical recycling of solid plastic waste*. *Waste management*, 2017. **69**: p. 24-58.
15. Schyns, Z.O. and M.P. Shaver, *Mechanical recycling of packaging plastics: A review*. *Macromolecular rapid communications*, 2021. **42**(3): p. 2000415.

16. Briassoulis, D., M. Hiskakis, and E. Babou, *Technical specifications for mechanical recycling of agricultural plastic waste*. Waste management, 2013. **33**(6): p. 1516-1530.
17. Maris, J., et al., *Mechanical recycling: Compatibilization of mixed thermoplastic wastes*. Polymer Degradation and Stability, 2018. **147**: p. 245-266.
18. Jiang, J., et al., *From plastic waste to wealth using chemical recycling: A review*. Journal of Environmental Chemical Engineering, 2022. **10**(1): p. 106867.
19. Han, M., *Depolymerization of PET bottle via methanolysis and hydrolysis*, in *Recycling of Polyethylene Terephthalate Bottles*. 2019, Elsevier. p. 85-108.
20. López-Fonseca, R., et al., *Chemical recycling of post-consumer PET wastes by glycolysis in the presence of metal salts*. Polymer Degradation and Stability, 2010. **95**(6): p. 1022-1028.
21. Yue, Q., et al., *Glycolysis of poly (ethylene terephthalate)(PET) using basic ionic liquids as catalysts*. Polymer Degradation and Stability, 2011. **96**(4): p. 399-403.
22. Oda, M., et al., *Enzymatic hydrolysis of PET: functional roles of three Ca²⁺ ions bound to a cutinase-like enzyme, Cut190*, and its engineering for improved activity*. Applied microbiology and biotechnology, 2018. **102**(23): p. 10067-10077.
23. Kurokawa, H., et al., *Methanolysis of polyethylene terephthalate (PET) in the presence of aluminium tiisopropoxide catalyst to form dimethyl terephthalate and ethylene glycol*. Polymer Degradation and Stability, 2003. **79**(3): p. 529-533.

24. Arhant, M., M. Le Gall, and P.-Y. Le Gac, *Fracture test to accelerate the prediction of polymer embrittlement during aging—Case of PET hydrolysis*. *Polymer Degradation and Stability*, 2022. **196**: p. 109848.
25. Brott, S., et al., *Engineering and evaluation of thermostable IsPETase variants for PET degradation*. *Engineering in life sciences*, 2022. **22**(3-4): p. 192-203.
26. Zope, V.S. and S. Mishra, *Kinetics of neutral hydrolytic depolymerization of PET (polyethylene terephthalate) waste at higher temperature and autogenous pressures*. *Journal of applied polymer science*, 2008. **110**(4): p. 2179-2183.
27. Wei, R., et al., *Mechanism-Based Design of Efficient PET Hydrolases*. *ACS catalysis*, 2022. **12**(6): p. 3382-3396.
28. Saadon, A.S., H. Kaco, and M.S. Sajab, *Depolymerization of Polyethylene Terephthalate (PET) from 3D Printed Waste via Thermal and Alkaline Hydrolysis*. 2021.
29. Wu, H.-S., *Strategic possibility routes of recycled PET*. *Polymers*, 2021. **13**(9): p. 1475.
30. Nisticò, R., *Polyethylene terephthalate (PET) in the packaging industry*. *Polymer Testing*, 2020. **90**: p. 106707.
31. Raheem, A.B., et al., *Current developments in chemical recycling of post-consumer polyethylene terephthalate wastes for new materials production: A review*. *Journal of cleaner production*, 2019. **225**: p. 1052-1064.

32. Shirke, A.N., et al., *Stabilizing leaf and branch compost cutinase (LCC) with glycosylation: mechanism and effect on PET hydrolysis*. *Biochemistry*, 2018. **57**(7): p. 1190-1200.
33. Chen, C.C., et al., *Structural studies reveal the molecular mechanism of PET ase*. *The FEBS journal*, 2018. **285**(20): p. 3717-3723.
34. Amarasekara, A.S. and B. Wiredu, *Aryl sulfonic acid catalyzed hydrolysis of cellulose in water*. *Applied Catalysis A: General*, 2012. **417**: p. 259-262.
35. Rat, M., et al., *Sulfonic acid functionalized periodic mesoporous organosilicas as acetalization catalysts*. *Microporous and mesoporous materials*, 2008. **112**(1-3): p. 26-31.
36. Miura, H., et al., *Quantitative evaluation of the effect of the hydrophobicity of the environment surrounding brønsted acid sites on their catalytic activity for the hydrolysis of organic molecules*. *Journal of the American Chemical Society*, 2018. **141**(4): p. 1636-1645.
37. de Dios Caputto, M.D., et al., *Chemical upcycling of poly (ethylene terephthalate) waste: Moving to a circular model*. *Journal of Polymer Science*, 2022.
38. Shojaei, B., M. Abtahi, and M. Najafi, *Chemical recycling of PET: A stepping-stone toward sustainability*. *Polymers for Advanced Technologies*, 2020. **31**(12): p. 2912-2938.

39. Quicker, P., M. Seitz, and J. Vogel, *Chemical recycling: A critical assessment of potential process approaches*. Waste Management & Research, 2022: p. 0734242X221084044.
40. An, W., et al., *Chemical recovery of thermosetting unsaturated polyester resins*. Green Chemistry, 2022.
41. Hu, K., et al., *Catalytic carbon and hydrogen cycles in plastics chemistry*. Chem Catalysis, 2022.
42. Martín, A.J., et al., *Catalytic processing of plastic waste on the rise*. Chem, 2021. **7**(6): p. 1487-1533.
43. Abedsoltan, H., et al., *Poly (4-styrenesulfonic acid): A recoverable and reusable catalyst for acid hydrolysis of polyethylene terephthalate*. Polymer, 2021. **222**: p. 123620.
44. Pickett, J.E. and D.J. Coyle, *Hydrolysis kinetics of condensation polymers under humidity aging conditions*. Polymer Degradation and Stability, 2013. **98**(7): p. 1311-1320.
45. Campanelli, J.R., M. Kamal, and D. Cooper, *A kinetic study of the hydrolytic degradation of polyethylene terephthalate at high temperatures*. Journal of applied polymer science, 1993. **48**(3): p. 443-451.

46. Ikenaga, K., T. Inoue, and K. Kusakabe, *Hydrolysis of PET by combining direct microwave heating with high pressure*. *Procedia engineering*, 2016. **148**: p. 314-318.
47. Van de Vyver, S., et al., *Recent advances in the catalytic conversion of cellulose*. *ChemCatChem*, 2011. **3**(1): p. 82-94.
48. Agarwal, S., A. Lathwal, and M. Nath, *Recent advances on cellulose sulfuric acid as sustainable and environmentally benign organocatalyst for organic transformations*. *Current Organocatalysis*, 2021. **8**(1): p. 72-92.
49. Abedsoltan, H. and M.R. Coleman, *Aryl sulfonic acid catalysts: Effect of pendant group structure on activity in hydrolysis of polyethylene terephthalate*. *Journal of Applied Polymer Science*, 2022: p. e52451.
50. Quaranta, E., D. Sgherza, and G. Tartaro, *Depolymerization of poly (bisphenol A carbonate) under mild conditions by solvent-free alcoholysis catalyzed by 1, 8-diazabicyclo [5.4. 0] undec-7-ene as a recyclable organocatalyst: a route to chemical recycling of waste polycarbonate*. *Green Chemistry*, 2017. **19**(22): p. 5422-5434.
51. Fukushima, K., et al., *Unexpected efficiency of cyclic amidine catalysts in depolymerizing poly (ethylene terephthalate)*. *Journal of Polymer Science Part A: Polymer Chemistry*, 2013. **51**(7): p. 1606-1611.
52. Nica, S., et al., *Glycolytic depolymerization of polyethylene terephthalate (PET) wastes*. *Revista de Chimie Bucharest*, 2015. **66**(8): p. 1105-1111.

53. To, A.T., P.W. Chung, and A. Katz, *Weak-acid sites catalyze the hydrolysis of crystalline cellulose to glucose in water: importance of post-synthetic functionalization of the carbon surface*. *Angewandte Chemie International Edition*, 2015. **54**(38): p. 11050-11053.
54. Charmot, A., P.-W. Chung, and A. Katz, *Catalytic hydrolysis of cellulose to glucose using weak-acid surface sites on postsynthetically modified carbon*. *ACS Sustainable Chemistry & Engineering*, 2014. **2**(12): p. 2866-2872.
55. Hocker, S., et al., *Polyamide hydrolysis accelerated by small weak organic acids*. *Polymer*, 2014. **55**(20): p. 5057-5064.
56. Agi, A., et al., *Ultrasound-assisted weak-acid hydrolysis of crystalline starch nanoparticles for chemical enhanced oil recovery*. *International journal of biological macromolecules*, 2020. **148**: p. 1251-1271.
57. Qi, X., et al., *Mechanochemical-assisted hydrolysis of pretreated rice straw into glucose and xylose in water by weakly acidic solid catalyst*. *Bioresource technology*, 2019. **273**: p. 687-691.
58. Yang, W., et al., *Hydrolysis of waste polyethylene terephthalate catalyzed by easily recyclable terephthalic acid*. *Waste Management*, 2021. **135**: p. 267-274.
59. Xue, Z., et al., *Thermal, electrochemical and radiolytic stabilities of ionic liquids*. *Physical Chemistry Chemical Physics*, 2018. **20**(13): p. 8382-8402.

60. Huang, Y., et al., *Thermal stability of ionic liquids in nitrogen and air environments*. The Journal of Chemical Thermodynamics, 2021. **161**: p. 106560.
61. de Jesus, S.S. and R. Maciel Filho, *Are ionic liquids eco-friendly?* Renewable and Sustainable Energy Reviews, 2022. **157**: p. 112039.
62. Ramajo, B., et al., *Long-term thermal stability of fatty acid anion-based ionic liquids*. Journal of Molecular Liquids, 2021. **328**: p. 115492.
63. Tsochatzis, E., J.A. Lopes, and M. Corredig, *Chemical testing of mechanically recycled polyethylene terephthalate for food packaging in the European Union*. Resources, Conservation and Recycling, 2022. **179**: p. 106096.
64. Babaahmadi, V., R.A. Abuzade, and M. Montazer, *Enhanced ultraviolet-protective textiles based on reduced graphene oxide-silver nanocomposites on polyethylene terephthalate using ultrasonic-assisted in-situ thermal synthesis*. Journal of Applied Polymer Science, 2022: p. 52196.
65. *Global polyethylene terephthalate (PET) market 2019 by manufacturers, regions, type, and application, Forecast 2024*. Available from: <https://www.marketwatch.com/press-release/polyethylene-terephthalate-pet-market-size-growth-drivers-and-trend-forecast-2022---future-business-trends-company-profiles-with-strategies-cagr-status-with-growth-rate-demand-analysis-with-covid-19-impact-2022-03-04>.
66. Ma, Y., et al., *Solid-state polymerization of PET: influence of nitrogen sweep and high vacuum*. Polymer, 2003. **44**(15): p. 4085-4096.

67. Cruz, S. and M. Zanin, *PET recycling: Evaluation of the solid state polymerization process*. Journal of applied polymer science, 2006. **99**(5): p. 2117-2123.
68. Lepoittevin, B. and P. Roger, *Poly (ethylene terephthalate)*. Handbook of engineering and speciality thermoplastics, 2011. **3**: p. 97-126.
69. Sousa, A.F., et al., *Polyethylene terephthalate: Copolyesters, composites, and renewable alternatives*. Poly (Ethylene Terephthalate) Based Blends, Composites and Nanocomposites, 2015: p. 113-141.
70. Toufaili, F.-A.E., *Catalytic and mechanistic studies of polyethylene terephthalate synthesis*. 2006.
71. Ronkay, F., et al., *Plastic waste from marine environment: Demonstration of possible routes for recycling by different manufacturing technologies*. Waste Management, 2021. **119**: p. 101-110.
72. Zhou, X.-j., et al., *Microplastic pollution of bottled water in China*. Journal of Water Process Engineering, 2021. **40**: p. 101884.
73. Rigamonti, L., et al., *Environmental evaluation of plastic waste management scenarios*. Resources, Conservation and Recycling, 2014. **85**: p. 42-53.
74. Wan, Y., et al., *Informal landfill contributes to the pollution of microplastics in the surrounding environment*. Environmental Pollution, 2022. **293**: p. 118586.

75. Chirayil, C.J., R.K. Mishra, and S. Thomas, *Materials Recovery, Direct Reuse and Incineration of PET Bottles*, in *Recycling of Polyethylene Terephthalate Bottles*. 2019, Elsevier. p. 37-60.
76. Yang, Z., et al., *Is incineration the terminator of plastics and microplastics?* Journal of Hazardous Materials, 2021. **401**: p. 123429.
77. Heidari, M., P.P. Garnaik, and A. Dutta, *The valorization of plastic via thermal means: industrial scale combustion methods*. *Plastics to Energy*, 2019: p. 295-312.
78. Canopoli, L., et al., *Physico-chemical properties of excavated plastic from landfill mining and current recycling routes*. *Waste management*, 2018. **76**: p. 55-67.
79. van Emmerik, T. and A. Schwarz, *Plastic debris in rivers*. *Wiley Interdisciplinary Reviews: Water*, 2020. **7**(1): p. e1398.
80. Silva, A.L., et al., *Microplastics in landfill leachates: The need for reconnaissance studies and remediation technologies*. *Case Studies in Chemical and Environmental Engineering*, 2021. **3**: p. 100072.
81. He, P., et al., *Municipal solid waste (MSW) landfill: A source of microplastics?- Evidence of microplastics in landfill leachate*. *Water research*, 2019. **159**: p. 38-45.
82. Nielsen, T.D., et al., *Politics and the plastic crisis: A review throughout the plastic life cycle*. *Wiley Interdisciplinary Reviews: Energy and Environment*, 2020. **9**(1): p. e360.

83. Kosior, E. and J. Mitchell, *Current industry position on plastic production and recycling*, in *Plastic Waste and Recycling*. 2020, Elsevier. p. 133-162.
84. Geyer, R., *Production, use, and fate of synthetic polymers*, in *Plastic waste and recycling*. 2020, Elsevier. p. 13-32.
85. Stubbins, A., et al., *Plastics in the Earth system*. *Science*, 2021. **373**(6550): p. 51-55.
86. Zheng, J. and S. Suh, *Strategies to reduce the global carbon footprint of plastics*. *Nature Climate Change*, 2019. **9**(5): p. 374-378.
87. Idumah, C.I. and I.C. Nwuzor, *Novel trends in plastic waste management*. *SN Applied Sciences*, 2019. **1**(11): p. 1-14.
88. Devasahayam, S., G.B. Raju, and C.M. Hussain, *Utilization and recycling of end of life plastics for sustainable and clean industrial processes including the iron and steel industry*. *Materials Science for Energy Technologies*, 2019. **2**(3): p. 634-646.
89. Ghosal, K. and C. Nayak, *Recent Advances in Chemical Recycling of Polyethylene Terephthalate Waste into Value Added Products for Sustainable Coating Solutions- Hope Vs Hype*. *Materials Advances*, 2022.
90. Sang, T., et al., *Polyethylene terephthalate degradation under natural and accelerated weathering conditions*. *European polymer journal*, 2020. **136**: p. 109873.

91. Tsironi, T.N., S.M. Chatzidakis, and N.G. Stoforos, *The future of polyethylene terephthalate bottles: Challenges and sustainability*. Packaging Technology and Science, 2022.
92. Tamburini, E., et al., *Plastic (PET) vs bioplastic (PLA) or refillable aluminium bottles—What is the most sustainable choice for drinking water? A life-cycle (LCA) analysis*. Environmental research, 2021. **196**: p. 110974.
93. Kang, M.J., et al., *A chemo-microbial hybrid process for the production of 2-pyrone-4, 6-dicarboxylic acid as a promising bioplastic monomer from PET waste*. Green Chemistry, 2020. **22**(11): p. 3461-3469.
94. Sid, S., et al., *Bio-sourced polymers as alternatives to conventional food packaging materials: A review*. Trends in Food Science & Technology, 2021. **115**: p. 87-104.
95. Wang, A., et al., *Performance of cost-effective PET packaging with light protective additives to limit photo-oxidation in UHT milk under refrigerated LED-lighted storage condition*. Food Packaging and Shelf Life, 2022. **31**: p. 100773.
96. Gerassimidou, S., et al., *Unpacking the complexity of the UK plastic packaging value chain: A stakeholder perspective*. Sustainable Production and Consumption, 2022. **30**: p. 657-673.
97. Smith, R.L., S. Takkellapati, and R.C. Riegerix, *Recycling of Plastics in the United States: Plastic Material Flows and Polyethylene Terephthalate (PET) Recycling Processes*. ACS Sustainable Chemistry & Engineering, 2022.

98. Gerassimidou, S., et al., *Unpacking the complexity of the PET drink bottles value chain: A chemicals perspective*. Journal of Hazardous Materials, 2022: p. 128410.
99. Meneses, R.A.M., et al., *Plastic recycling and their use as raw material for the synthesis of carbonaceous materials*. Heliyon, 2022: p. e09028.
100. Ignatyev, I.A., W. Thielemans, and B. Vander Beke, *Recycling of polymers: a review*. ChemSusChem, 2014. **7**(6): p. 1579-1593.
101. Wäger, P.A. and R. Hischer, *Life cycle assessment of post-consumer plastics production from waste electrical and electronic equipment (WEEE) treatment residues in a Central European plastics recycling plant*. Science of the Total Environment, 2015. **529**: p. 158-167.
102. Gopalakrishna, K. and N. Reddy, *Regulations on Recycling PET Bottles, in Recycling of Polyethylene Terephthalate Bottles*. 2019, Elsevier. p. 23-35.
103. Tshifularo, C.A. and A. Patnaik, *Recycling of plastics into textile raw materials and products, in Sustainable technologies for fashion and textiles*. 2020, Elsevier. p. 311-326.
104. Navarro, R., et al., *The influence of polyethylene in the mechanical recycling of polyethylene terephthalate*. Journal of Materials Processing Technology, 2008. **195**(1-3): p. 110-116.

105. Barthélémy, E., et al., *Safety evaluation of mechanical recycling processes used to produce polyethylene terephthalate (PET) intended for food contact applications*. Food Additives & Contaminants: Part A, 2014. **31**(3): p. 490-497.
106. Chaudhari, U.S., et al., *Systems analysis approach to polyethylene terephthalate and olefin plastics supply chains in the circular economy: A review of data sets and models*. ACS Sustainable Chemistry & Engineering, 2021. **9**(22): p. 7403-7421.
107. Elamri, A., et al., *Progress in polyethylene terephthalate recycling*. 2017, Nova Science Publishers.
108. Jeswani, H., et al., *Life cycle environmental impacts of chemical recycling via pyrolysis of mixed plastic waste in comparison with mechanical recycling and energy recovery*. Science of the Total Environment, 2021. **769**: p. 144483.
109. Brouwer, M.T., F. Alvarado Chacon, and E.U. Thoden van Velzen, *Effect of recycled content and rPET quality on the properties of PET bottles, part III: Modelling of repetitive recycling*. Packaging Technology and Science, 2020. **33**(9): p. 373-383.
110. Zhang, R., et al., *PET bottles recycling in China: An LCA coupled with LCC case study of blanket production made of waste PET bottles*. Journal of environmental management, 2020. **260**: p. 110062.
111. Molnar, B. and F. Ronkay, *Effect of solid-state polycondensation on crystalline structure and mechanical properties of recycled polyethylene-terephthalate*. Polymer Bulletin, 2019. **76**(5): p. 2387-2398.

112. Guo, W., et al., *Low temperature solid-state extrusion of recycled poly (ethylene terephthalate) bottle scraps*. Journal of applied polymer science, 2006. **102**(3): p. 2692-2699.
113. Huang, L., L. Pan, and T. Inoue, *Effect of solid-state shearing of poly (ethylene terephthalate) on isothermal crystallization and fiber structure formation*. Journal of applied polymer science, 2007. **104**(2): p. 787-791.
114. Crippa, M. and B. Morico, *PET depolymerization: a novel process for plastic waste chemical recycling*, in *Studies in Surface Science and Catalysis*. 2020, Elsevier. p. 215-229.
115. Chu, M., et al., *Rational Design of Chemical Catalysis for Plastic Recycling*. ACS Catalysis, 2022. **12**(8): p. 4659-4679.
116. Smith, R.L., S. Takkellapati, and R.C. Riegerix, *Recycling of Plastics in the United States: Plastic Material Flows and Polyethylene Terephthalate (PET) Recycling Processes*. ACS Sustainable Chemistry & Engineering, 2022. **10**(6): p. 2084-2096.
117. Yao, H., et al., *Colorless BHET obtained from PET by modified mesoporous catalyst ZnO/SBA-15*. Chemical Engineering Science, 2022. **248**: p. 117109.
118. Bascucci, C., et al., *Investigating thermomechanical recycling of poly (ethylene terephthalate) containing phosphorus flame retardants*. Polymer Degradation and Stability, 2022. **195**: p. 109783.

119. Tarannum, N., et al., *Chemical depolymerization of recycled PET to oxadiazole and hydrazone derivatives: Synthesis, characterization, molecular docking and DFT study*. Journal of King Saud University-Science, 2022. **34**(1): p. 101739.
120. Barnard, E., J.J.R. Arias, and W. Thielemans, *Chemolytic depolymerisation of PET: a review*. Green Chemistry, 2021. **23**(11): p. 3765-3789.
121. Siddiqui, M.N., et al., *Chemical Recycling of PET in the Presence of the Bio-Based Polymers, PLA, PHB and PEF: A Review*. Sustainability, 2021. **13**(19): p. 10528.
122. Arturi, K.R., et al., *Recovery of value-added chemicals by solvolysis of unsaturated polyester resin*. Journal of Cleaner Production, 2018. **170**: p. 131-136.
123. Armenise, S., et al., *Plastic waste recycling via pyrolysis: A bibliometric survey and literature review*. Journal of Analytical and Applied Pyrolysis, 2021. **158**: p. 105265.
124. Peng, Y., et al., *A review on catalytic pyrolysis of plastic wastes to high-value products*. Energy Conversion and Management, 2022. **254**: p. 115243.
125. Lebedeva, E., et al., *Application of Low-Temperature Solvolysis for Processing of Reinforced Carbon Plastics*. Russian Journal of Applied Chemistry, 2020. **93**(6): p. 845-853.
126. Kaminsky, W., *Chemical recycling of plastics by fluidized bed pyrolysis*. Fuel Communications, 2021. **8**: p. 100023.

127. Osman, A.I., et al., *Pyrolysis kinetic modelling of abundant plastic waste (PET) and in-situ emission monitoring*. Environmental Sciences Europe, 2020. **32**(1): p. 1-12.
128. Suriapparao, D.V., D.A. Kumar, and R. Vinu, *Microwave co-pyrolysis of PET bottle waste and rice husk: effect of plastic waste loading on product formation*. Sustainable Energy Technologies and Assessments, 2022. **49**: p. 101781.
129. Zhang, H., et al., *Upcycling of PET waste into methane-rich gas and hierarchical porous carbon for high-performance supercapacitor by autogenic pressure pyrolysis and activation*. Science of the Total Environment, 2021. **772**: p. 145309.
130. Gebre, S.H., M.G. Sendeku, and M. Bahri, *Recent Trends in the Pyrolysis of Non-Degradable Waste Plastics*. ChemistryOpen, 2021. **10**(12): p. 1202-1226.
131. Diaz-Silvarrey, L.S., A. McMahon, and A.N. Phan, *Benzoic acid recovery via waste poly (ethylene terephthalate)(PET) catalytic pyrolysis using sulphated zirconia catalyst*. Journal of analytical and applied pyrolysis, 2018. **134**: p. 621-631.
132. Mortezaeikia, V., O. Tavakoli, and M.S. Khodaparasti, *A review on kinetic study approach for pyrolysis of plastic wastes using thermogravimetric analysis*. Journal of Analytical and Applied Pyrolysis, 2021. **160**: p. 105340.
133. Jahirul, M., et al., *Transport fuel from waste plastics pyrolysis—A review on technologies, challenges and opportunities*. Energy Conversion and Management, 2022. **258**: p. 115451.

134. Jia, H., et al., *Catalytic fast pyrolysis of poly (ethylene terephthalate)(PET) with zeolite and nickel chloride*. *Polymers*, 2020. **12**(3): p. 705.
135. Kumagai, S., et al., *Catalytic Pyrolysis of Poly (ethylene terephthalate) in the Presence of Metal Oxides for Aromatic Hydrocarbon Recovery Using Tandem μ -Reactor-GC/MS*. *Energy & Fuels*, 2020. **34**(2): p. 2492-2500.
136. Shahi, A., B. Roozbehani, and M. Mirdrikvand, *Catalytic pyrolysis of waste polyethylene terephthalate granules using a Lewis-Brønsted acid sites catalyst*. *Clean Technologies and Environmental Policy*, 2022: p. 1-9.
137. Benhaliliba, M., *ZnO a multifunctional material: Physical properties, spectroscopic ellipsometry and surface examination*. *Optik*, 2021. **241**: p. 167197.
138. Williams, P.T., *Hydrogen and carbon nanotubes from pyrolysis-catalysis of waste plastics: A review*. *Waste and Biomass Valorization*, 2021. **12**(1): p. 1-28.
139. Kusenberg, M., et al., *A comprehensive experimental investigation of plastic waste pyrolysis oil quality and its dependence on the plastic waste composition*. *Fuel Processing Technology*, 2022. **227**: p. 107090.
140. Dogu, O., et al., *The chemistry of chemical recycling of solid plastic waste via pyrolysis and gasification: State-of-the-art, challenges, and future directions*. *Progress in Energy and Combustion Science*, 2021. **84**: p. 100901.
141. Thiounn, T. and R.C. Smith, *Advances and approaches for chemical recycling of plastic waste*. *Journal of Polymer Science*, 2020. **58**(10): p. 1347-1364.

142. Sherwood, J., *Closed-loop recycling of polymers using solvents*. Johnson Matthey Technology Review, 2020: p. 4-15.
143. Wang, Q., et al., *Deep eutectic solvents as highly active catalysts for the fast and mild glycolysis of poly (ethylene terephthalate)(PET)*. Green Chemistry, 2015. **17**(4): p. 2473-2479.
144. Pestana, S.C., et al., *Natural eutectic solvents for sustainable recycling of poly (ethyleneterephthalate): closing the circle*. Green Chemistry, 2021. **23**(23): p. 9460-9464.
145. Ghasemi, M.H., et al., *Mechanistic aspects of poly (ethylene terephthalate) recycling—toward enabling high quality sustainability decisions in waste management*. Environmental Science and Pollution Research, 2021. **28**(32): p. 43074-43101.
146. Shamsi, R., et al., *Hopes beyond PET recycling: Environmentally clean and engineeringly applicable*. Journal of Polymers and the Environment, 2019. **27**(11): p. 2490-2508.
147. Lee, A. and M.S. Liew, *Tertiary recycling of plastics waste: an analysis of feedstock, chemical and biological degradation methods*. Journal of Material Cycles and Waste Management, 2021. **23**(1): p. 32-43.
148. Xin, J., et al., *Progress in the catalytic glycolysis of polyethylene terephthalate*. Journal of Environmental Management, 2021. **296**: p. 113267.

149. Zhu, M., et al., *Investigation of solid catalysts for glycolysis of polyethylene terephthalate*. Chemical engineering journal, 2012. **185**: p. 168-177.
150. Kim, Y., et al., *Optimizing PET Glycolysis with an Oyster Shell-Derived Catalyst Using Response Surface Methodology*. Polymers, 2022. **14**(4): p. 656.
151. Fan, C., et al., *Efficient glycolysis of PET catalyzed by a metal-free phosphazene base: the important role of EG*. Green Chemistry, 2022.
152. Azeem, M., M.B. Fournet, and O.A. Attallah, *Ultrafast 99% Polyethylene terephthalate depolymerization into value added monomers using sequential glycolysis-hydrolysis under microwave irradiation*. Arabian Journal of Chemistry, 2022. **15**(7): p. 103903.
153. Lei, D., et al., *Rapid Glycolysis of Waste Polyethylene Terephthalate Fibers via a Stepwise Feeding Process*. Industrial & Engineering Chemistry Research, 2022. **61**(14): p. 4794-4802.
154. Ekart, M.P., W.S. Murdoch Jr, and T.M. Pell, *A glycolysis process for recycling of post-consumer pet*. 2000, Google Patents.
155. Parrott, M., *Chemical recycling of polyethylene terephthalate by microwave irradiation*. 2020, Google Patents.
156. Ekart, M.P. and T.M. Pell Jr, *Process including glycolysis and subsequent purification for recycling polyester materials*. 1997, Google Patents.

157. Smith, B.L., P. Nayar, and G. Shaw, *Process for recycling polyester materials*. 2007, Google Patents.
158. Macdowell, J.T., *Process of reclaiming linear terephthalate polyester*. 1965, Google Patents.
159. Payne, J. and M.D. Jones, *The chemical recycling of polyesters for a circular plastics economy: challenges and emerging opportunities*. ChemSusChem, 2021. **14**(19): p. 4041-4070.
160. Capeletti, M.R. and F.J. Passamonti, *Optimization of reaction parameters in the conversion of PET to produce BHET*. Polymer Engineering & Science, 2018. **58**(9): p. 1500-1507.
161. Wang, T., et al., *Metal ions immobilized on polymer ionic liquid as novel efficient and facile recycled catalyst for glycolysis of PET*. Polymer Degradation and Stability, 2021. **194**: p. 109751.
162. Li, Y., et al., *Zinc-doped ferrite nanoparticles as magnetic recyclable catalysts for scale-up glycolysis of poly (ethylene terephthalate) wastes*. Advanced Powder Technology, 2022. **33**(3): p. 103444.
163. Deng, L., et al., *New effective catalysts for glycolysis of polyethylene terephthalate waste: Tropine and tropine-zinc acetate complex*. Journal of Molecular Liquids, 2021. **334**: p. 116419.

164. Eshaq, G. and A. ElMetwally, *(Mg–Zn)–Al layered double hydroxide as a regenerable catalyst for the catalytic glycolysis of polyethylene terephthalate*. Journal of Molecular Liquids, 2016. **214**: p. 1-6.
165. Yunita, I., et al., *Effective catalysts derived from waste ostrich eggshells for glycolysis of post-consumer PET bottles*. Chemical Papers, 2019. **73**(6): p. 1547-1560.
166. Shuangjun, C., et al., *Glycolysis of poly (ethylene terephthalate) waste catalyzed by mixed Lewis acidic ionic liquids*. Journal of Thermal Analysis and Calorimetry, 2021. **143**(5): p. 3489-3497.
167. Pham, C.T., et al., *The advancement of bis (2-hydroxyethyl) terephthalate recovered from post-consumer poly (ethylene terephthalate) bottles compared to commercial polyol for preparation of high performance polyurethane*. Journal of Industrial and Engineering Chemistry, 2021. **93**: p. 196-209.
168. Nicholson, S.R., et al., *The critical role of process analysis in chemical recycling and upcycling of waste plastics*. Annual Review of Chemical and Biomolecular Engineering, 2022. **13**.
169. Huang, J., et al., *Removal of trace amount impurities in glycolytic monomer of polyethylene terephthalate by recrystallization*. Journal of Environmental Chemical Engineering, 2021. **9**(5): p. 106277.

170. Guo, Z., E. Adolfsson, and P.L. Tam, *Nanostructured micro particles as a low-cost and sustainable catalyst in the recycling of PET fiber waste by the glycolysis method*. Waste Management, 2021. **126**: p. 559-566.
171. Abdelaal, M.Y., T.R. Sobahi, and M.S.I. Makki, *Chemical transformation of pet waste through glycolysis*. Construction and Building Materials, 2011. **25**(8): p. 3267-3271.
172. Wang, J., et al., *Synthesis of diisooctyl terephthalate (DOTP) plasticizer*. Huaxue Shijie, 1991. **32**: p. 208-210.
173. Liu, F., et al., *Alcoholysis of poly (ethylene terephthalate) to produce dioctyl terephthalate with sub-and super-critical isooctyl alcohol*. Journal of Analytical and Applied Pyrolysis, 2013. **99**: p. 16-22.
174. Liu, S., et al., *Isooctanol alcoholysis of waste polyethylene terephthalate in acidic ionic liquid*. Journal of Polymer Research, 2013. **20**(12): p. 1-6.
175. Mendes, L., M. Dias, and T. Rodrigues, *Chemical recycling of PET waste with multifunctional pentaerythritol in the melt state*. Journal of Polymers and the Environment, 2011. **19**(1): p. 254-262.
176. Chen, J., et al., *Alcoholysis of PET to produce dioctyl terephthalate by isooctyl alcohol with ionic liquid as cosolvent*. Polymer degradation and stability, 2014. **107**: p. 178-183.

177. Erwin, H., S. Erhard, and L. Rudolf, *Regeneration of terephthalic acid dimethyl ester from polyethylene terephthalate*. 1962, Google Patents.
178. Jang, J.Y., K. Sadeghi, and J. Seo, *Chain-Extending Modification for Value-Added Recycled PET: A Review*. *Polymer Reviews*, 2022: p. 1-30.
179. Laldinpui, Z., et al., *Methanolysis of PET Waste Using Heterogeneous Catalyst of Bio-waste Origin*. *Journal of Polymers and the Environment*, 2021: p. 1-15.
180. Pham, D.D. and J. Cho, *Low-energy catalytic methanolysis of poly(ethyleneterephthalate)*. *Green Chemistry*, 2021. **23**(1): p. 511-525.
181. Sánchez, A.C. and S.R. Collinson, *The selective recycling of mixed plastic waste of polylactic acid and polyethylene terephthalate by control of process conditions*. *European Polymer Journal*, 2011. **47**(10): p. 1970-1976.
182. Mishra, S. and A.S. Goje, *Kinetic and thermodynamic study of methanolysis of poly(ethylene terephthalate) waste powder*. *Polymer international*, 2003. **52**(3): p. 337-342.
183. Du, J.-T., et al., *ZnO nanodispersion as pseudohomogeneous catalyst for alcoholysis of polyethylene terephthalate*. *Chemical Engineering Science*, 2020. **220**: p. 115642.
184. Liu, Q., R. Li, and T. Fang, *Investigating and modeling PET methanolysis under supercritical conditions by response surface methodology approach*. *Chemical Engineering Journal*, 2015. **270**: p. 535-541.

185. Yang, Y., et al., *Study on methanolytic depolymerization of PET with supercritical methanol for chemical recycling*. Polymer degradation and stability, 2002. **75**(1): p. 185-191.
186. Goto, M., et al., *Degradation kinetics of polyethylene terephthalate in supercritical methanol*. AIChE journal, 2002. **48**(1): p. 136-144.
187. Goto, M., *Chemical recycling of plastics using sub-and supercritical fluids*. The Journal of Supercritical Fluids, 2009. **47**(3): p. 500-507.
188. Genta, M., M. Goto, and M. Sasaki, *Heterogeneous continuous kinetics modeling of PET depolymerization in supercritical methanol*. The Journal of Supercritical Fluids, 2010. **52**(3): p. 266-275.
189. Kim, B.K., et al., *Depolymerization of polyethyleneterephthalate in supercritical methanol*. Journal of applied polymer science, 2001. **81**(9): p. 2102-2108.
190. De Castro, R.E., et al., *Depolymerization of poly (ethylene terephthalate) wastes using ethanol and ethanol/water in supercritical conditions*. Journal of applied polymer science, 2006. **101**(3): p. 2009-2016.
191. *Eastman will build a \$250 million plastics recycling plant*. Available from: <https://cen.acs.org/environment/recycling/Eastman-build-250-million-plastics/99/web/2021/02>.

192. Zhou, J., et al., *Aminolysis of polyethylene terephthalate fabric by a method involving the gradual concentration of dilute ethylenediamine*. *Colloids and Surfaces A: Physicochemical and Engineering Aspects*, 2017. **513**: p. 146-152.
193. Hoang, C.N. and Y.H. Dang, *Aminolysis of poly (ethylene terephthalate) waste with ethylenediamine and characterization of α , ω -diamine products*. *Polymer degradation and stability*, 2013. **98**(3): p. 697-708.
194. Shukla, S. and A.M. Harad, *Aminolysis of polyethylene terephthalate waste*. *Polymer degradation and stability*, 2006. **91**(8): p. 1850-1854.
195. Musale, R.M. and S.R. Shukla, *Deep eutectic solvent as effective catalyst for aminolysis of polyethylene terephthalate (PET) waste*. *International Journal of Plastics Technology*, 2016. **20**(1): p. 106-120.
196. Palekar, V.S., R.V. Shah, and S. Shukla, *Ionic liquid-catalyzed aminolysis of poly (ethylene terephthalate) waste*. *Journal of applied polymer science*, 2012. **126**(3): p. 1174-1181.
197. Tawfik, M.E., N.M. Ahmed, and S.B. Eskander, *Aminolysis of poly (ethylene terephthalate) wastes based on sunlight and utilization of the end product [bis (2-hydroxyethylene) terephthalamide] as an ingredient in the anticorrosive paints for the protection of steel structures*. *Journal of Applied Polymer Science*, 2011. **120**(5): p. 2842-2855.

198. Elsaheed, S.M. and R.K. Farag, *Synthesis and characterization of unsaturated polyesters based on the aminolysis of poly (ethylene terephthalate)*. Journal of applied polymer science, 2009. **112**(6): p. 3327-3336.
199. More, A.P., et al., *Studies of different techniques of aminolysis of poly (ethylene terephthalate) with ethylenediamine*. Polymer Bulletin, 2017. **74**(8): p. 3269-3282.
200. Lorusso, E., et al., *Investigation of aminolysis routes on PET fabrics using different amine-based materials*. Nano Select, 2021.
201. Bulak, E. and I. Acar, *The use of aminolysis, aminoglycolysis, and simultaneous aminolysis–hydrolysis products of waste PET for production of paint binder*. Polymer Engineering & Science, 2014. **54**(10): p. 2272-2281.
202. Bech, L., et al., *Chemical surface modification of poly (ethylene terephthalate) fibers by aminolysis and grafting of carbohydrates*. Journal of Polymer Science Part A: Polymer Chemistry, 2007. **45**(11): p. 2172-2183.
203. Soni, R., S. Singh, and K. Dutt, *Studies on synthesis and characterization of N-alkyl terephthalamides using different amines from polyethylene terephthalate waste*. Journal of applied polymer science, 2010. **115**(5): p. 3074-3080.
204. Zhu, X., et al., *Effects of coal and ammonium polyphosphate on thermal degradation and flame retardancy of polyethylene terephthalate*. Journal of polymer research, 2010. **17**(5): p. 621-629.

205. Vavilova, S.Y., N. Prorokova, and Y.A. Kalinnikov, *Nature of the effect of decreasing the electrical resistance of polyethylene terephthalate with aqueous solutions of ammonia*. Fibre Chemistry, 1998. **30**(3): p. 172-174.
206. Zheng, Z., et al., *Surface characterization of polyethylene terephthalate films treated by ammonia low-temperature plasma*. Applied Surface Science, 2012. **258**(18): p. 7207-7212.
207. Xu, L., et al., *Catalytic fast pyrolysis of polyethylene terephthalate plastic for the selective production of terephthalonitrile under ammonia atmosphere*. Waste Management, 2019. **92**: p. 97-106.
208. Xu, L., et al., *Selective production of terephthalonitrile and benzonitrile via pyrolysis of polyethylene terephthalate (PET) with ammonia over Ca (OH) 2/Al2O3 catalysts*. Catalysts, 2019. **9**(5): p. 436.
209. Khoonkari, M., et al., *Chemical recycling of PET wastes with different catalysts*. International Journal of Polymer Science, 2015. **2015**.
210. Arai, R., et al., *Reaction kinetics of hydrothermal depolymerization of poly (ethylene naphthalate), poly (ethylene terephthalate), and polycarbonate with aqueous ammonia solution*. Chemical engineering science, 2010. **65**(1): p. 36-41.
211. Mittal, A., et al., *Scanning electron microscopic study of hazardous waste flakes of polyethylene terephthalate (PET) by aminolysis and ammonolysis*. Journal of hazardous materials, 2010. **178**(1-3): p. 390-396.

212. Chan, K. and A. Zinchenko, *Conversion of waste bottles' PET to a hydrogel adsorbent via PET aminolysis*. Journal of Environmental Chemical Engineering, 2021. **9**(5): p. 106129.
213. Zhu, Y., Z. Mao, and C. Gao, *Aminolysis-based surface modification of polyesters for biomedical applications*. RSC advances, 2013. **3**(8): p. 2509-2519.
214. Gupta, P. and S. Bhandari, *Chemical depolymerization of PET bottles via ammonolysis and aminolysis*, in *Recycling of Polyethylene Terephthalate Bottles*. 2019, Elsevier. p. 109-134.
215. Fukushima, K., et al., *Advanced chemical recycling of poly (ethylene terephthalate) through organocatalytic aminolysis*. Polymer Chemistry, 2013. **4**(5): p. 1610-1616.
216. Kárpáti, L., et al., *Synthesis and characterization of isophorondiamine based epoxy hardeners from aminolysis of PET*. eXPRESS Polymer Letters, 2019. **13**(7).
217. Vogt, B.D., K.K. Stokes, and S.K. Kumar, *Why is recycling of postconsumer plastics so challenging?* ACS Applied Polymer Materials, 2021. **3**(9): p. 4325-4346.
218. Pivnenko, K., et al. *Challenges in plastics recycling*. in *Proceedings of the Sardinia*. 2015.
219. Silva, A.L.P., et al., *Increased plastic pollution due to COVID-19 pandemic: Challenges and recommendations*. Chemical Engineering Journal, 2021. **405**: p. 126683.

220. North, E.J. and R.U. Halden, *Plastics and environmental health: the road ahead*. Reviews on environmental health, 2013. **28**(1): p. 1-8.
221. Wang, S., et al., *Sodium titanium tris (glycolate) as a catalyst for the chemical recycling of poly (ethylene terephthalate) via glycolysis and repolycondensation*. Polymer Degradation and Stability, 2015. **114**: p. 105-114.
222. Kim, D.H., et al., *One-pot chemo-bioprocess of PET depolymerization and recycling enabled by a biocompatible catalyst, betaine*. ACS Catalysis, 2021. **11**(7): p. 3996-4008.
223. Pingale, N. and S. Shukla, *Microwave assisted ecofriendly recycling of poly (ethylene terephthalate) bottle waste*. European Polymer Journal, 2008. **44**(12): p. 4151-4156.
224. Stewart, R., *Going green: eco-friendly materials and recycling on growth paths*. Plastics Engineering, 2008. **64**(1): p. 16-24.
225. Sojobi, A.O., S.E. Nwobodo, and O.J. Aladegboye, *Recycling of polyethylene terephthalate (PET) plastic bottle wastes in bituminous asphaltic concrete*. Cogent engineering, 2016. **3**(1): p. 1133480.
226. Choi, S. and H.-M. Choi, *Eco-friendly, expeditious depolymerization of PET in the blend fabrics by using a bio-based deep eutectic solvent under microwave irradiation for composition identification*. Fibers and Polymers, 2019. **20**(4): p. 752-759.

227. Samak, N.A., et al., *Recent advances in biocatalysts engineering for polyethylene terephthalate plastic waste green recycling*. *Environment International*, 2020. **145**: p. 106144.
228. Abdel Hameed, R., et al., *Green Recycling of Poly (ethylene terephthalate) Waste as Corrosion Inhibitor for Steel in Marine Environment*. *Egyptian Journal of Chemistry*, 2021. **64**(5): p. 2685-2695.
229. Nkwachukwu, O.I., et al., *Focus on potential environmental issues on plastic world towards a sustainable plastic recycling in developing countries*. *International Journal of Industrial Chemistry*, 2013. **4**(1): p. 1-13.
230. Sandin, G. and G.M. Peters, *Environmental impact of textile reuse and recycling—A review*. *Journal of cleaner production*, 2018. **184**: p. 353-365.
231. Herrero Acero, E., et al., *Enzymatic surface hydrolysis of PET: effect of structural diversity on kinetic properties of cutinases from Thermobifida*. *Macromolecules*, 2011. **44**(12): p. 4632-4640.
232. Liebminger, S., et al., *Hydrolysis of PET and bis-(benzoyloxyethyl) terephthalate with a new polyesterase from Penicillium citrinum*. *Biocatalysis and Biotransformation*, 2007. **25**(2-4): p. 171-177.
233. Puspitasari, N., S.-L. Tsai, and C.-K. Lee, *Fungal hydrophobin RolA enhanced PETase hydrolysis of polyethylene terephthalate*. *Applied Biochemistry and Biotechnology*, 2021. **193**(5): p. 1284-1295.

234. Kawai, F., *The current state of research on PET hydrolyzing enzymes available for biorecycling*. Catalysts, 2021. **11**(2): p. 206.
235. de Queiros Eugenio, E., et al., *Experimental and mathematical modeling approaches for biocatalytic post-consumer poly (ethylene terephthalate) hydrolysis*. Journal of Biotechnology, 2021. **341**: p. 76-85.
236. Zhou, Y., et al., *Challenges and opportunities in bioremediation of micro-nano plastics: A review*. Science of The Total Environment, 2022. **802**: p. 149823.
237. Delangiz, N., et al., *Can polymer-degrading microorganisms solve the bottleneck of plastics' environmental challenges?* Chemosphere, 2022: p. 133709.
238. Stanica-Ezeanu, D. and D. Matei, *Natural depolymerization of waste poly (ethylene terephthalate) by neutral hydrolysis in marine water*. Scientific reports, 2021. **11**(1): p. 1-7.
239. Ali, S.S., et al., *Plastic wastes biodegradation: mechanisms, challenges and future prospects*. Science of the Total Environment, 2021. **780**: p. 146590.
240. Beech, J.L., et al., *A flexible kinetic assay efficiently sorts prospective biocatalysts for PET plastic subunit hydrolysis*. RSC advances, 2022. **12**(13): p. 8119-8130.
241. Li, Y., et al., *Towards Making Poly (ethylene terephthalate) Degradable in Aqueous Environment*. Macromolecular Materials and Engineering, 2022: p. 2100832.

242. Amarasekara, A.S., J.A. Gonzalez, and V.C. Nwankwo, *Sulfonic acid group functionalized Brønsted acidic ionic liquid catalyzed depolymerization of poly (ethylene terephthalate) in water*. Journal of Ionic Liquids, 2022. **2**(1): p. 100021.
243. Geyer, B., G. Lorenz, and A. Kandelbauer, *Recycling of poly (ethylene terephthalate)-A review focusing on chemical methods*. Express Polymer Letters, 2016. **10**(7).
244. Paszun, D. and T. Szychaj, *Chemical recycling of poly (ethylene terephthalate)*. Industrial & engineering chemistry research, 1997. **36**(4): p. 1373-1383.
245. Rahimi, A. and J.M. García, *Chemical recycling of waste plastics for new materials production*. Nature Reviews Chemistry, 2017. **1**(6): p. 1-11.
246. Malik, N., et al., *An overview on PET waste recycling for application in packaging*. International Journal of Plastics Technology, 2017. **21**(1): p. 1-24.
247. Shanmugam, V., et al., *Polymer recycling in additive manufacturing: An opportunity for the circular economy*. Materials Circular Economy, 2020. **2**(1): p. 1-11.
248. Campanelli, J., D. Cooper, and M. Kamal, *Catalyzed hydrolysis of polyethylene terephthalate melts*. Journal of Applied Polymer Science, 1994. **53**(8): p. 985-991.
249. Mancini, S.D. and M. Zanin, *Optimization of neutral hydrolysis reaction of post-consumer PET for chemical recycling*. Progress in Rubber Plastics and Recycling Technology, 2004. **20**(2): p. 117-132.

250. Quartinello, F., et al., *Synergistic chemo-enzymatic hydrolysis of poly (ethylene terephthalate) from textile waste*. Microbial biotechnology, 2017. **10**(6): p. 1376-1383.
251. Zhu, B., D. Wang, and N. Wei, *Enzyme discovery and engineering for sustainable plastic recycling*. Trends in biotechnology, 2022. **40**(1): p. 22-37.
252. Sato, O., et al., *Chemical recycling process of poly (ethylene terephthalate) in high-temperature liquid water*. Journal of chemical engineering of Japan, 2010. **43**(3): p. 313-317.
253. Liu, Y., M. Wang, and Z. Pan, *Catalytic depolymerization of polyethylene terephthalate in hot compressed water*. The Journal of Supercritical Fluids, 2012. **62**: p. 226-231.
254. Mancini, S.D., et al., *Solid-state hydrolysis of postconsumer polyethylene terephthalate after plasma treatment*. Journal of Applied Polymer Science, 2013. **127**(3): p. 1989-1996.
255. Čorak, I., et al., *Sustainable Alkaline Hydrolysis of Polyester Fabric at Low Temperature*. Materials, 2022. **15**(4): p. 1530.
256. Kao, C.Y., W.H. Cheng, and B.Z. Wan, *Investigation of alkaline hydrolysis of polyethylene terephthalate by differential scanning calorimetry and thermogravimetric analysis*. Journal of applied polymer science, 1998. **70**(10): p. 1939-1945.

257. Wan, B.-Z., C.-Y. Kao, and W.-H. Cheng, *Kinetics of depolymerization of poly (ethylene terephthalate) in a potassium hydroxide solution*. Industrial & engineering chemistry research, 2001. **40**(2): p. 509-514.
258. Goje, A., et al., *Chemical recycling, kinetics, and thermodynamics of hydrolysis of poly (ethylene terephthalate) waste with nonaqueous potassium hydroxide solution*. Polymer-Plastics Technology and Engineering, 2004. **43**(2): p. 369-388.
259. Collins, M. and S. Zeronian, *The molecular weight distribution and oligomers of sodium hydroxide hydrolyzed poly (ethylene terephthalate)*. Journal of applied polymer science, 1992. **45**(5): p. 797-804.
260. Holmes, S. and S. Zeronian, *Surface area of aqueous sodium hydroxide hydrolyzed high-speed spun poly (ethylene terephthalate) fibers*. Journal of applied polymer science, 1995. **55**(11): p. 1573-1581.
261. Mancini, S.D., et al., *Additional steps in mechanical recycling of PET*. Journal of Cleaner Production, 2010. **18**(1): p. 92-100.
262. Chaonan, L. and C. Jihua, *The study of the recovery of highly purified terephthalic acid from alkali weight-reduction wastewater*. International journal of environment and pollution, 2007. **29**(4): p. 484-494.
263. Al-Sabagh, A., et al., *Greener routes for recycling of polyethylene terephthalate*. Egyptian Journal of Petroleum, 2016. **25**(1): p. 53-64.

264. Murthy, N., S. Wilson, and J. Sy, *Biodegradation of polymers*. Polymer Science: A Comprehensive Reference, 10 Volume Set, 2012: p. 547-560.
265. Bee, S.-L., et al., *Approaches to improve therapeutic efficacy of biodegradable PLA/PLGA microspheres: a review*. Polymer Reviews, 2018. **58**(3): p. 495-536.
266. *Base-Catalyzed Hydrolysis of Esters*. 2022; Available from: <https://www.chemistrysteps.com/ester-hydrolysis-acid-and-base-catalyzed-mechanism/>.
267. Pitat, J., V. Holcik, and M. Bacak, *A method of processing waste of polyethylene terephthalate by hydrolysis*. GB Patent, 1959. **822**: p. 834.
268. Lazarus, S.D., I.C. Twilley, and O.E. Snider, *Simultaneous depolymerization of polycaprolactam and polyester with recovery of caprolactam*. 1967, Google Patents.
269. Nikolaevich, L., I. Vladimirovna, and M. Zulfatovich, *Method for Waste PET Alkaline Hydrolysis with Terephthalic Acid Production*. RU Patent, 2017. **2**.
270. Mishra, S., V.S. Zope, and A.S. Goje, *Kinetic and thermodynamic studies of depolymerisation of poly (ethylene terephthalate) by saponification reaction*. Polymer international, 2002. **51**(12): p. 1310-1315.
271. Karayannidis, G., A. Chatziavgoustis, and D. Achilias, *Poly (ethylene terephthalate) recycling and recovery of pure terephthalic acid by alkaline hydrolysis*. Advances in Polymer Technology: Journal of the Polymer Processing Institute, 2002. **21**(4): p. 250-259.

272. Kosmidis, V.A., D.S. Achilias, and G.P. Karayannidis, *Poly (ethylene terephthalate) recycling and recovery of pure terephthalic acid. Kinetics of a phase transfer catalyzed alkaline hydrolysis*. *Macromolecular Materials and Engineering*, 2001. **286**(10): p. 640-647.
273. López-Fonseca, R., et al., *A kinetic study of the depolymerisation of poly (ethylene terephthalate) by phase transfer catalysed alkaline hydrolysis*. *Journal of Chemical Technology & Biotechnology: International Research in Process, Environmental & Clean Technology*, 2009. **84**(1): p. 92-99.
274. Naik, S.D. and L. Doraiswamy, *Mathematical modeling of solid-liquid phase-transfer catalysis*. *Chemical engineering science*, 1997. **52**(24): p. 4533-4546.
275. Van Kruchten, E.M.G.A., *Quaternary phosphonium salt catalysts in catalytic hydrolysis of alkylene oxides*. 2000, Google Patents.
276. López-Fonseca, R., J. González-Velasco, and J. Gutiérrez-Ortiz, *A shrinking core model for the alkaline hydrolysis of PET assisted by tributylhexadecylphosphonium bromide*. *Chemical Engineering Journal*, 2009. **146**(2): p. 287-294.
277. Khalaf, H.I. and O.A. Hasan, *Effect of quaternary ammonium salt as a phase transfer catalyst for the microwave depolymerization of polyethylene terephthalate waste bottles*. *Chemical Engineering Journal*, 2012. **192**: p. 45-48.
278. Achilias, D. and G. Karayannidis, *The chemical recycling of PET in the framework of sustainable development*. *Water, air and soil pollution: Focus*, 2004. **4**(4): p. 385-396.

279. Welle, F., *Twenty years of PET bottle to bottle recycling—An overview*. Resources, Conservation and Recycling, 2011. **55**(11): p. 865-875.
280. Siddiqui, M.N., et al., *Hydrolytic depolymerization of PET in a microwave reactor*. Macromolecular Materials and Engineering, 2010. **295**(6): p. 575-584.
281. Paliwal, N.R. and A.K. Mungray, *Ultrasound assisted alkaline hydrolysis of poly (ethylene terephthalate) in presence of phase transfer catalyst*. Polymer degradation and stability, 2013. **98**(10): p. 2094-2101.
282. Chen, W., et al., *Biomass-derived γ -valerolactone: Efficient dissolution and accelerated alkaline hydrolysis of polyethylene terephthalate*. Green Chemistry, 2021. **23**(11): p. 4065-4073.
283. Wang, Y., et al., *Towards recycling purpose: converting PET plastic waste back to terephthalic acid using pH-responsive phase transfer catalyst*. Chinese Journal of Chemical Engineering, 2021.
284. Ügdüler, S., et al., *Towards closed-loop recycling of multilayer and coloured PET plastic waste by alkaline hydrolysis*. Green chemistry, 2020. **22**(16): p. 5376-5394.
285. Kumagai, S., et al., *Alkaline hydrolysis of PVC-coated PET fibers for simultaneous recycling of PET and PVC*. Journal of Material Cycles and Waste Management, 2018. **20**(1): p. 439-449.

286. Das, S.K., et al., *Plastic recycling of polyethylene terephthalate (PET) and polyhydroxybutyrate (PHB)—A comprehensive review*. *Materials Circular Economy*, 2021. **3**(1): p. 1-22.
287. George, N. and T. Kurian, *Recent developments in the chemical recycling of postconsumer poly (ethylene terephthalate) waste*. *Industrial & Engineering Chemistry Research*, 2014. **53**(37): p. 14185-14198.
288. Yoshioka, T., T. Motoki, and A. Okuwaki, *Kinetics of hydrolysis of poly (ethylene terephthalate) powder in sulfuric acid by a modified shrinking-core model*. *Industrial & engineering chemistry research*, 2001. **40**(1): p. 75-79.
289. Yoshioka, T., N. Okayama, and A. Okuwaki, *Kinetics of hydrolysis of PET powder in nitric acid by a modified shrinking-core model*. *Industrial & engineering chemistry research*, 1998. **37**(2): p. 336-340.
290. Mancini, S.D. and M. Zanin, *Post consumer pet depolymerization by acid hydrolysis*. *Polymer-Plastics Technology and Engineering*, 2007. **46**(2): p. 135-144.
291. Mishra, S., A. Goje, and V. Zope, *Chemical recycling, kinetics, and thermodynamics of poly (ethylene terephthalate)(PET) waste powder by nitric acid hydrolysis*. *Polymer Reaction Engineering*, 2003. **11**(1): p. 79-99.
292. Carta, D., G. Cao, and C. D'Angeli, *Chemical recycling of poly (ethylene terephthalate)(PET) by hydrolysis and glycolysis*. *Environmental Science and Pollution Research*, 2003. **10**(6): p. 390-394.

293. Tabekh, H., Y. Kouksi, and Z. Ajji, *Chemical recycling of poly (ethylene terephthalate) using sulfuric acid*. *Revue Roumaine de Chimie*, 2012. **57**(12): p. 1031-1036.
294. de Carvalho, G.M., E.C. Muniz, and A.F. Rubira, *Hydrolysis of post-consume poly (ethylene terephthalate) with sulfuric acid and product characterization by WAXD, ¹³C NMR and DSC*. *Polymer degradation and Stability*, 2006. **91**(6): p. 1326-1332.
295. Santos, L.A. and L.C. Mendes, *ACID-HYDROLYSIS OF POST-CONSUMER PET USING VARIABLE ROUTES*.
296. Brown Jr, G.E. and R.C. O'brien, *Method for recovering terephthalic acid and ethylene glycol from polyester materials*. 1976, Google Patents.
297. Li, X.K., et al., *Reaction kinetics and mechanism of catalyzed hydrolysis of waste PET using solid acid catalyst in supercritical CO₂*. *AIChE Journal*, 2015. **61**(1): p. 200-214.
298. Pusztaszeri, S.F., *Method for recovery of terephthalic acid from polyester scrap*. 1982, Google Patents.
299. Gao, R., H. Pan, and J. Lian, *Recent advances in the discovery, characterization, and engineering of poly (ethylene terephthalate)(PET) hydrolases*. *Enzyme and Microbial Technology*, 2021. **150**: p. 109868.

300. Kawai, F., T. Kawabata, and M. Oda, *Current knowledge on enzymatic PET degradation and its possible application to waste stream management and other fields*. Applied microbiology and biotechnology, 2019. **103**(11): p. 4253-4268.
301. Barth, M., et al., *Effect of hydrolysis products on the enzymatic degradation of polyethylene terephthalate nanoparticles by a polyester hydrolase from Thermobifida fusca*. Biochemical engineering journal, 2015. **93**: p. 222-228.
302. Sulaiman, S., et al., *Isolation of a novel cutinase homolog with polyethylene terephthalate-degrading activity from leaf-branch compost by using a metagenomic approach*. Applied and Environmental Microbiology, 2012. **78**(5): p. 1556-1562.
303. Carniel, A., et al., *Lipase from Candida antarctica (CALB) and cutinase from Humicola insolens act synergistically for PET hydrolysis to terephthalic acid*. Process Biochemistry, 2017. **59**: p. 84-90.
304. Liu, P., et al., *Potential one-step strategy for PET degradation and PHB biosynthesis through co-cultivation of two engineered microorganisms*. Engineering Microbiology, 2021. **1**: p. 100003.
305. Ribitsch, D., et al., *A new esterase from Thermobifida halotolerans hydrolyses polyethylene terephthalate (PET) and polylactic acid (PLA)*. Polymers, 2012. **4**(1): p. 617-629.

306. Guebitz, G.M. and A. Cavaco-Paulo, *Enzymes go big: surface hydrolysis and functionalisation of synthetic polymers*. Trends in biotechnology, 2008. **26**(1): p. 32-38.
307. Barth, M., et al., *A dual enzyme system composed of a polyester hydrolase and a carboxylesterase enhances the biocatalytic degradation of polyethylene terephthalate films*. Biotechnology Journal, 2016. **11**(8): p. 1082-1087.
308. Billig, S., et al., *Hydrolysis of cyclic poly (ethylene terephthalate) trimers by a carboxylesterase from Thermobifida fusca KW3*. Applied microbiology and biotechnology, 2010. **87**(5): p. 1753-1764.
309. de Castro, A.M., et al., *Screening of commercial enzymes for poly (ethylene terephthalate)(PET) hydrolysis and synergy studies on different substrate sources*. Journal of Industrial Microbiology and Biotechnology, 2017. **44**(6): p. 835-844.
310. Carniel, A., V. de Abreu Waldow, and A.M. de Castro, *A comprehensive and critical review on key elements to implement enzymatic PET depolymerization for recycling purposes*. Biotechnology Advances, 2021. **52**: p. 107811.
311. Wei, R. and W. Zimmermann, *Microbial enzymes for the recycling of recalcitrant petroleum-based plastics: how far are we?* Microbial biotechnology, 2017. **10**(6): p. 1308-1322.
312. Mathew, J.J., et al., *Microbial degradation of polyethylene terphthalate (PET): An outlook study*. Journal of Medicinal Plants, 2021. **9**(5): p. 31-40.

313. Koshti, R., L. Mehta, and N. Samarth, *Biological recycling of polyethylene terephthalate: a mini-review*. Journal of Polymers and the Environment, 2018. **26**(8): p. 3520-3529.
314. Ohmura, S.D., et al., *Depolymerization of waste PET with phosphoric acid-modified silica gel under microwave irradiation*. Journal of Polymers and the Environment, 2017. **25**(2): p. 250-257.
315. Kang, M.J., et al., *Depolymerization of PET into terephthalic acid in neutral media catalyzed by the ZSM-5 acidic catalyst*. Chemical Engineering Journal, 2020. **398**: p. 125655.
316. Granados, M.L., et al., *Poly (styrenesulphonic) acid: an active and reusable acid catalyst soluble in polar solvents*. Green chemistry, 2011. **13**(11): p. 3203-3212.
317. Liu, M., et al., *Degradation of waste polycarbonate via hydrolytic strategy to recover monomer (bisphenol A) catalyzed by DBU-based ionic liquids under metal- and solvent-free conditions*. Polymer Degradation and Stability, 2018. **157**: p. 9-14.
318. Cândido, A.A., et al., *Mechanistic investigation of DBU-based ionic liquids for aza-michael reaction: mass spectrometry and DFT studies of catalyst role*. Journal of the Brazilian Chemical Society, 2020. **31**: p. 1796-1804.
319. Gao, F., et al., *CO₂ absorption by DBU-based protic ionic liquids: Basicity of anion dictates the absorption capacity and mechanism*. Frontiers in chemistry, 2019. **6**: p. 658.

320. Chen, X. and A. Ying, *DBU derived ionic liquids and their application in organic synthetic reactions*. *Ionic Liquids: Applications and Perspectives*, 2011: p. 305-330.
321. Sheppard, K., *High school students' understanding of titrations and related acid-base phenomena*. *Chemistry Education Research and Practice*, 2006. **7**(1): p. 32-45.
322. Borsci, S., et al., *Usability study of pH strips for nasogastric tube placement*. *PloS one*, 2017. **12**(11): p. e0189013.
323. Iacono, S.D., et al. *pH strip reader for beer samples based on image analysis*. in *2020 IEEE International Workshop on Metrology for Agriculture and Forestry (MetroAgriFor)*. 2020. IEEE.
324. Singh, S., et al., *Recycling of waste poly (ethylene terephthalate) bottles by alkaline hydrolysis and recovery of pure nanospindle-shaped terephthalic acid*. *Journal of nanoscience and nanotechnology*, 2018. **18**(8): p. 5804-5809.
325. Redman-Furey, N., et al., *An evaluation of primary water standards by TG/DTA and vapor sorption analysis*. *Journal of thermal analysis and calorimetry*, 2010. **102**(2): p. 633-639.
326. Gaffney, J.S., N.A. Marley, and D.E. Jones, *Fourier transform infrared (FTIR) spectroscopy*. *Characterization of Materials*, 2002: p. 1-33.

327. Lewis, S., A. Lewis, and P. Lewis, *Prediction of glycoprotein secondary structure using ATR-FTIR*. *Vibrational Spectroscopy*, 2013. **69**: p. 21-29.
328. Wang, J.-Q., et al., *A review of NMR analysis in polysaccharide structure and conformation: Progress, challenge and perspective*. *Food Research International*, 2021. **143**: p. 110290.
329. Tan, H.-b. and Y.-f. Wang, *Synthesis, NMR analysis and X-ray crystal structure of 3, 9-bis (4-(trifluoromethyl) phenyl)-3, 9-diazatetraasterane*. *Journal of Molecular Structure*, 2020. **1220**: p. 128751.
330. Drzeżdżon, J., et al., *A review of new approaches to analytical methods to determine the structure and morphology of polymers*. *TrAC Trends in Analytical Chemistry*, 2019. **118**: p. 470-476.
331. Chao, D., et al., *SEM study of the morphology of high molecular weight polyaniline*. *Synthetic Metals*, 2005. **150**(1): p. 47-51.
332. González, G.P., P.F. Hernando, and J.D. Alegría, *A morphological study of molecularly imprinted polymers using the scanning electron microscope*. *Analytica chimica acta*, 2006. **557**(1-2): p. 179-183.
333. Bjorksten, J., *Polyesters and their applications*. 1956: Reinhold Publishing Corporation.
334. *Global polyethylene terephthalate (PET) market 2019 by manufacturers, regions, type, and application, Forecast 2024*. [cited 2020; Available from:

<https://www.marketwatch.com/press-release/polyethylene-terephthalate-pet-market-2019---global-trends-statistics-size-share-regional-analysis-by-key-players-industry-forecast-by-categories-platform-end---user-2019-08-27>

335. ; Available from: <https://www.plasticsnews.com/news/napcor-us-lacks-recycled-pet-meet-consumer-brands-pledges>
336. Fang, P., et al., *High-efficiency glycolysis of poly (ethylene terephthalate) by sandwich-structure polyoxometalate catalyst with two active sites*. 2018. **156**: p. 22-31.
337. Leng, Z., R.K. Padhan, and A.J.o.c.p. Sreeram, *Production of a sustainable paving material through chemical recycling of waste PET into crumb rubber modified asphalt*. *Journal of cleaner production*, 2018. **180**: p. 682-688.
338. Nelms, S.E., et al., *Plastic and marine turtles: a review and call for research*. 2016. **73**(2): p. 165-181.
339. Raheem, A.B., et al., *Current developments in chemical recycling of post-consumer polyethylene terephthalate wastes for new materials production: a review*. 2019. **225**: p. 1052-1064.
340. Scheirs, J.J.J.W. and J. Sons Ltd, Baffins Lane, Chichester, Sussex PO 19 1 UD, UK, . 591, *Polymer recycling: science, technology and applications*. 1998.
341. Wilcox, C., et al., *A quantitative analysis linking sea turtle mortality and plastic debris ingestion*. 2018. **8**(1): p. 1-11.

342. Nait-Ali, L.K., et al., *Kinetic analysis and modelling of PET macromolecular changes during its mechanical recycling by extrusion*. 2011. **96**(2): p. 236-246.
343. Gu, F., et al., *From waste plastics to industrial raw materials: A life cycle assessment of mechanical plastic recycling practice based on a real-world case study*. 2017. **601**: p. 1192-1207.
344. Nikles, D.E., M.S.J.M.M. Farahat, and Engineering, *New motivation for the depolymerization products derived from poly (ethylene terephthalate)(PET) waste: A review*. 2005. **290**(1): p. 13-30.
345. Venkatachalam, S., et al., *Degradation and recyclability of poly (ethylene terephthalate)*, in *Polyester*. 2012, InTech Rijeka, Croatia. p. 75-98.
346. Awaja, F. and D.J.E.P.J. Pavel, *Recycling of PET*. 2005. **41**(7): p. 1453-1477.
347. Bartolome, L., et al., *Recent developments in the chemical recycling of PET*. 2012. **406**.
348. López-Fonseca, R., et al., *Chemical recycling of post-consumer PET wastes by glycolysis in the presence of metal salts*. 2010. **95**(6): p. 1022-1028.
349. Yue, Q., et al., *Glycolysis of poly (ethylene terephthalate)(PET) using basic ionic liquids as catalysts*. 2011. **96**(4): p. 399-403.
350. Zhang, L., et al., *Hydrolysis of poly (ethylene terephthalate) waste bottles in the presence of dual functional phase transfer catalysts*. 2013. **130**(4): p. 2790-2795.

351. Mishra, S. and A.S.J.P.i. Goje, *Kinetic and thermodynamic study of methanolysis of poly (ethylene terephthalate) waste powder*. 2003. **52**(3): p. 337-342.
352. Palekar, V.S., R.V. Shah, and S.J.J.o.a.p.s. Shukla, *Ionic liquid-catalyzed aminolysis of poly (ethylene terephthalate) waste*. 2012. **126**(3): p. 1174-1181.
353. Soni, R. and S.J.J.o.a.p.s. Singh, *Synthesis and characterization of terephthalamides from poly (ethylene terephthalate) waste*. 2005. **96**(5): p. 1515-1528.
354. Wang, Y., et al., *Zinc-catalyzed ester bond cleavage: Chemical degradation of polyethylene terephthalate*. 2019. **208**: p. 1469-1475.
355. Li, X.K., et al., *Reaction kinetics and mechanism of catalyzed hydrolysis of waste PET using solid acid catalyst in supercritical CO₂*. 2015. **61**(1): p. 200-214.
356. Ikenaga, K., T. Inoue, and K.J.P.e. Kusakabe, *Hydrolysis of PET by combining direct microwave heating with high pressure*. 2016. **148**: p. 314-318.
357. Spaseska, D., M.J.J.o.t.U.o.C.T. Civkaroska, and Metallurgy, *Alkaline hydrolysis of poly (ethylene terephthalate) recycled from the postconsumer soft-drink bottles*. 2010. **45**(4): p. 379-384.
358. Wan, B.-Z., et al., *Kinetics of depolymerization of poly (ethylene terephthalate) in a potassium hydroxide solution*. 2001. **40**(2): p. 509-514.

359. Hu, L.-C., et al., *Alkali-decomposition of poly (ethylene terephthalate) in mixed media of nonaqueous alcohol and ether. Study on recycling of poly (ethylene terephthalate)*. Polymer journal, 1997. **29**(9): p. 708-712.
360. Collins, M. and S.J.J.o.a.p.s. Zeronian, *The molecular weight distribution and oligomers of sodium hydroxide hydrolyzed poly (ethylene terephthalate)*. 1992. **45**(5): p. 797-804.
361. Oku, A., L.C. Hu, and E.J.J.o.A.P.S. Yamada, *Alkali decomposition of poly (ethylene terephthalate) with sodium hydroxide in nonaqueous ethylene glycol: a study on recycling of terephthalic acid and ethylene glycol*. 1997. **63**(5): p. 595-601.
362. Mandoki, J.W., *Depolymerization of condensation polymers*. 1986, Google Patents.
363. Campanelli, J.R., M. Kamal, and D.J.J.o.A.P.S. Cooper, *A kinetic study of the hydrolytic degradation of polyethylene terephthalate at high temperatures*. 1993. **48**(3): p. 443-451.
364. Grause, G., et al., *Hydrolysis of poly (ethylene terephthalate) in a fluidised bed reactor*. 2004. **85**(1): p. 571-575.
365. Mancini, S.D., M.J.P.-P.T. Zanin, and Engineering, *Post consumer pet depolymerization by acid hydrolysis*. 2007. **46**(2): p. 135-144.

366. Mishra, S., et al., *Chemical recycling, kinetics, and thermodynamics of hydrolysis of poly (ethylene terephthalate)(PET) waste in sulfuric acid in presence of phosphoric acid*. 2003. **42**(4): p. 581-603.
367. Moghbeli, M.R., S. Namayandeh, and S.H.I.I.J.o.C.R.E. Hashemabadi, *Wet hydrolysis of waste polyethylene terephthalate thermoplastic resin with sulfuric acid and cfd simulation for high viscous liquid mixing*. 2010. **8**(1).
368. Al-tamimi, R.K., et al., *Post consumer poly (ethylene terephthalate) depolymerization by waste of battery acid hydrolysis*. 2011. **2**(2): p. 88-93.
369. Tabekh, H., Y. Koudsi, and Z.J.R.R.C. Ajji, *Chemical recycling of poly (ethylene terephthalate) using sulfuric acid*. 2012. **57**(12): p. 1029-1034.
370. Yoshioka, T., T. Sato, and A.J.J.o.A.P.S. Okuwaki, *Hydrolysis of waste PET by sulfuric acid at 150 C for a chemical recycling*. 1994. **52**(9): p. 1353-1355.
371. Yoshioka, T., et al., *Kinetics of hydrolysis of poly (ethylene terephthalate) powder in sulfuric acid by a modified shrinking-core model*. 2001. **40**(1): p. 75-79.
372. Yoshioka, T., et al., *Kinetics of hydrolysis of PET powder in nitric acid by a modified shrinking-core model*. 1998. **37**(2): p. 336-340.
373. Ravens, D.J.P., *The chemical reactivity of poly (ethylene terephthalate): Heterogeneous hydrolysis by hydrochloric acid*. 1960. **1**: p. 375-383.
374. Davies, T., et al., *The kinetics of the hydrolysis of polyethylene terephthalate film*. 1962. **66**(1): p. 175-176.

375. Amarasekara, A.S. and B.J.A.C.A.G. Wiredu, *Aryl sulfonic acid catalyzed hydrolysis of cellulose in water*. 2012. **417**: p. 259-262.
376. Granados, M.L., et al., *Poly (styrenesulphonic) acid: an active and reusable acid catalyst soluble in polar solvents*. 2011. **13**(11): p. 3203-3212.
377. Xue, Z., et al., *Advances in the conversion of glucose and cellulose to 5-hydroxymethylfurfural over heterogeneous catalysts*. 2016. **6**(101): p. 98874-98892.
378. Alonso-Fagúndez, N., et al., *Poly-(styrene sulphonic acid): An acid catalyst from polystyrene waste for reactions of interest in biomass valorization*. 2014. **234**: p. 285-294.
379. Rubio, A.C.A., et al., *Homogeneous and reusable superacid polymer catalyst useful for the synthesis of 5-hydroxymethylfurfural from glucose*. 2020, Google Patents.
380. Cheong, S.I., et al., *Physical adsorption of water-soluble polymers on hydrophobic polymeric membrane surfaces via salting-out effect*. 2013. **21**(6): p. 629-635.
381. Blokhuis, A.M., K.J.J.o.c. Djurhuus, and i. science, *Adsorption of poly (styrene sulfonate) of different molecular weights on α -alumina: effect of added sodium dodecyl sulfate*. 2006. **296**(1): p. 64-70.
382. Cousin, P. and P.J.J.o.P.S.P.B.P.P. Smith, *Dynamic mechanical properties of sulfonated polystyrene/alumina composites*. 1994. **32**(3): p. 459-468.

383. Coughlin, J.E., et al., *Sulfonation of polystyrene: Toward the "ideal" polyelectrolyte*. 2013. **51**(11): p. 2416-2424.
384. Kwok, D.Y., A.W.J.A.i.c. Neumann, and i. science, *Contact angle measurement and contact angle interpretation*. 1999. **81**(3): p. 167-249.
385. Pavlov, D., et al., *Influence of H₂SO₄ concentration on the mechanism of the processes and on the electrochemical activity of the Pb/PbO₂/PbSO₄ electrode*. 2004. **137**(2): p. 288-308.
386. Siril, P., H.E. Cross, and D.J.J.o.M.C.A.C. Brown, *New polystyrene sulfonic acid resin catalysts with enhanced acidic and catalytic properties*. 2008. **279**(1): p. 63-68.
387. Harmer, M.A. and Q.J.A.C.A.G. Sun, *Solid acid catalysis using ion-exchange resins*. 2001. **221**(1-2): p. 45-62.
388. Tejero, J., et al., *Zeolite catalysed dehydration of alcohol to linear ether*, in *Studies in surface science and catalysis*. 2008, Elsevier. p. 1115-1118.
389. Ravens, D. and I.J.T.o.t.F.S. Ward, *Chemical reactivity of polyethylene terephthalate. Hydrolysis and esterification reactions in the solid phase*. 1961. **57**: p. 150-159.
390. Ayyappan, K., et al., *Catalytic hydrolysis of ethyl acetate using cation exchange resin (Amberlyst-15): a kinetic study*. 2009. **4**(1): p. 16.
391. Newalkar, B., et al., *Kinetics of ethylacetate hydrolysis on mordenite*. 1993.

392. Namba, S., N. Hosonuma, and T.J.J.o.C. Yashima, *Catalytic application of hydrophobic properties of high-silica zeolites: I. Hydrolysis of ethyl acetate in aqueous solution*. 1981. **72**(1): p. 16-20.
393. Shimizu, K.-i., et al., *Acidic properties of sulfonic acid-functionalized FSM-16 mesoporous silica and its catalytic efficiency for acetalization of carbonyl compounds*. 2005. **231**(1): p. 131-138.
394. Rat, M., et al., *Sulfonic acid functionalized periodic mesoporous organosilicas as acetalization catalysts*. 2008. **112**(1-3): p. 26-31.
395. Heiss-Blanquet, S., et al., *Effect of pretreatment and enzymatic hydrolysis of wheat straw on cell wall composition, hydrophobicity and cellulase adsorption*. 2011. **102**(10): p. 5938-5946.
396. Miura, H., et al., *Quantitative Evaluation of the Effect of the Hydrophobicity of the Environment Surrounding Brønsted Acid Sites on Their Catalytic Activity for the Hydrolysis of Organic Molecules*. 2018. **141**(4): p. 1636-1645.
397. Chibowski, S., M.J.A.S. Wiśniewska, and Technology, *Study of the adsorption mechanism and the structure of adsorbed layers of polyelectrolytes at the metal oxide/solution interface*. 2001. **19**(5): p. 409-421.
398. Sen, A.K., S. Roy, and V.A.J.P.i. Juvekar, *Effect of structure on solution and interfacial properties of sodium polystyrene sulfonate (NaPSS)*. 2007. **56**(2): p. 167-174.

399. Sádaba, I., et al., *Silica-poly (styrenesulphonic acid) nanocomposites for the catalytic dehydration of xylose to furfural*. Applied Catalysis B: Environmental, 2014. **150**: p. 421-431.
400. Stan, C.S., et al., *Synthesis and characterization of PSSA-polyaniline composite with an enhanced processability in thin films*. Open Chemistry, 2015. **13**(1).
401. Göktepe, F., A. Bozkurt, and Ş.T. Günday, *Synthesis and proton conductivity of poly (styrene sulfonic acid)/heterocycle-based membranes*. Polymer international, 2008. **57**(1): p. 133-138.
402. Yan, W., et al., *Preparation of partially reduced graphene oxide nanosheets/poly (sodium 4-styrenesulfonate) composite with high capacitance*. Electrochimica Acta, 2014. **147**: p. 257-264.
403. Singh, A.K., R. Bedi, and B.S. Kaith, *Composite materials based on recycled polyethylene terephthalate and their properties—A comprehensive review*. Composites Part B: Engineering, 2021: p. 108928.
404. Umasabor, R.I. and S.C. Daniel, *The effect of using polyethylene terephthalate as an additive on the flexural and compressive strength of concrete*. Heliyon, 2020. **6**(8): p. e04700.
405. Subramanian, K., et al., *Environmental life cycle assessment of textile bio-recycling—valorizing cotton-polyester textile waste to pet fiber and glucose syrup*. Resources, Conservation and Recycling, 2020. **161**: p. 104989.

406. Quintero, A.V., et al., *Capacitive strain sensors inkjet-printed on pet fibers for integration in industrial textile*. *Procedia engineering*, 2015. **120**: p. 279-282.
407. Shukla, S., A.M. Harad, and L.S. Jawale, *Recycling of waste PET into useful textile auxiliaries*. *Waste Management*, 2008. **28**(1): p. 51-56.
408. Nisticò, R., *Polyethylene terephthalate (PET) in the packaging industry*. *Polymer Testing*, 2020: p. 106707.
409. Fernández-Menéndez, T., et al., *Industrially produced PET nanocomposites with enhanced properties for food packaging applications*. *Polymer Testing*, 2020. **90**: p. 106729.
410. Junior, W.J.F.L., et al., *Reuse of refillable PET packaging: Approaches to safety and quality in soft drink processing*. *Food Control*, 2019. **100**: p. 329-334.
411. Cardozo, I.M.M., et al., *Exploratory analysis of the presence of 14 carbonyl compounds in bottled mineral water in polyethylene terephthalate (PET) containers*. *Food Chemistry*, 2021. **365**: p. 130475.
412. Kankanige, D. and S. Babel, *Smaller-sized micro-plastics (MPs) contamination in single-use PET-bottled water in Thailand*. *Science of the Total Environment*, 2020. **717**: p. 137232.
413. Limbo, S., et al., *Storage of pasteurized milk in clear PET bottles combined with light exposure on a retail display case: A possible strategy to define the shelf life and support a recyclable packaging*. *Food Chemistry*, 2020. **329**: p. 127116.

414. Ros-Chumillas, M., et al., *Quality and shelf life of orange juice aseptically packaged in PET bottles*. Journal of Food Engineering, 2007. **79**(1): p. 234-242.
415. Haider, S. and I. Hafeez, *A step toward smart city and green transportation: Eco-friendly waste PET management to enhance adhesion properties of asphalt mixture*. Construction and Building Materials, 2021. **304**: p. 124702.
416. Gileno, L.A. and L.F.R. Turci, *Life cycle assessment for PET-bottle recycling in Brazil: B2B and B2F routes*. Cleaner Environmental Systems, 2021: p. 100057.
417. Alfahdawi, I.H., et al., *Influence of PET wastes on the environment and high strength concrete properties exposed to high temperatures*. Construction and Building Materials, 2019. **225**: p. 358-370.
418. Das, P. and P. Tiwari, *Thermal degradation study of waste polyethylene terephthalate (PET) under inert and oxidative environments*. Thermochimica Acta, 2019. **679**: p. 178340.
419. Choudhary, K., K.S. Sangwan, and D. Goyal, *Environment and economic impacts assessment of PET waste recycling with conventional and renewable sources of energy*. Procedia CIRP, 2019. **80**: p. 422-427.
420. Li, Y., et al., *Rural household food waste characteristics and driving factors in China*. Resources, Conservation and Recycling, 2021. **164**: p. 105209.

421. Benavides, P.T., et al., *Exploring comparative energy and environmental benefits of virgin, recycled, and bio-derived PET bottles*. ACS Sustainable Chemistry & Engineering, 2018. **6**(8): p. 9725-9733.
422. Thompson, R.C., et al., *Plastics, the environment and human health: current consensus and future trends*. Philosophical transactions of the royal society B: biological sciences, 2009. **364**(1526): p. 2153-2166.
423. Chen, L., R.E. Pelton, and T.M. Smith, *Comparative life cycle assessment of fossil and bio-based polyethylene terephthalate (PET) bottles*. Journal of Cleaner Production, 2016. **137**: p. 667-676.
424. Gomes, T.S., L.L. Visconte, and E.B. Pacheco, *Life cycle assessment of polyethylene terephthalate packaging: An overview*. Journal of Polymers and the Environment, 2019. **27**(3): p. 533-548.
425. Chiari, L. and A. Zecca, *Constraints of fossil fuels depletion on global warming projections*. Energy Policy, 2011. **39**(9): p. 5026-5034.
426. Gervet, B., *The use of crude oil in plastic making contributes to global warming*. Lulea: Lulea University of Technology, 2007.
427. Mülhaupt, R., *Green polymer chemistry and bio-based plastics: dreams and reality*. Macromolecular Chemistry and Physics, 2013. **214**(2): p. 159-174.
428. Awaja, F. and D. Pavel, *Recycling of PET*. European polymer journal, 2005. **41**(7): p. 1453-1477.

429. Candido, S.E.A., M. Sacomano Neto, and M.R. Côrtes, *How social inequalities shape markets: lessons from the configuration of PET recycling practices in Brazil*. Business & Society, 2021: p. 0007650321989063.
430. Shamsi, R., et al., *Hopes beyond PET recycling: environmentally clean and engineeringly applicable*. Journal of Polymers and the Environment, 2019. **27**(11): p. 2490-2508.
431. Wang, Z., et al., *A pseudo-homogeneous system for PET glycolysis using a colloidal catalyst of graphite carbon nitride in ethylene glycol*. Polymer Degradation and Stability, 2021: p. 109638.
432. Wang, R., et al., *A new class of catalysts for the glycolysis of PET: Deep eutectic solvent@ ZIF-8 composite*. Polymer Degradation and Stability, 2021. **183**: p. 109463.
433. de Castro, A.M., et al., *Enzyme-catalyzed simultaneous hydrolysis-glycolysis reactions reveals tunability on PET depolymerization products*. Biochemical Engineering Journal, 2018. **137**: p. 239-246.
434. Kint, D.P., et al., *Poly (ethylene terephthalate) copolymers containing nitroterephthalic units. III. Methanolytic degradation*. Journal of Polymer Science Part A: Polymer Chemistry, 2002. **40**(14): p. 2276-2285.
435. Bartolome, L., et al., *Recent developments in the chemical recycling of PET*. Material recycling-trends and perspectives, 2012. **406**.

436. Lee, J., et al., *Chemical recycling of plastic waste via thermocatalytic routes*. Journal of Cleaner Production, 2021: p. 128989.
437. Chanda, M., *Chemical aspects of polymer recycling*. Advanced Industrial and Engineering Polymer Research, 2021.
438. Aguado, A., et al., *Chemical depolymerisation of PET complex waste: hydrolysis vs. glycolysis*. Journal of Material Cycles and Waste Management, 2014. **16**(2): p. 201-210.
439. Lee, H.L., C.W. Chiu, and T. Lee, *Engineering terephthalic acid product from recycling of PET bottles waste for downstream operations*. Chemical Engineering Journal Advances, 2021. **5**: p. 100079.
440. Collias, D.I., et al., *Biobased terephthalic acid technologies: a literature review*. Industrial Biotechnology, 2014. **10**(2): p. 91-105.
441. Filella, M., *Antimony and PET bottles: Checking facts*. Chemosphere, 2020: p. 127732.
442. Gao, R., H. Pan, and J. Lian, *Recent Advances in the Discovery, Characterization, and Engineering of Poly (ethylene terephthalate)(PET) Hydrolases*. Enzyme and Microbial Technology, 2021: p. 109868.
443. Barnard, E., J.J.R. Arias, and W. Thielemans, *Chemolytic depolymerisation of PET: a review*. Green Chemistry, 2021.

444. Spaseska, D. and M. Civkaroska, *Alkaline hydrolysis of poly (ethylene terephthalate) recycled from the postconsumer soft-drink bottles*. Journal of the university of chemical technology and metallurgy, 2010. **45**(4): p. 379-384.
445. Oku, A., L.C. Hu, and E. Yamada, *Alkali decomposition of poly (ethylene terephthalate) with sodium hydroxide in nonaqueous ethylene glycol: a study on recycling of terephthalic acid and ethylene glycol*. Journal of Applied Polymer Science, 1997. **63**(5): p. 595-601.
446. Al-tamimi, R.K., et al., *Post consumer poly (ethylene terephthalate) depolymerization by waste of battery acid hydrolysis*. Journal of Materials and Environmental Science, 2011. **2**(2): p. 88-93.
447. Mishra, S., A. Goje, and V. Zope, *Chemical recycling, kinetics, and thermodynamics of hydrolysis of poly (ethylene terephthalate)(PET) waste in sulfuric acid in presence of phosphoric acid*. Polymer-Plastics Technology and Engineering, 2003. **42**(4): p. 581-603.
448. Kan, Y., et al., *IsPETase Is a Novel Biocatalyst for Poly (ethylene terephthalate)(PET) Hydrolysis*. ChemBioChem, 2021. **22**(10): p. 1706-1716.
449. Güçlü, G., et al., *Simultaneous glycolysis and hydrolysis of polyethylene terephthalate and characterization of products by differential scanning calorimetry*. Polymer, 2003. **44**(25): p. 7609-7616.
450. Amarasekara, A.S. and B. Wiredu, *Degradation of cellulose in dilute aqueous solutions of acidic ionic liquid 1-(1-propylsulfonic)-3-methylimidazolium chloride,*

- and p-toluenesulfonic acid at moderate temperatures and pressures. Industrial & engineering chemistry research, 2011. 50(21): p. 12276-12280.*
451. Amarasekara, A.S. and O.S. Owereh, *Synthesis of a sulfonic acid functionalized acidic ionic liquid modified silica catalyst and applications in the hydrolysis of cellulose. Catalysis Communications, 2010. 11(13): p. 1072-1075.*
452. Amarasekara, A.S. and B. Wiredu, *Sulfonic acid group functionalized ionic liquid catalyzed hydrolysis of cellulose in water: structure activity relationships. Sustain Energy, 2014. 2: p. 102-107.*
453. Tan, X., et al., *Sulfonic acid-functionalized heterogeneous catalytic materials for efficient biodiesel production: A review. Journal of Environmental Chemical Engineering, 2020: p. 104719.*
454. Sohn, H., *Fluid-Solid Reactions. 2020: Elsevier.*
455. Ayyappan, K., et al., *Catalytic hydrolysis of ethyl acetate using cation exchange resin (Amberlyst-15): a kinetic study. Bulletin of Chemical Reaction Engineering & Catalysis, 2009. 4(1): p. 16.*
456. Kwok, D.Y. and A.W. Neumann, *Contact angle measurement and contact angle interpretation. Advances in colloid and interface science, 1999. 81(3): p. 167-249.*
457. Zhang, L., *Kinetics of hydrolysis of poly (ethylene terephthalate) wastes catalyzed by dual functional phase transfer catalyst: A mechanism of chain-end scission. European polymer journal, 2014. 60: p. 1-5.*

458. Yoshioka, T., T. Sato, and A. Okuwaki, *Hydrolysis of waste PET by sulfuric acid at 150 C for a chemical recycling*. Journal of Applied Polymer Science, 1994. **52**(9): p. 1353-1355.
459. Zhang, Z.-w., G.-d. Zhang, and C.-p. Mo, *Study on the microscopic adsorption of sulfur molecules onto {10 $\bar{1}$ 4} calcite surface*. Colloids and Surfaces A: Physicochemical and Engineering Aspects, 2021. **630**: p. 127630.
460. Namba, S., N. Hosonuma, and T. Yashima, *Catalytic application of hydrophobic properties of high-silica zeolites: I. Hydrolysis of ethyl acetate in aqueous solution*. Journal of Catalysis, 1981. **72**(1): p. 16-20.
461. Sangster, J.M., *Octanol-water partition coefficients: fundamentals and physical chemistry*. Vol. 1. 1997: John Wiley & Sons.
462. Abedsoltan, H., Z. Zoghi, and A.H. Mohammadi, *Prediction of terephthalic acid (TPA) yield in aqueous hydrolysis of polyethylene terephthalate (PET)*. arXiv preprint arXiv:2201.12657, 2022.
463. Peñalver, R., et al., *Authentication of recycled plastic content in water bottles using volatile fingerprint and chemometrics*. Chemosphere, 2022. **297**: p. 134156.
464. Verma, S., et al., *Recent Advances for Fabricating Smart Electromagnetic Interference Shielding Textile: A Comprehensive Review*. Electronic Materials Letters, 2022: p. 1-14.

465. Salhotra, S., R. Khitoliya, and S.K. Arora, *Assessing the applicability of GBFS-coated PET-fibers as a construction material: An innovative way of waste management*. *Materials Today: Proceedings*, 2022. **48**: p. 1015-1020.
466. Chamoun, M., *Investigating of HDPE & PET materials useability in electric cabling ducts for the car industry*. 2022.
467. Chu, J., et al., *A life-cycle perspective for analyzing carbon neutrality potential of polyethylene terephthalate (PET) plastics in China*. *Journal of Cleaner Production*, 2022. **330**: p. 129872.
468. Haas, V., et al., *Developing future visions for bio-plastics substituting PET—A backcasting approach*. *Sustainable Production and Consumption*, 2022. **31**: p. 370-383.
469. Kim, T., et al., *Life Cycle Greenhouse Gas Emissions and Water and Fossil-Fuel Consumptions for Polyethylene Furanoate and Its Coproducts from Wheat Straw*. *ACS Sustainable Chemistry & Engineering*, 2022. **10**(8): p. 2830-2843.
470. Grause, G., *Depolymerisation of Fossil Fuel and Biomass-derived Polyesters*, in *Production of Biofuels and Chemicals from Sustainable Recycling of Organic Solid Waste*. 2022, Springer. p. 283-316.
471. Guo, J., et al., *Fabrication of superhydrophobic and flame-retardant polyethylene terephthalate fabric through a fluorine-free layer-by-layer technique*. *International Journal of Chemical Reactor Engineering*, 2022.

472. Doyle, L. and I. Weidlich, *Moisture Uptake and Effects of Hygrothermal Exposure on Closed-Cell Semicrystalline Polyethylene Terephthalate Foam*. *Polymer Degradation and Stability*, 2022: p. 110009.
473. Colletti, S., *Valorization of biomass: synthesis of polyfunctional aromatic derivatives for the chemical recycling of PET waste*. 2022.
474. Candido, S.E.A., M. Sacomano Neto, and M.R. Côrtes, *How social inequalities shape markets: lessons from the configuration of PET recycling practices in Brazil*. *Business & Society*, 2022. **61**(3): p. 539-571.
475. Mendiburu-Valor, E., et al., *Valorization of urban and marine PET waste by optimized chemical recycling*. *Resources, Conservation and Recycling*, 2022. **184**: p. 106413.
476. Liu, J. and J. Yin, *Carbon Dioxide Synergistic Enhancement of Supercritical Methanol on PET Depolymerization for Chemical Recovery*. *Industrial & Engineering Chemistry Research*, 2022.
477. Singh, A., et al., *Recent Innovations in Chemical Recycling of Polyethylene Terephthalate Waste: A Circular Economy Approach Toward Sustainability*, in *Handbook of Solid Waste Management: Sustainability through Circular Economy*. 2022, Springer. p. 1149-1176.
478. Wang, Z., et al., *Cyanamide as a Highly Efficient Organocatalyst for the Glycolysis Recycling of PET*. *ACS Sustainable Chemistry & Engineering*, 2022.

479. Fan, C., et al., *Efficient glycolysis of PET catalyzed by a metal-free phosphazene base: the important role of EG⁻* Electronic supplementary information (ESI) available. See. *Green Chemistry*, 2022. **24**(3): p. 1294-1301.
480. Krisbiantoro, P.A., et al., *Catalytic Glycolysis of Polyethylene Terephthalate (PET) by Solvent-Free Mechanochemically Synthesized MFe₂O₄ (M= Co, Ni, Cu and Zn) Spinel*. *Chemical Engineering Journal*, 2022: p. 137926.
481. Jiang, Z., et al., *Poly (ionic liquid) s as efficient and recyclable catalysts for methanolysis of PET*. *Polymer Degradation and Stability*, 2022. **199**: p. 109905.
482. Laldinpuui, Z., et al., *Methanolysis of PET Waste Using Heterogeneous Catalyst of Bio-waste Origin*. *Journal of Polymers and the Environment*, 2022. **30**(4): p. 1600-1614.
483. Pasula, R.R., et al., *The influences of substrates' physical properties on enzymatic PET hydrolysis: Implications for PET hydrolase engineering*. *Engineering Biology*, 2022. **6**(1): p. 17-22.
484. Arnling Bååth, J., et al., *Sabatier Principle for Rationalizing Enzymatic Hydrolysis of a Synthetic Polyester*. *JACS Au*, 2022.
485. Tollini, F., et al., *Influence of the Catalytic System on the Methanolysis of Polyethylene Terephthalate at Mild Conditions: A Systematic Investigation*. *Chemical Engineering Science*, 2022: p. 117875.

486. James, A. and S. De, *Cation- π and hydrophobic interaction controlled PET recognition in double mutated cutinase—identification of a novel binding subsite for better catalytic activity*. RSC Advances, 2022. **12**(32): p. 20563-20577.
487. Han, M., et al., *Photocatalytic Upcycling of Poly (ethylene terephthalate) Plastic to High-Value Chemicals*. Applied Catalysis B: Environmental, 2022: p. 121662.
488. Liu, L., et al., *Optimization of Poly (ethylene terephthalate) Fiber Degradation by Response Surface Methodology Using an Amino Acid Ionic Liquid Catalyst*. ACS Engineering Au, 2022.
489. Senra, E.M., et al., *Influence of a Catalyst in Obtaining a Post-Consumer Pet-Based Alkyd Resin That Meets Circular Economy Principles*. Journal of Polymers and the Environment, 2022: p. 1-18.
490. Huang, J., et al., *Chemical recycling of plastic waste for sustainable material management: A prospective review on catalysts and processes*. Renewable and Sustainable Energy Reviews, 2022. **154**: p. 111866.
491. Sharifian, S. and N. Asasian-Kolur, *Polyethylene terephthalate (PET) waste to carbon materials: Theory, methods and applications*. Journal of Analytical and Applied Pyrolysis, 2022: p. 105496.
492. Wang, L., et al., *Glycolysis of PET using 1, 3-dimethylimidazolium-2-carboxylate as an organocatalyst*. ACS Sustainable Chemistry & Engineering, 2020. **8**(35): p. 13362-13368.

493. Silva, C.V.G., et al., *PET glycolysis optimization using ionic liquid [Bmin] ZnCl₃ as catalyst and kinetic evaluation*. *Polímeros*, 2018. **28**: p. 450-459.
494. Ju, Z., et al., *Theoretical studies on glycolysis of poly (ethylene terephthalate) in ionic liquids*. *RSC advances*, 2018. **8**(15): p. 8209-8219.
495. Tang, S., et al., *MgO/NaY as modified mesoporous catalyst for methanolysis of polyethylene terephthalate wastes*. *Journal of Environmental Chemical Engineering*, 2022: p. 107927.
496. Liu, C., et al., *Unveiling the microenvironments between ionic liquids and methanol for alcoholysis of poly (ethylene terephthalate)*. *Chemical Engineering Science*, 2022. **247**: p. 117024.
497. Shi, K., et al., *Preparation of Diacid Comprising Ionic Liquid Catalyst and Its Application in Catalytic Degradation of PET*. *Catalysis Letters*, 2022. **152**(4): p. 1182-1193.
498. Wang, H., et al., *Degradation of poly (ethylene terephthalate) using ionic liquids*. *Green Chemistry*, 2009. **11**(10): p. 1568-1575.
499. Quaranta, E., C.C. Minischetti, and G. Tartaro, *Chemical Recycling of Poly (bisphenol A carbonate) by Glycolysis under 1, 8-Diazabicyclo [5.4. 0] undec-7-ene Catalysis*. *ACS omega*, 2018. **3**(7): p. 7261-7268.
500. Do, T., E.R. Baral, and J.G. Kim, *Chemical recycling of poly (bisphenol A carbonate): 1, 5, 7-Triazabicyclo [4.4. 0]-dec-5-ene catalyzed alcoholysis for*

- highly efficient bisphenol A and organic carbonate recovery*. Polymer, 2018. **143**: p. 106-114.
501. Speight, J.G., *Lange's handbook of chemistry*. 2017: McGraw-Hill Education.
502. Kaupmees, K., A. Trummal, and I. Leito, *Basicities of strong bases in water: a computational study*. Croatica Chemica Acta, 2014. **87**(4): p. 385-395.
503. Kütt, A., et al., *pKa values in organic chemistry—Making maximum use of the available data*. Tetrahedron letters, 2018. **59**(42): p. 3738-3748.
504. Samuelsen, L., et al., *Determination of acidity constants for weak acids and bases by isothermal titration calorimetry*. Journal of Pharmaceutical and Biomedical Analysis, 2020. **184**: p. 113206.
505. Pilarski, B., et al., *General analytical procedure for determination of acidity parameters of weak acids and bases*. Journal of Analytical Methods in Chemistry, 2015. **2015**.
506. Yang, X., S.R. Liew, and R. Bai, *Simultaneous alkaline hydrolysis and non-solvent induced phase separation method for polyacrylonitrile (PAN) membrane with highly hydrophilic and enhanced anti-fouling performance*. Journal of Membrane Science, 2021. **635**: p. 119499.
507. Yuan, Y. and T.R. Lee, *Contact angle and wetting properties*, in *Surface science techniques*. 2013, Springer. p. 3-34.

508. Law, K.-Y. and H. Zhao, *Surface wetting: characterization, contact angle, and fundamentals*. 2016: Springer International Publishing Basel, Switzerland.
509. Li, R. and Y. Shan, *Contact angle and local wetting at contact line*. *Langmuir*, 2012. **28**(44): p. 15624-15628.
510. Liu, N., et al. *Catalysis Investigation of PET Depolymerization with Brønsted Acidic Ionic Liquid under Microwave Irradiation*. in *Advanced Materials Research*. 2014. Trans Tech Publ.
511. Liu, B., et al., *Lewis acid–base synergistic catalysis for polyethylene terephthalate degradation by 1, 3-Dimethylurea/Zn (OAc)₂ deep eutectic solvent*. *ACS Sustainable Chemistry & Engineering*, 2018. **7**(3): p. 3292-3300.
512. Dzhubarov, G.V., et al., *A kinetic study on the depolymerization of polyethylene terephthalate waste with crude glycerol*. *Chemical Papers*, 2021. **75**(11): p. 6035-6046.
513. Chamas, A., et al., *Degradation rates of plastics in the environment*. *ACS Sustainable Chemistry & Engineering*, 2020. **8**(9): p. 3494-3511.
514. Biermann, L., et al., *Development of a continuous PET depolymerization process as a basis for a back-to-monomer recycling method*. *Green Processing and Synthesis*, 2021. **10**(1): p. 361-373.

515. Mahadevan Subramanya, S., Y. Mu, and P.E. Savage, *Effect of Cellulose and Polypropylene on Hydrolysis of Polyethylene Terephthalate for Chemical Recycling*. ACS Engineering Au, 2022.
516. Zhang, S., et al., *Cosolvent-promoted selective non-aqueous hydrolysis of PET wastes and facile product separation*. Green Chemistry, 2022. **24**(8): p. 3284-3292.
517. Yang, W., et al., *Easily recoverable and reusable p-toluenesulfonic acid for faster hydrolysis of waste polyethylene terephthalate*. Green Chemistry, 2022. **24**(3): p. 1362-1372.
518. Eugenio, E.d.Q., et al., *Kinetic modeling of the post-consumer poly (ethylene terephthalate) hydrolysis catalyzed by cutinase from Humicola insolens*. Journal of Polymers and the Environment, 2022. **30**(4): p. 1627-1637.
519. Trejo-Carbajal, N., K.I. Ambriz-Luna, and A.M. Herrera-González, *Efficient method and mechanism of depolymerization of PET under conventional heating and microwave radiation using t-BuNH₂/Lewis acids*. European Polymer Journal, 2022: p. 111388.
520. Sonnendecker, C., et al., *Low Carbon Footprint Recycling of Post-Consumer PET Plastic with a Metagenomic Polyester Hydrolase*. ChemSusChem, 2022. **15**(9): p. e202101062.
521. Jalali, S., M. Montazer, and R.M.A. Malek, *A novel semi-bionanofibers through Introducing tragacanth Gum into PET attaining rapid wetting and degradation*. Fibers and Polymers, 2018. **19**(10): p. 2088-2096.

522. Alonso-Fagúndez, N., et al., *Poly-(styrene sulphonic acid): An acid catalyst from polystyrene waste for reactions of interest in biomass valorization*. *Catalysis Today*, 2014. **234**: p. 285-294.
523. Kumar, A. and T.R. Rao, *Kinetics of hydrolysis of polyethylene terephthalate pellets in nitric acid*. *Journal of applied polymer science*, 2003. **87**(11): p. 1781-1783.
524. Salmi, T., et al., *Kinetic modeling of hemicellulose hydrolysis in the presence of homogeneous and heterogeneous catalysts*. *AIChE Journal*, 2014. **60**(3): p. 1066-1077.
525. Thompson, D., F. Vilbrandt, and W. Gray, *The effect of insonation on the specific reaction rate constant in the acid hydrolysis of ethyl acetate*. *The Journal of the Acoustical Society of America*, 1953. **25**(3): p. 485-490.
526. Anuradha, V., et al., *p-Toluenesulfonic acid catalyzed regiospecific nitration of phenols with metal nitrates*. *Tetrahedron letters*, 2006. **47**(28): p. 4933-4935.
527. Yoshioka, T., M. Ota, and A. Okuwaki, *Conversion of a used poly (ethylene terephthalate) bottle into oxalic acid and terephthalic acid by oxygen oxidation in alkaline solutions at elevated temperatures*. *Industrial & engineering chemistry research*, 2003. **42**(4): p. 675-679.
528. Arias, J.J.R. and W. Thielemans, *Instantaneous hydrolysis of PET bottles: an efficient pathway for the chemical recycling of condensation polymers*. *Green Chemistry*, 2021. **23**(24): p. 9945-9956.

529. Lima, P., R. Angélica, and R. Neves, *Dissolution kinetics of metakaolin in sulfuric acid: comparison between heterogeneous and homogeneous reaction methods*. Applied Clay Science, 2014. **88**: p. 159-162.
530. Chan, R. and R. McIntosh, *THE HETEROGENEOUS AND HOMOGENEOUS THERMAL DECOMPOSITIONS OF NICKEL CARBONYL*. Canadian Journal of Chemistry, 1962. **40**(5): p. 845-855.
531. Jyoti, G., et al., *Homogeneous and heterogeneous catalyzed esterification of acrylic acid with ethanol: reaction kinetics and modeling*. International Journal of Chemical Kinetics, 2018. **50**(5): p. 370-380.
532. Ramírez-Verduzco, L., J. De los Reyes, and E. Torres-García, *Solvent Effect in Homogeneous and Heterogeneous Reactions To Remove Dibenzothiophene by an Oxidation– Extraction Scheme*. Industrial & engineering chemistry research, 2008. **47**(15): p. 5353-5361.
533. Lin, X., et al., *Review on Development of Ionic Liquids in Lignocellulosic Biomass Refining*. Journal of Molecular Liquids, 2022: p. 119326.
534. Nardelli, F., et al., *Thermal Stability of Ionic Liquids: Effect of Metals*. Applied Sciences, 2022. **12**(3): p. 1652.
535. Pei, Y., et al., *Ionic liquids for advanced materials*. Materials Today Nano, 2022. **17**: p. 100159.

536. Khurana, J.M., B. Nand, and P. Saluja, *1, 8-Diazabicyclo [5.4. 0] undec-7-ene: A Highly Efficient Catalyst for One-Pot Synthesis of Substituted Tetrahydro-4H-chromenes, Tetrahydro [b] pyrans, Pyrano [d] pyrimidines, and 4H-Pyrans in Aqueous Medium*. *Journal of Heterocyclic Chemistry*, 2014. **51**(3): p. 618-624.
537. Lasemi, Z., et al., *1, 8-Diazabicyclo [5.4. 0] undec-7-ene functionalized cellulose nanofibers as an efficient and reusable nanocatalyst for the synthesis of tetraketones in aqueous medium*. *Research on Chemical Intermediates*, 2020. **46**(7): p. 3667-3682.
538. Pschenitzka, M., S. Meister, and B. Rieger, *Positive effect of 1, 8-diazabicyclo [5.4. 0] undec-7-ene (DBU) on homogeneous photocatalytic reduction of CO₂*. *Chemical Communications*, 2018. **54**(27): p. 3323-3326.
539. Ara, G., et al., *1, 8-Diazabicyclo [5.4. 0]-undec-7-ene based protic ionic liquids and their binary systems with molecular solvents catalyzed Michael addition reaction*. *New Journal of Chemistry*, 2020. **44**(32): p. 13701-13706.
540. Song, M., X. Zhu, and Y. Xu, *Electric conductivity of binary solutions of DBU lactic acid ionic liquid*. *Physics and Chemistry of Liquids*, 2020. **58**(1): p. 1-7.
541. Wang, S., et al., *Electrical Conductivities of DBU-Based Ionic Liquid in Its Binary Solutions with Nonaqueous Molecular Solvents*. *Journal of Solution Chemistry*, 2021. **50**(4): p. 558-575.
542. Zhu, X., M. Song, and Y. Xu, *DBU-based protic ionic liquids for CO₂ capture*. *ACS Sustainable Chemistry & Engineering*, 2017. **5**(9): p. 8192-8198.

543. Dubelley, F., et al., *Predictive durability of polyethylene terephthalate toward hydrolysis over large temperature and relative humidity ranges*. *Polymer*, 2018. **142**: p. 285-292.
544. Maurya, A., A. Bhattacharya, and S.K. Khare, *Enzymatic remediation of polyethylene terephthalate (PET)-based polymers for effective management of plastic wastes: an overview*. *Frontiers in Bioengineering and Biotechnology*, 2020. **8**: p. 602325.
545. Amézqueta, S., et al., *Octanol-water partition constant*. *Liquid-phase extraction*, 2020: p. 183-208.
546. Poole, S.K. and C.F. Poole, *Separation methods for estimating octanol-water partition coefficients*. *Journal of Chromatography B*, 2003. **797**(1-2): p. 3-19.
547. Machatha, S.G. and S.H. Yalkowsky, *Comparison of the octanol/water partition coefficients calculated by ClogP®, ACDlogP and KowWin® to experimentally determined values*. *International journal of pharmaceutics*, 2005. **294**(1-2): p. 185-192.
548. Ropel, L., et al., *Octanol-water partition coefficients of imidazolium-based ionic liquids*. *Green Chemistry*, 2005. **7**(2): p. 83-90.
549. Rothwell, J.A., A.J. Day, and M.R. Morgan, *Experimental determination of octanol-water partition coefficients of quercetin and related flavonoids*. *Journal of agricultural and food chemistry*, 2005. **53**(11): p. 4355-4360.

550. Schönsee, C.D. and T.D. Bucheli, *Experimental determination of octanol–water partition coefficients of selected natural toxins*. Journal of Chemical & Engineering Data, 2020. **65**(4): p. 1946-1953.
551. Nedyalkova, M.A., et al., *Calculating the partition coefficients of organic solvents in octanol/water and octanol/air*. Journal of chemical information and modeling, 2019. **59**(5): p. 2257-2263.

Appendix A

Supporting Information for Chapter 6

6.6 Supporting Information for Chapter 6

6.6.1 TGA results for individual components

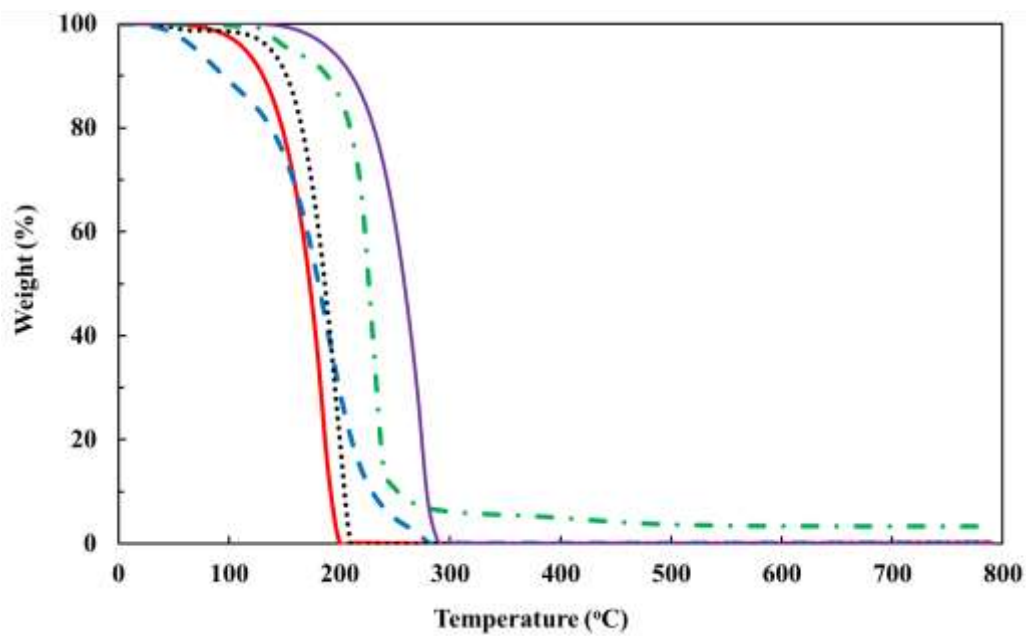


Figure A-6-S1: TGA curves for DBU (—), H₂SO₄ (—), LA (---), OA (...), and CA

(—•).

6.6.2 TGA results for DBU-acid ionic liquids, synthesized in water

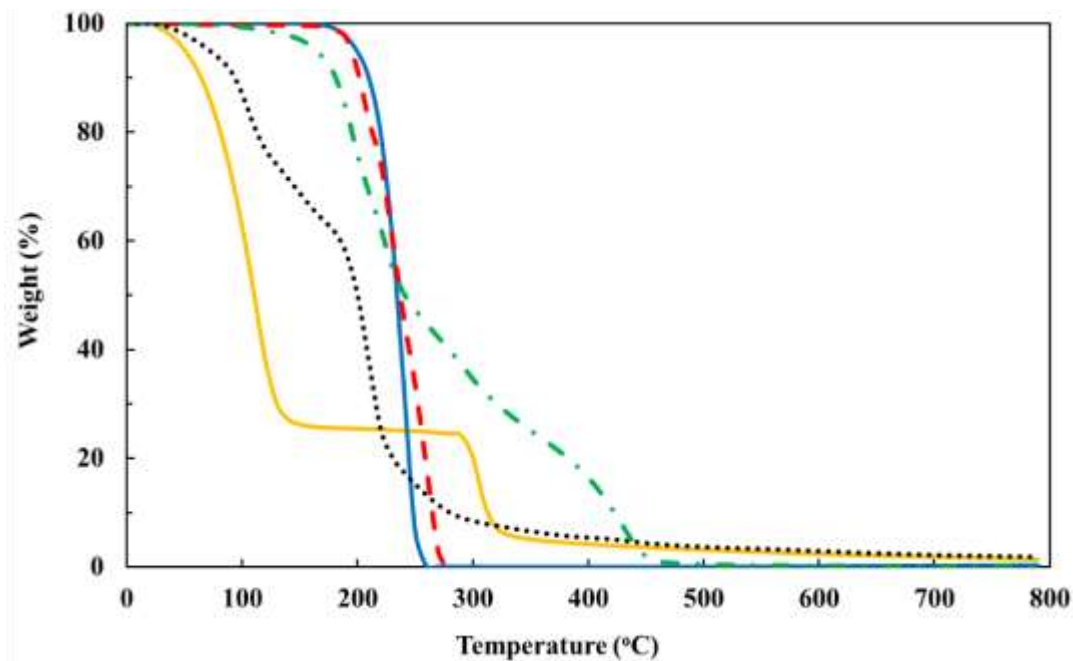


Figure A-6-S2: TGA curves for DBU-SO₄ (—), DBU-OA-equimolar (—), DBU-OA-titration (---), DBU-CA-equimolar (—•), and DBU-CA-titration (···), synthesized in water.

6.6.3 TGA results for DBU-acid ionic liquids, synthesized in organic solvents

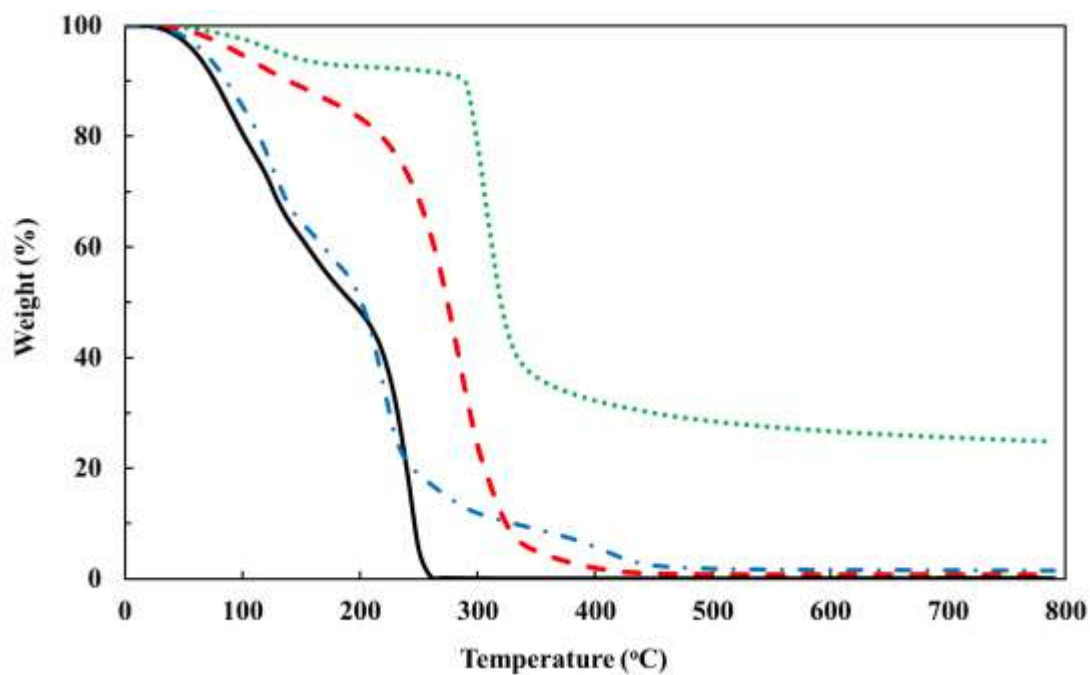


Figure A-6-S3: TGA curves for DBU-SO₄ (····), DBU-LA (---), DBU-OA (—), and DBU-CA (—•), synthesized in organic solvents.

6.6.4 Titration results for individual components: DBU, LA, OA, and CA

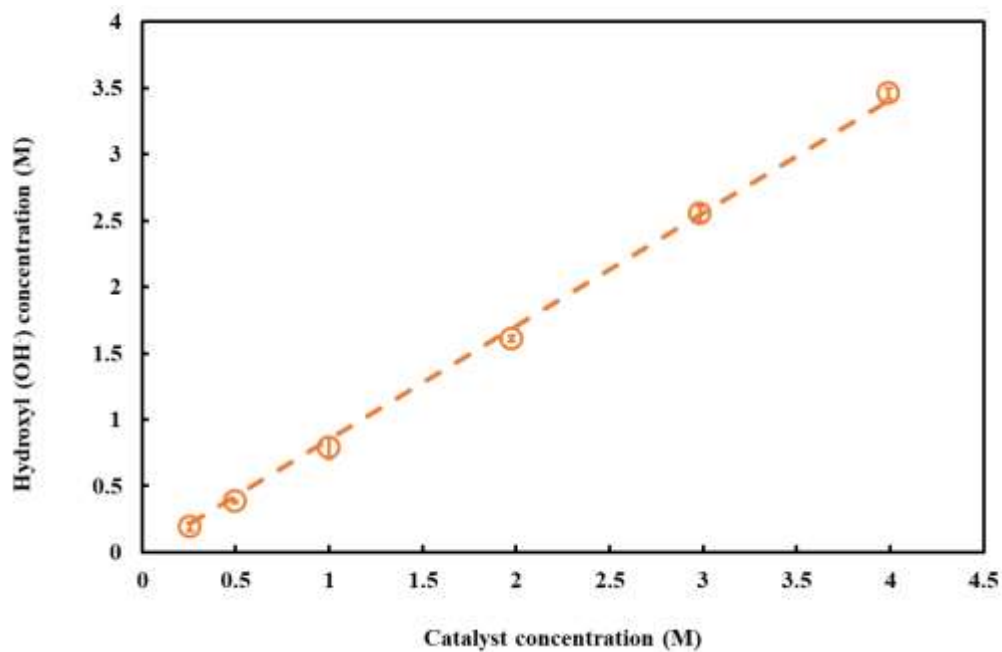


Figure A-6-S4: The hydroxyl (OH⁻) concentration as a function of the concentration of DBU (O, ---), the dashed line is linear fitting; $[\text{OH}^-] = 0.85 * [\text{DBU}]$, $R^2 = 0.9993$.

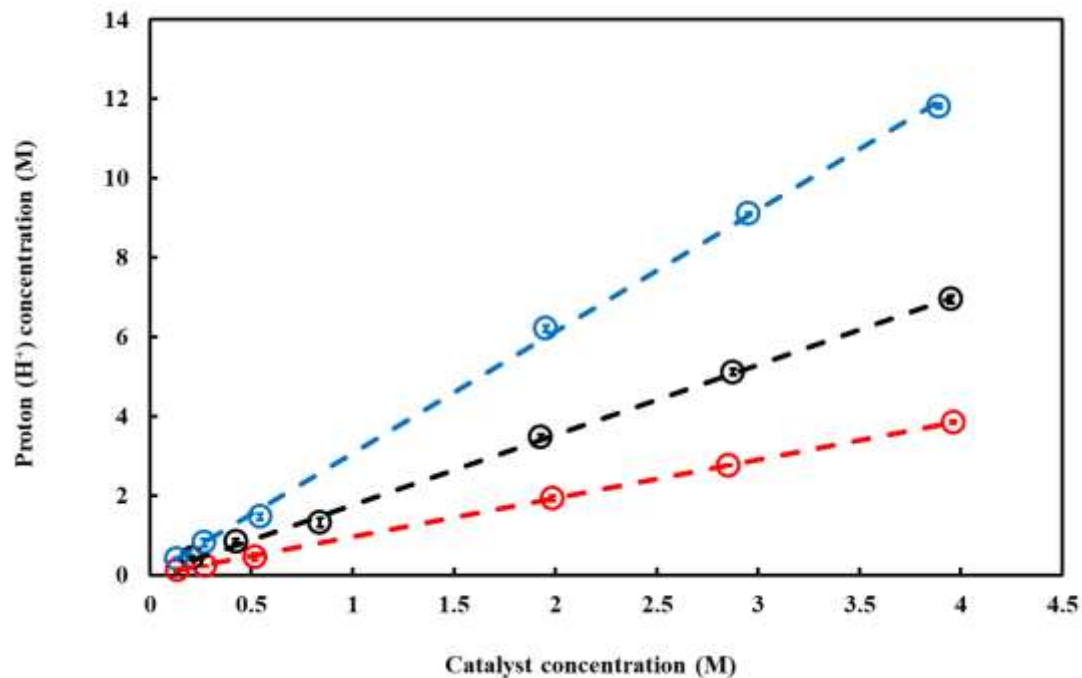


Figure A-6-S5: The proton (H^+) concentration as a function of the concentrations of LA

(O, ---), OA (O, ---), and CA (O, ---), the dashed lines are linear fitting; $[H^+]_{LA} = 0.97$

* $[LA]$, $R^2_{LA} = 0.9999$; $[H^+]_{OA} = 1.77 * [OA]$, $R^2_{OA} = 0.9994$; $[H^+]_{CA} = 3.07 * [CA]$, $R^2_{CA} = 0.9996$.

6.6.5 Titration results for DBU-acid ionic liquids, synthesized in water

Table A-6-S1: Results of pH tape strips and estimated [H⁺] values for the synthesized DBU-SO₄ in water, equimolar ratio of DBU to H₂SO₄.









Concentration (M)	pH tape result	pH	Estimated [H ⁺] (M)
4		1	10 ⁻¹
2		2	10 ⁻²
1		3	10 ⁻³
0.5		3	10 ⁻³
0.25		3	10 ⁻³
0.125		3	10 ⁻³

Table A-6-S2: Results of pH tape strips and estimated [H⁺] values for the synthesized DBU-OA in water, equimolar ratio of DBU to OA.











Concentration (M)	pH tape result	pH	Estimated [H ⁺] (M)
4		2	10 ⁻²
2		2	10 ⁻²
1		2	10 ⁻²
0.5		3	10 ⁻³
0.25		3	10 ⁻³
0.125		3	10 ⁻³

Table A-6-S3: Results of pH tape strips and estimated [H⁺] values for the synthesized DBU-OA in water, titration molar ratio of DBU (2.08) to OA (1).



Concentration (M)	pH tape result	pH	Estimated [H ⁺] (M)
4		2	10 ⁻²
2		3	10 ⁻³

1		3	10^{-3}
0.5		3	10^{-3}
0.25		3	10^{-3}
0.125		3	10^{-3}

Table A-6-S4: Results of pH tape strips and estimated $[H^+]$ values for the synthesized DBU-CA in water, equimolar ratio of DBU to CA.



Concentration (M)	pH tape result	pH	Estimated $[H^+]$ (M)
4		5	10^{-5}
2		5	10^{-5}
1		5	10^{-5}
0.5		5	10^{-5}
0.25		5	10^{-5}
0.125		5	10^{-5}

Table A-6-S5: Results of pH tape strips and estimated [H⁺] values for the synthesized DBU-CA in water, titration molar ratio of DBU (3.61) to CA (1).



Concentration (M)	pH tape result	pH	Estimated [H ⁺] (M)
4	[Yellowish-green color]	6	10 ⁻⁶
2	[Yellowish-green color]	6	10 ⁻⁶
1	[Yellowish-green color]	6	10 ⁻⁶
0.5	[Yellowish-green color]	6	10 ⁻⁶
0.25	[Green color]	7	10 ⁻⁷
0.125	[Green color]	7	10 ⁻⁷

6.6.6 Titration results for DBU-acid ionic liquids, synthesized in organic solvents

Table A-6-S6: Results of pH tape strips and estimated $[H^+]$ values for the synthesized DBU-SO₄ in organic solvent, equimolar ratio of DBU to H₂SO₄.









Concentration (M)	pH tape result	pH	Estimated $[H^+]$ (M)
4		1	10^{-1}
2		2	10^{-2}
1		3	10^{-3}
0.5		3	10^{-3}
0.25		3	10^{-3}
0.125		3	10^{-3}

Table A-6-S7: Results of pH tape strips and estimated [OH⁻] values for the synthesized DBU-LA, equimolar ratio of DBU to LA.






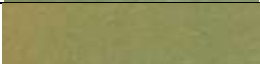
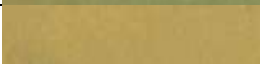
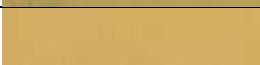

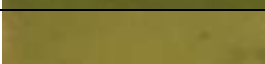

Concentration (M)	pH tape result	pH	Estimated [OH ⁻] (M)
4		10	10 ⁻⁴
2		10	10 ⁻⁴
1		9	10 ⁻⁵
0.5		9	10 ⁻⁵
0.25		8	10 ⁻⁶
0.125		8	10 ⁻⁶

Table A-6-S8: Results of pH tape strips and estimated [OH⁻] values for the synthesized DBU-OA in organic solvent, structural molar ratio of DBU (2) to H₂SO₄ (1).



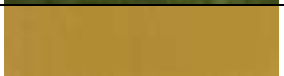

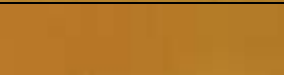



Concentration (M)	pH tape result	pH	Estimated [OH ⁻] (M)
4		10	10 ⁻⁴
2		9	10 ⁻⁵
1		8	10 ⁻⁶

0.5		8	10^{-6}
0.25		8	10^{-6}
0.125		7	10^{-7}

Table A-6-S8: Results of pH tape strips and estimated [OH⁻] values for the synthesized DBU-CA in organic solvent, structural molar ratio of DBU (3) to CA (1).



Concentration (M)	pH tape result	pH	Estimated [OH ⁻] (M)
4		10	10^{-4}
2		10	10^{-4}
1		8	10^{-6}
0.5		8	10^{-6}
0.25		7	10^{-7}
0.125		7	10^{-7}

6.6.7 Shrinking core model fitting to the TPA yield (%) kinetics data- Individual Components, $T_R = 150^\circ\text{C}$

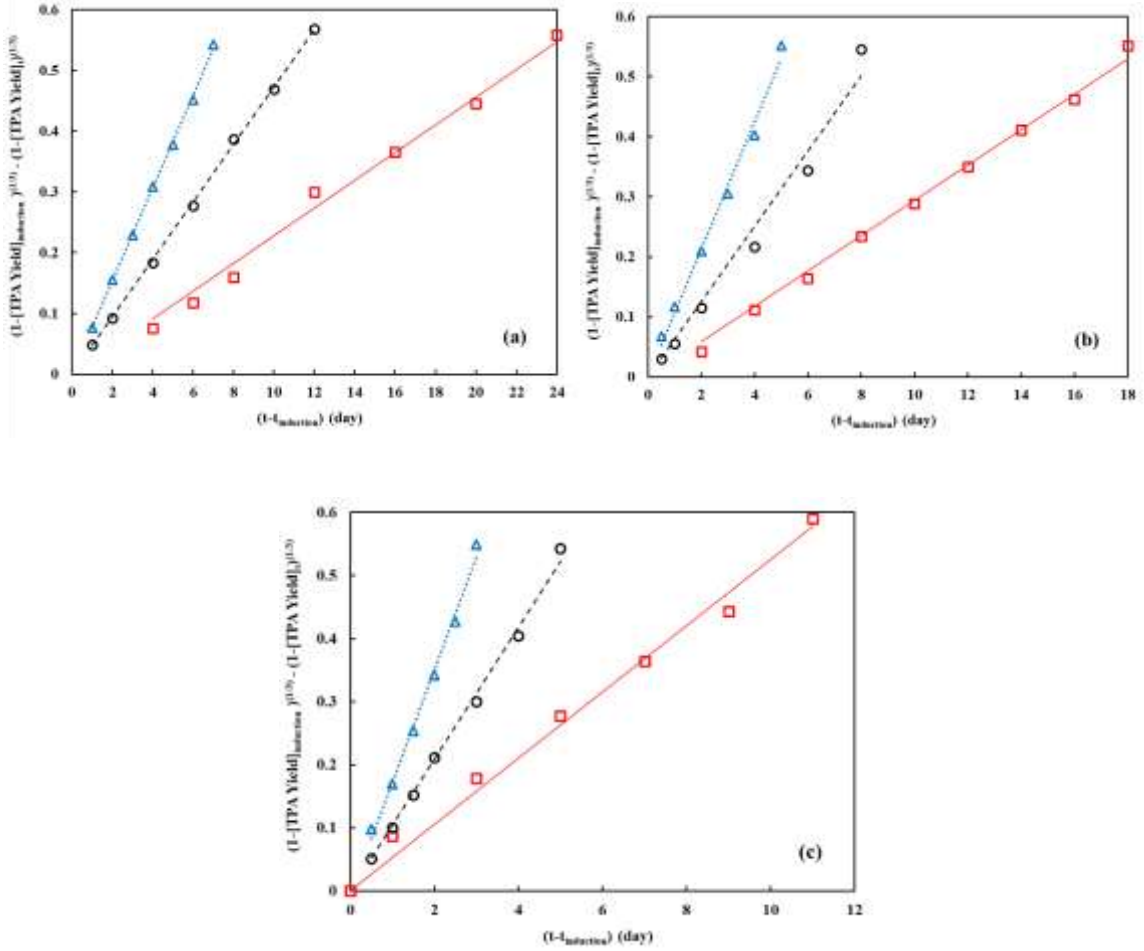


Figure A-6-S6: Fit of shrinking core model to the TPA yield kinetic data at $T_R = 150^\circ\text{C}$ for (a) 1M, (b) 2M, and (c) 4M solutions of LA (\square , —), OA (\circ , ---), and CA (Δ , ...).

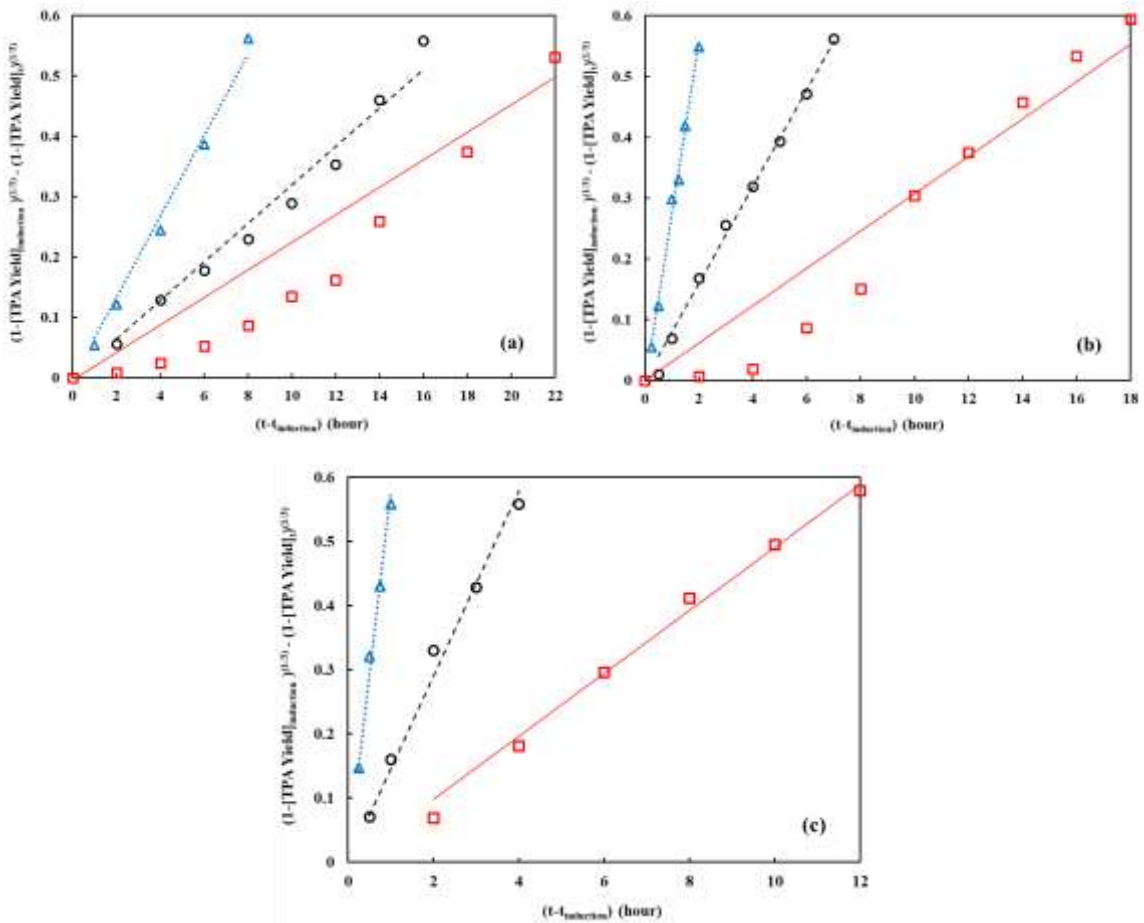


Figure A-6-S7: Fit of shrinking core model to the TPA yield kinetic data at $T_R = 150^\circ\text{C}$ for (a) 1M, (b) 2M, and (c) 4M solutions of DBU-LA (\square , —), DBU-OA (\circ , ---), and DBU-CA (Δ , ...). The lines illustrate the fit of shrinking core model.

6.6.8 PET conversion (%) kinetics data for solutions of individual components, $T_R=150^\circ\text{C}$

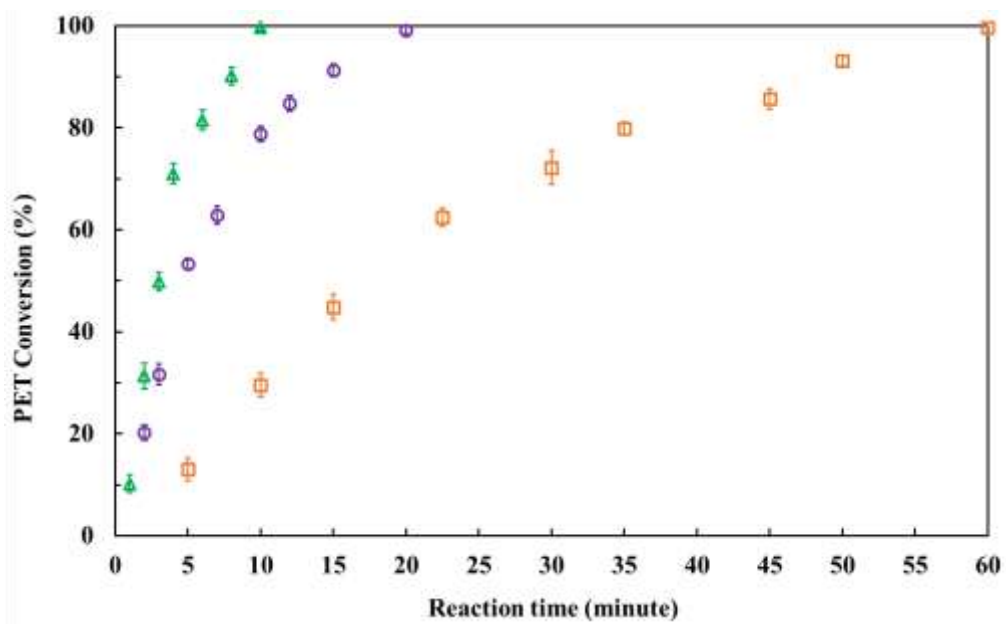


Figure A-6-S8: PET conversion kinetics data at $T_R=150^\circ\text{C}$ for 1M (\square), 2M (\circ), and 4M (Δ) solutions of DBU.

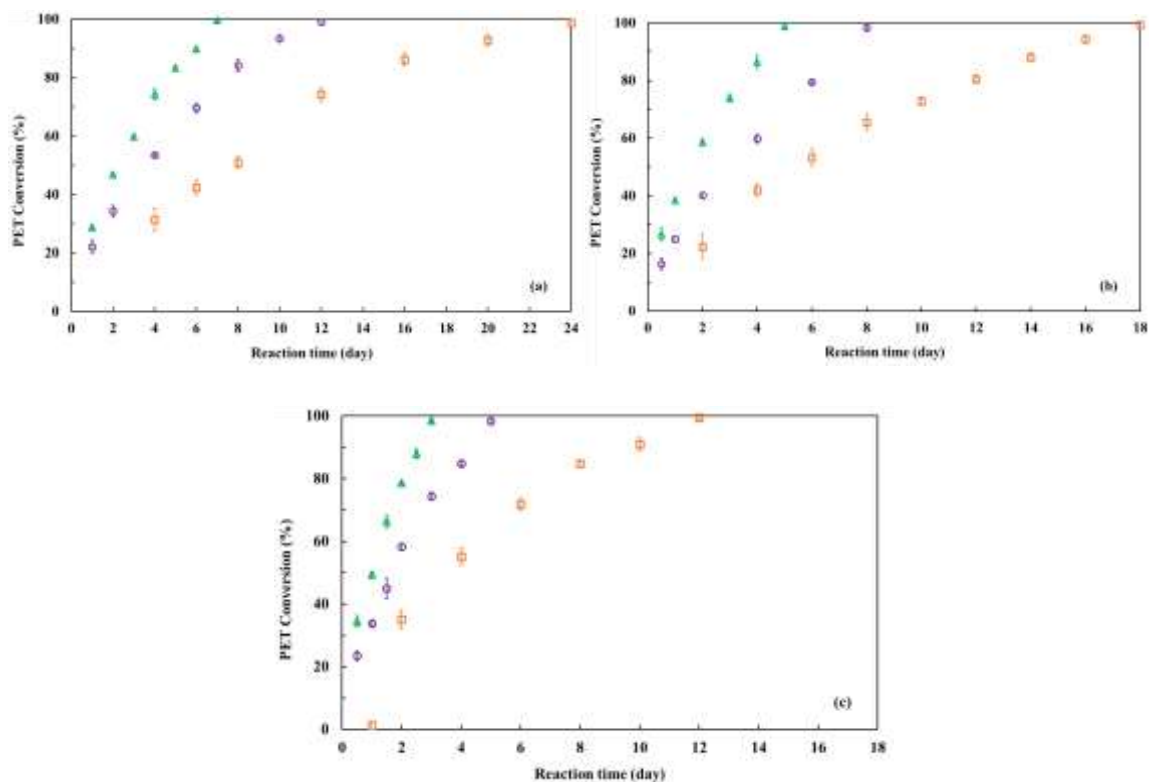


Figure A-6-S9: PET conversion kinetics data at $T_R = 150^\circ\text{C}$ for (a) 1M, (b) 2M, and (c) 4M solutions of LA (\square), OA (\circ), and CA (Δ).

6.6.9 Specific reaction rate constants for tested catalysts, $T_R = 150^\circ\text{C}$

Table A-6-S9: Specific reaction rate constants (k_{sp} values), PET hydrolysis at $T_R = 150^\circ\text{C}$.

Catalyst type	k_{sp} [kg PET. m. (mol catalyst) $^{-1}$. s $^{-1}$] * (10^{11})
DBU	5730
LA	2.40
OA	4.71
CA	7.98
DBU-LA	68.6
DBU-OA	213
DBU-CA	965

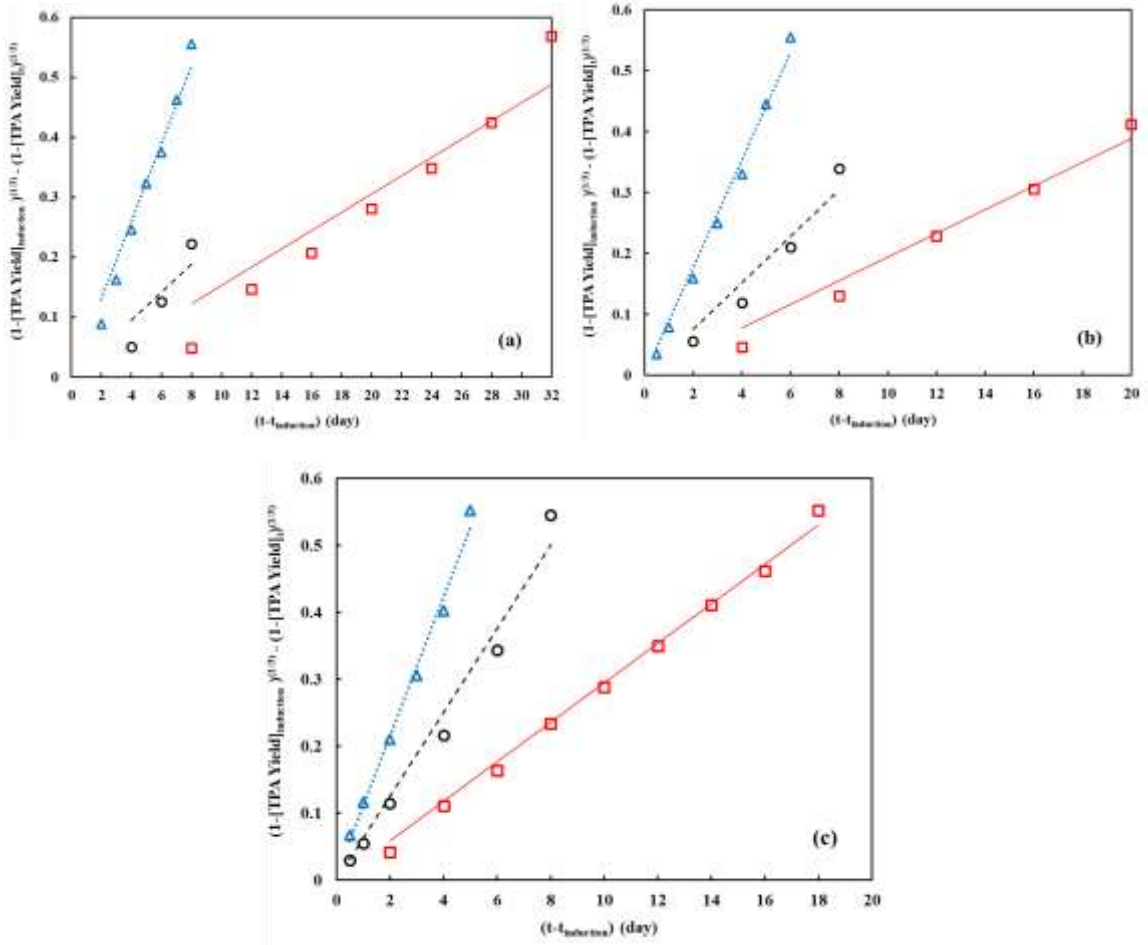


Figure A-6-S10: Fit of shrinking core model to the TPA yield kinetic data, 2M solutions of LA (\square , —), OA (\circ , ---), and CA (Δ , ...) at (a) $T_R = 130^\circ C$ (b) $T_R = 140^\circ C$, and (c) $T_R = 150^\circ C$.

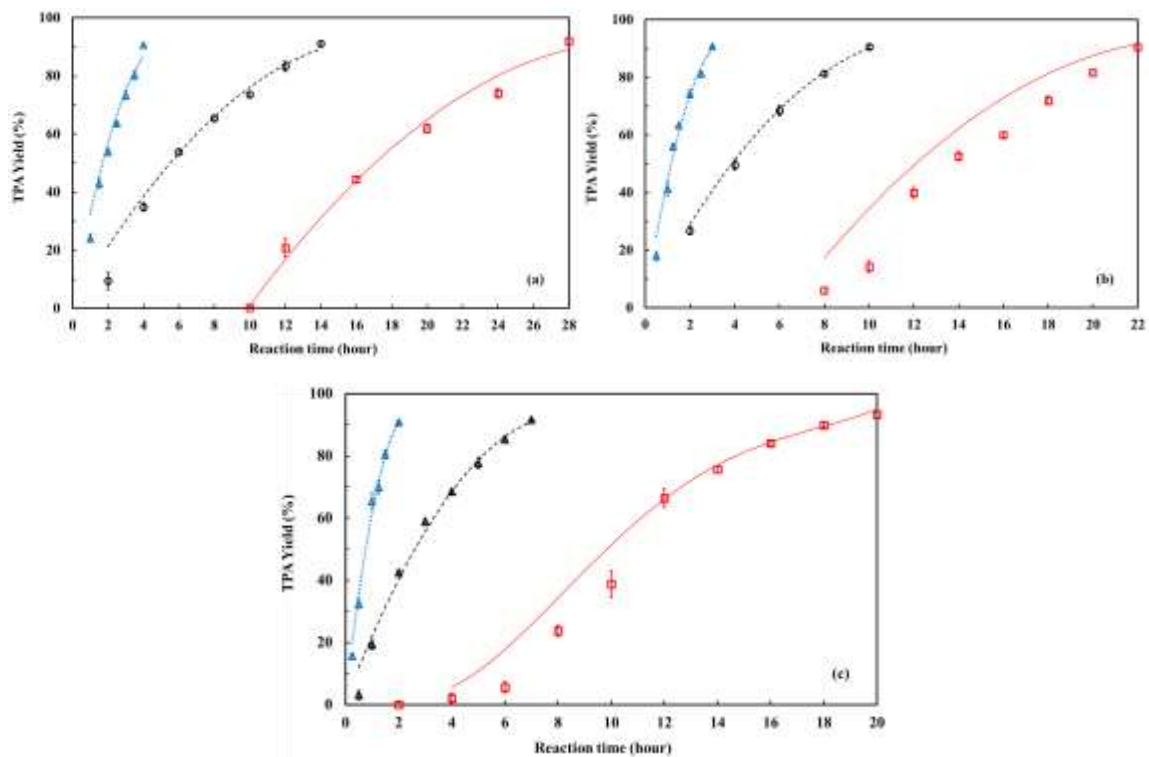


Figure A-6-S11: Fit of shrinking core model to the TPA yield kinetic data for 2M solutions of DBU-LA (\square , —), DBU-OA (\circ , ---), and DBU-CA (Δ , \dots) at (a) $T_R = 130^\circ\text{C}$ (b) $T_R = 140^\circ\text{C}$, and (c) $T_R = 150^\circ\text{C}$.

6.6.10 PET conversion (%) kinetics data, 2M solutions of individual components

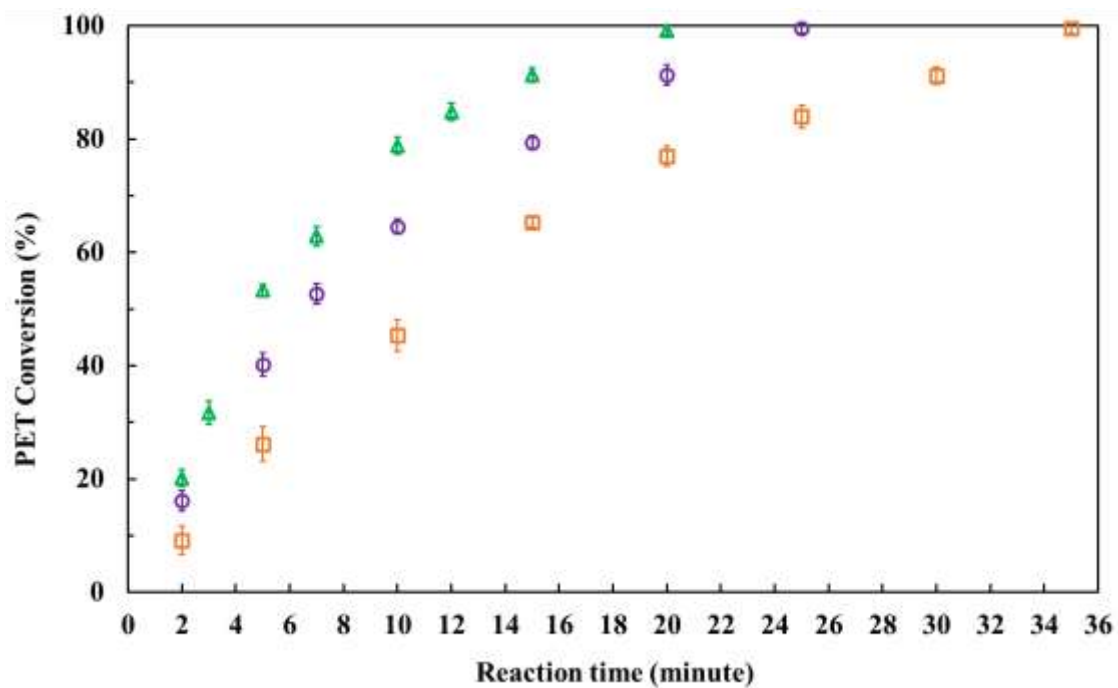


Figure A-6-S12: PET conversion kinetics data for 2M solutions of DBU at $T_R=130^\circ\text{C}$ (□), $T_R=140^\circ\text{C}$ (○), and $T_R=130^\circ\text{C}$ (Δ) solutions of DBU.

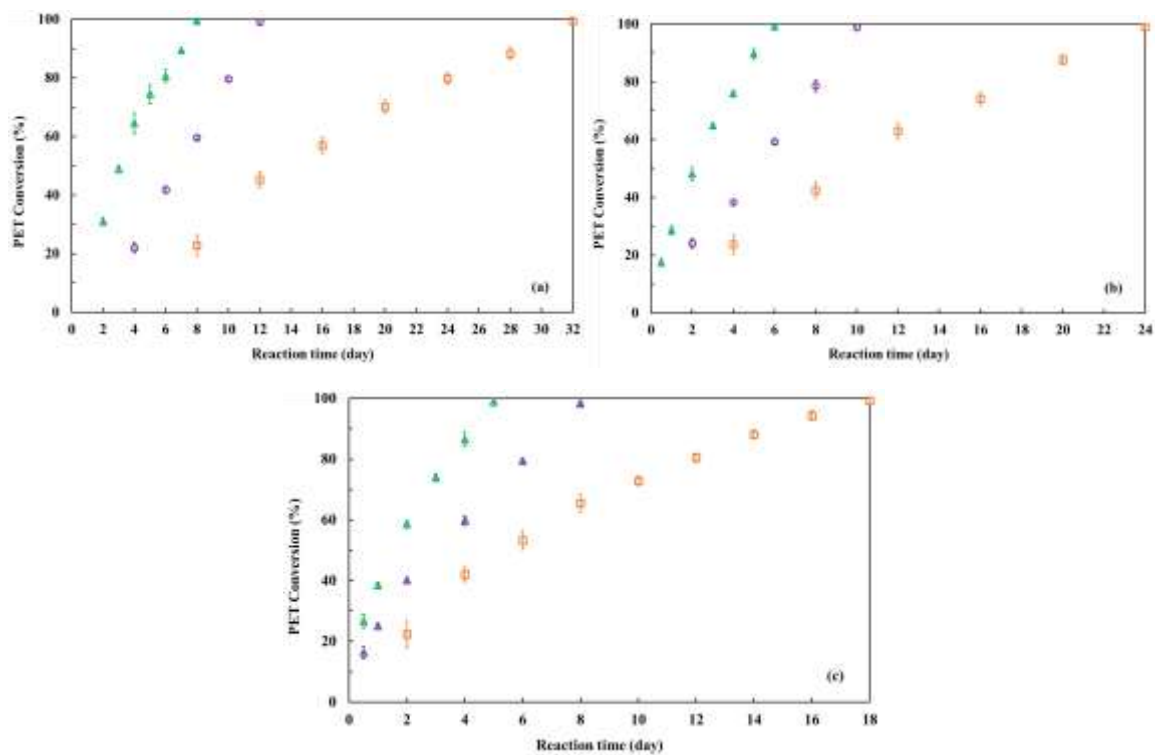


Figure A-6-S13: Effect of reaction temperature on PET conversion at (a) $T_R=130^\circ\text{C}$, (b) $T_R=140^\circ\text{C}$, and (c) $T_R=150^\circ\text{C}$ for 2M solutions of LA (\square), OA (\circ), and CA (\triangle).

6.6.11 Specific reaction rate constants, 2M solutions of the catalysts

Table A-6-S10: Specific reaction rate constants (k_{sp} values) as a function of the reaction temperature for 2M catalyst solutions for PET hydrolysis.

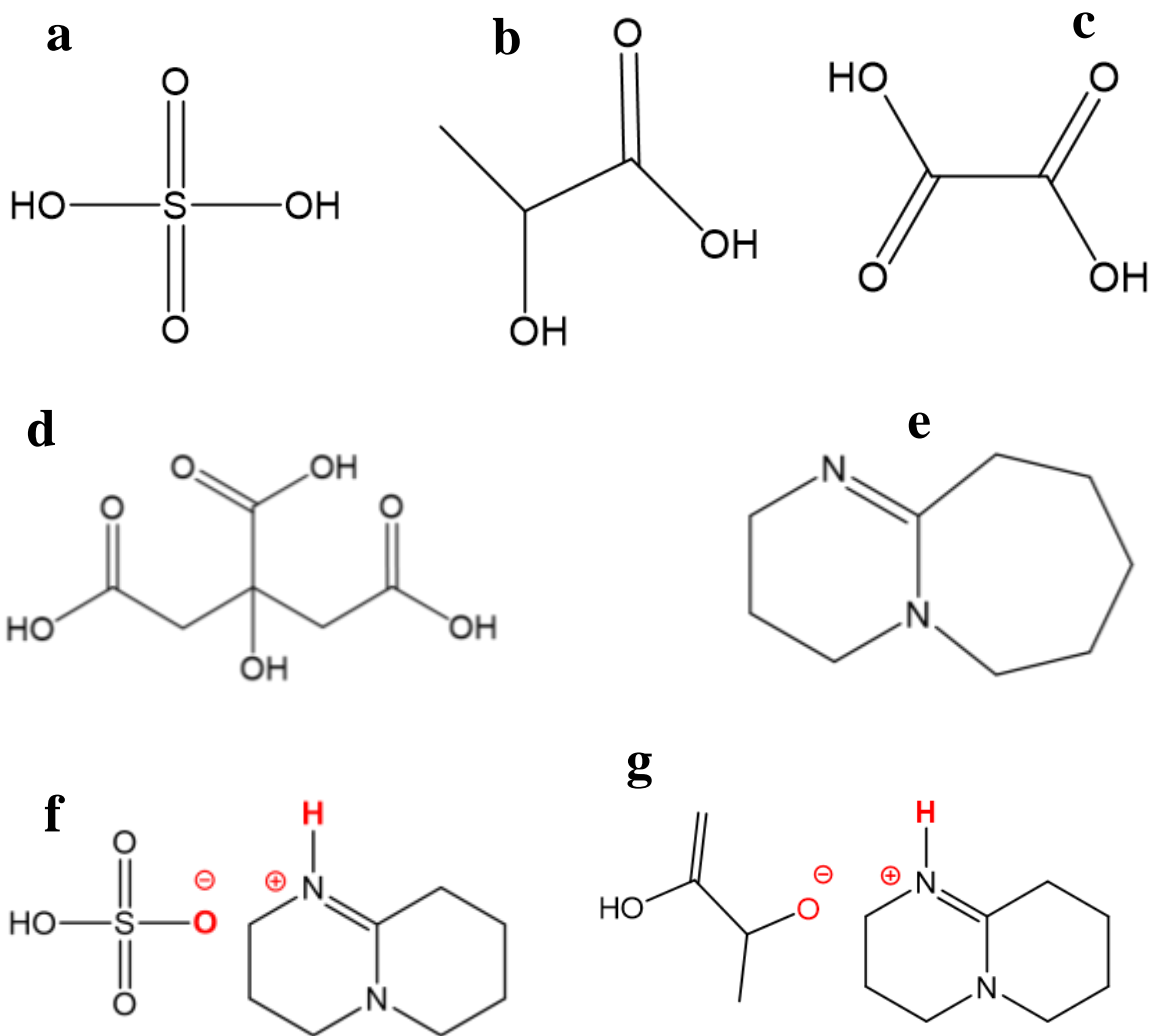
2M Catalyst Solution	DBU	LA	OA	CA	DBU-LA	DBU-OA	DBU-CA
	*k_{sp}	*k_{sp}	*k_{sp}	*k_{sp}	*k_{sp}	*k_{sp}	*k_{sp}
130	2770	1.74	2.89	7.81	84.5	109	355
140	3960	2.60	4.63	10.7	105	155	519
150	5260	3.47	7.52	12.7	117	231	797

$$*[k_{sp}] = [kg\ PET.\ m.\ (mol\ catalyst)^{-1}.\ s^{-1}] * 10^{11}$$

Appendix B

The chemical structures of tested catalysts in Chapter 6

The chemical structures of catalysts including sulfuric acid, the weak acids, and the synthesized DBU-acid ionic liquids are illustrated in **Figure B**.



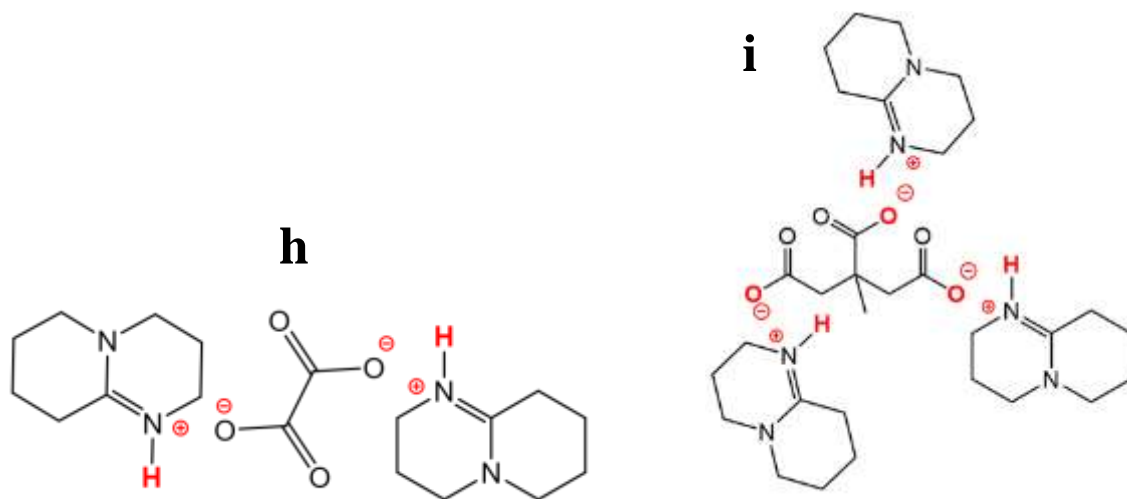


Figure B: The chemical structures of catalysts a. sulfuric acid (H₂SO₄), b. lactic acid (LA), c. oxalic acid (OA), d. citric acid (CA), e. 1,8-Diazabicyclo (5.4.0) undec-7-ene (DBU),

f. DBU-SO₄, g. DBU-LA, h. DBU-OA, and i. DBU-CA.

Appendix C

FTIR results for Chapter 6

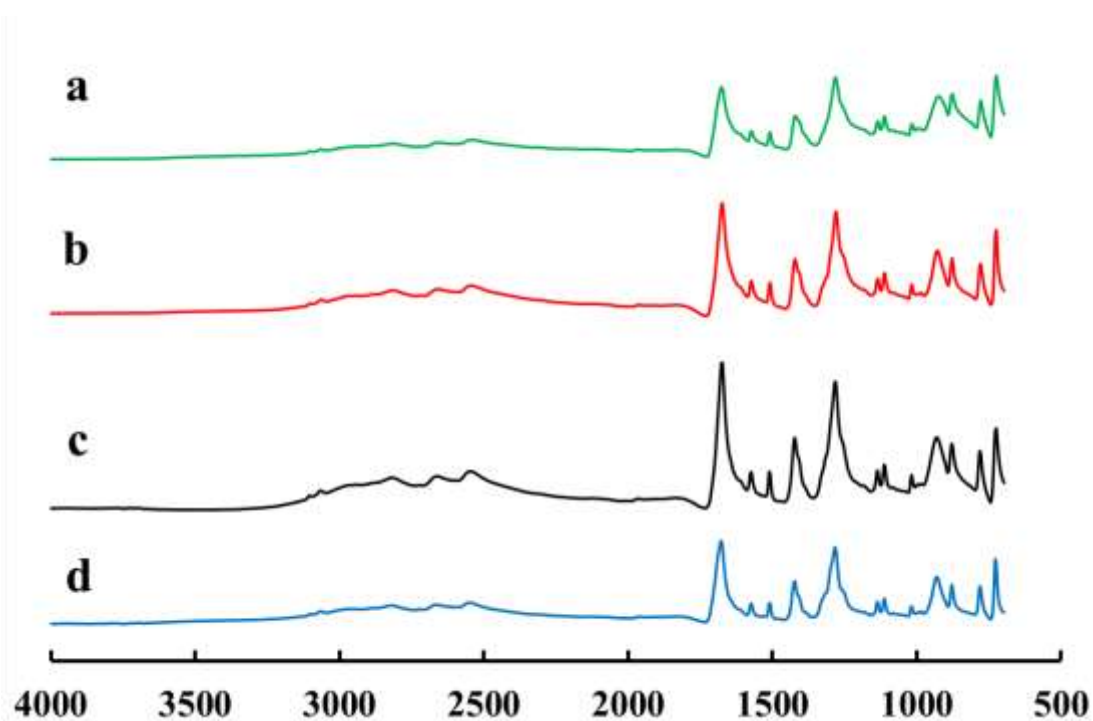


Figure C-1: The FTIR spectra for a. commercial TPA (—) [49] and recovered TPA samples from the hydrolysis of PET with 2M aqueous catalyst solutions of b. LA (—), c. OA (—), and d. CA (—), ($T_R = 150^\circ\text{C}$).

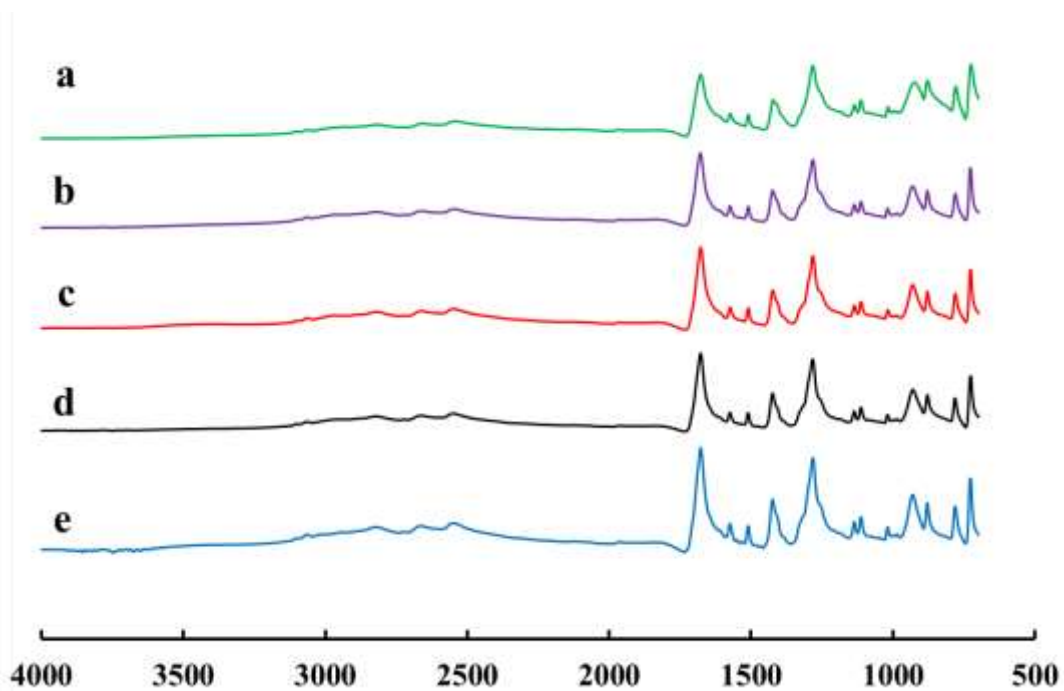


Figure C-2: The FTIR spectra for a. commercial TPA (—) [49] and recovered TPA samples from the hydrolysis of PET with 2M aqueous catalyst solutions of b. DBU (—), c. DBU-LA (—), d. DBU-OA (—), and e. DBU-CA (—), ($T_R = 150^\circ\text{C}$).

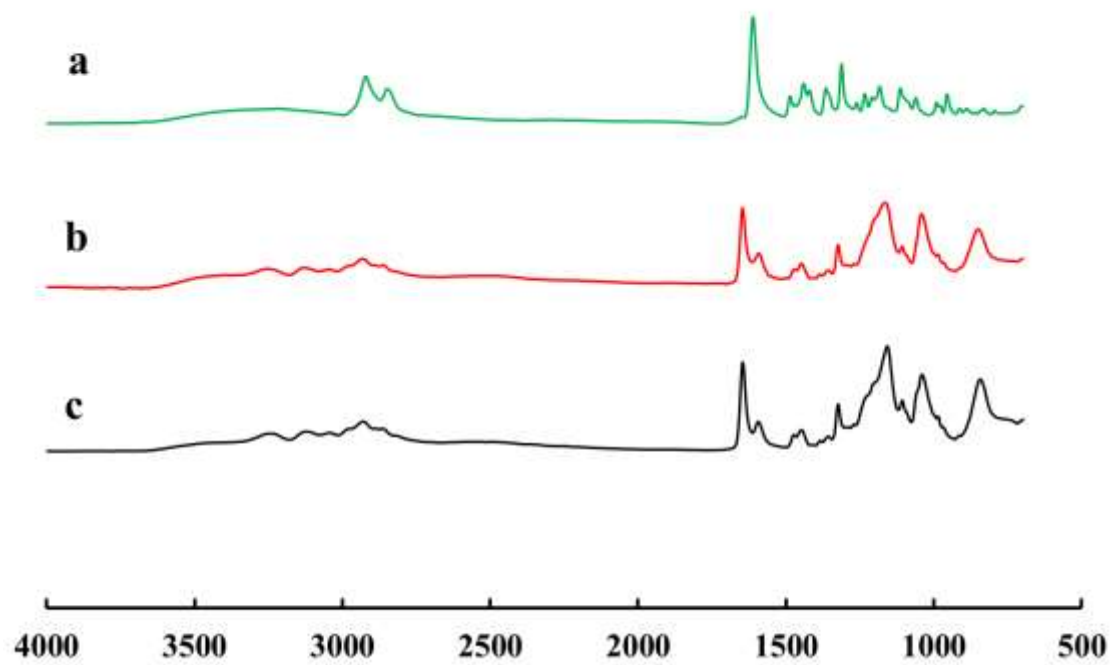


Figure C-3: The FTIR spectra for a. DBU (—), b. DBU-SO₄ synthesized in water (—), and c. DBU-SO₄ synthesized in organic solvent (—).

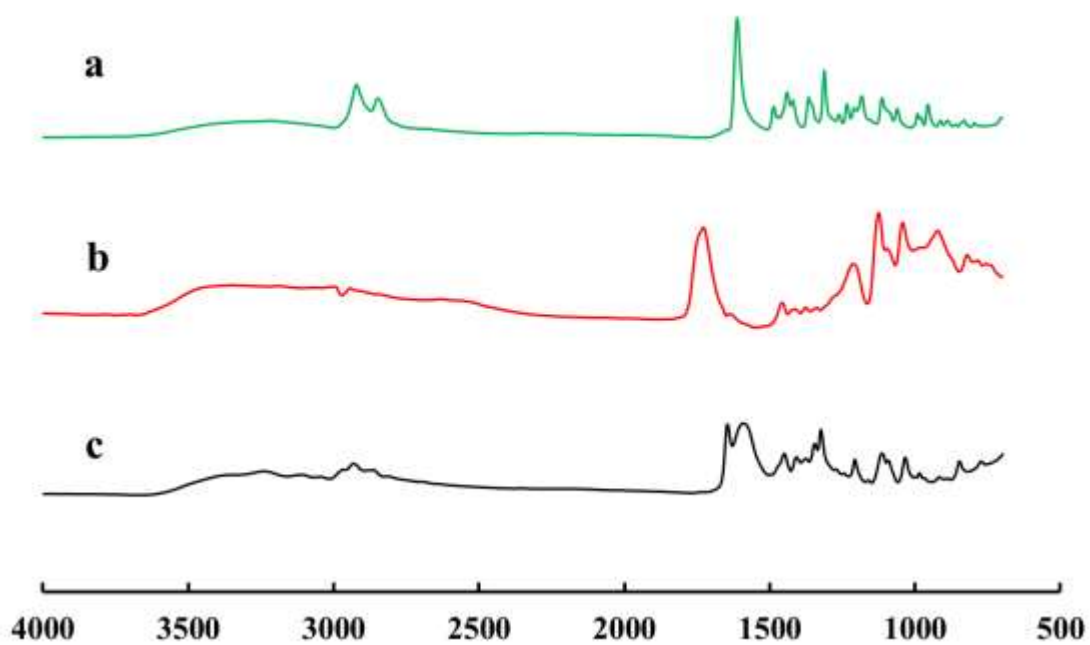


Figure C-4: The FTIR spectra for a. DBU (—), b. lactic acid (LA) (—), and
c. synthesized DBU-LA (—).

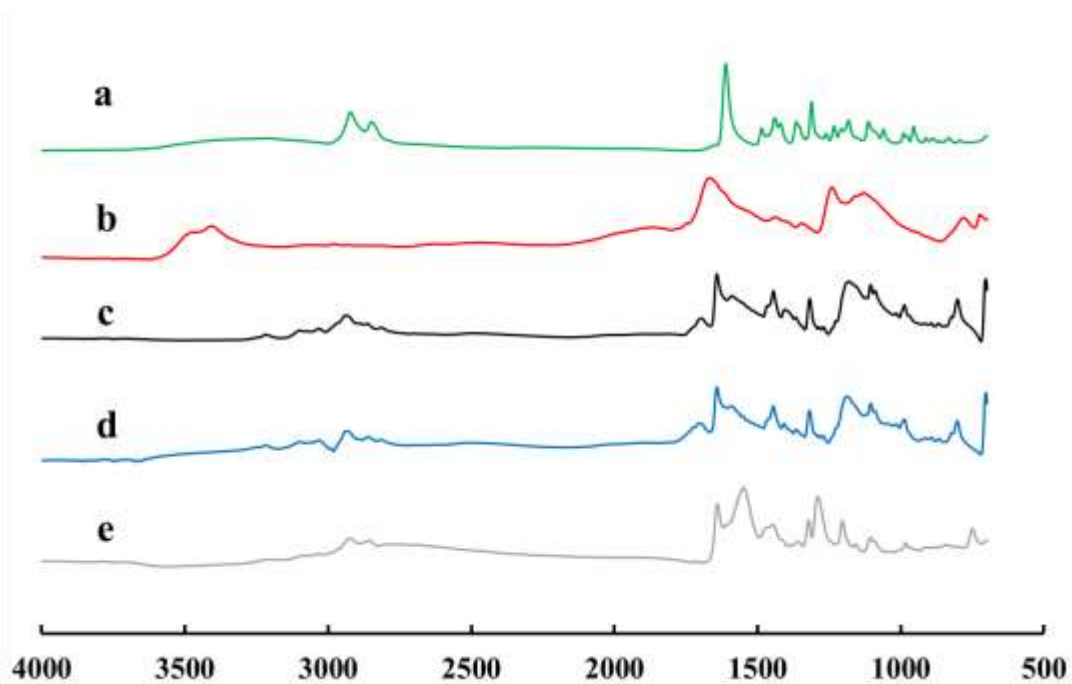


Figure C-5: The FTIR spectra for a. DBU (—), b. oxalic acid (OA) (—),

c. DBU-OA-equimolar synthesized in water (—),

d. DBU-OA-titration synthesized in water (—), and

e. DBU-OA synthesized in methanol (—).

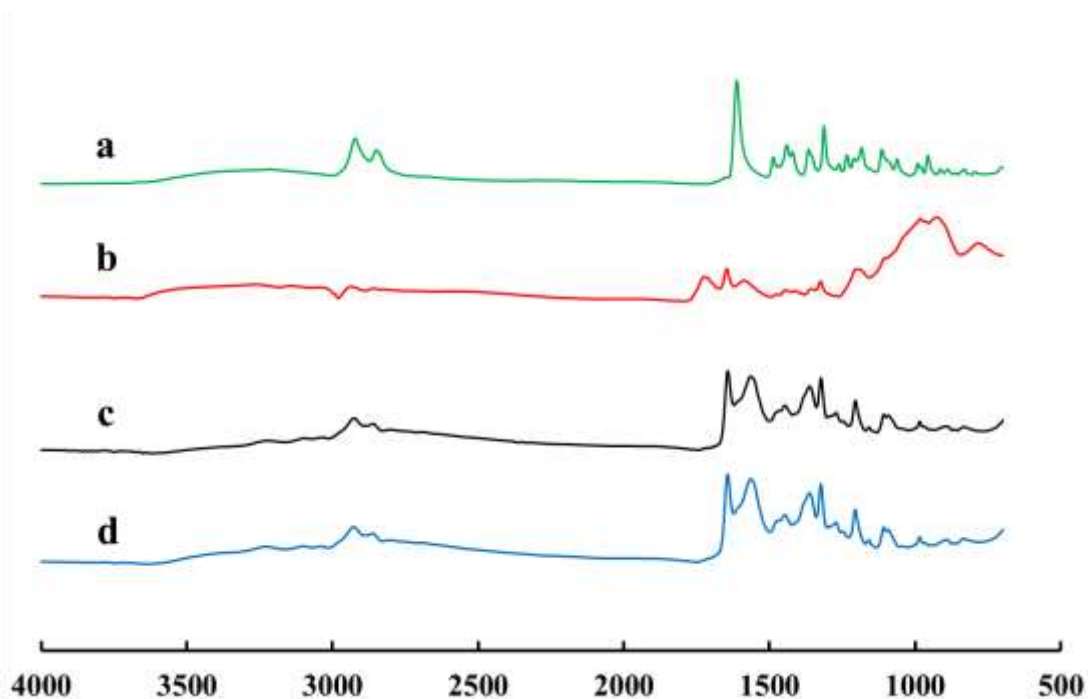
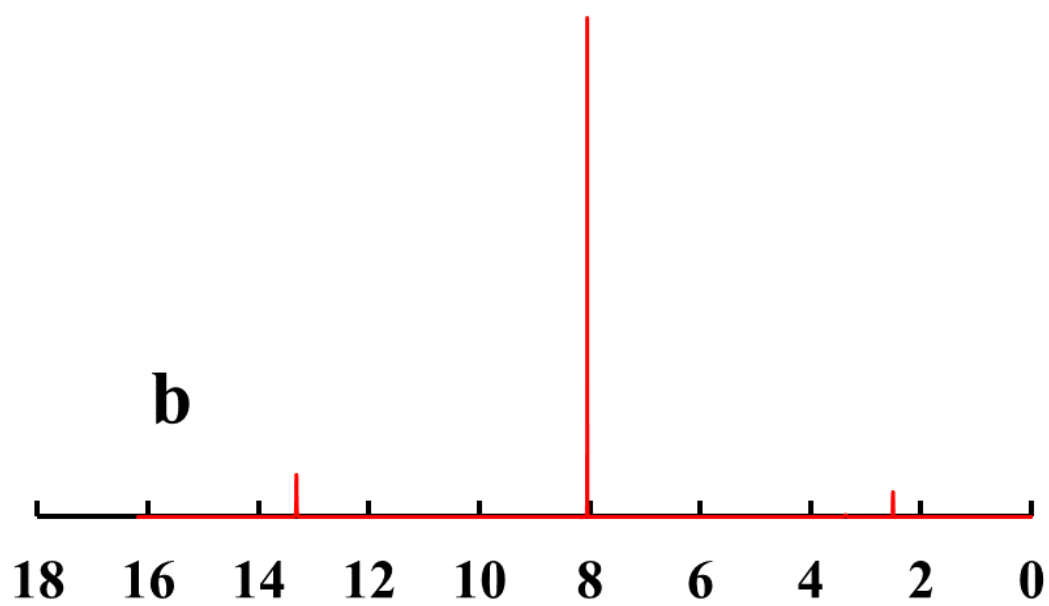
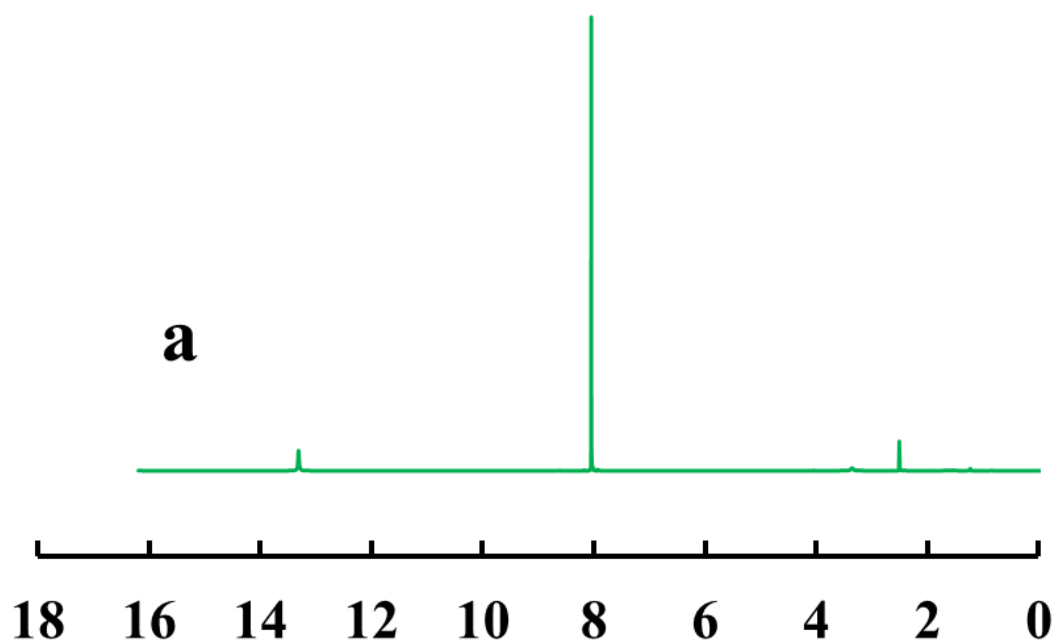


Figure C-6: The FTIR spectra for a. DBU (—), b. DBU-CA-equimolar synthesized in water (—), c. DBU-CA-titration synthesized in water (—), and d. DBU-CA synthesized in methanol (—).

Appendix D

^1H NMR results for Chapter 6



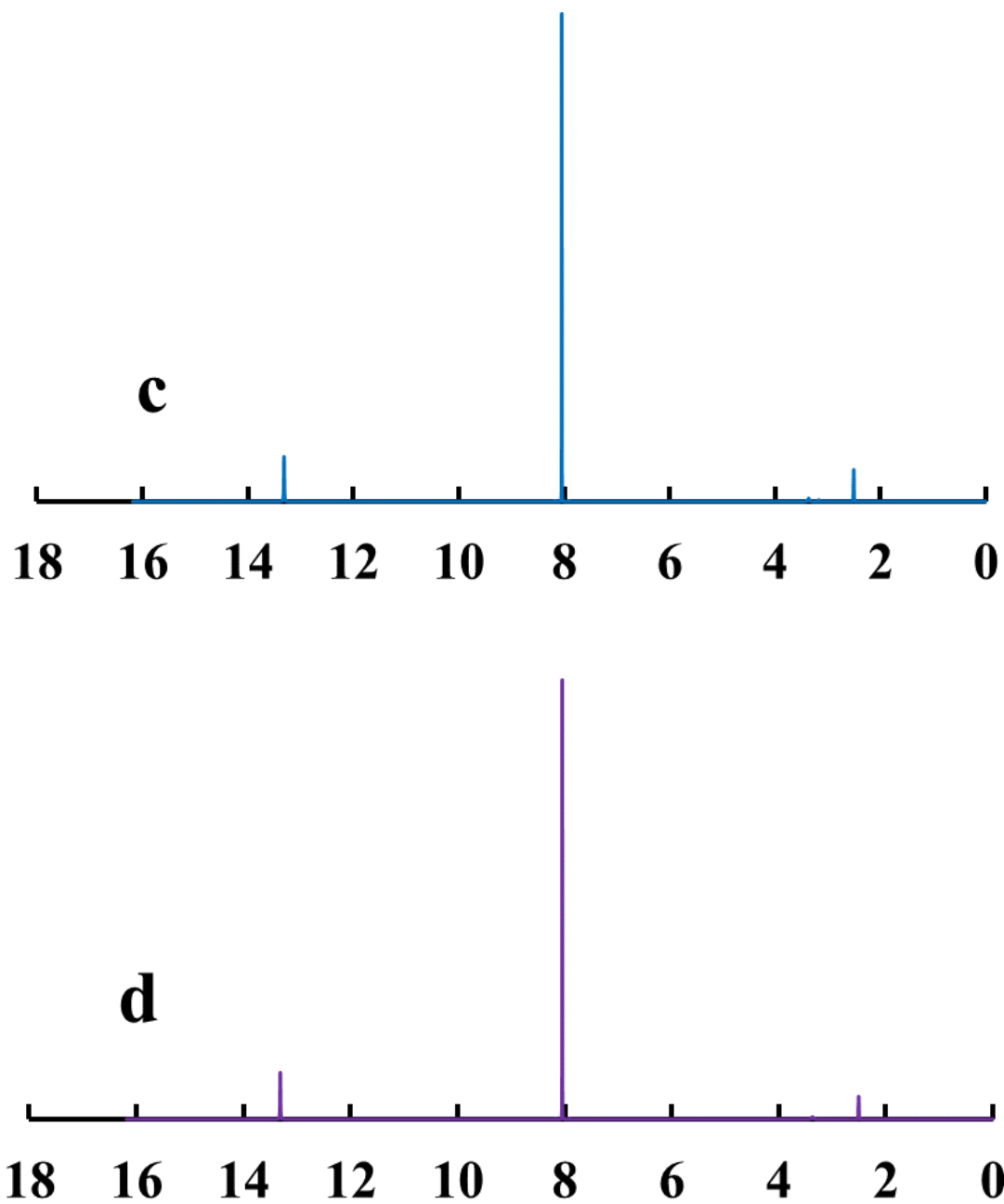
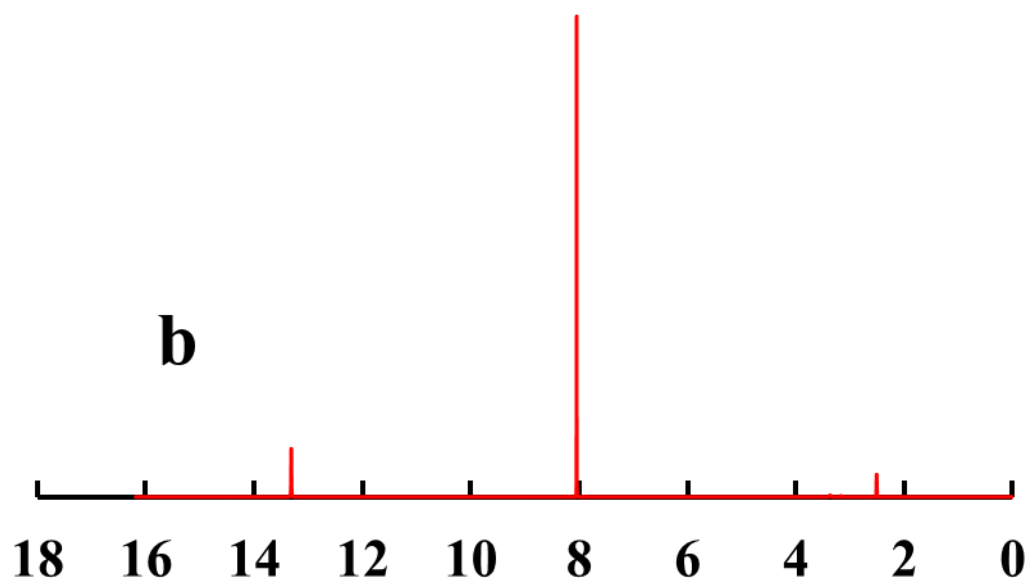
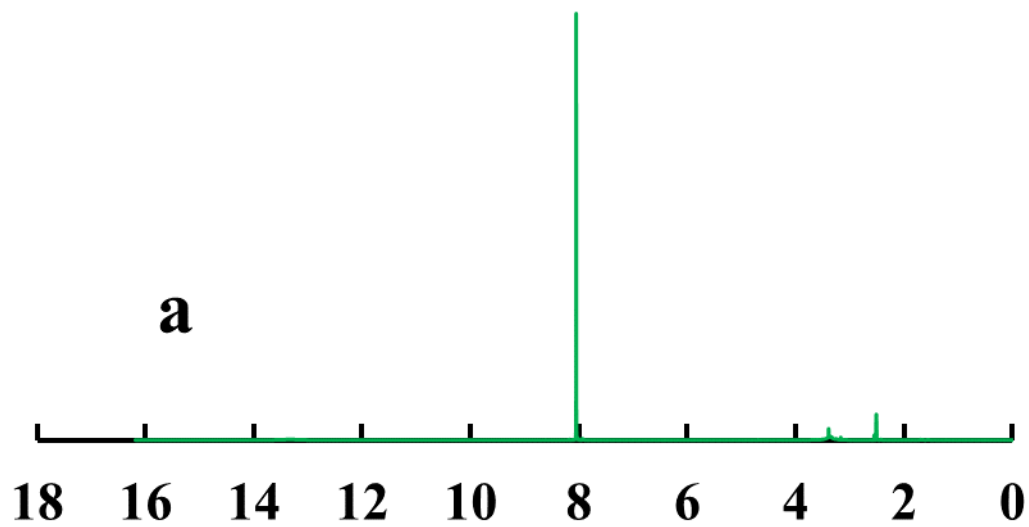


Figure D-1: The ^1H NMR spectra of a. commercial TPA (—) [43, 49] and recovered TPA samples from the hydrolysis of PET with 2M aqueous catalyst solutions of b. LA (—), c. OA (—), and d. CA (—), ($T_{\text{R}} = 150^\circ\text{C}$).



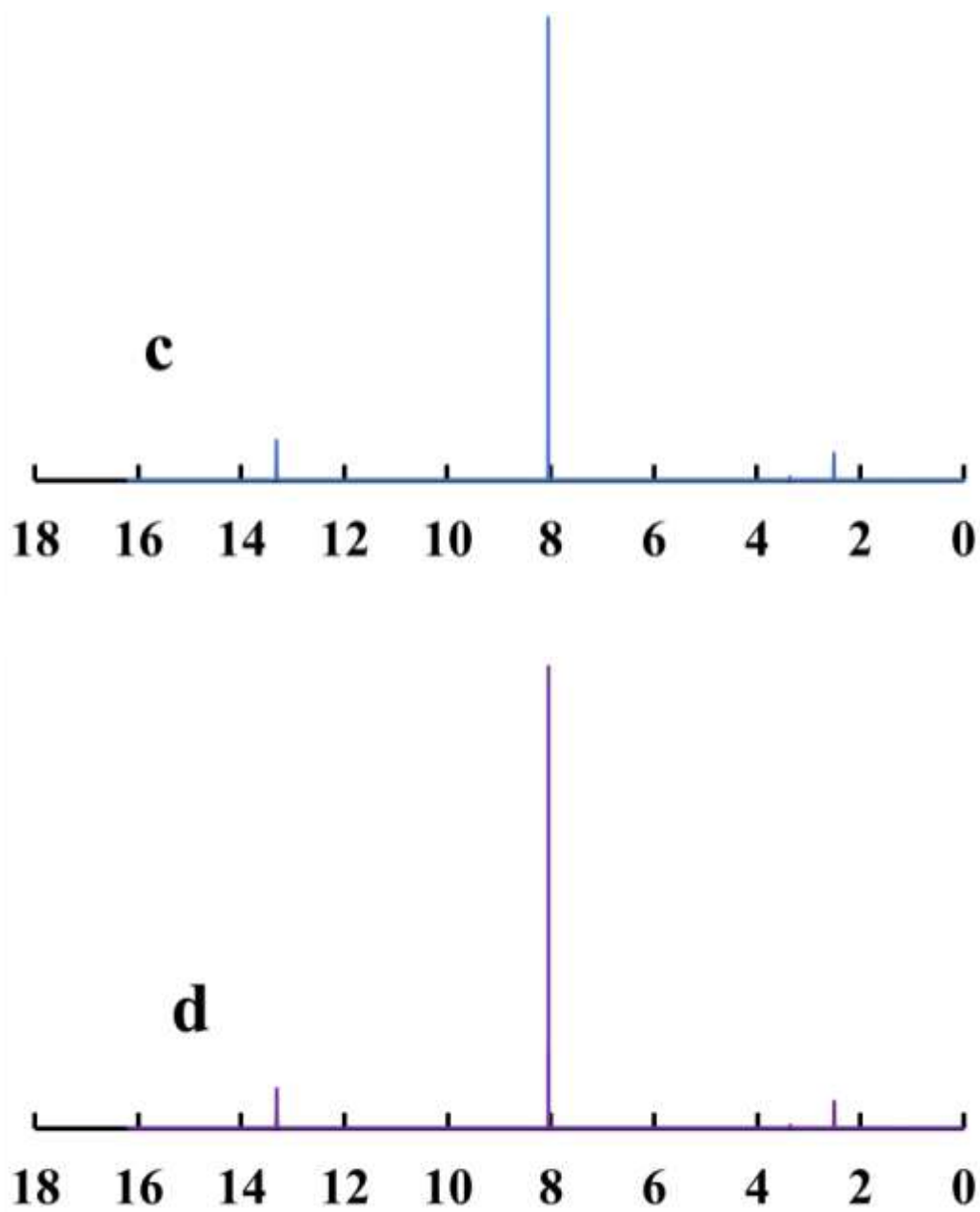


Figure D-2: The ^1H NMR spectra of the recovered TPA samples from the hydrolysis of PET with 2M aqueous catalyst solutions of a. DBU (—) b. DBU-LA (—), c. DBU-OA (—), and d. DBU-CA (—), ($T_{\text{R}} = 150^\circ\text{C}$).

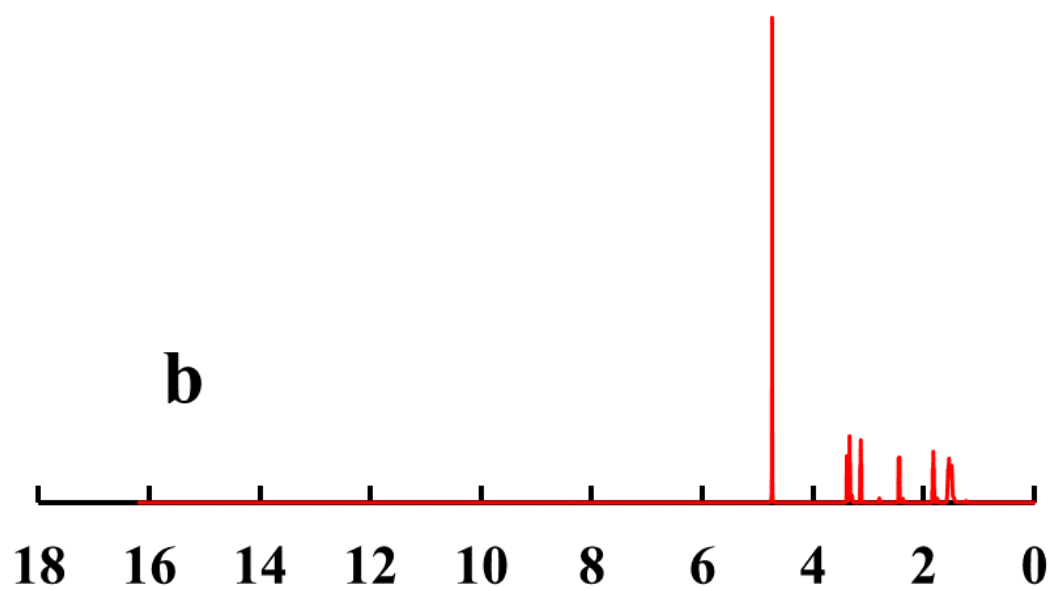
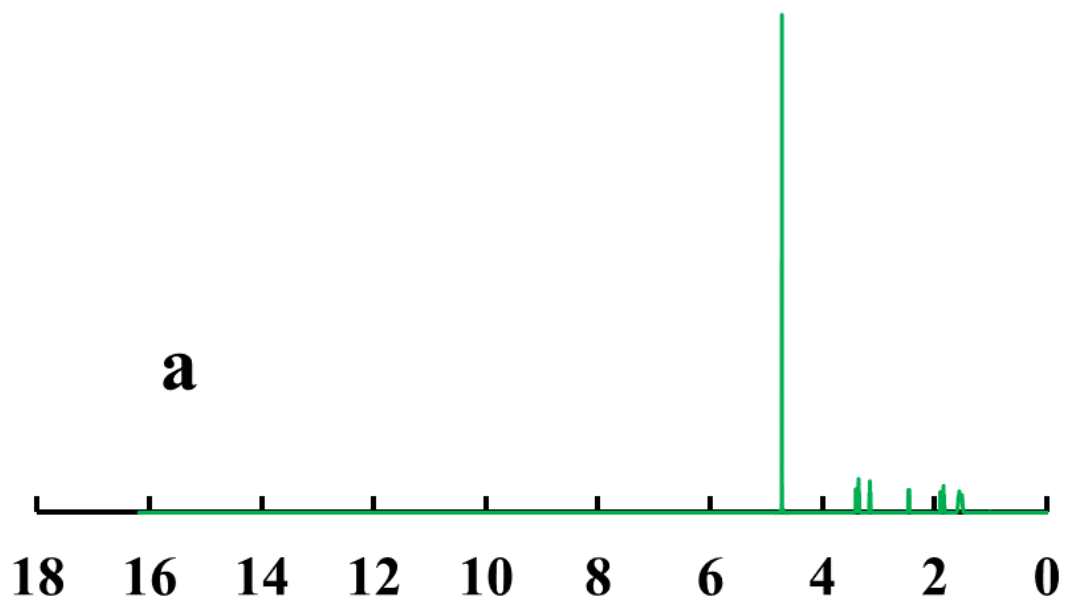


Figure D-3: The ¹H NMR spectra of a. DBU-SO₄ synthesized in organic solvent (—) and

b. DBU-SO₄ synthesized in water (—).

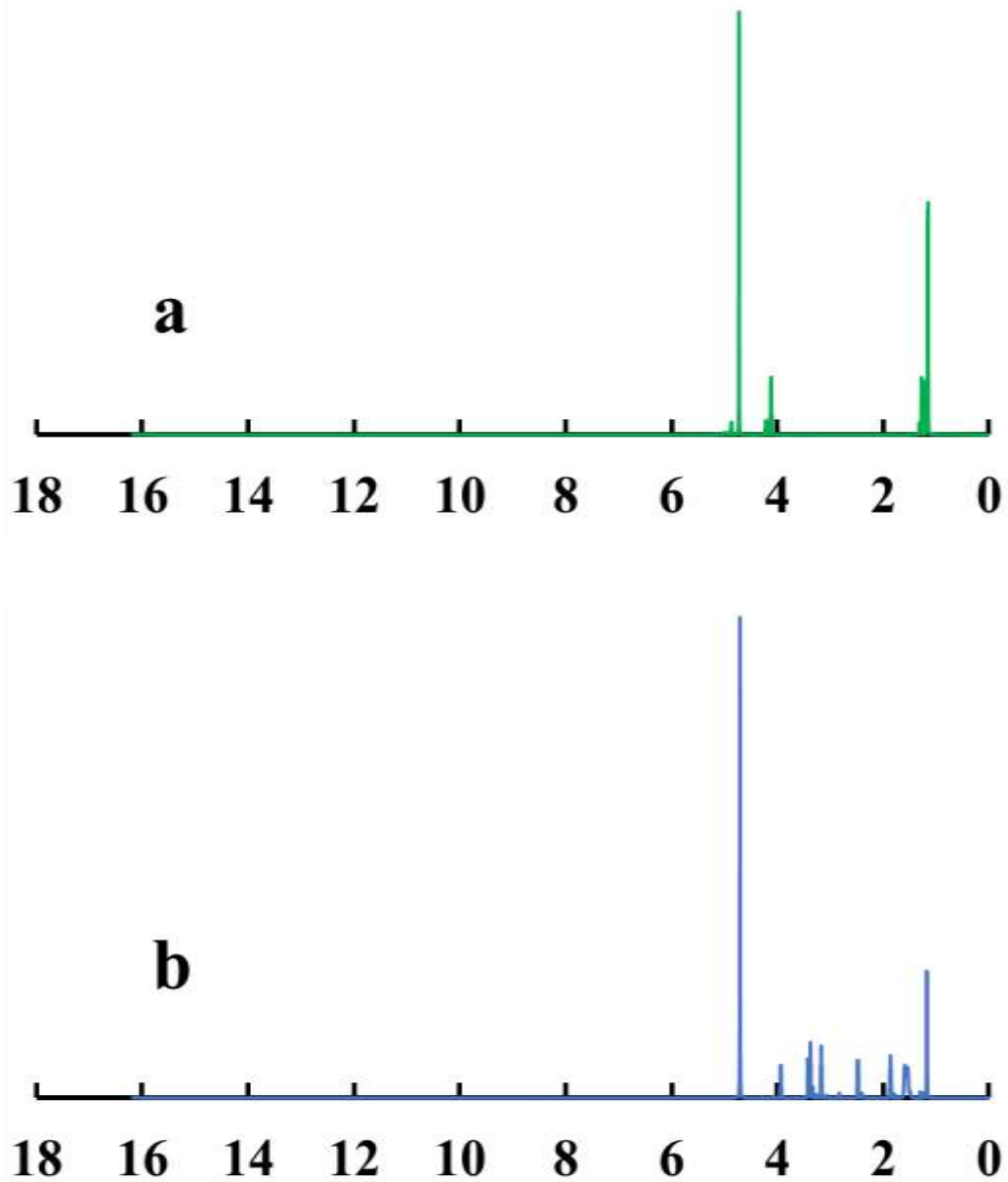
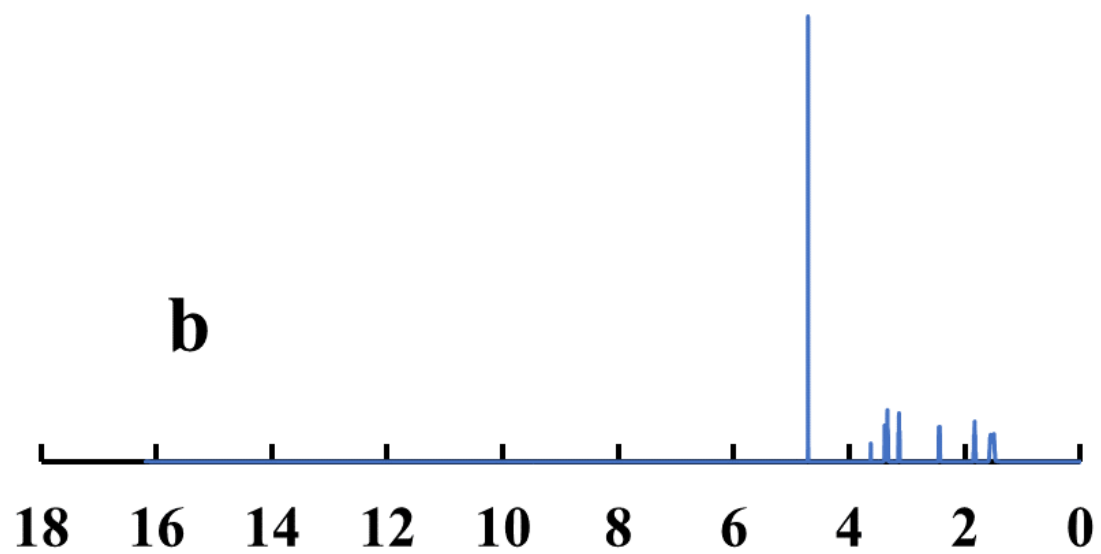
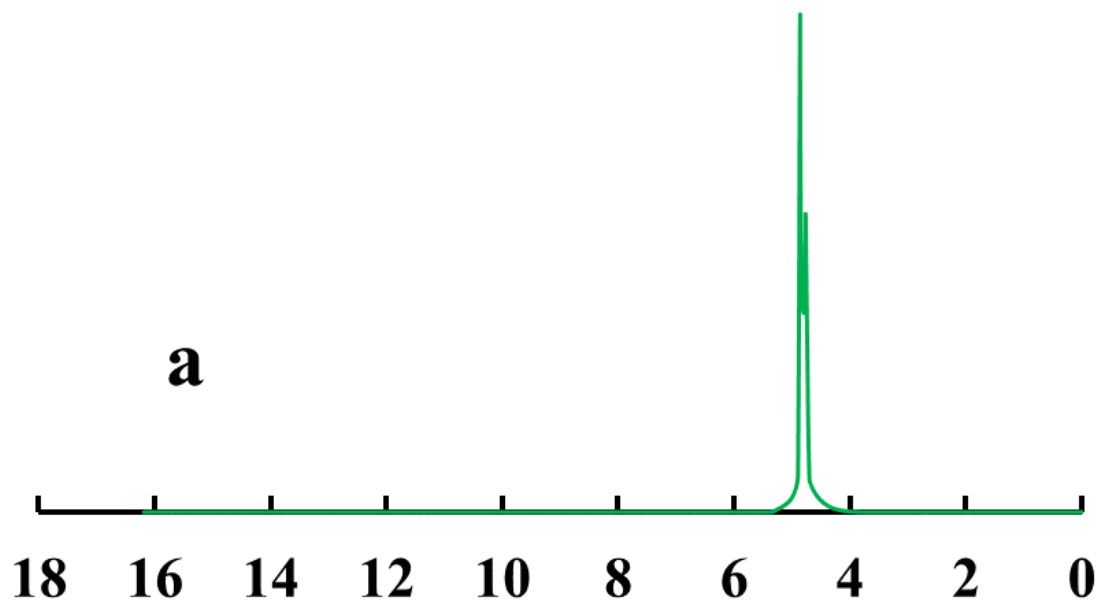


Figure D-4: The ^1H NMR spectra of a. lactic acid (LA) (—) and
b. synthesized DBU-LA (—).



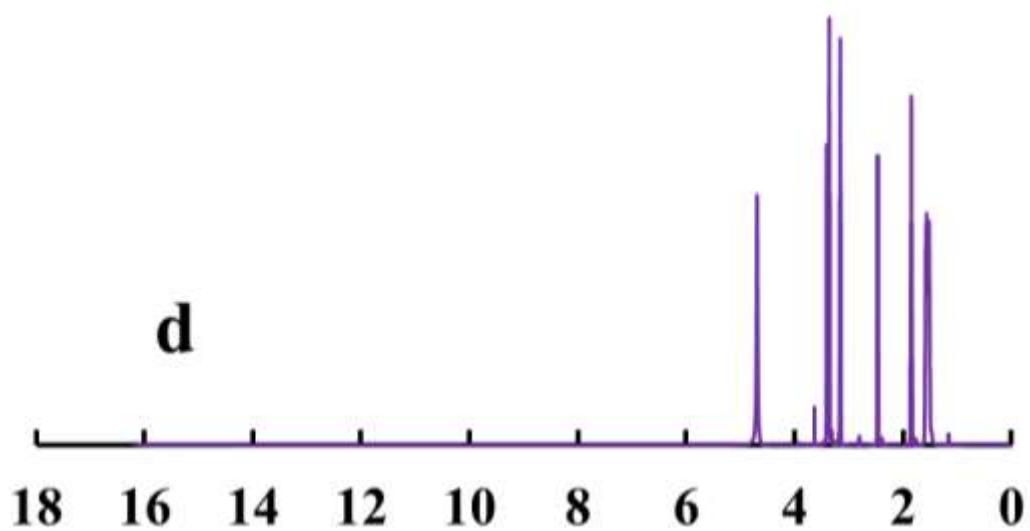
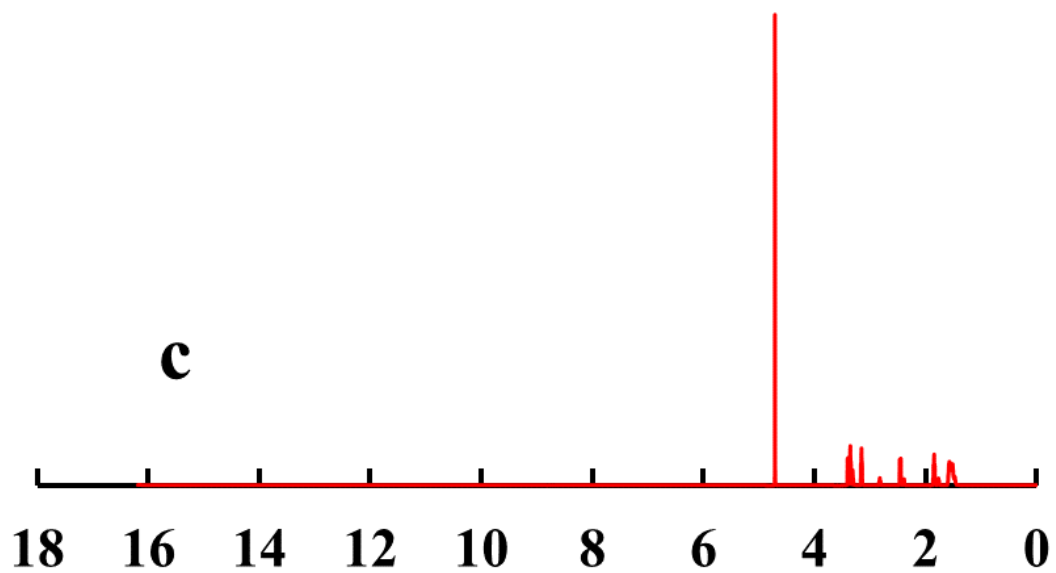
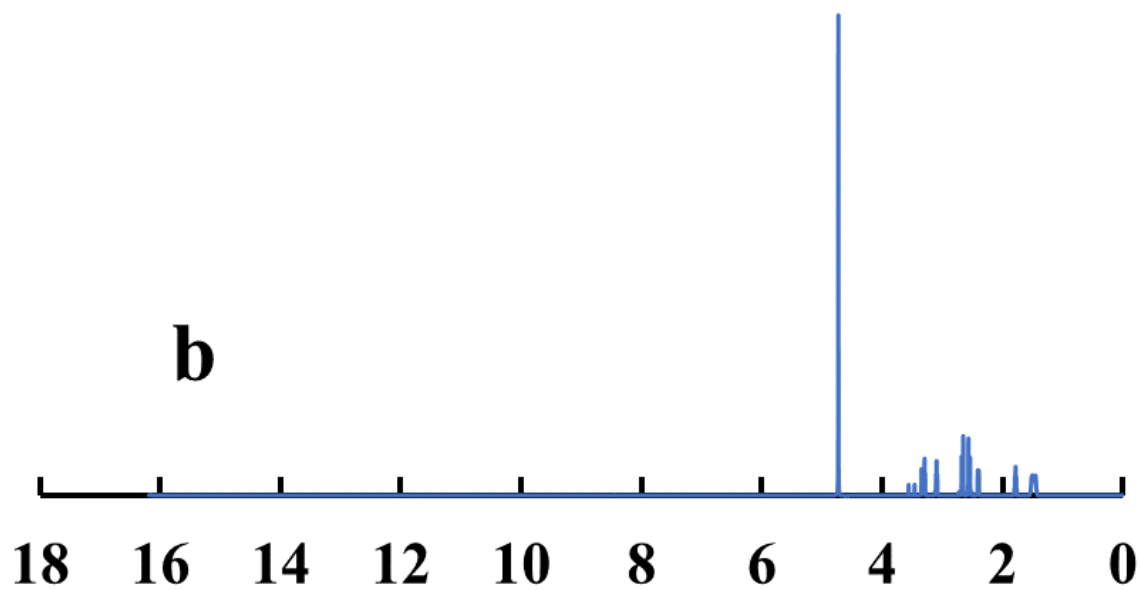
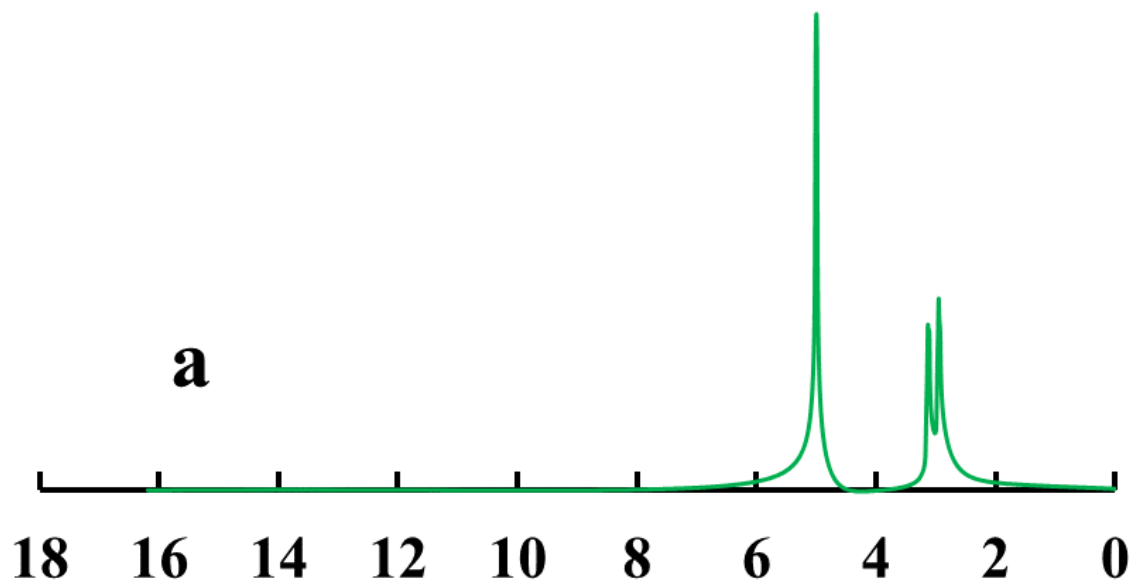


Figure D-5: The ^1H NMR spectra of a. oxalic acid (OA) (—),
 b. DBU-OA-equimolar synthesized in water (—), c. DBU-OA-titration synthesized in
 water (—), d. DBU-OA synthesized in methanol (—).



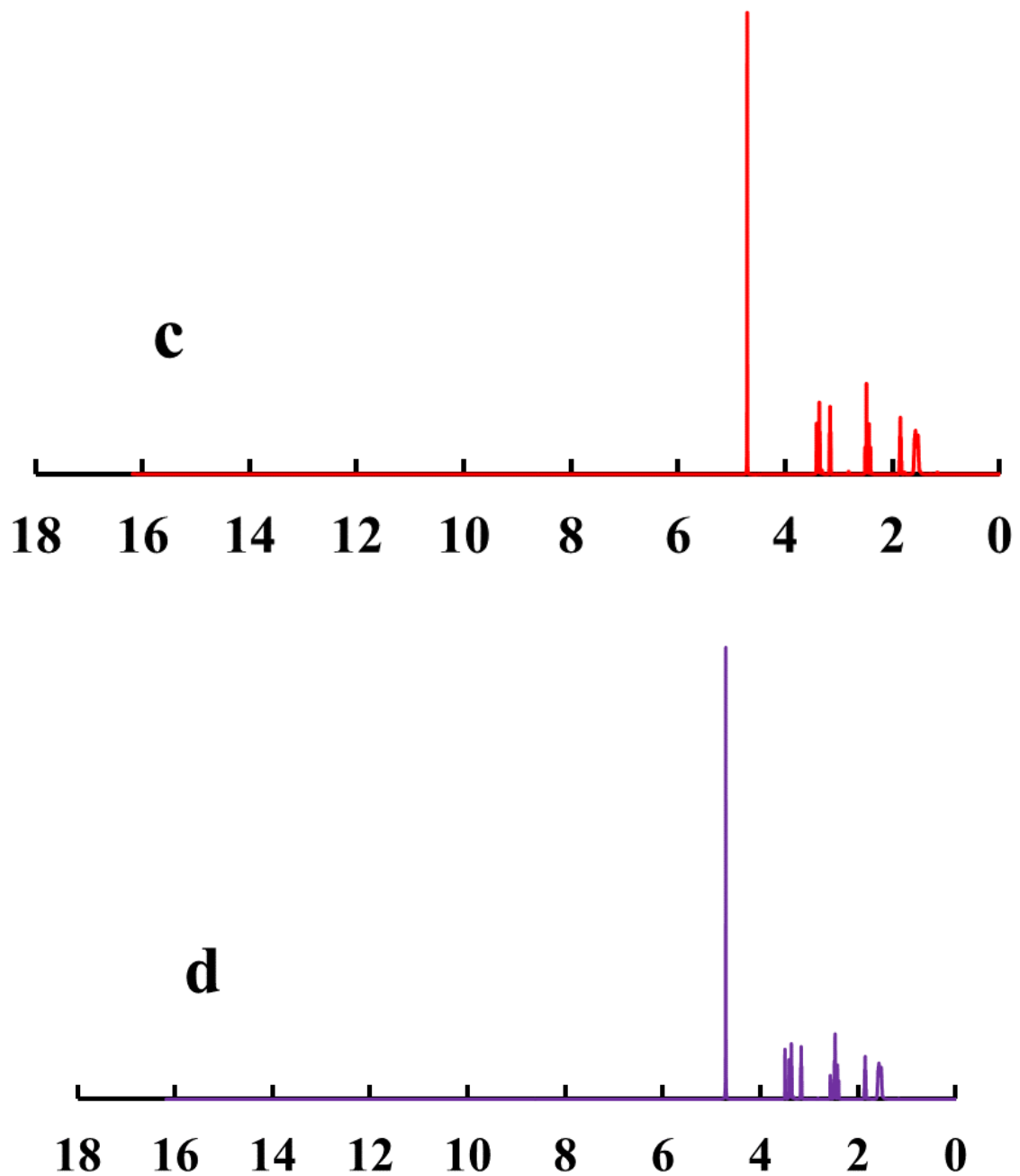


Figure D-6: The ^1H NMR spectra of a. citric acid (CA) (—),
 b. DBU-CA-equimolar synthesized in water (—), c. DBU-CA-titration synthesized in
 water (—), d. DBU-CA synthesized in methanol (—).

Appendix E

TGA results for DBU and DBU-acid ionic liquids

The TGA curves for DBU and DBU-acid ionic liquids that were synthesized in methanol are illustrated in **Figure E**. As noted, the complete thermal degradation of DBU occurred at 200°C. However, the complete thermal degradations for DBU-LA, DBU-OA, and DBU-CA were at temperatures of 450°C, 260°C, and 500°C, respectively. The TGA curves confirmed the DBU-acid ionic liquids have higher thermal stability than DBU.

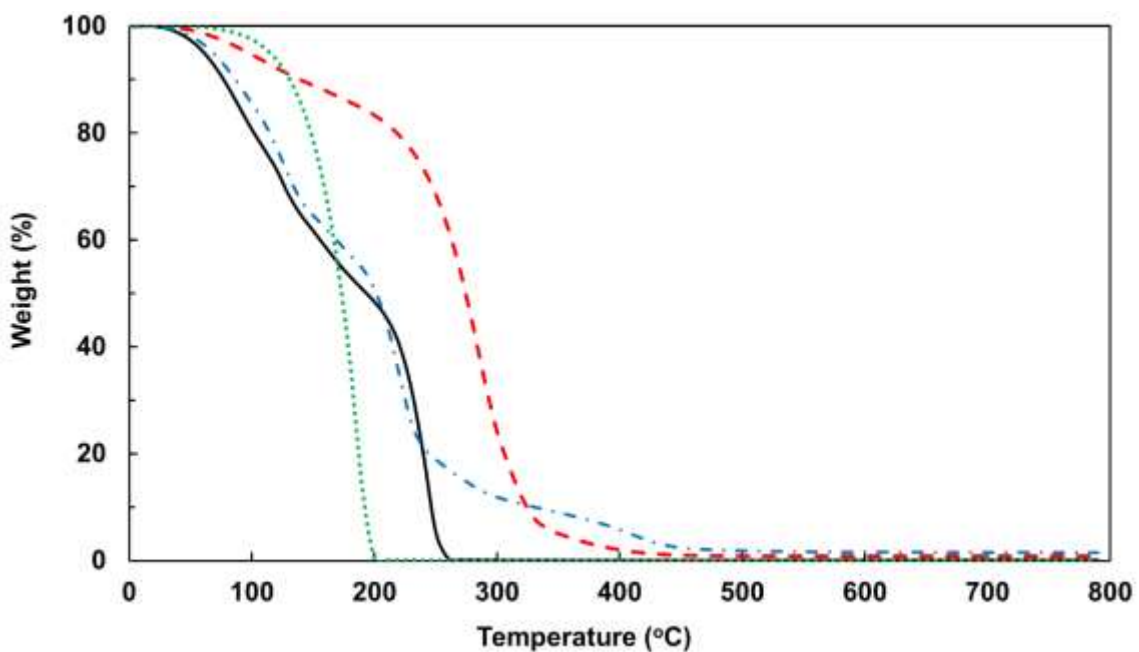


Figure E: The TGA curves for DBU (...) and DBU-acid ionic liquids synthesized in methanol: DBU-LA (---), DBU-OA (—), and (DBU-CA (—•)).

Appendix F

Comparisons of tested catalysts for hydrolysis of PET

The concentration effect on achieving more than 90% TPA yield for PET hydrolysis, using the aqueous solutions of proposed catalysts, are illustrated in **Figure F-1** (for LA, OA, and CA) and **Figure F-2** (for the rest except DBU), respectively. The DBU had super activity in hydrolysis of PET [43, 49]. For the reaction temperature of 150°C, the required times to achieve more than 90% TPA yield were 60, 20, and 10 minutes for aqueous solutions of DBU with 1, 2, and 4 M concentrations of DBU, respectively.

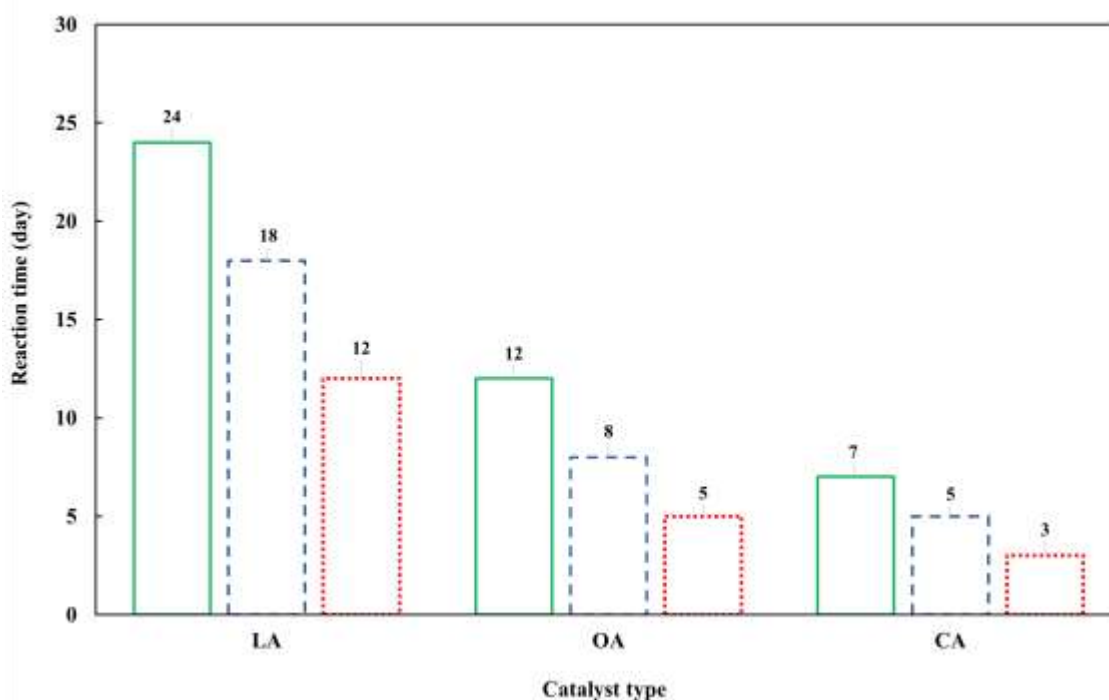


Figure F-1: The required time to achieve more than 90% TPA yield as a function of the catalyst concentration, 1M (—), 2M (---), 4M (...), aqueous solutions of LA, OA, and CA,

Reaction temperature = 150°C (Hydrolysis of PET in water) [43, 49].

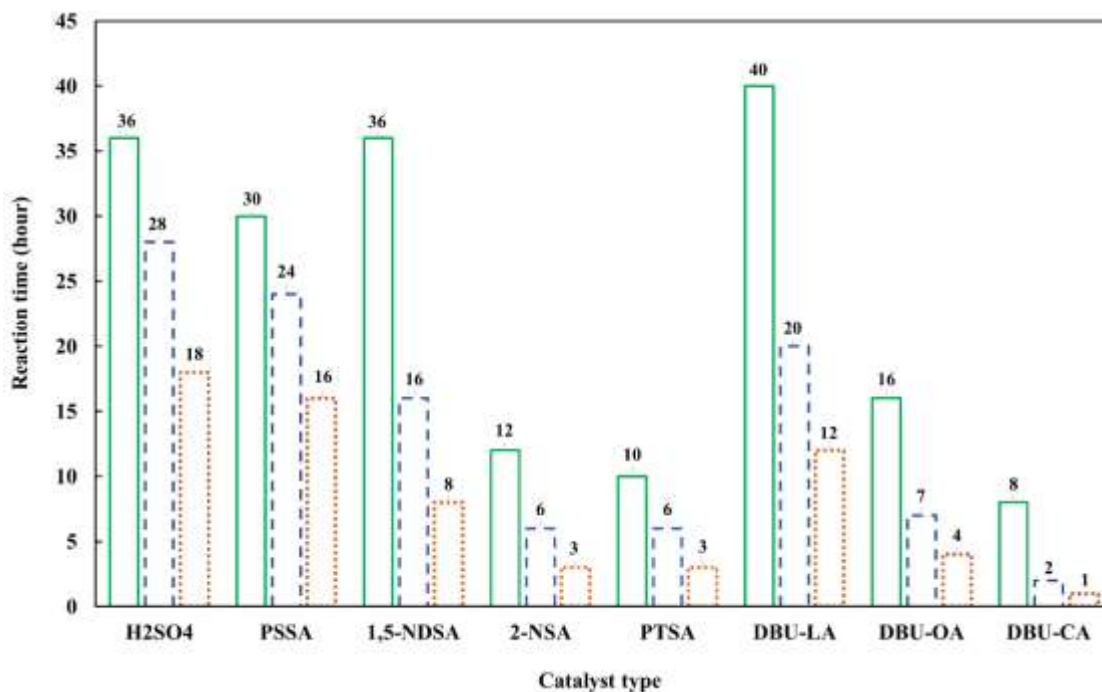


Figure F-2: The required time to achieve more than 90% TPA yield as a function of the catalyst concentration, 1M (—), 2M (---), 4M (···), aqueous solutions of H₂SO₄, PSSA, (1,5-NDSA), 2-NSA, DBU-LA, DBU-OA, and DBU-CA,

Reaction temperature = 150°C (Hydrolysis of PET in water) [43, 49].

The temperature effect on achieving more than 90% TPA yield for PET hydrolysis, using 2M of proposed catalyst concentrations in water, are illustrated in **Figure F-3** (for LA, OA, and CA) and **Figure F-4** (for the rest except DBU), respectively. The DBU had super activity in hydrolysis of PET [43, 49]. For the 2M DBU concentration in water, the required times to achieve more than 90% TPA yield were 35, 25, and 20 minutes for the reaction temperatures of 130°C, 140°C, and 150°C, respectively.

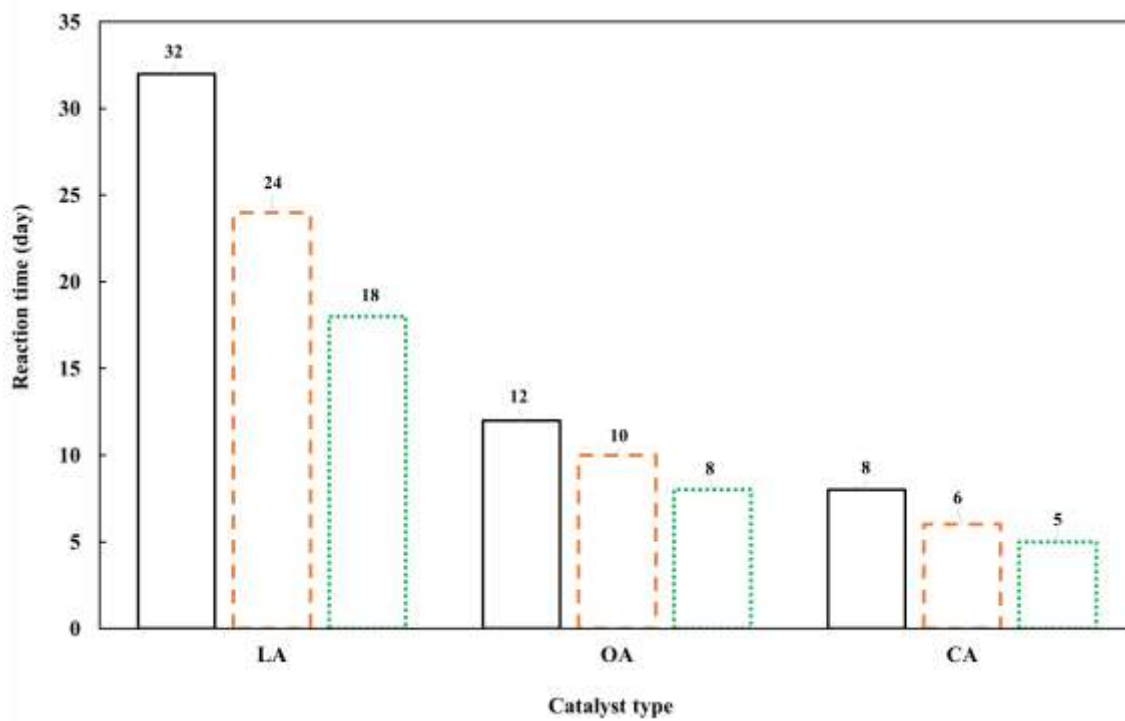


Figure F-3: The required time to achieve more than 90% TPA yield as a function of the reaction temperature, 130°C (—), 140°C (---), 150°C (...), 2M aqueous solutions of LA, OA, and CA,

Catalyst concentration = 2M (Hydrolysis of PET in water) [43, 49].

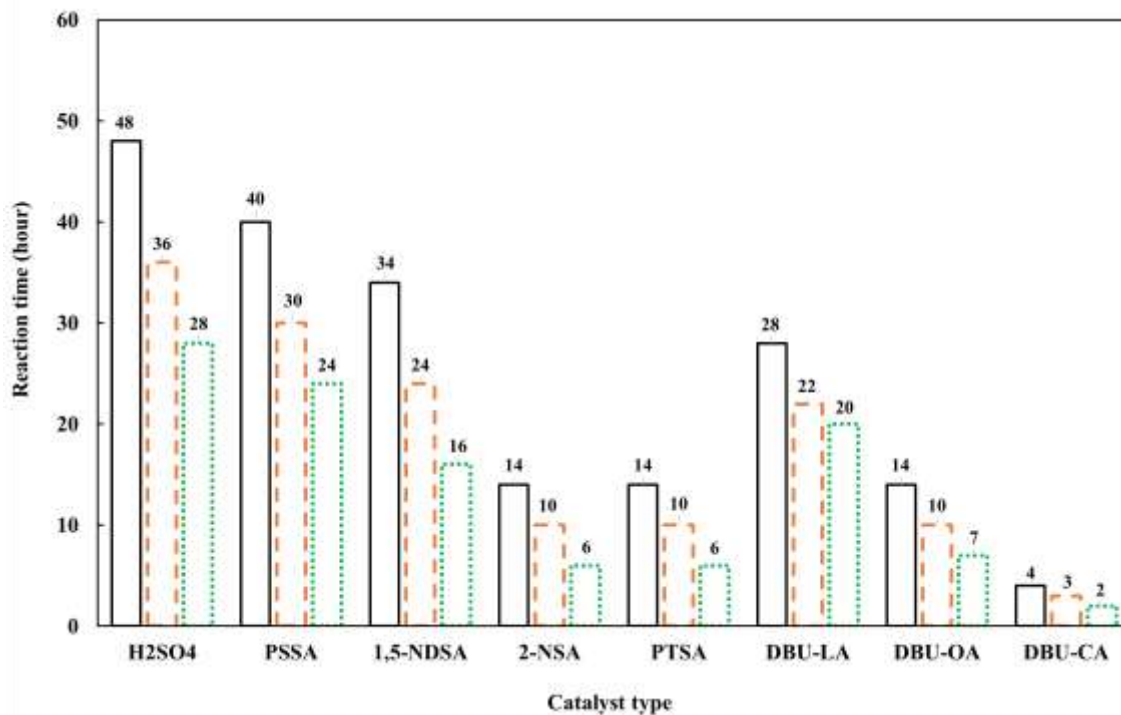


Figure F-4: The required time to achieve more than 90% TPA yield as a function of the reaction temperature, 130°C (—), 140°C (---), 150°C (...), 2M aqueous solutions of H₂SO₄, PSSA, (1,5-NDSA), 2-NSA, DBU-LA, DBU-OA, and DBU-CA,

Catalyst concentration = 2M (Hydrolysis of PET in water) [43, 49].

Appendix G

Octanol/water partition coefficient (P) values

To indirectly study the system of PET hydrolysis, the system of octanol/water was considered. This type of approach to study the hydrophobicity of a system by considering a similar system was reported for the hydrolysis of cellulose [34]. The method was adopted for the hydrolysis of PET [49]. The logarithmic partition coefficient (Log P) is the ratio of the concentration of unionized part of the catalyst in octanol to water for octanol/water system [34, 49]. The Log P values of tested catalysts for hydrolysis of PET were calculated by using the online software, ChemAxon™ [335]. The apparent reaction rate constants (K values) as the function of the Log P values are illustrated in **Figure G**.

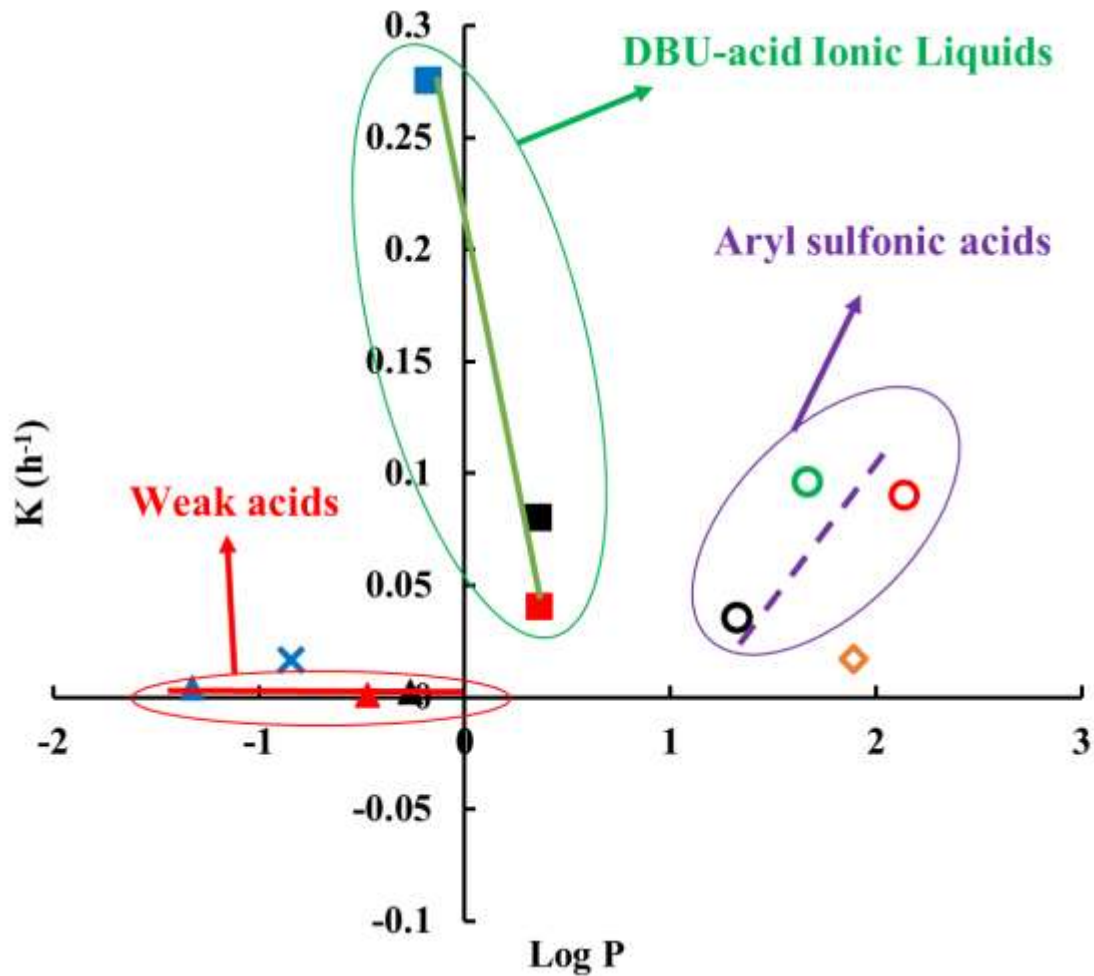


Figure G: Apparent reaction rate constants (K values) as the function of $\text{Log } P$ for 2M solutions of catalysts H_2SO_4 (X), PSSA (◇), PTSA (○), 2-NSA (○), 1,5-NDSA (○), LA (▲), OA (▲), CA (▲), DBU-LA (■), DBU-OA (■), and DBU-CA (■),

Reaction temperature = 150°C (Hydrolysis of PET in water) [43, 49].

Appendix H

Apparent reaction rate constant as the function of the contact angle value

The apparent reaction rate constants as the function of the contact angle values are depicted in **Figure H**. As illustrated, there are linear correlations between the contact angle value and the reaction rate constant. As the contact angle value decreases, due to the higher catalyst concentration, the apparent reaction rate constant increases [43, 49].

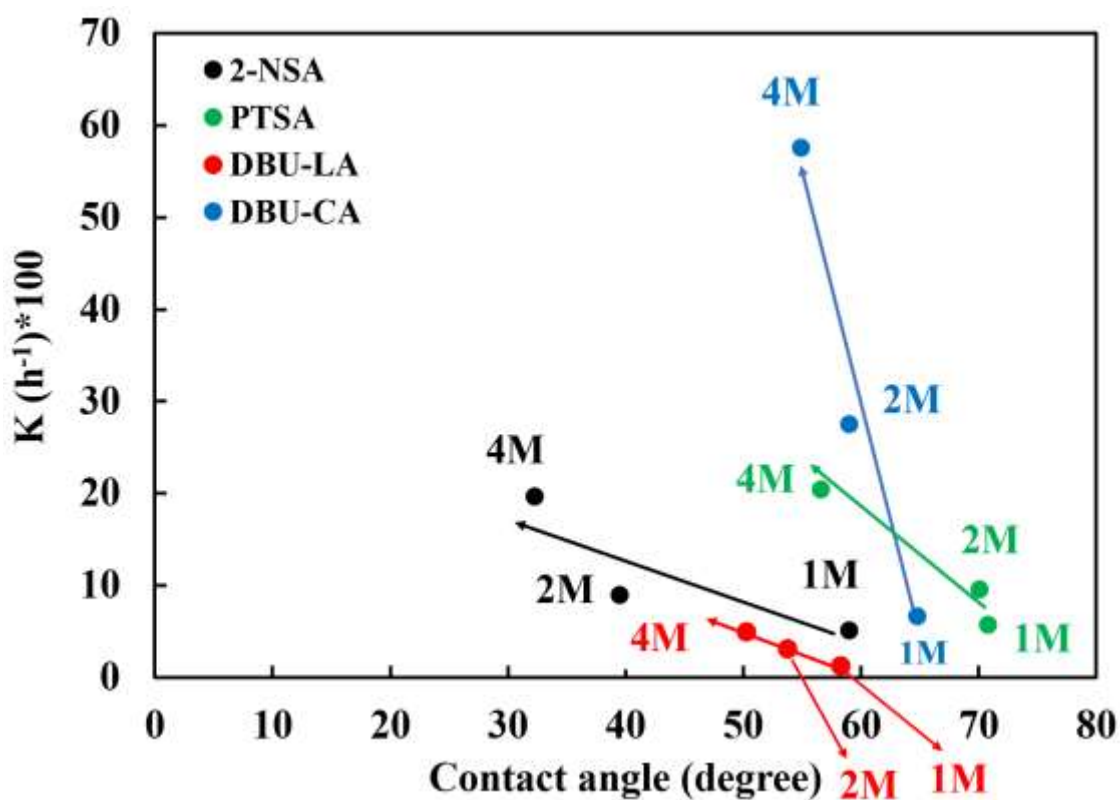


Figure H: The apparent reaction rate constants as the function of the contact angle values for aqueous catalyst solutions of 2-NSA (●), PTSA (●), DBU-LA (●), and DBU-CA (●)

[43, 49].